2

BR-M85010462

DOE/NV/10174--4

DE85 010462

TECHNICAL SUPPORT FOR GEOPRESSURED-GEOTHERMAL WELL ACTIVITIES IN LOUISIANA

ANNUAL REPORT
for the period
1 November 1982 to 31 October 1983

C. G. Groat
Program Coordinator

31 October 1984

Work Performed under Contract
DE-AC08-81NV10174

Louisiana State University
Office for Research
Louisiana Geological Survey
University Station, Box G
Baton Rouge, LA 70893

MASTER

DISTRIBUTION OF THIS DOCUMENT IS UNLIMITED

DISCLAIMER

This report was prepared as an account of work sponsored by an agency of the United States Government. Neither the United States Government nor any agency Thereof, nor any of their employees, makes any warranty, express or implied, or assumes any legal liability or responsibility for the accuracy, completeness, or usefulness of any information, apparatus, product, or process disclosed, or represents that its use would not infringe privately owned rights. Reference herein to any specific commercial product, process, or service by trade name, trademark, manufacturer, or otherwise does not necessarily constitute or imply its endorsement, recommendation, or favoring by the United States Government or any agency thereof. The views and opinions of authors expressed herein do not necessarily state or reflect those of the United States Government or any agency thereof.

DISCLAIMER

Portions of this document may be illegible in electronic image products. Images are produced from the best available original document.

DISCLAIMER

This report was prepared as an account of work sponsored by the United States Government. Neither the United States nor the United States Department of Energy, nor any of their employees, makes any warranty, express or implied, or assumes any legal liability or responsibility for the accuracy, completeness, or usefulness of any information, apparatus, product, or process disclosed, or represents that its use would not infringe privately owned rights. Reference herein to any specific commercial product, process, or service by trade name, mark, manufacturer, or otherwise, does not necessarily constitute or imply its endorsement, recommendations, or favoring by the United States Government or any agency thereof. The views and opinions of authors expressed herein do not necessarily state or reflect those of the United States Government or any agency thereof.

Printed in the United States of America

Available from:

National Technical Information Service
U.S. Department of Commerce
5285 Port Royal Road
Springfield, Virginia 22161

Price: Printed copy A09
Microfiche A01

DOE/NV/10174-4

TECHNICAL SUPPORT FOR GEOPRESSURED-GEOTHERMAL WELL ACTIVITIES IN LOUISIANA

ANNUAL REPORT
for the period
1 November 1982 to 31 October 1983

C. G. Groat
Program Coordinator

Louisiana State University
Office for Research
Louisiana Geological Survey
University Station, Box G
Baton Rouge, LA 70893

Prepared for the
U.S. Department of Energy
Division of Geothermal Energy
Under Contract DE-AC08-81NV10174

CONTENTS

	Page
PREFACE	v
ENVIRONMENTAL MONITORING	1
Water Quality Monitoring	1
Subsidence Monitoring	13
Microseismic Monitoring	34
REPORT DISTRIBUTION	79

PREFACE

This annual report describes environmental monitoring activities carried out by Louisiana State University (LSU) under U.S. Department of Energy Contract DE-AC08-81NV10174 for the period 1 November 1982 through 31 October 1983. Other aspects of the LSU technical support program have been completed and were covered in final form in reports immediately preceding this one. During the period included in this report, the Louisiana Geological Survey, aided by subcontractors, monitored microseismic activity, land-surface elevations, and surface and ground-water quality at three designed geopressured-geothermal test well sites in Louisiana. Don Stevenson supervised microseismic monitoring activities, and Drukell Trahan coordinated water quality and land-surface elevation studies. This report is a progress report in the sense that it discusses program components, provides data, and presents preliminary interpretations. The monitoring program continues and will be the subject of subsequent annual reports.

C. G. Groat

ENVIRONMENTAL MONITORING

WATER QUALITY MONITORING

by D. B. Trahan

Abstract

Historic ground-water chemistry studies in southwestern Louisiana provide a comparison of past chemical characteristics with the results of present ground-water quality monitoring. Temporal and spatial variations in ground-water chemistry may represent changes in water quality induced by natural or domestic processes.

Total dissolved solids (TDS) concentrations of analyzed ground waters at Parcperdue were less than 300 mg/L. For Sweet Lake, TDS concentrations ranged from 400 to 1200 mg/L, and for Rockefeller Refuge, from 1500 to 4000 mg/L TDS. These values are consistent with historic isohalines, which indicate the position of the saltwater interface before 1967. This interface dips to the north from 0 ft MSL along the coast to -2000 ft MSL in northern Calcasieu Parish.

Piper diagrams of major cations and anions in selected natural waters allow for the distinction of these waters according to depth and variation with time. Aquifer recharge is indicated at Parcperdue due to the close chemical association of surface and ground waters. Coastal surface waters and seawaters are chemically similar to geothermal brines except for magnesium content, which is relatively lower in geothermal brines. Ground waters and inland surface waters are distinct from geothermal brines in all cation and anion percentages. The most distinguishing parameters may be magnesium and sulfate. Relative contents of magnesium and sulfate generally decrease and increase with depth, respectively.

Variations in water chemistry at the geopressured-geothermal test sites are probably related to natural causes, the most important of which is saltwater intrusion. It is also possible that contamination may be caused by the migration of natural brines or by the injection of oil-field wastes with depth. Further work with mixing diagrams and statistical analyses will allow for a distinction between these phenomena.

Introduction

The third year of geothermal testing in south Louisiana saw many changes which affected the status, development, and continuation of the environmental monitoring program. The closing of the Parcperdue geopressured-geothermal test site led to the termination of water quality monitoring there. Except for surface contamination caused by a leaky brine disposal pit, it is doubtful that there was enough production or subsurface injection to adversely impact the natural waters in the area. Historical subsurface injection from other sources has been shallower and possibly volumetrically greater so that, if detected, contamination of natural water by brine may not be blamed solely on geopressured-geothermal production. The same concern can be voiced for the other sites, although water quality monitoring is continuing.

Expansion of the water quality data base is crucial. Changes in water quality due to brine contamination can only be assessed after examining the water's natural characteristics. For this, we have relied on statistical and graphical methods which group parameters into origin-related families and trace the changes in major and key constituents through time. In addition, data which may relate natural water quality characteristics to geologic variability are presented. Permeability anomalies may allow saltwater intrusion or freshwater recharge in a tested aquifer. These phenomena are distinguishable to some degree in our analyses.

Discussion

Extensive research was done in the late 1960s on the water quality characteristics of ground waters in southwestern Louisiana (Harder and others, 1967; Winslow, Hillier, and Turcan, 1968). A concentrated effort was made to establish the position of the saltwater interface, but little was done to establish the rate of movement. By comparing data from the present project with data obtained in earlier studies, some observations can be made about this important phenomenon.

The regional position of the freshwater-saltwater interface and the limits of fresh water are shown in Figure 1, and total dissolved solids (TDS) contents with depth are shown in Figure 2. From these diagrams, the approximate TDS concentrations of ground waters near the geopressured-geothermal test sites can be interpolated. The resulting values represent the chemical characteristics of these waters prior to 1967-68. A comparison with more recent data should indicate a change caused by the movement of the saltwater interface.

At Parcperdue, the altitude of the base of fresh water is approximately -275 m (-900 ft) MSL (Fig. 1). An increase in dissolved solids content with depth is indicated by the altitudes of the 1000-, 3000-, and 10,000-mg/L dissolved solids surfaces (Fig. 2). The observation wells used to monitor changes in water quality are greater than -61 m (-200 ft) LSD (land surface datum). Assuming that no significant saltwater intrusion has occurred since 1968, the shallow ground waters at Parcperdue should still be fresh.

The map showing the base of fresh water (Fig. 1) is based on chloride content. Water with a chloride content less than 250 mg/L is considered to be fresh. The most recent water quality analyses for Parcperdue ground waters gave an average chloride concentration of only 12 mg/L. This indicates that the saltwater interface is still some distance away from the test site or that

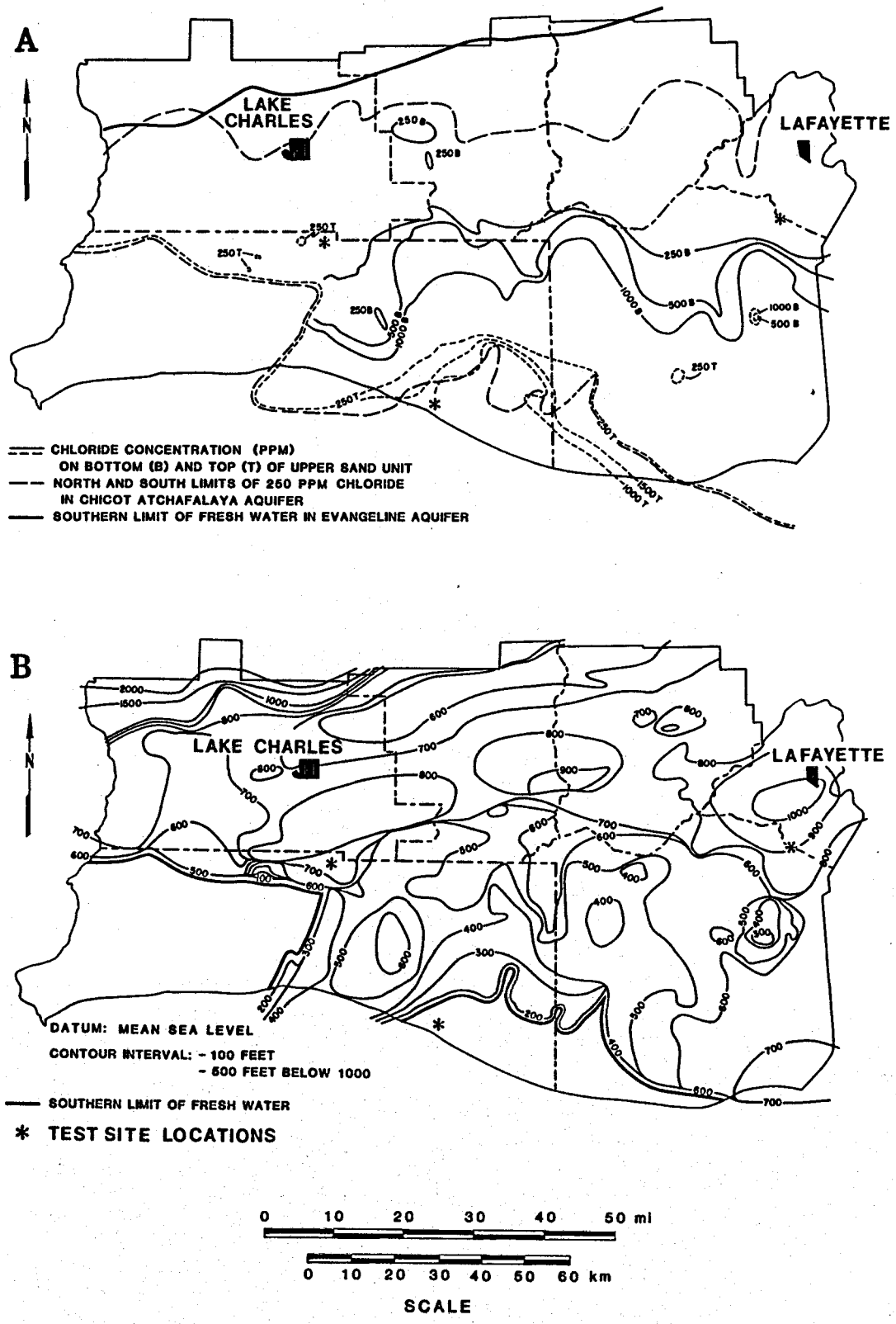

FIGURE 1. Freshwater-saltwater interface in the Chicot aquifer (A) and the base of fresh water (B), southwestern Louisiana (after Harder, Kilburn, and Whitman, 1967). Asterisks indicate test site locations.

4

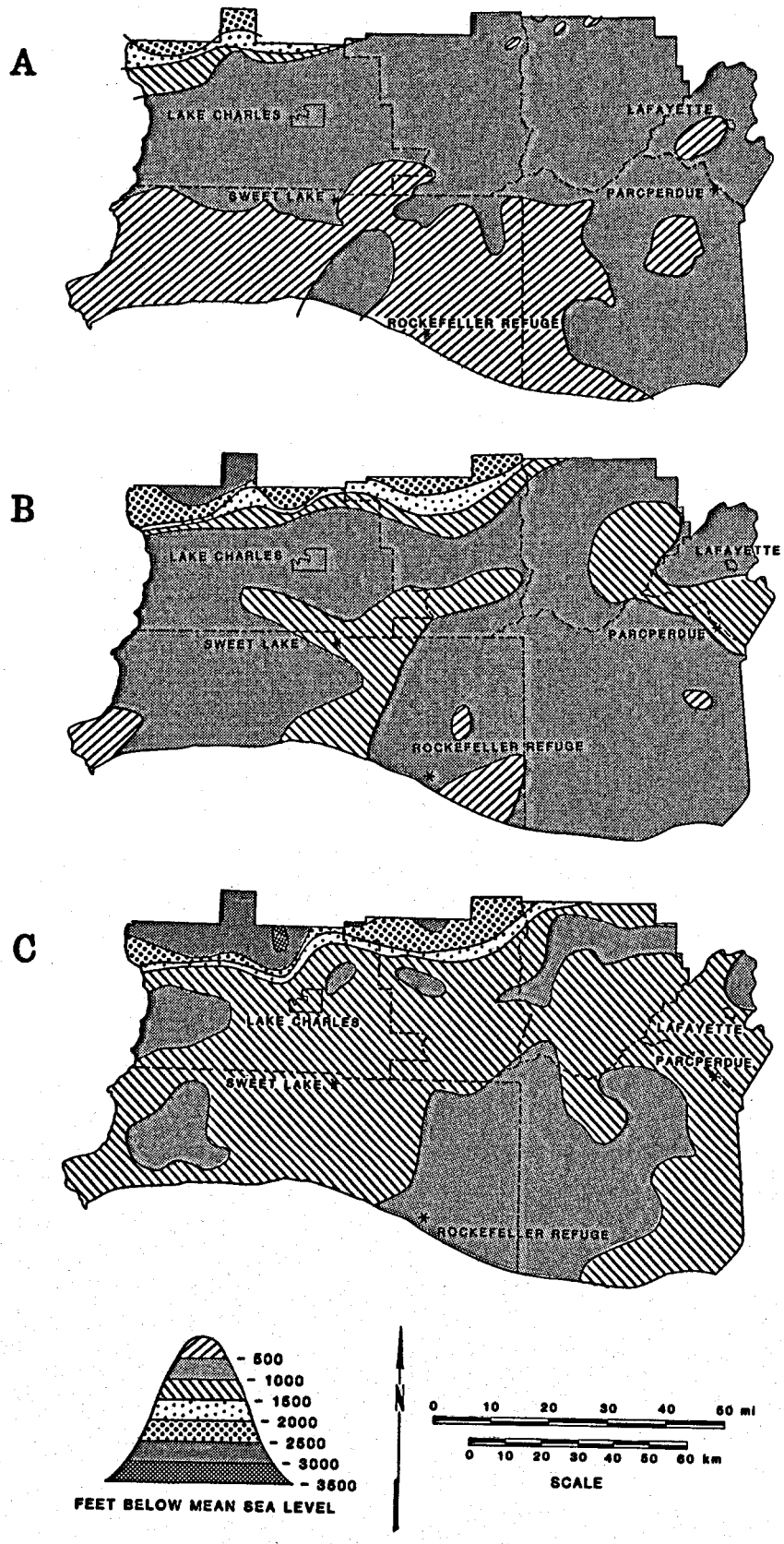

FIGURE 2. Altitudes of dissolved solids surfaces: A) 1000 mg/L (after Harder, Kilburn, and Whitman, 1967), B) 3000 mg/L (after Winslow, Hillier, and Turcan, 1968), and C) 10,000 mg/L (after Winslow, Hillier, and Turcan, 1968).

perhaps recharge in the area is sufficient to keep pace with saltwater intrusion.

The base of fresh water is shallower at Sweet Lake than at Parcperdue (Fig. 1). In 1967, the 250-mg/L isohaline was approximately -183 m (-600 ft) MSL. In November 1983 chloride concentrations in project observation wells were below the laboratory detection limit of 1.0 mg/L. The Sweet Lake test site may be in an area of very active ground-water recharge, as indicated by an anomalously deep saltwater interface shown by the altitude of the 3000-mg/L dissolved solids surface (Fig. 2).

According to Figure 1, the Rockefeller Refuge test site is located completely outside of the limit of fresh water in southwestern Louisiana. Project analyses of the November 1983 samples gave chloride contents of 48 and 13 mg/L for the 94-m (310-ft) and the 201-m (660-ft) wells, respectively; however, the respective TDS concentrations were 3500 and 1500 mg/L. The 1000-mg/L dissolved solids surface is shown to be less than -152 m (-500 ft) MSL (Fig. 2), which is consistent with our analysis.

A common method of illustrating the general chemical characteristics of natural waters is the trilinear plot (Piper, 1944), which is a diagram divided into three fields representing the relative concentrations of major cations, anions, and cation-anion pairs (Fig. 3). In the lower left triangle, the percentage reacting values (PRVs) of the major cations calcium (Ca), magnesium (Mg), and sodium (Na) are plotted as a single point. In the lower right triangle, the PRVs of the major anions chloride (Cl), sulfate (SO_4), and bicarbonate (HCO_3) are plotted. The intersection of the rays from these two fields in the central diamond indicates the relative concentrations of the most common cation-anion pairs, such as sodium bicarbonate ($NaHCO_3$), sodium chloride (NaCl), and calcium carbonate ($CaCO_3$). The local field, designated as A (Fig. 3), contains the PRVs of major dissolved constituents in project

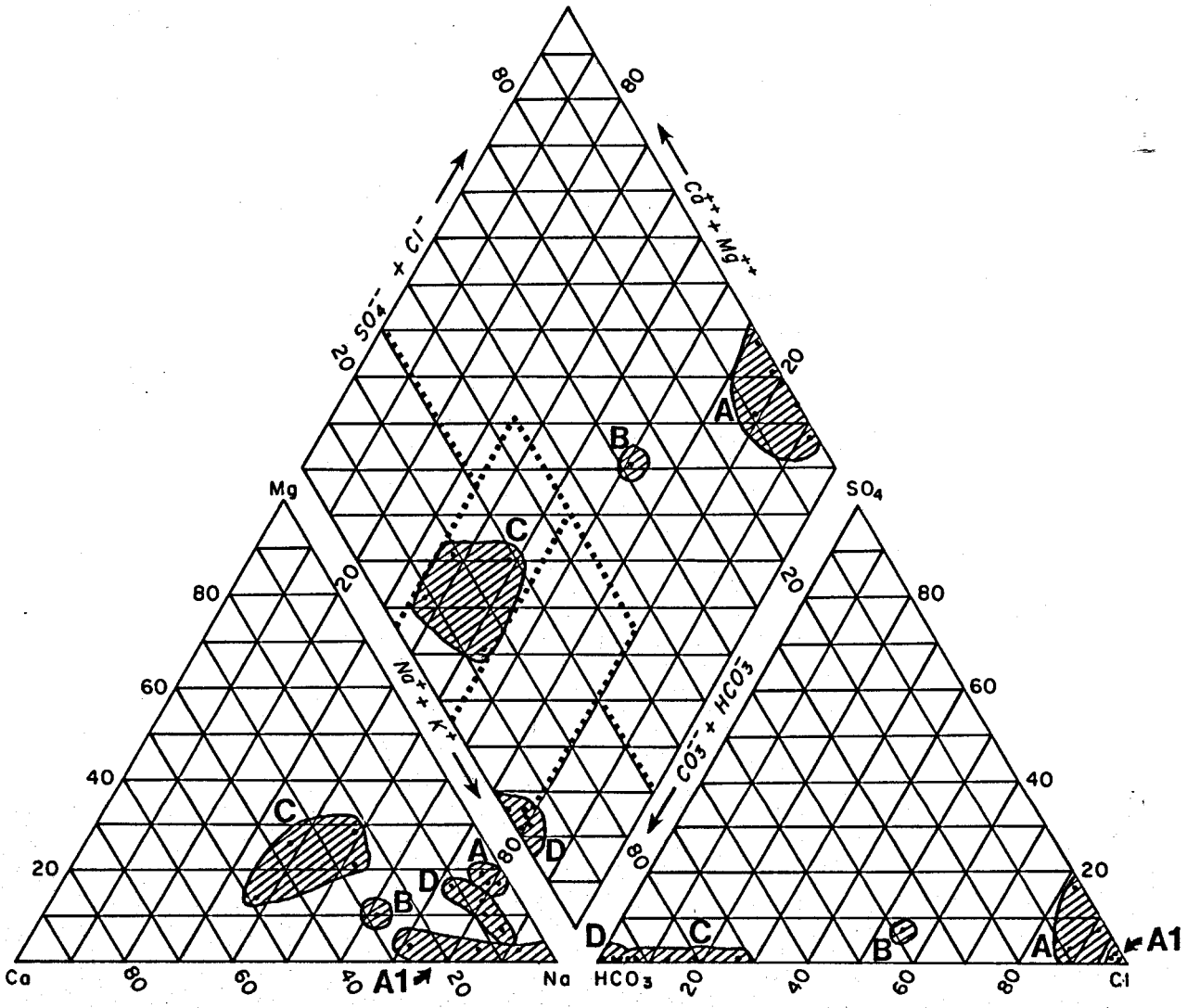

FIGURE 3. Trilinear plot of dissolved constituents from natural waters in southwestern Louisiana.

A = Seawater and surface waters in marshlands
A_1 = Geopressured-geothermal brines
B = Sweet Lake drainage
C = Parcperdue surface and ground waters
D = Sweet Lake and Rockefeller Refuge shallow ground waters

brines, average seawater, and surface waters in the southwestern Louisiana marshlands. A single point, plotted as B, represents water from drainage of the Sweet Lake site. C is a grouping of surface and subsurface waters at Parcperdue, and D represents shallow ground waters from Sweet Lake and Rockefeller Refuge. Also indicated are the general characteristics of waters in the major southwestern Louisiana aquifers identified by Harder and others (1967).

A definite gradation is indicated from seawater and brines to surface waters to ground waters in the anion triangle and the central diamond. This illustrates the relative bicarbonate (HCO_3) enrichment in fresh surface and shallow subsurface waters. The grouping of all Parcperdue near-surface waters substantiates a conclusion made earlier in the DOE geopressured-geothermal environmental monitoring phase: that shallow ground waters underlying the Parcperdue test site are hydrologically connected to the surface and that recharge probably occurs in the Vermilion River west of the prospect.

All near-surface waters at Parcperdue fall within the range of concentrations reported by Harder and others (1967) to be characteristic of the Chicot aquifer. This aquifer is probably commonly connected to the surface and receives sufficient recharge to maintain a relatively high ratio of calcium to sodium. Ground waters from Sweet Lake and Rockefeller Refuge plot very close to the limit separating Evangeline aquifer waters from blended Chicot-Evangeline waters. The lower chloride content of these waters may indicate a low rate of saltwater intrusion in these aquifers; however, TDS content is high, which may indicate a diagenetic process whereby chloride from seawater is taken out of solution.

Diagenetic processes are probably responsible for the variations indicated in the cation and anion triangles. A relative decrease in the concentration of magnesium with depth is indicated for seawater, ground waters, and brines.

This decrease may possibly be due to the role of magnesium in cation exchange reactions.

Summary

Several natural and man-induced processes may be responsible for the spatial and temporal variations which have been illustrated by the environmental monitoring data. Water quality variability may be due to saltwater intrusion, waste dispersion, or natural diagenetic processes. Furthermore, oil field brines may find their way into shallow subsurface waters up faults or by molecular diffusion through semipermeable shale membranes.

The saltwater interface has been shown to follow a northwest-southeast trend in southwestern Louisiana (Harder and others, 1967). Although some local variation may be due to fluid production (oil, gas, or ground water), the regional variability is probably related to Pleistocene and older deltaic progradation, as elements of these systems tend to be tangent to the strike of the saltwater interface (Fig. 4). The anomaly which causes displacement of the interface to the south on the 3000-mg/L dissolved solids surface (Fig. 2) may be due to an area of recharge to the north or may be a relatively impermeable volume of sediment through which the flow of saline water is impeded.

Present water quality characteristics at the geopressured-geothermal test sites are consistent with those found in earlier studies (Harder and others, 1967; Winslow, Hillier, and Turcan, 1968). Harder and others (1967) calculated the rate of movement of the saltwater interface at limited, selected points in southwestern Louisiana. The rate of movement was found to be best illustrated by a yearly change of 1 to 5 mg/L in chloride content. Our data seem to substantiate that claim; however, we have also shown that TDS content may increase at a faster rate, possibly due to diagenetic processes. Movement of the saltwater interface in some areas may be masked.

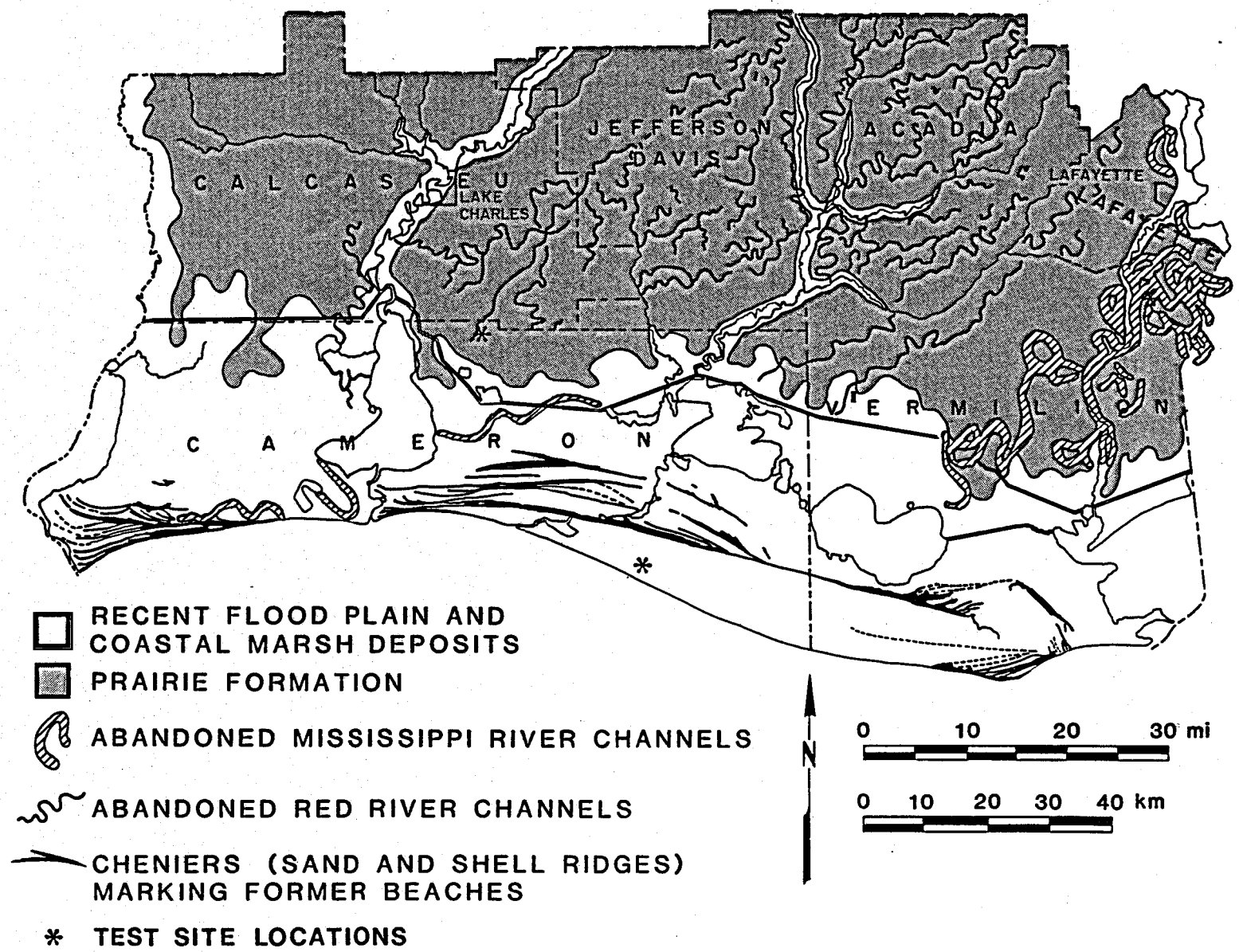

FIGURE 4. Geologic and physiographic features of southwestern Louisiana (after Jones, Turcan, and Skibitzke, 1956).

Brine contamination may come from two sources, if detected. Subsurface injection of oil field brines is a common practice in south Louisiana. Brine contamination may occur when well casings rupture or after disposal when brine migrates up faults or through leaky aquitards. Another possible source of brine contamination may be natural due to movement of the brine from its origin up deep faults or by slow leakage through semipermeable shale membranes. The overpressuring of some brines in the subsurface may facilitate such a mechanism, although movement will be very slow, and diagenetic processes will significantly alter the composition of fluids during migration.

A trilinear analysis of natural waters may contribute greatly to an understanding of mixing and diagenetic processes. One goal of this program is to determine the parameter most affected by these processes. Our preliminary analysis indicates that magnesium may play a major role in the genesis of ground waters; sulfate content may be of secondary importance. Mixing diagrams will be used in future studies to identify and distinguish between variations caused by saltwater intrusion, brine migration, or both.

References

Harder, A. H., C. Kilburn, H. M. Whitman, and S. M. Rogers, 1967, Effects of ground-water withdrawals on water levels and saltwater encroachment in southwestern Louisiana: Dept. Conservation, La. Geol. Survey, and Dept. Public Works, Water Resources Bull. no. 10, 56 p.

Jones, P. H., A. N. Turcan, Jr., and H. E. Skibitzke, 1956, Ground-water resources, in P. H. Jones and others, Water resources of southwestern Louisiana: U.S. Geol. Survey, Water-Supply Paper 1364, pl. 1.

Piper, A. M., 1944, A graphic procedure in the geochemical interpretation of water analyses: Trans. Am. Geophysical Union, vol. 215, p. 914-29.

Winslow, A. G., D. E. Hillier, and A. N. Turcan, Jr., 1968, Saline ground water in Louisiana: U.S. Geol. Survey, Hydrologic Inv. Atlas HA-310, 4 maps.

SUBSIDENCE MONITORING

by D. B. Trahan

Abstract

Benchmark networks have been installed around each of the U.S. Department of Energy geopressured-geothermal test sites in southwestern Louisiana. These networks are periodically surveyed to detect subsidence which may be attributable to depressurization of the geopressured-geothermal reservoirs. The acquired leveling data have been adjusted to account for regional base-line movement determined in another study.

The effects of geopressured-geothermal development can only be assessed after carefully examining other potential causes of subsidence. The histories of oil and gas production and ground-water withdrawal around the geopressured-geothermal test site at Parcperdue indicate that oil, gas, and ground-water production may contribute much more to anomalous subsidence than recent geopressured-geothermal brine production.

A trend-surface analysis of leveling data for the Parcperdue test site allowed for the separation of a regional component of movement attributable to uplift in the Iberian structural axis to the east and subsidence above a Pleistocene depocenter to the west of the test site. Residual deviations from the regional trend may be associated with the temporary loading and compaction of surface soils caused by the weight of drilling equipment and with ground-water withdrawal.

Introduction

Subsidence monitoring is continuing at all sites as scheduled. Because subsidence rates may reflect increased historical fluid production in these areas, best future efforts would be aimed at the use of models which take into consideration the production from individual wells and fields. Correlations

could be made with fluid volumes, reservoir geometries, and pressure changes during production. Some of these data have been obtained as a key element of the geopressured-geothermal program, but only for the geopressured-geothermal wells. Preliminary data are presented here for other wells and fields in the Parcperdue area. Similar data for the other sites are being gathered.

Discussion

The effect of geopressured-geothermal production on subsidence rates may be assessed only after careful examination of historical production of oil, gas, and ground water in the area surrounding each test site. Because of a potential time lag between production and subsidence, consideration must be given to some minimum backlog of data. For our purpose, an arbitrary period of six years has been chosen. In addition, cumulative production from each field has been considered. Subsidence monitoring is most complete in the area around the Parcperdue geopressured-geothermal test site, and those data are examined here.

The fields producing oil, gas, or both near the Parcperdue test site are Parcperdue and North Parcperdue (Fig. 5). The North Parcperdue field, dating back to 1972, has the greatest total historical production. Cumulative production to October 1983 is given below:

Crude:	209,166 bbl (barrels)
Condensate:	2,109,384 bbl
Natural gas:	74,677,992 MCF (thousand cubic feet)
Casing-head gas:	703,349 MCF

Monthly production data from January 1978 to October 1983 are given in Table 1. Yearly production for this period averages about 250,000 bbl of liquid petroleum (figures are for condensate alone up to July 1982, then for condensate and crude to the end of record). Total monthly production per year increased through the period (Table 2). A similar trend is apparent for gas production.

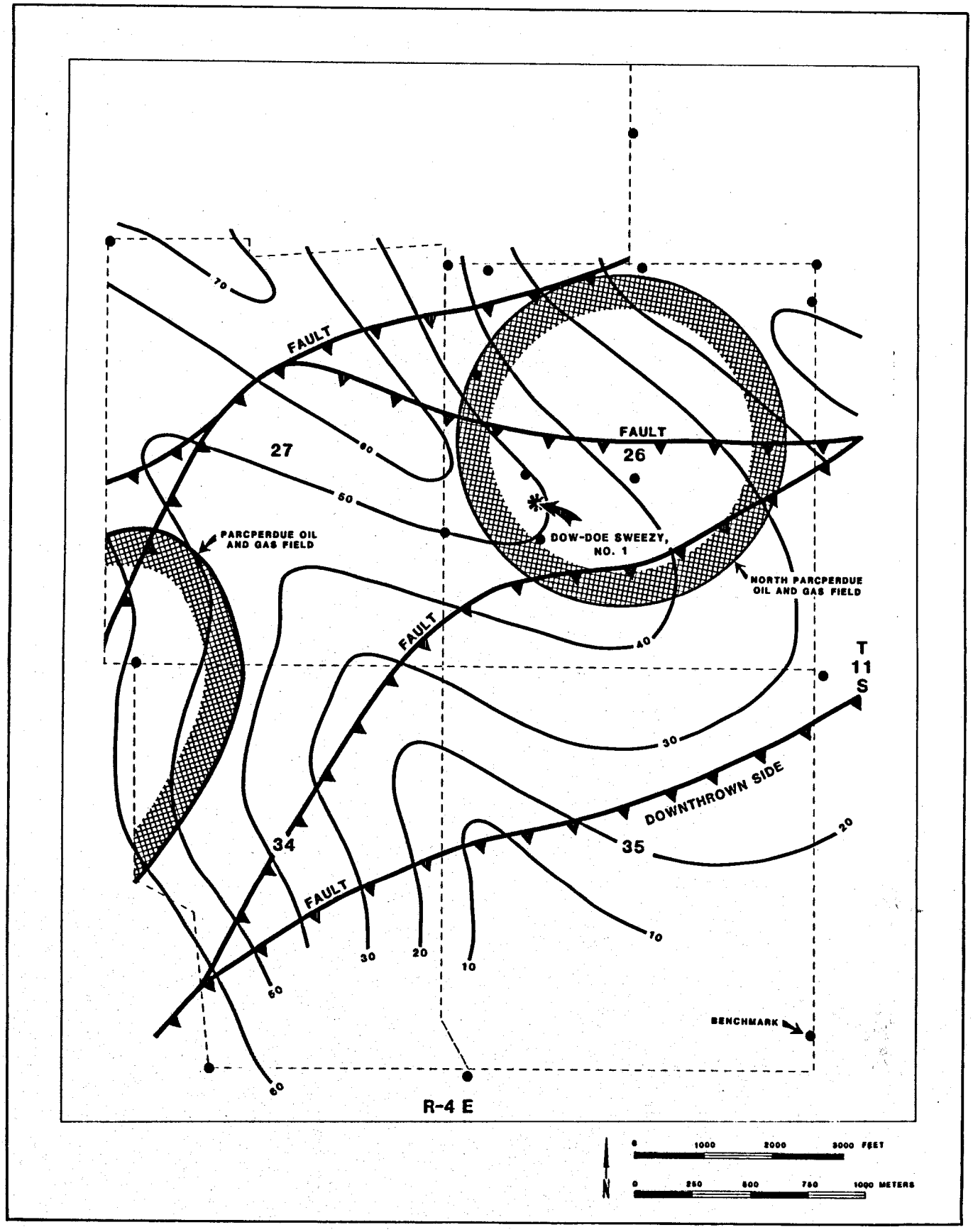

FIGURE 5. Net sand isopach of Cibicides jeffersonensis sandstone, Parcperdue oil and gas fields, Louisiana.

TABLE 1. Production of liquid petroleum (in barrels) from North Parcperdue field (Figures for January 1978 through June 1982 are for condensate only; figures for crude and condensate are combined as of July 1982.)

YEAR	Jan.	Feb.	Mar.	Apr.	May	June	July
1978	4,613	3,495	3,813	3,652	3,250	2,464	1,967
1979	19,007	14,440	15,332	12,532	12,781	12,144	18,409
1980	21,199	20,834	19,415	18,022	20,792	21,103	22,404
1981	20,151	16,906	17,477	17,146	18,288	17,736	18,998
1982	28,346	25,051	28,176	28,227	45,336	37,962	31,417
1983	37,265	33,953	36,666	35,486	36,107	35,932	32,760

YEAR	Aug.	Sept.	Oct.	Nov.	Dec.	Total	Average
1978	857	280	343	448	6,057	31,239	2,603
1979	19,111	18,526	21,402	20,335	20,698	204,717	17,060
1980	21,931	23,028	24,784	20,595	21,290	255,397	21,283
1981	18,996	17,994	20,890	23,987	27,180	235,749	19,646
1982	27,647	29,069	29,296	29,827	30,557	370,911	30,909
1983	32,458	31,807	24,736	---	---	337,170	28,097

Table 2. Production of natural gas (in thousands of cubic feet) from the North Parcperdue field. (Figures for natural and casing-head gas are combined as of July 1982.)

YEAR	Jan.	Feb.	Mar.	Apr.	May	June	July
1978	179,700	144,904	166,947	155,757	149,302	115,844	100,575
1979	518,161	581,654	474,361	255,157	262,540	253,299	504,263
1980	694,773	646,404	513,193	471,032	617,052	664,018	688,802
1981	597,537	476,600	469,838	491,540	524,832	506,600	546,848
1982	1,437,415	1,288,569	1,381,845	1,368,730	1,598,032	1,319,992	1,107,584
1983	1,311,464	1,164,429	1,296,182	1,273,905	1,219,300	1,301,371	1,095,594

YEAR	Aug.	Sept.	Oct.	Nov.	Dec.	Total	Average
1978	54,314	37,031	37,723	50,906	179,462	1,372,015	114,335
1979	516,799	542,078	691,722	673,374	707,090	5,980,498	498,374
1980	665,297	711,068	776,055	625,463	633,724	7,706,881	642,240
1981	567,351	555,226	675,080	1,239,699	1,395,373	8,046,524	670,544
1982	917,281	1,012,311	1,030,654	1,080,751	1,147,449	14,690,613	1,224,218
1983	1,143,973	1,136,626	858,266	11,801,110	---	23,602,220	2,145,656

Of the 15 wells drilled in the North Parcperdue field, 3 were dry holes that are now plugged; 3 have been plugged and abandoned (of these, 2 produced for some time); and 9 are producing (Table 3). The perforated intervals in the producing wells range from 3658 to 4877 m (12,000-16,000 ft) deep and average 4552 m (14,933 ft). The thicknesses of these intervals range from 2 to 19 m (7-62 ft) and average 9 m (29 ft). Ten of these wells have produced gas and only one has produced crude oil.

The Parcperdue field, the oldest field in the area (1959), is located about 1067 m (3500 ft) west of the North Parcperdue field. Although Parcperdue was discovered much earlier than North Parcperdue, its production history has been somewhat limited. The Parcperdue field now produces only crude oil and casing-head gas in much lower quantities than North Parcperdue. Since its discovery, the Parcperdue field has produced the following cumulative totals:

Crude:	1,352,403 bbl
Condensate:	50,292 bbl
Natural gas:	2,345,889 MCF
Casing-head gas:	3,608,197 MCF

Crude production, which decreased steadily from January 1978 to September 1982, varied from 370 to 110 bbl per month per year (Table 4). Production of casing-head gas was more variable, beginning at 765 MCF per month in 1978 and then decreasing roughly one order of magnitude in 1979, 1980, and for half of 1981. Production increased more than tenfold in August 1981 and has remained steady for most of the remaining record (Table 5).

The Parcperdue field has been relatively nonproductive. Seven wells drilled in the field were dry, two wells produced but were then plugged and abandoned, one is producing, and one is temporarily shut in (Table 6). The average depth to the producing intervals is 4088 m (13,411 ft), and the intervals are 1.5 to 4 m (5-14 ft) thick. Two wells have produced crude oil and one

TABLE 3. Data for wells in the North Parcperdue oil and gas field.

	Section Township, and Range	North Latitude	West Longitude	Perforated Interval Bottom Depth and Thickness (ft)	Total Depth (ft)	Type Fluid Produced*	Completion Date (mo/d/yr)
DRY AND PLUGGED	22,11 S.,04 E.	30°04'23"	92°02'43"	0	17,500	0	09/27/76
	26,11 S.,04 E.	30°03'19"	92°02'06"	0	17,736	0	03/26/74
	27,11 S.,04 E.	—	—	0	16,014	0	0
PLUGGED & ABANDONED	23,11 S.,04 E.	30°04'12"	92°01'52"	15,814 & 56	17,190	2	06/12/74
	27,11 S.,04 E.	30°03'53"	92°02'38"	15,590 & 17	18,000	2	08/06/73
	55,11 S.,04 E.	—	—	0	17,850	0	0
ACTIVE — PRODUCING	26,11 S.,04 E.	30°03'47"	92°02'15"	15,720 & 32	16,560	2	09/17/72
	26,11 S.,04 E.	30°03'42"	92°02'15"	13,196 & 42	13,317	2	09/04/78
	27,11 S.,04 E.	30°03'36"	92°03'09"	14,424 & 12	15,750	2	03/23/73
	52,11 S.,04 E.	30°03'03"	92°03'37"	15,553 & 62	15,650	2	07/13/78
	54,11 S.,04 E.	—	—	15,820 & 43	16,526	2	04/15/81
	54,11 S.,04 E.	—	—	13,110 & 26	13,250	1	04/06/82
	55,11 S.,04 E.	—	—	15,820 & 7	16,923	2	10/05/81
	55,11 S.,04 E.	—	—	15,798 & 16	16,040	2	11/03/82
	40,12 S.,04 E.	—	—	13,736 & 9	17,975	2	06/10/82

*0 = no fluid or brine only
1 = oil
2 = gas

TABLE 4. Crude oil production (in barrels) from the Parcperdue field.

YEAR	Jan.	Feb.	Mar.	Apr.	May	June	July
1978	425	393	382	402	394	384	351
1979	307	282	298	306	208	295	303
1980	295	284	287	275	279	254	243
1981	218	213	227	109	196	187	206
1982	136	165	188	170	185	160	167
1983	171	154	169	153	164	6	42

YEAR	Aug.	Sept.	Oct.	Nov.	Dec.	Total	Average
1978	314	365	367	362	303	4442	372
1979	298	285	290	281	302	3455	288
1980	240	232	244	230	247	3110	259
1981	176	197	180	187	185	2281	190
1982	173	161	169	164	171	2009	167
1983	74	58	---	---	---	991	110

TABLE 5. Production of casing-head gas (in thousands of cubic feet) from the Parcperdue field.

YEAR	Jan.	Feb.	Mar.	Apr.	May	June
1978	765	765	765	765	765	765
1979	73	73	73	73	73	73
1980	70	70	70	70	70	70
1981	70	70	70	70	70	70
1982	793	1023	1078	900	943	1031
1983	1097	1087	1108	982	1057	36

YEAR	July	Aug.	Sept.	Oct.	Nov.	Dec.
1978	765	765	765	765	765	765
1979	73	73	73	73	73	73
1980	20	70	70	70	70	70
1981	70	891	934	844	1168	1289
1982	1198	926	893	1039	1055	1098
1983	292	705	687	---	---	---

TABLE 6. Data for wells drilled in the Parcperdue oil and gas field.

	Section Township, and Range	North Latitude	West Longitude	Perforated Interval Bottom Depth and Thickness (ft)	Total Depth (ft)	Type Fluid Produced*	Completion Date (mo/d/yr)
DRY & PLUGGED	27,11 S.,04 E.	30°03'03"	92°03'00"	0	12,450	0	09/10/66
	33,11 S.,04 E.	30°02'45"	92°03'28"	0	15,274	0	11/19/65
	34,11 S.,04 E.	30°02'59"	92°03'11"	0	12,400	0	10/21/77
	35,11 S.,04 E.	30°02'40"	92°02'17"	0	17,330	0	04/16/75
	35,11 S.,04 E.	—	—	0	18,150	0	03/23/82
	41,12 S.,04 E.	30°01'41"	92°03'09"	0	18,224	0	03/17/71
	41,12 S.,04 E.	30°01'55"	92°03'11"	0	12,795	0	01/21/79
PLUGGED & ABANDONED	34,11 S.,04 E.	30°02'54"	92°02'47"	13,283 & 5	13,620	1	03/12/59
	34,11 S.,04 E.	30°02'33"	92°02'56"	14,818 & 8	15,368	2	12/28/59
ACTIVE—PRODUCING	34,11 S.,04 E.	30°02'50"	92°03'04"	12,297 & 9	13,500	1	10/21/67
SHUT-IN, PRODUCTIVE	34,11 S.,04 E.	30°02'50"	92°03'04"	13,280 & 14	13,500	1	10/12/59
GEOPRESSURED	26,11 S.,04 E.	—	—	13,406 & 57	13,612	0	08/16/81
SALTWATER DISPOSAL	26,11 S.,04 E.	—	—	4,660 & 140	5,011	-	02/28/82
	26,11 S.,04 E.	—	—	2,076 & 20	2,150	-	10/31/74

*0 = no fluid or brine only
1 = oil
2 = gas

has produced gas. The geopressured-geothermal well has produced from an interval 17 m (57 ft) thick at a depth of 4086 m (13,406 ft). This well produced 1,940,000 bbl of brine and 31,500 MCF of gas during its short production history. Two saltwater disposal wells inject oil field brines into shallow aquifers above the Parcperdue field. The DOE saltwater disposal well injected into an interval 1420 m (4660 ft) deep and 43 m (140 ft) thick. Another well, exact location unknown, injects fluids into a shallower horizon 655 m (2150 ft) deep and 6 m (20 ft) thick.

The limits of the producing fields (Fig. 5) are generalized. Production is actually concentrated along a band approximately 152 to 305 m (500-1000 ft) wide, which is bounded to the north by the northernmost fault defining the Parcperdue fault block. All wells producing in this trend are considered to be in the North Parcperdue field. Another trend, which is 305 to 610 m (1000-2000 ft) wide, extends from the major trend to the southwest through sec. 34, T. 11 S., R. 4 E. Most wells in this trend are considered to be in the Parcperdue field.

The chief use of ground water in the Parcperdue area has historically been rice irrigation. Although total rice acreage has decreased during the last few years, rice irrigation still outweighed other uses during the period 1978-83. Ground-water production was estimated by calculating rice acreage during each of the years shown (Table 7). A review of aerial photographs, discussions with various area agricultural officials, and crop-yield reports revealed the locations and acreages supplied by each well. The amount of water required for rice irrigation has been estimated at 30 acre-in. per year. By multiplying the acreage supplied by each well by this factor, ground-water production was calculated (Table 7).

Water from six wells is used to irrigate rice primarily in April and May. Total ground-water production in the area from April 1978 to May 1983 was

TABLE 7. Ground-water production (in millions of barrels) from rice irrigation wells near the Parcperdue geopressured-geothermal prospect.

	Well Number								
YEAR	1	2	3	4	5	6	7	8	9
1978	4.76	----	5.98	0.27	----	----	0.78	1.76	----
1979	4.84	----	3.72	----	----	----	----	1.10	----
1980	4.84	0.23	3.03	0.28	----	----	----	0.45	----
1981	4.67	----	3.95	0.61	----	----	----	2.23	----
1982	4.17	1.37	3.56	0.52	----	----	----	1.87	----
1983	2.33	1.82	2.12	----	----	----	----	0.85	----
TOTAL	25.61	3.42	22.36	1.68	----	----	0.78	8.26	----

approximately 62,110,000 bbl, most of which was concentrated at two wells (Table 7). Average production by well was 10,350,000 bbl for the same period. The two major producing wells each discharged about 4,000,000 bbl of water per year. These wells are 70 to 91 m (230-300 ft) deep and are located 3.2 km (2 mi) southeast and 2.4 km (1.5 mi) south-southwest of the test site, respectively (Fig. 6).

The subsidence monitoring data for the Parcperdue test site has been referenced to the movement of a benchmark in Lafayette along a survey line which traverses south Louisiana from Orange, Texas, to Baldwin, Louisiana. Base-line movement along this line was determined in a separate study which referenced all movements from north to south Louisiana to the movement of the Monroe uplift in northeastern Louisiana. That study is in Appendix A.

The Symap procedure (Dougenik and Sheehan, 1977) was used to contour the velocities of movement and to establish weighted trend surfaces for the periods 1980-81 and 1981-83. In both instances, the second-order trend surface was most significant and indicated a general southeast-northwest trend toward greater subsidence in the area (Figs. 7 and 8). This trend is possibly due to uplift of the Five-Island salt dome ridge to the east and southeast and to subsidence of a depocenter formed by Pleistocene Red River alluviation to the west and northwest of the test site.

Residuals off the general trend are considered to represent subsidence anomalies not associated with regional subsidence. The residuals mapped on the 1980-81 velocity surface (Fig. 9) are consistent with the unweighted contour pattern (Fig. 10), indicating significant variability from the general trend. One subsidence anomaly, centered in the Parcperdue test site, may be due to the temporary loading and compaction of the surface caused by the weight of the drilling equipment. That same anomaly is not evident for the second period of monitoring probably due to the release of the static load after removal of the

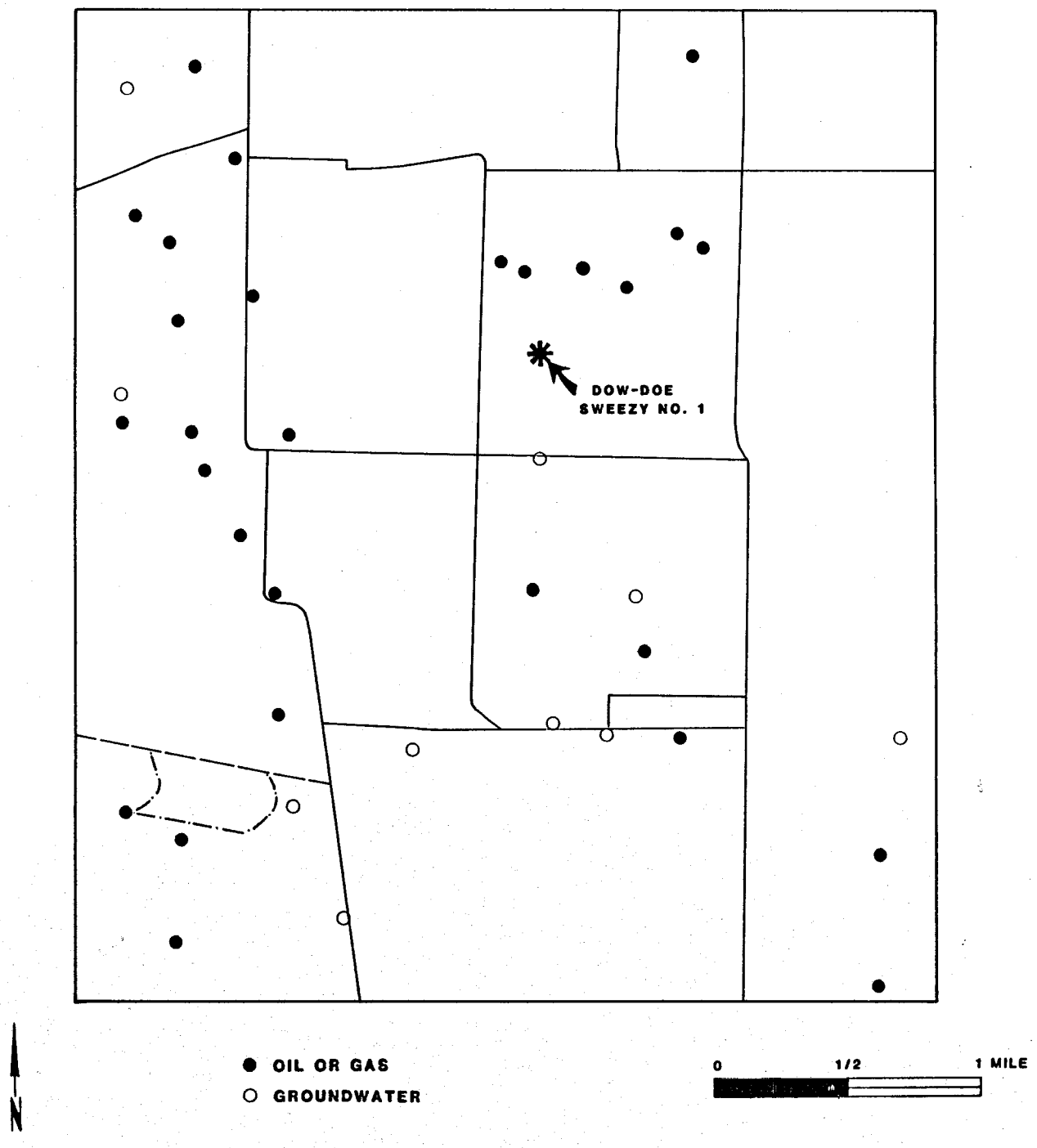

FIGURE 6. Fluid production near the Parcperdue geopressured-geothermal prospect.

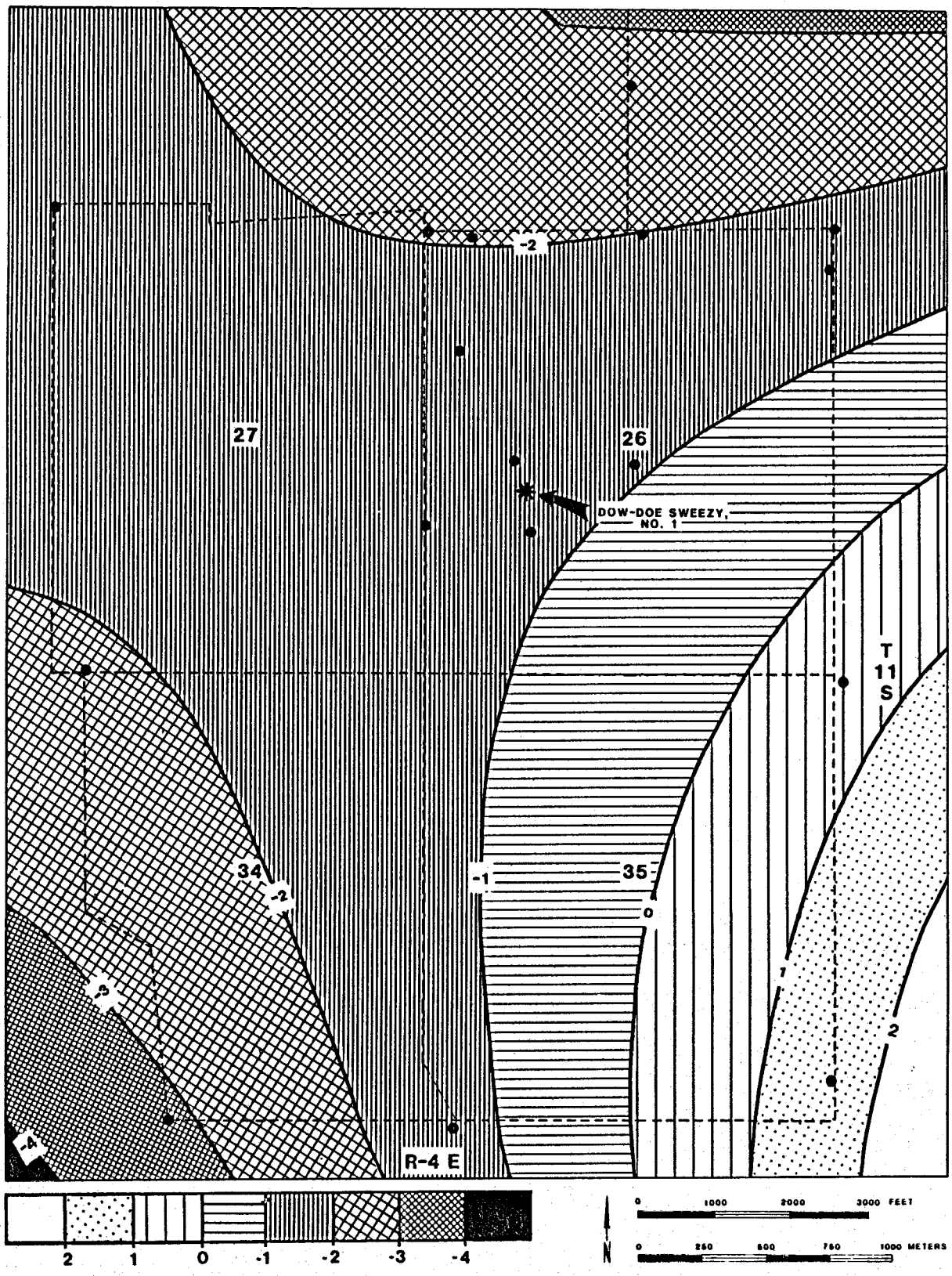

FIGURE 7. Weighted second-order trend surface, change in elevation (mm/yr), Parcperdue geopressured-geothermal test site, 1980-81.

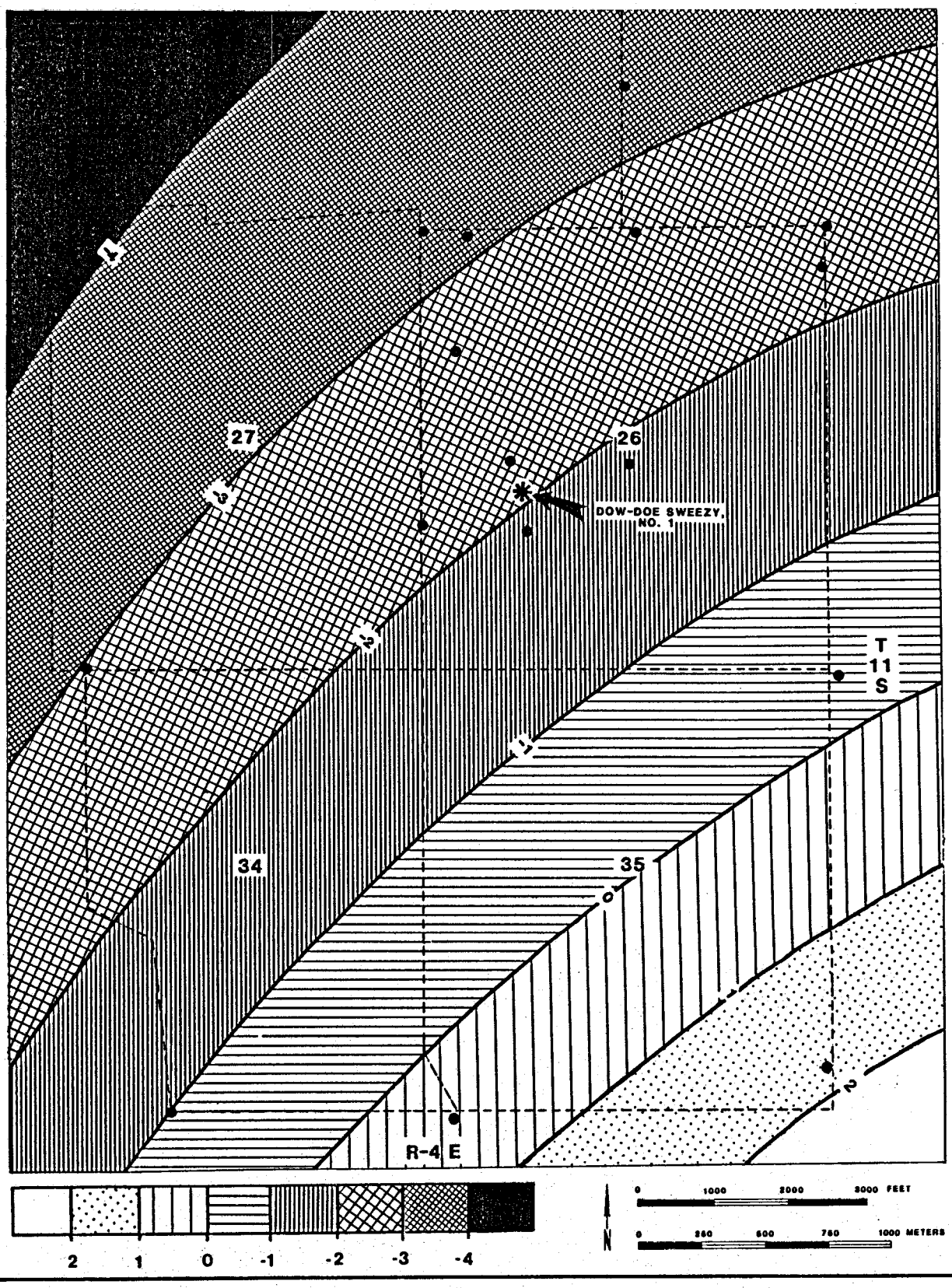

FIGURE 8. Weighted second-order trend surface, change in elevation (mm/yr), Parcperdue geopressured-geothermal test site, 1981-83.

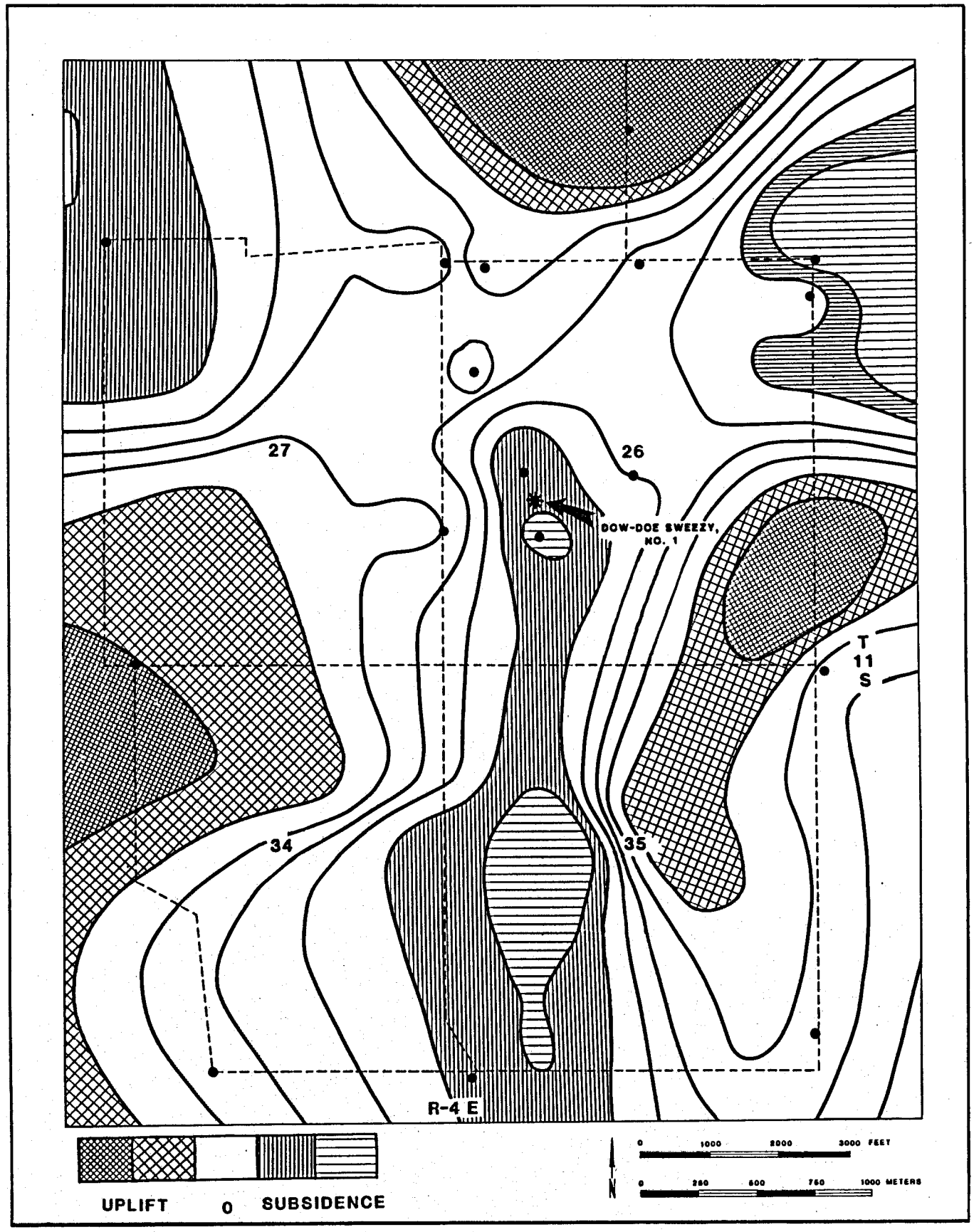

FIGURE 9. Second-order residual surface, change in elevation (mm/yr), Parcperdue geopressured-geothermal test site, 1980-81.

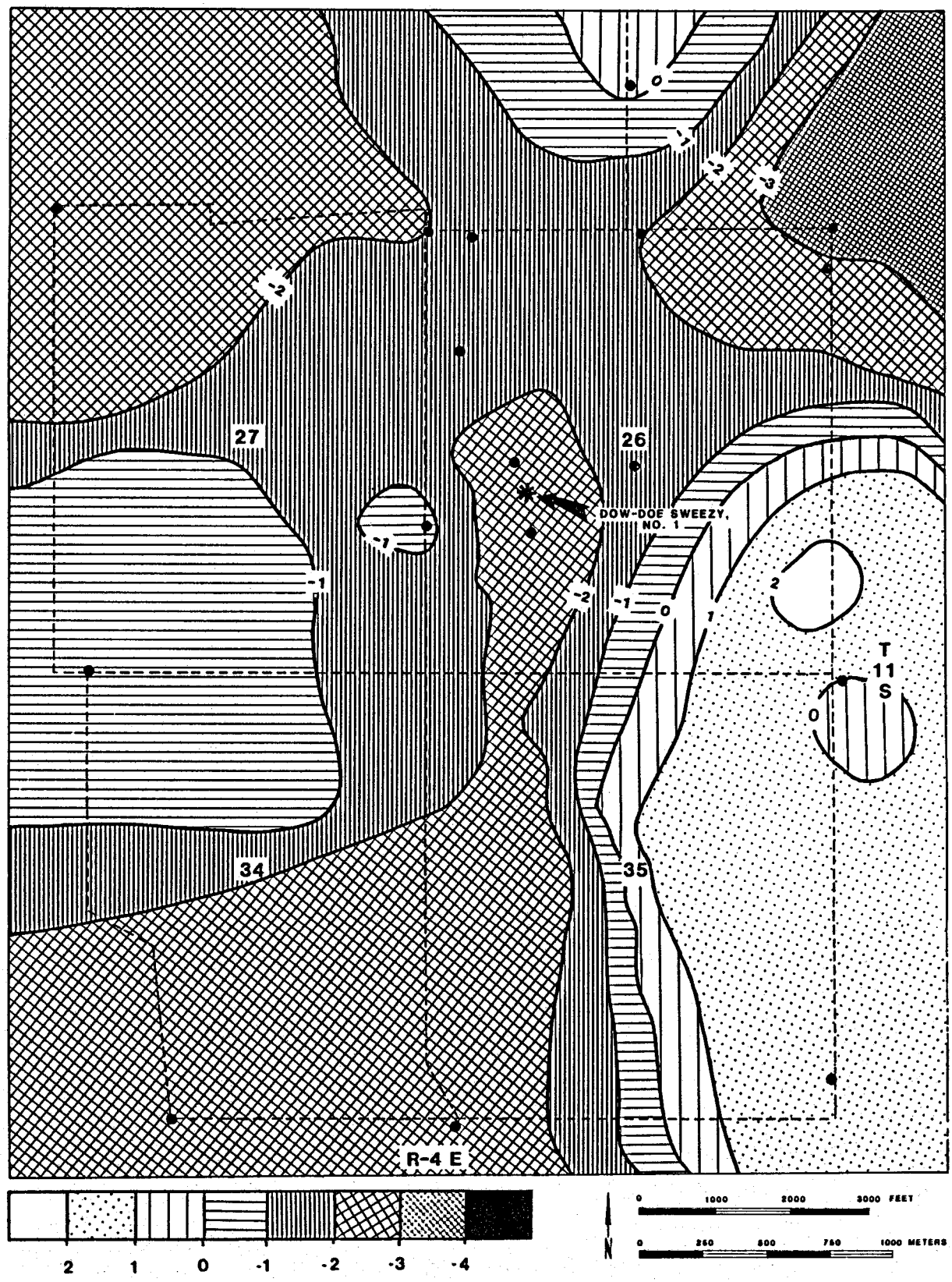

FIGURE 10. Contoured velocity surface, change in elevation (mm/yr), Parcperdue geopressured-geothermal test site, 1980-81.

drilling equipment (Fig. 11). However, one anomaly, located about 1.6 km (1 mi) south of the test site, is persistent during both periods. This anomaly would coincide well with the Parcperdue producing trend if the stresses above the compacting reservoir were offset to the east.

Summary

The analysis of subsidence will continue as more data become available for Parcperdue and the other design well prospects. The important considerations in oil-field subsidence analyses are 1) the reduction in reservoir pressure, 2) the rate and degree of pore pressure reduction, and 3) the uniaxial compaction coefficient (Geertsma, 1973).

The reduction in reservoir pressure is a function of the mobility, solubility, density, and compressibility of fluids as well as reservoir boundary conditions. Pore pressure reductions depend on the permeability distribution, well locations, and production rate. The compaction coefficient depends on rock type (the number, size, and shape of grain contacts in sandstones), degree of cementation, porosity, and depth of burial.

The effect of geopressured-geothermal development on subsidence rates will not be instantaneous. A lag in the transfer of stresses to the surface is expected for geopressured-geothermal development and for other fluid production activities. The effect of historical fluid production may be apparent in our data. Modeling studies which take into consideration the production histories of the producing fields, changes in pressures, depths, production volumes, and other factors will be attempted in the future. Some of the data necessary for such an analysis are presented here, although much more will be necessary.

Ground-water production may also cause subsidence of the land surface; however, the mechanism for compaction is different than that for deeper oil and/or gas reservoirs. In most cases, changes in pressure in shallow aquifers

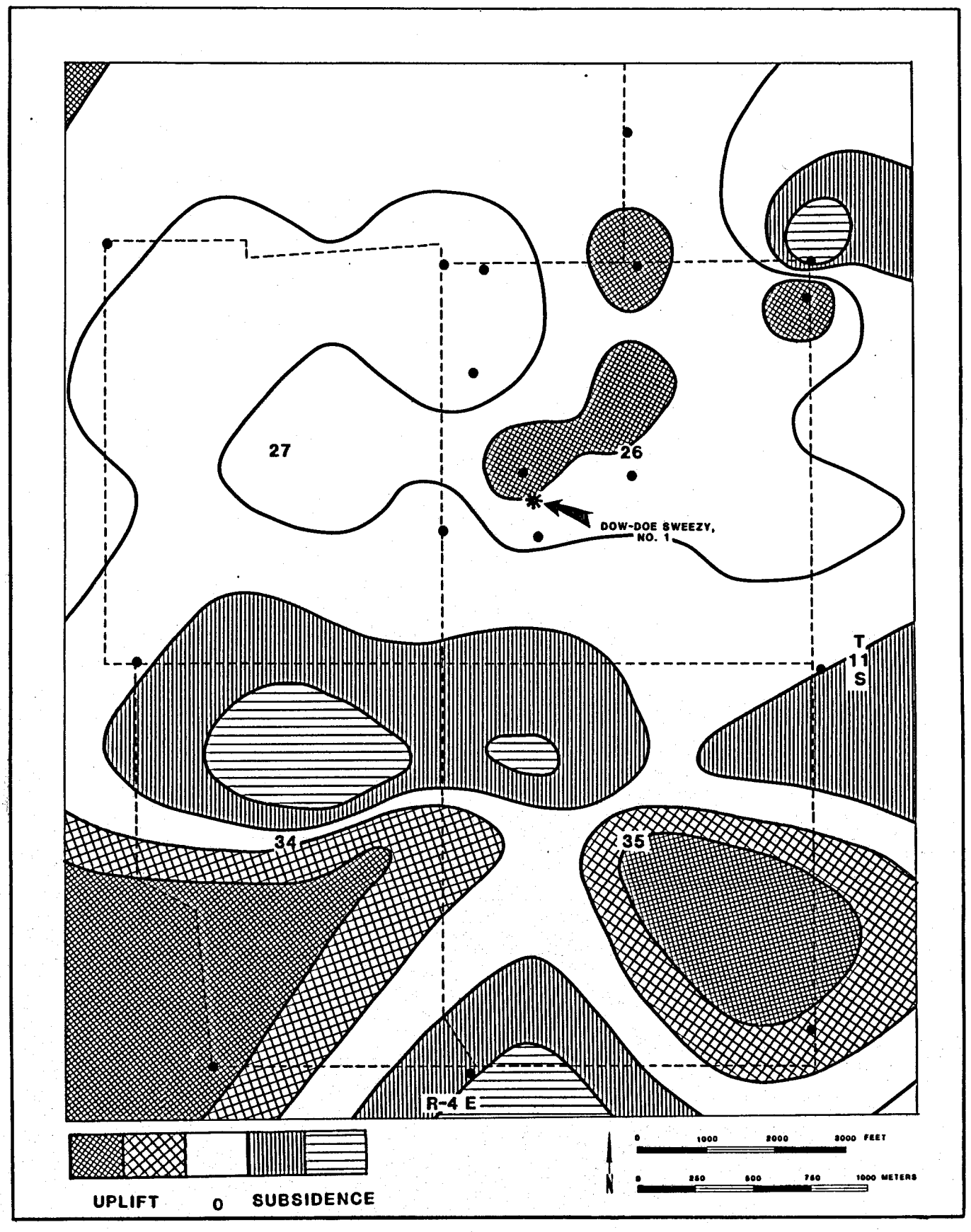

FIGURE 11. Second-order residual surface, change in elevation (mm/yr), Parcperdue geopressured-geothermal test site, 1981-83.

are small due to a relatively steady recharge into these aquifers. Subsidence may occur if the piezometric head is lowered significantly due to a low water budget (that is, discharge exceeds recharge). Therefore, future work will also include an analysis of these conditions.

References

Dougenick, J. A., and D. E. Sheehan, 1977, Symap user's manual: Laboratory for Computer Graphics and Spatial Analysis, Graduate School of Design, Harvard.

Geertsma, J., 1973, Land subsidence above compacting oil and gas reservoirs: Jour. Petr. Technology, June, p. 734–44.

MICROSEISMIC MONITORING

by D. A. Stevenson

Abstract

Microseismic monitoring arrays have been established around three U.S. Department of Energy geopressured-geothermal wells to assess the effects well development may have on subsidence and growth fault activation. Continuous microseismic monitoring has been ongoing since August 1980 at the Parcperdue and Sweet Lake prospects; the Rockefeller Refuge array has been operating since June 1981.

The results obtained from this monitoring have shown some unusual characteristics associated with Gulf Coast seismic activity. Observed activity can be classified into two dominant types, one with identifiable body phases and the other with only surface wave signatures. The latter event type comprises over 99% of the 1000+ microseismic event locations presented to us by our subcontractors. Two problems have been encountered with respect to the slow-moving surface wave signature events. The first is that location and depth accuracy is extremely inaccurate. The second is that rainfall and weather-associated frontal passages seem to be closely related to periods of seismic activity at all three wells. The second problem makes it extremely difficult to separate earth origin events from atmospheric acoustic events, such as thunderstorms, since both phenomena occupy much the same velocity range and seismic signature on recording instruments.

After relatively short periods and low levels of flow testing at Parcperdue and Sweet Lake, seismic monitoring has shown no plausible correlation to inferred growth fault locations of periods of flow testing. We hope to see longer terms and higher volumes of flow testing at Rockefeller Refuge, which should give us a truer indication of induced seismicity attributed to geopressured-geothermal development.

Introduction

The Louisiana Geological Survey and Louisiana State University conducted base-line seismic studies at the U.S. Department of Energy Parcperdue, Sweet Lake, and Rockefeller Refuge prospects to investigate microseismicity associated with geopressured-geothermal fluid production. These monitoring programs were designed, first, to establish the nature of the local seismic activity prior to production and, second, to determine if well activities induce changes in the rate of local fault movement. This section describes the results obtained from microseismic monitoring at Parcperdue, Sweet Lake, and Rockefeller Refuge up to 30 September 1983. Much of the information presented in the Sweet Lake and Rockefeller Refuge subsections are taken from quarterly reports submitted to the university by the subcontractor, Woodward-Clyde Consultants.

Parcperdue

The Parcperdue microseismic array consists of five continuously recording seismograph stations in the North Parcperdue gas field of Vermilion Parish, Louisiana. The L. R. Sweezy geopressured-geothermal wells comprising this portion of the project were shut in on 5 February 1983. The final report, as submitted by our subcontractor for the entire microseismic recording period January 1980 through November 1983, is included in Appendix B.

Sweet Lake

The Sweet Lake microseismic monitoring network consists of eight permanent field stations (Fig. 12) which are maintained by the university subcontractor, Woodward-Clyde Consultants. Location coordinates are given in Table 8. Data collected at each field station are multiplexed and transmitted over telephone lines to the central recording facility in Baton Rouge, Louisiana.

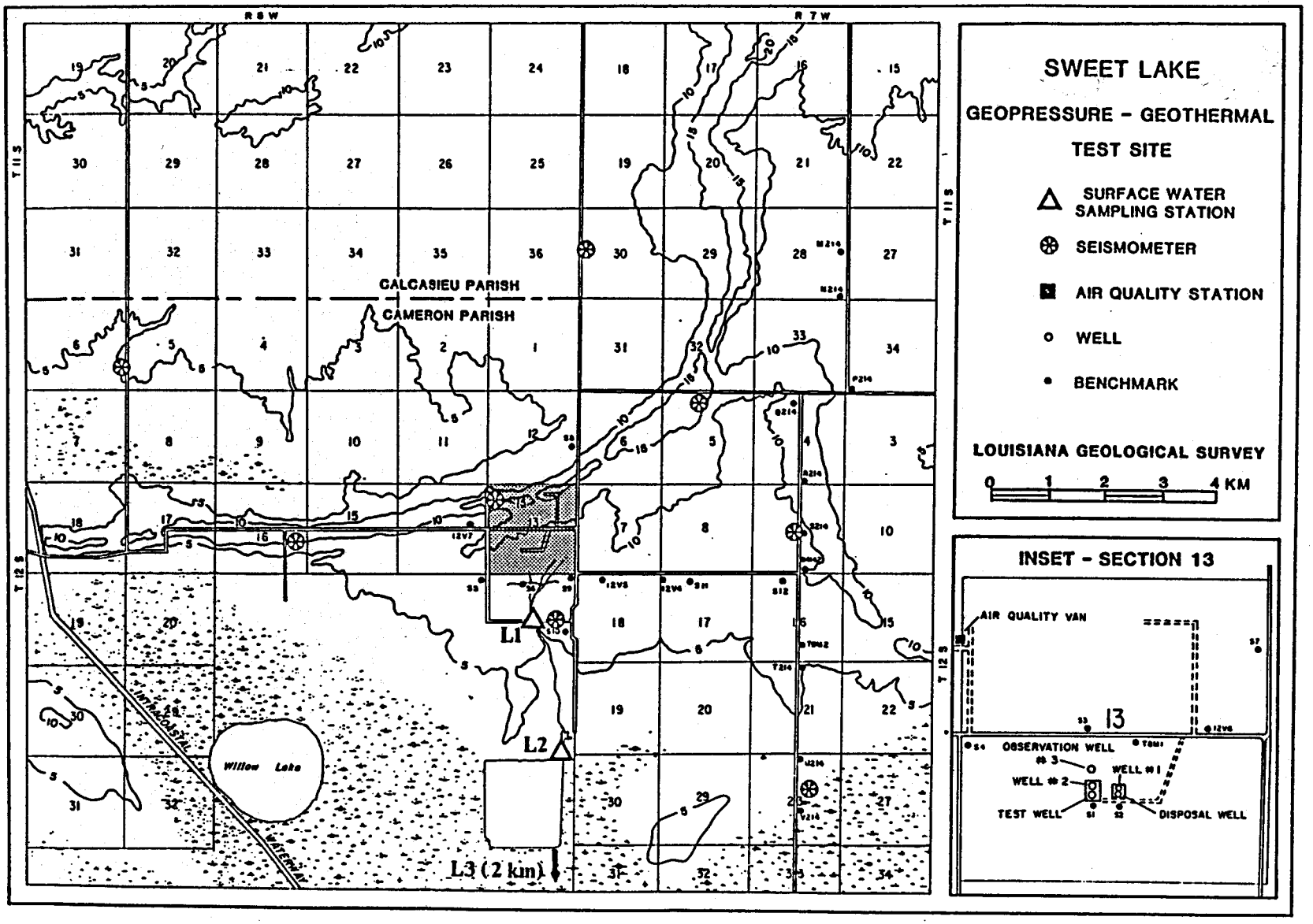

FIGURE 12. Area map of Sweet Lake geopressured-geothermal test site showing locations of observation stations.

TABLE 8. Sweet Lake microseismic monitoring network station coordinates.

Station Name	North Latitude	West Longitude
CPT	30°02'37"	93°12'47"
CPF	30°00'04"	93°08'02"
CLB	30°01'16"	93°08'43"
SFY	30°00'50"	93°10'56"
HWN	30°01'05"	93°05'19"
WLR	30°03'34"	93°07'41"
JCF	30°02'16"	93°07'01"
HWS	29°59'33"	93°05'17"

At the central recording facility, all data are continuously recorded on magnetic tape, and selected station data are simultaneously recorded on three drum recorders. Drum records are scanned daily to detect possible natural seismic activity. Upon detection, all station data are played back from the magnetic tape into hard copy format through an oscillograph. These hard copies of station data are further reviewed and analyzed to obtain hypocenter locations and other information. Data reduction is accomplished using a modified version of the earthquake location program FASTHYPO.

Characteristics of Seismic Wave Arrivals

Seismic events recorded by the south Louisiana seismic monitoring networks are not representative of microearthquakes recorded by networks in other environments. Microearthquakes in other environments are typically characterized by a P-wave arrival (primary compressional/dilatational), an S-wave arrival (secondary shear) and, in some instances, a surface wave arrival. At Sweet Lake, however, typically only one arrival is observed. This arrival is usually impulsive and has a frequency of 5 to 15 Hz (Fig. 13). The arrival appears to be travelling with a velocity of about 0.35 km/s (kilometers per second). This velocity is similar to the velocity of fundamental mode Rayleigh waves computed by using a velocity model derived for a portion of the Gulf Coast in Texas. Because the sediment velocities in south Louisiana are similar to those in coastal Texas, we have concluded that the recorded arrivals may be fundamental mode Rayleigh waves.

P- and S-wave arrivals are observed for seismic events that can be identified as explosions detonated for geophysical surveys. The P-wave velocity determined from these near-surface events is about 1.5 km/s.

Location of Seismic Events

Microearthquakes are located using a modified version of the computer program FASTHYPO (Herrman, 1979). This program uses an iterative least squares

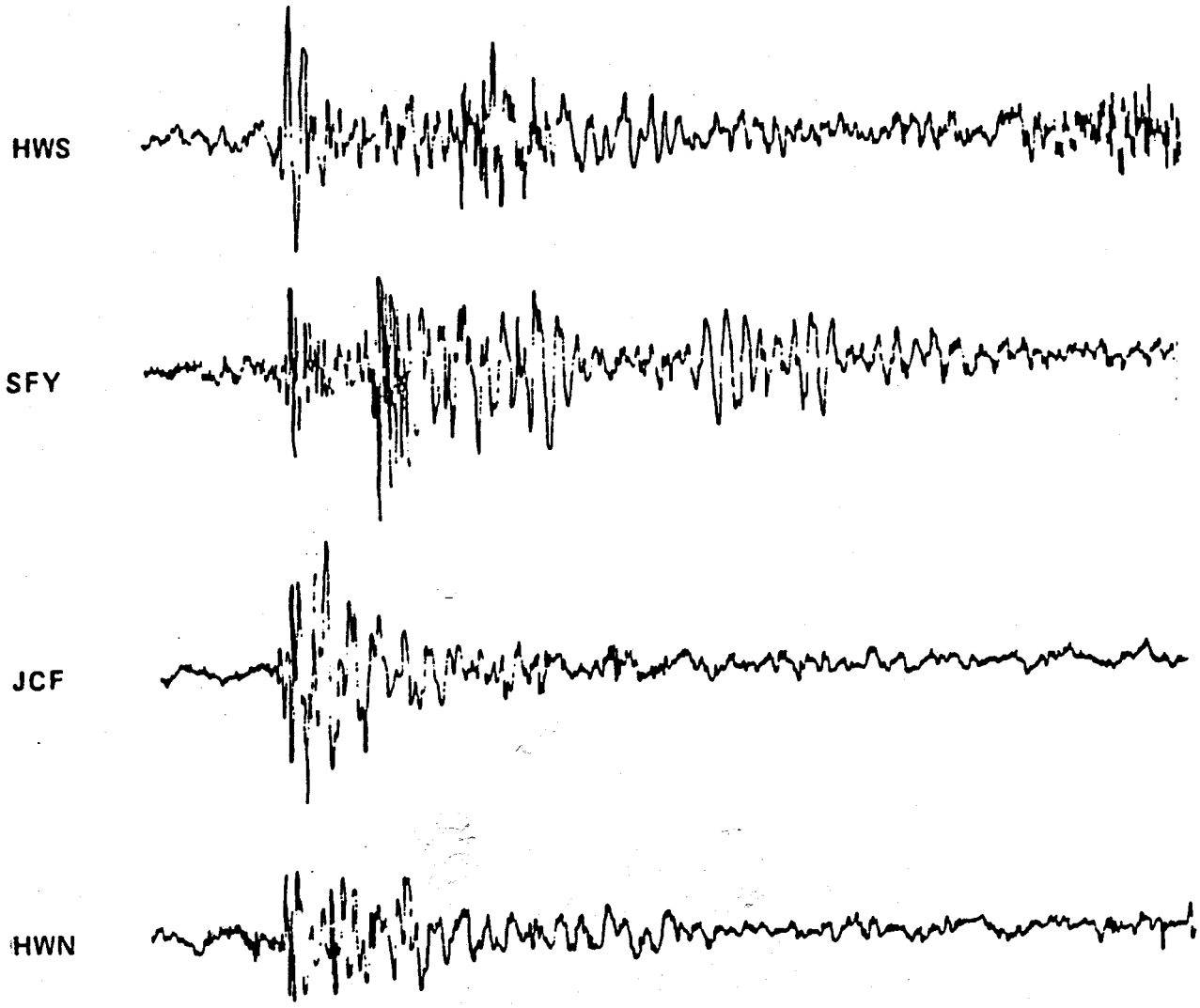

FIGURE 13. Characteristic seismographs recommended by the Sweet Lake network.

procedure to minimize the root mean square (RMS) residual of the travel times. Input to the program usually consists of arrival times for P- and S-waves and a plane-layered velocity model. Because P- and S-waves are not observed for microearthquakes detected by the seismic network at Sweet Lake, a procedure has been adopted using the impulsive Rayleigh wave arrivals to locate the events. Arrival times of the Rayleigh waves are treated as P-wave arrivals, and a half-space with a velocity of 0.342 km/s is used as the velocity model. Locations determined by this method must be considered uncertain, but for events within the array they are probably fairly accurate.

Depth is left unconstrained in the location procedure. Most calculated depths range from 0 to about 8 km, but the significance, if any, of computed depths based on surface wave arrivals is questionable at best. Impulsive wave arrival times can be read with a precision of better than 0.1 s in most cases. Differences in the calculated travel times for two events located in the center of the array but at depths of 0 and 4 km, respectively, would be on the order of 4 s for a half-space with a velocity of 0.342 km/s. Thus, calculated depths cannot be explained as the result of uncertainties in arrival time readings. If compensations for the larger travel times are made by changing the velocity of the half-space rather than the depth, a velocity decrease of about 20% would be required. Another possibility is that energy recorded as a Rayleigh wave travelled along part of its path as a body wave. In this case, the different travel times would result from the different percentage of travel path that was transversed as a body wave. The depths computed in this case may not be meaningful, but relative depths would be correct in a qualitative sense.

Magnitudes

Magnitudes are calculated on the basis of event duration. Duration is measured as the time from the onset of the arrival to the point at which the

arrival recedes into background noise. The following formula is used for magnitude calculation:

$$m_D = -2.22 + 1.18 \log(D)$$

This formula was derived for use in the Mississippi embayment by the Tennessee Earthquake Information Center. Its applicability to the south Louisiana region has not been tested. While magnitudes that are computed may not be valid in terms of their absolute values, they do give a sense of the relative size of events.

Magnitudes calculated for microearthquakes recorded by the Sweet Lake network indicate that all detected events are small. Calculated magnitudes are typically less than 1 (m_D) for the events detected.

Another measure of the size of microseismicity recorded at the Sweet Lake site may be found in "felt reports" of the local residents. Local blasts, using charges of up to 25 pounds of explosives, are routinely detonated during seismic prospecting in the area. These blasts are often felt by local residents. There are no felt reports of microearthquakes at the Sweet Lake site.

Seismicity and Well Production

Microearthquakes were first detected by the monitoring network at Sweet Lake in June 1981. This activity followed approximately one year of seismic quiescence, as observed on network records. The detection level of the network may, however, have changed during that time. In late May and early June of 1981, station gains and filter settings were adjusted to increase the sensitivity of the network. While some very small events may have been missed prior to June 1981, activity similar to that detected beginning in June 1981 would have been evident on the records if it had occurred. No such activity was detected in a detailed review of the network records.

The time history of seismic activity at Sweet Lake is characterized by a constant low background level of seismicity punctuated by bursts of earthquakes

(Fig. 14). These bursts consisted of at least 5 events; in one case, 35 events occurred within 15 km of the wells during a single day. The first such burst of activity occurred four days prior to perforation of the disposal well (Fig. 15). The next burst occurred two days after the disposal well was perforated. No activity occurred when the production well was perforated.

Other bursts of activity may correlate in time with large, rapid changes in the fluid pressure, as measured at the wellhead of the production and disposal wells (Figs. 15-24). Most bursts occur two to three days after the measured pressure change, but some precede the change by less than a day.

There may be a correlation between the level of seismic activity in June 1981 and the activity at the wells (perforation, flow, and reservoir limit testing) (Fig. 25). However, seismic activity continued beyond the end of the initial flow test in February 1982. In fact, some of the largest bursts of activity occurred after the reservoir limit test ended (Fig. 25). Daily drilling reports from Magma Gulf-Technadril describing activity at the wells subsequent to the termination of the flow test may suggest that some of the bursts of seismicity were related to well activity (Fig. 26). While the largest burst of seismicity, which occurred on Julian Day 107, is not related to drilling or flow activity, a large unexplained pressure increase was noted at the wellhead of the disposal well on the next day (day 108). There is no correlation between seismic bursts and well activity after April 1982 because the well was shut in until September 1983.

Spatial Distribution of Microearthquakes

The spatial distribution of all earthquakes within about 10 km of the wells does not show any clear relation to the locations of growth faults inferred for depths of 3600 to 4600 m (Fig. 27). Examination of events that occurred only during the reservoir limit test leads to the same conclusion

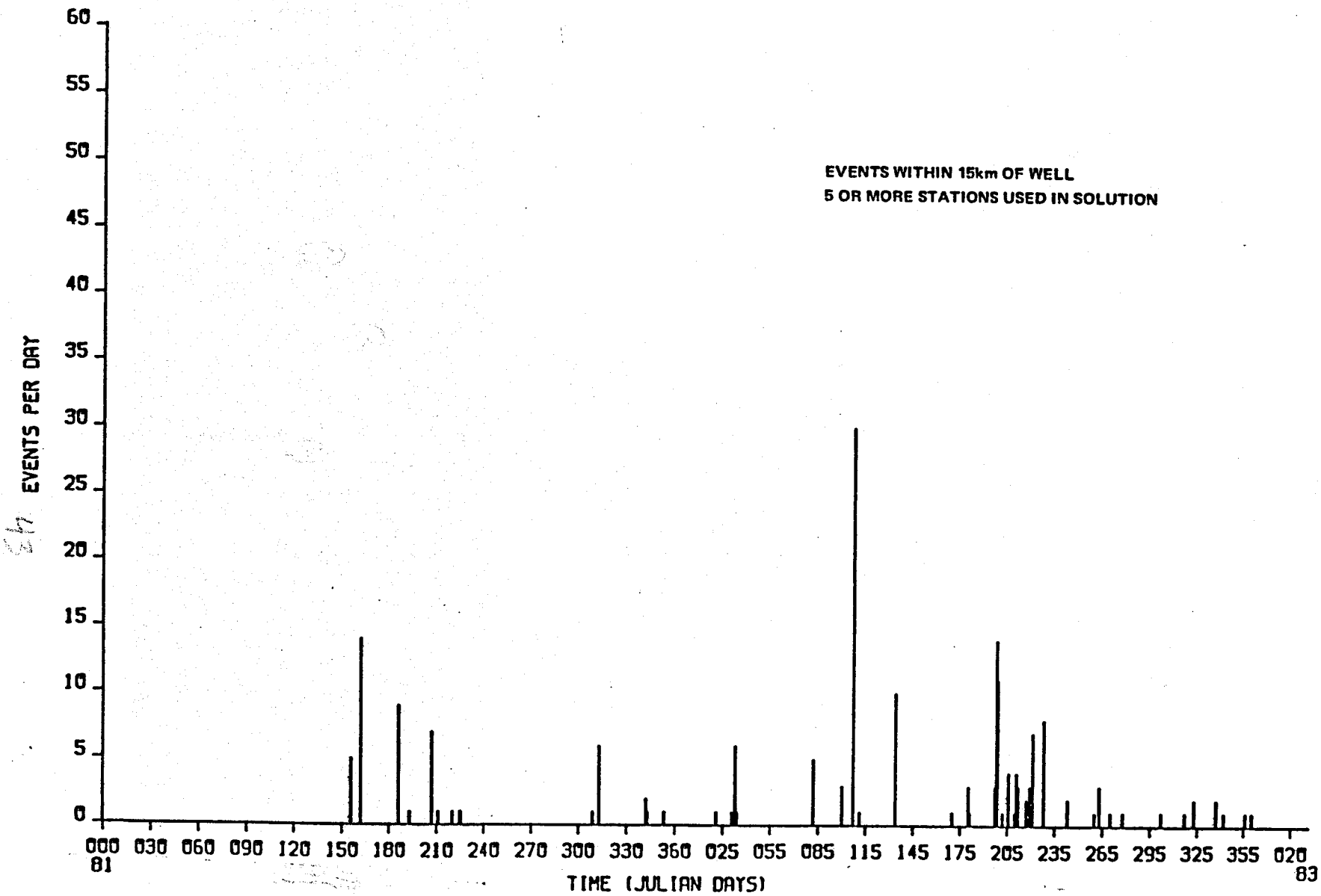

FIGURE 14. Time history of seismic activity, Sweet Lake test well.

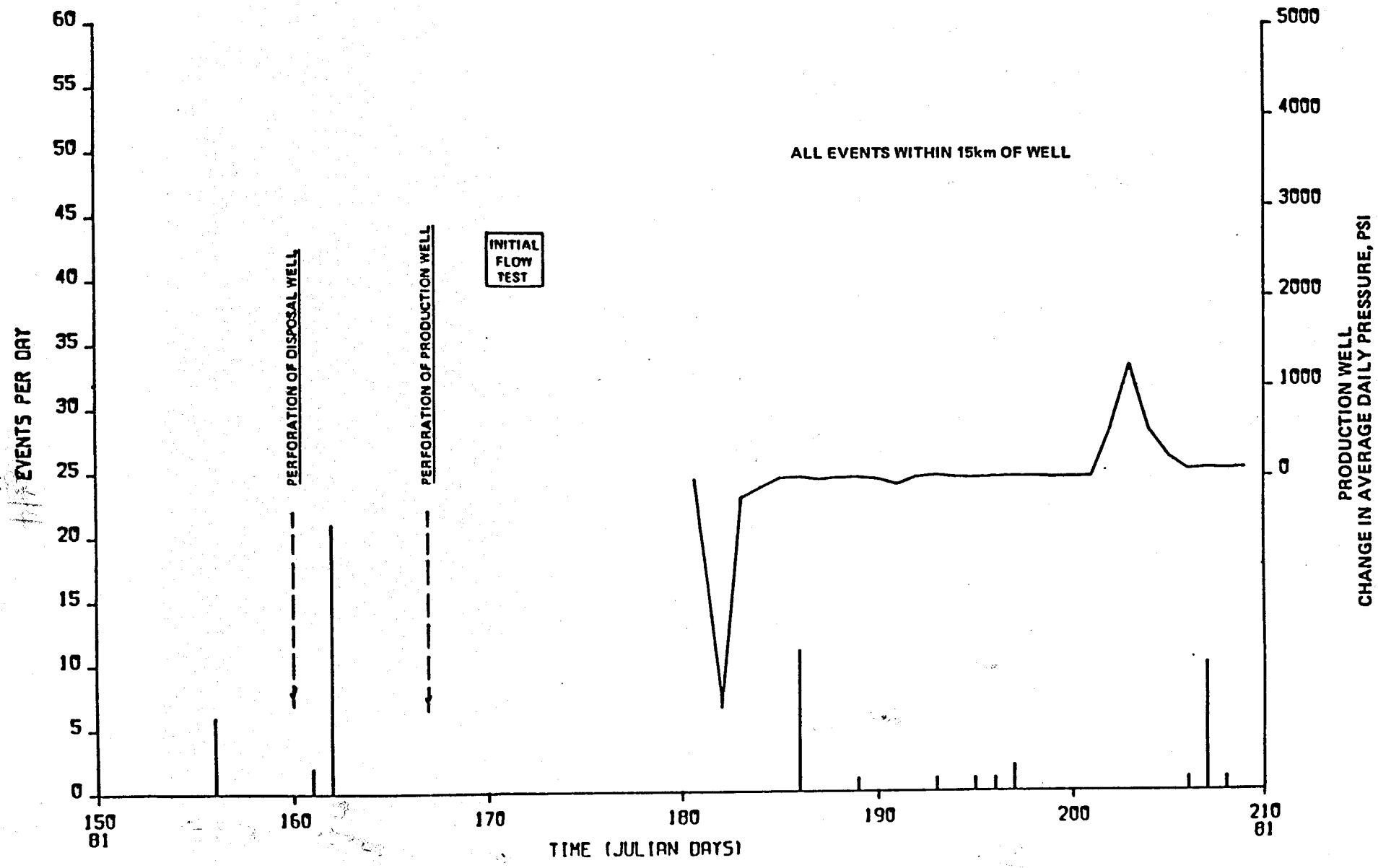

FIGURE 15. Seismic activity and changes in well pressure, Sweet Lake test well.

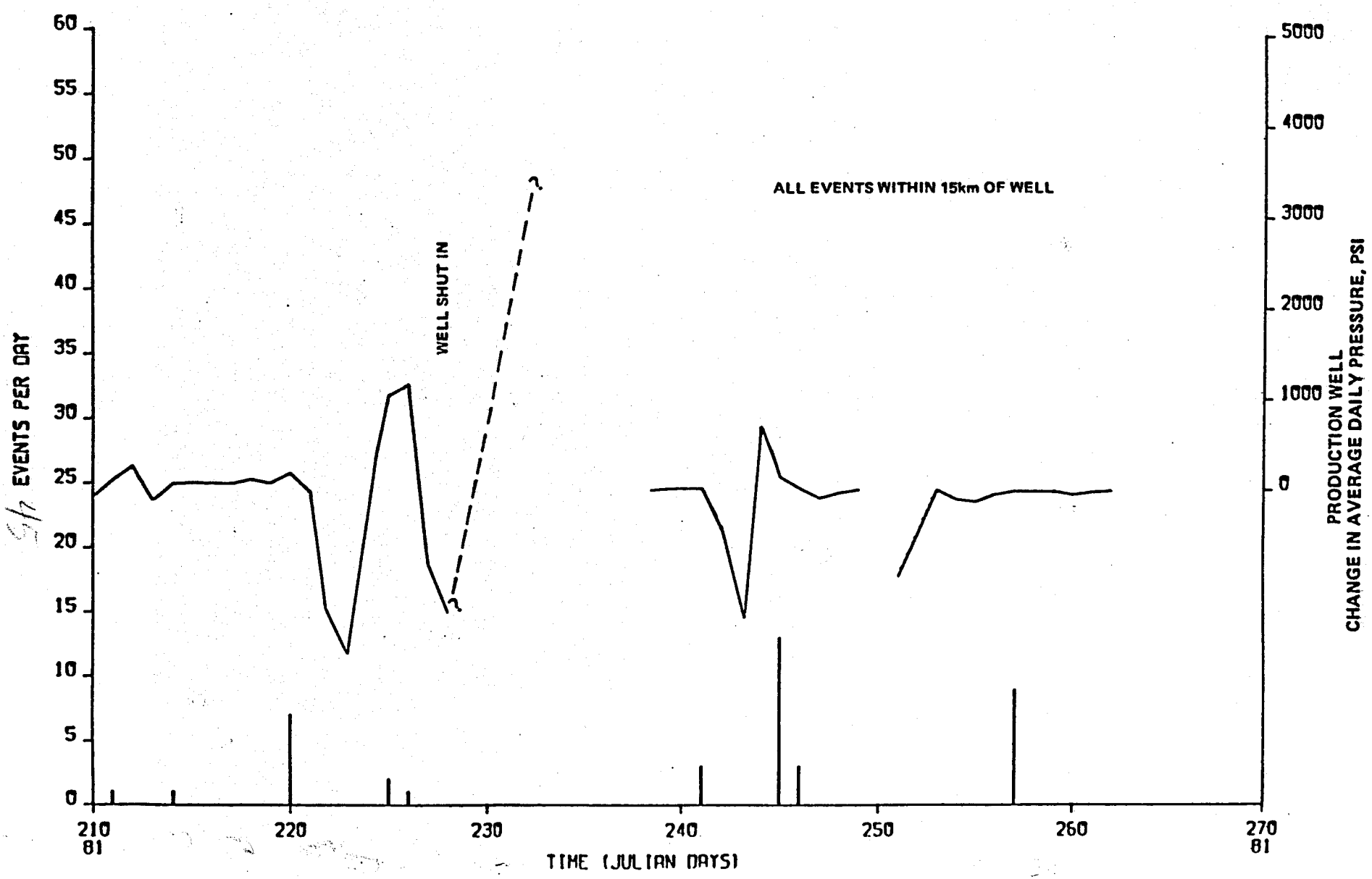

FIGURE 16. Seismic activity and changes in well pressure, Sweet Lake test well.

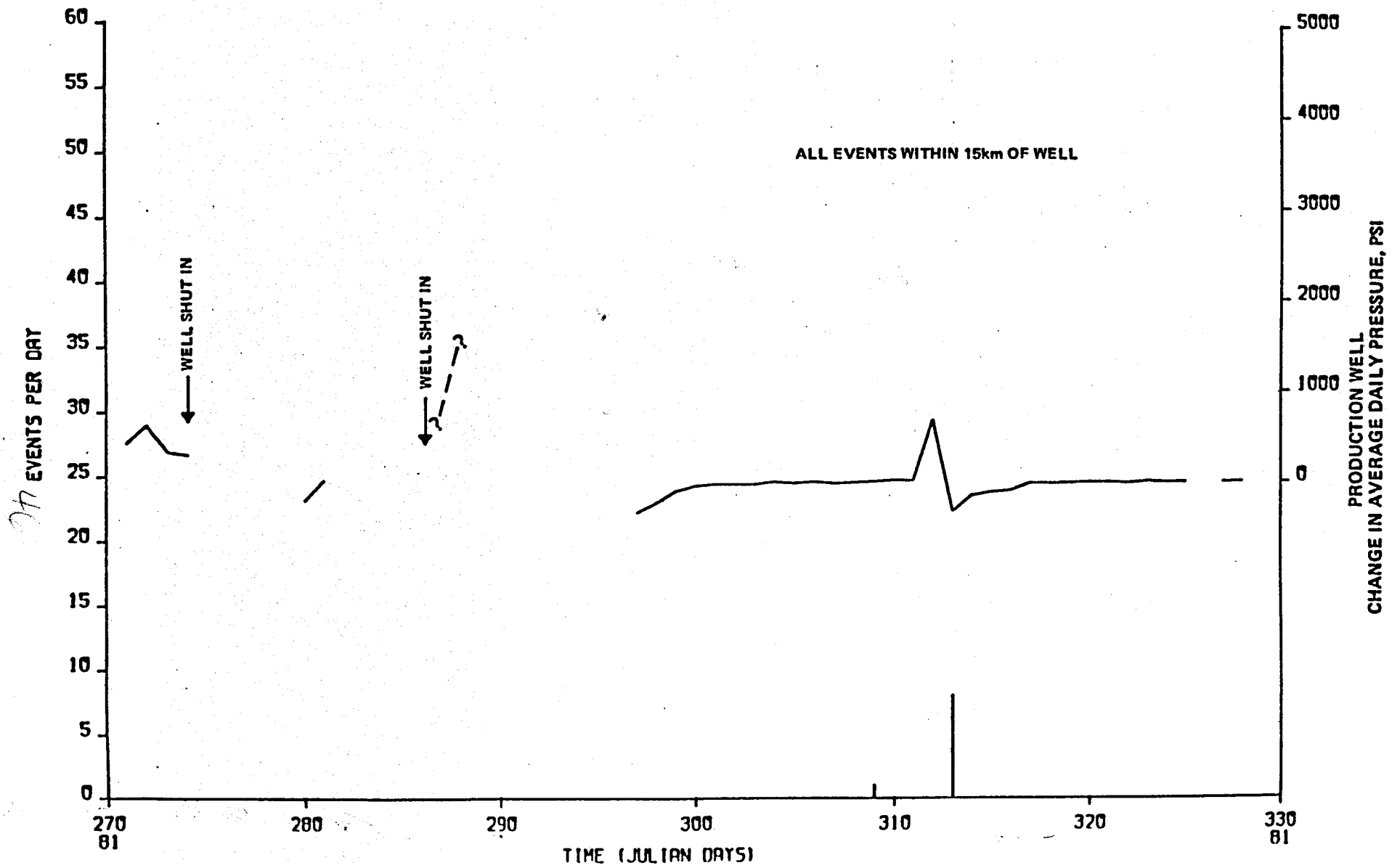

FIGURE 17. Seismic activity and changes in well pressure, Sweet Lake test well.

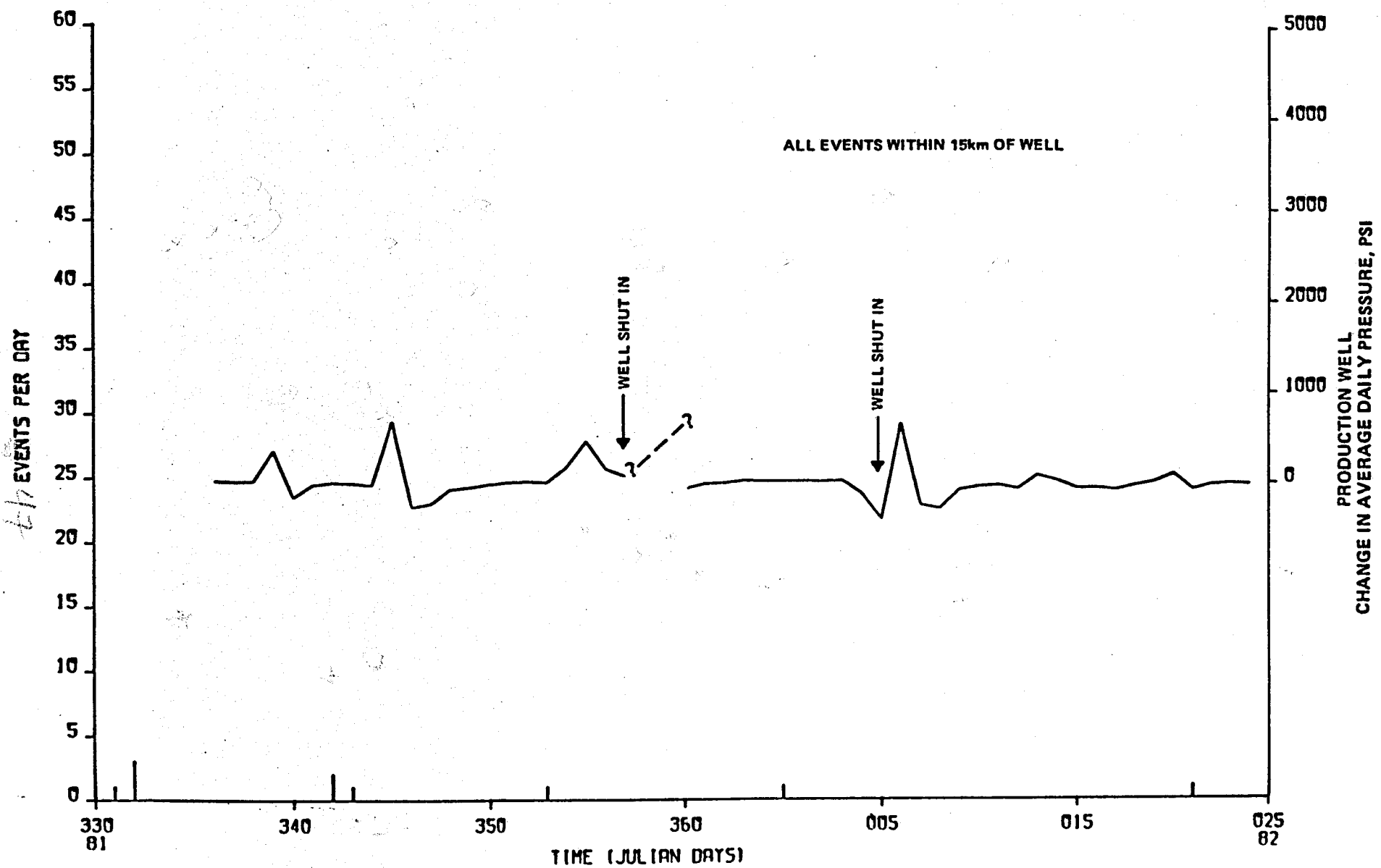

FIGURE 18. Seismic activity and changes in well pressure, Sweet Lake test well.

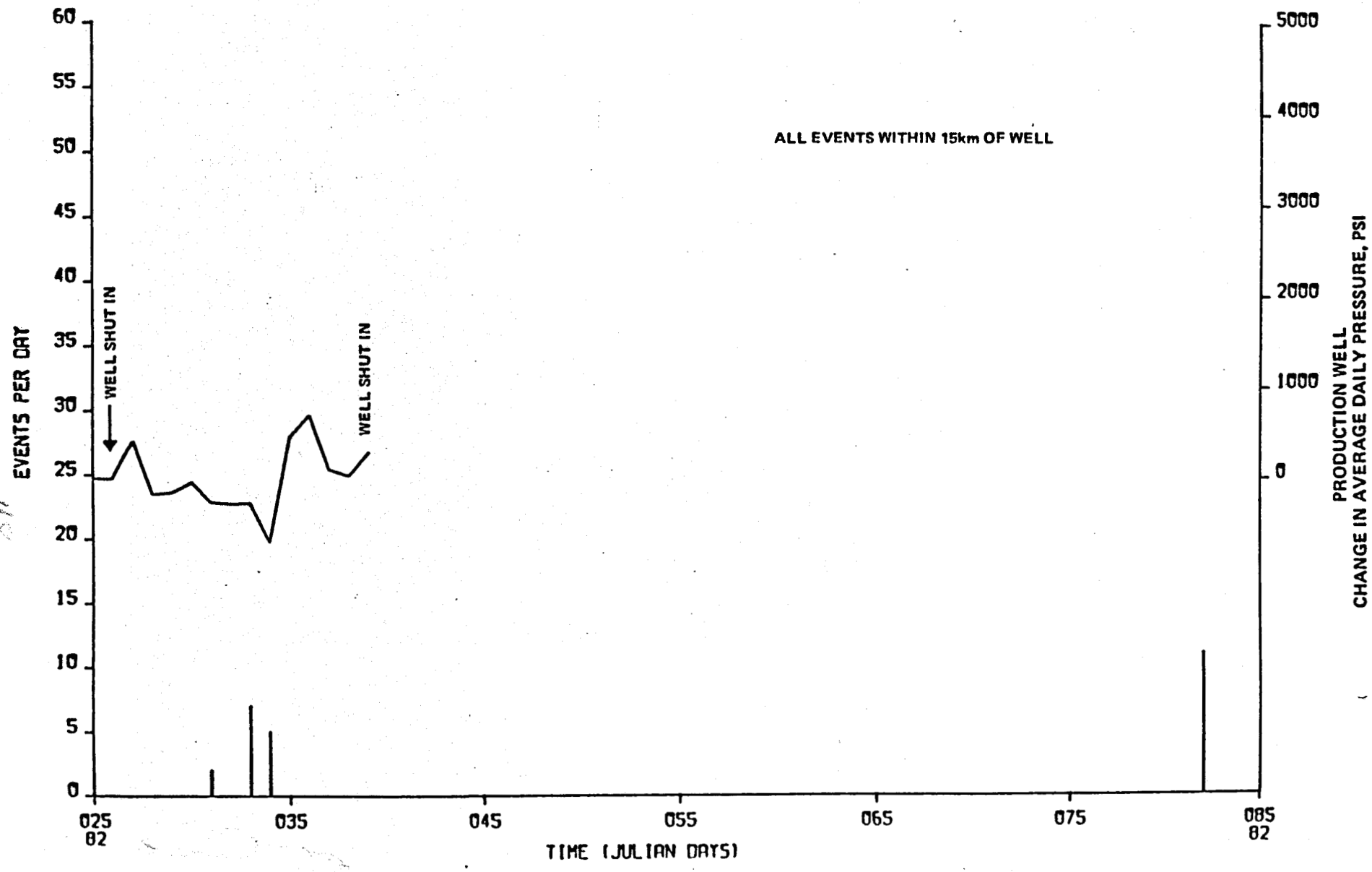

FIGURE 19. Seismic activity and changes in well pressure, Sweet Lake test well.

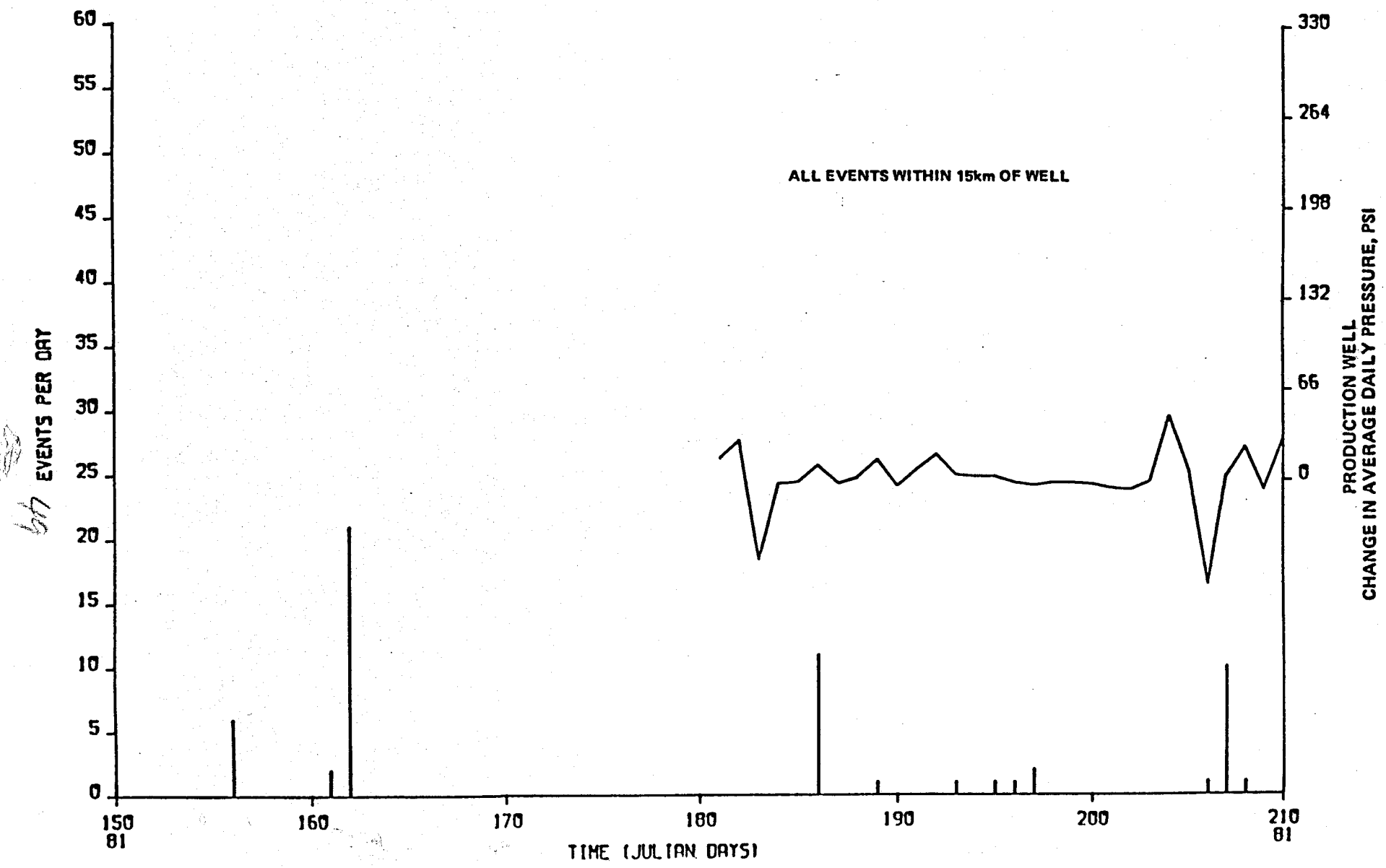

FIGURE 20. Seismic activity and changes in well pressure, Sweet Lake test well.

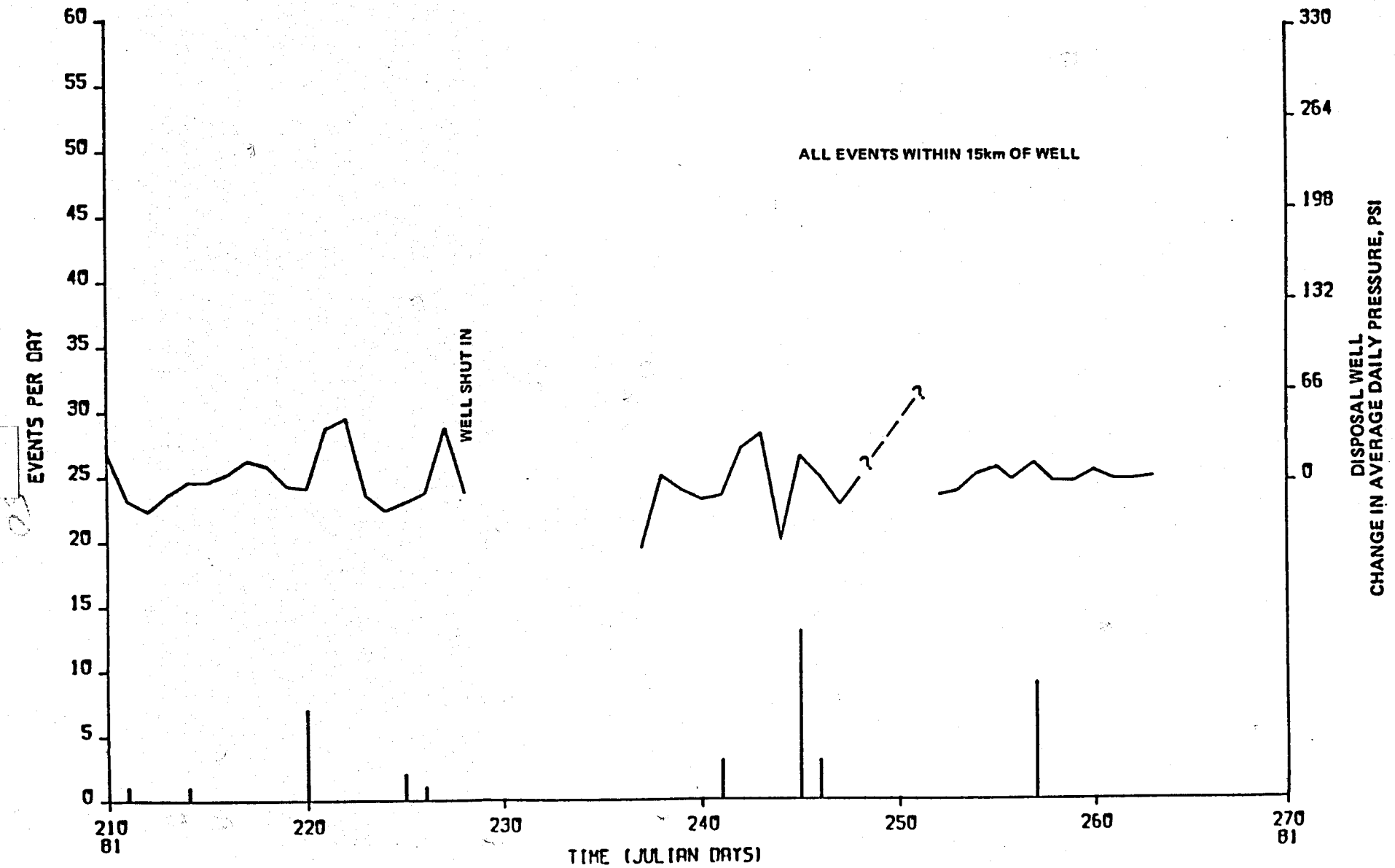

FIGURE 21. Seismic activity and changes in well pressure, Sweet Lake test well.

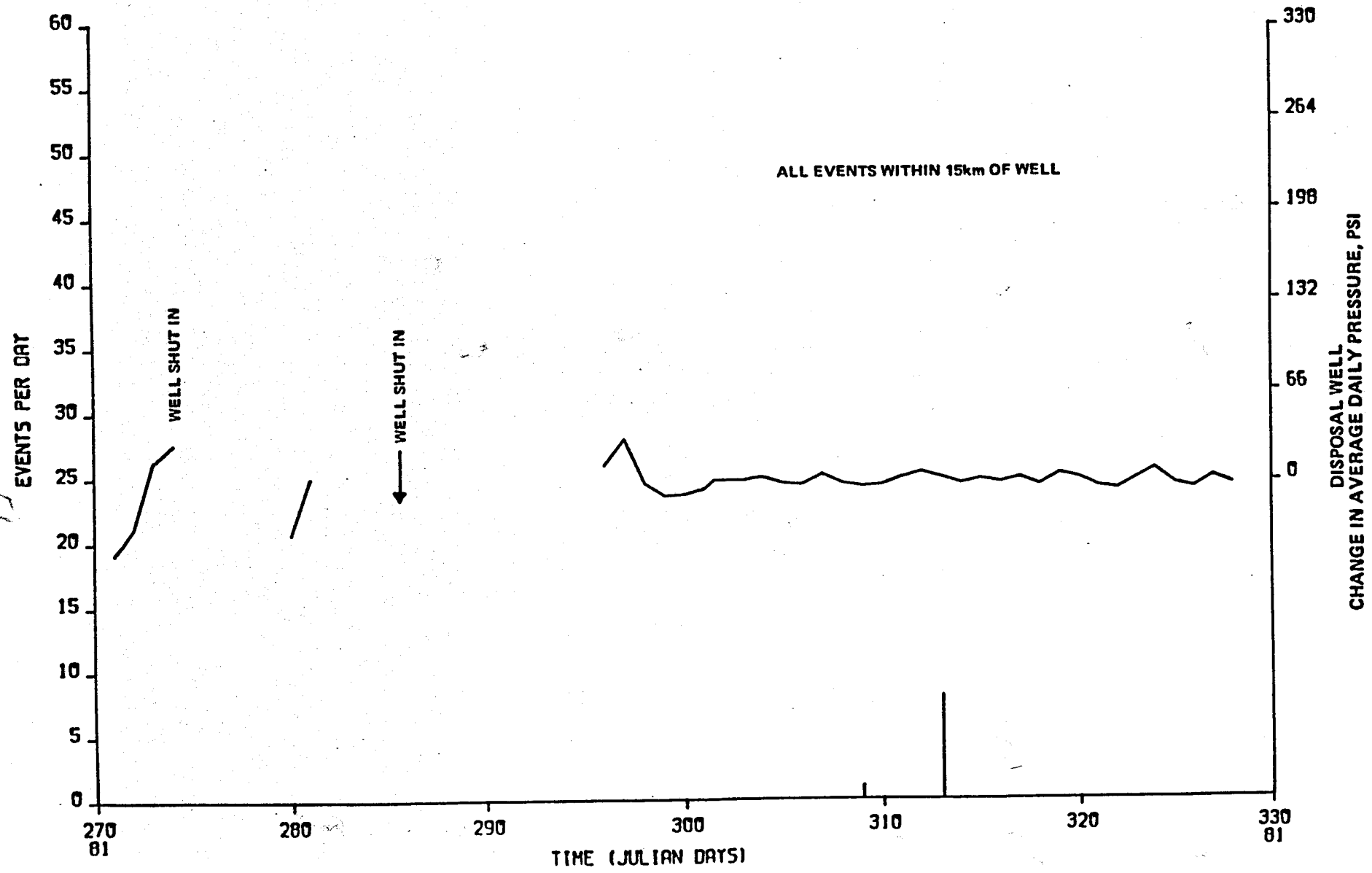

FIGURE 22. Seismic activity and changes in well pressure, Sweet Lake test well.

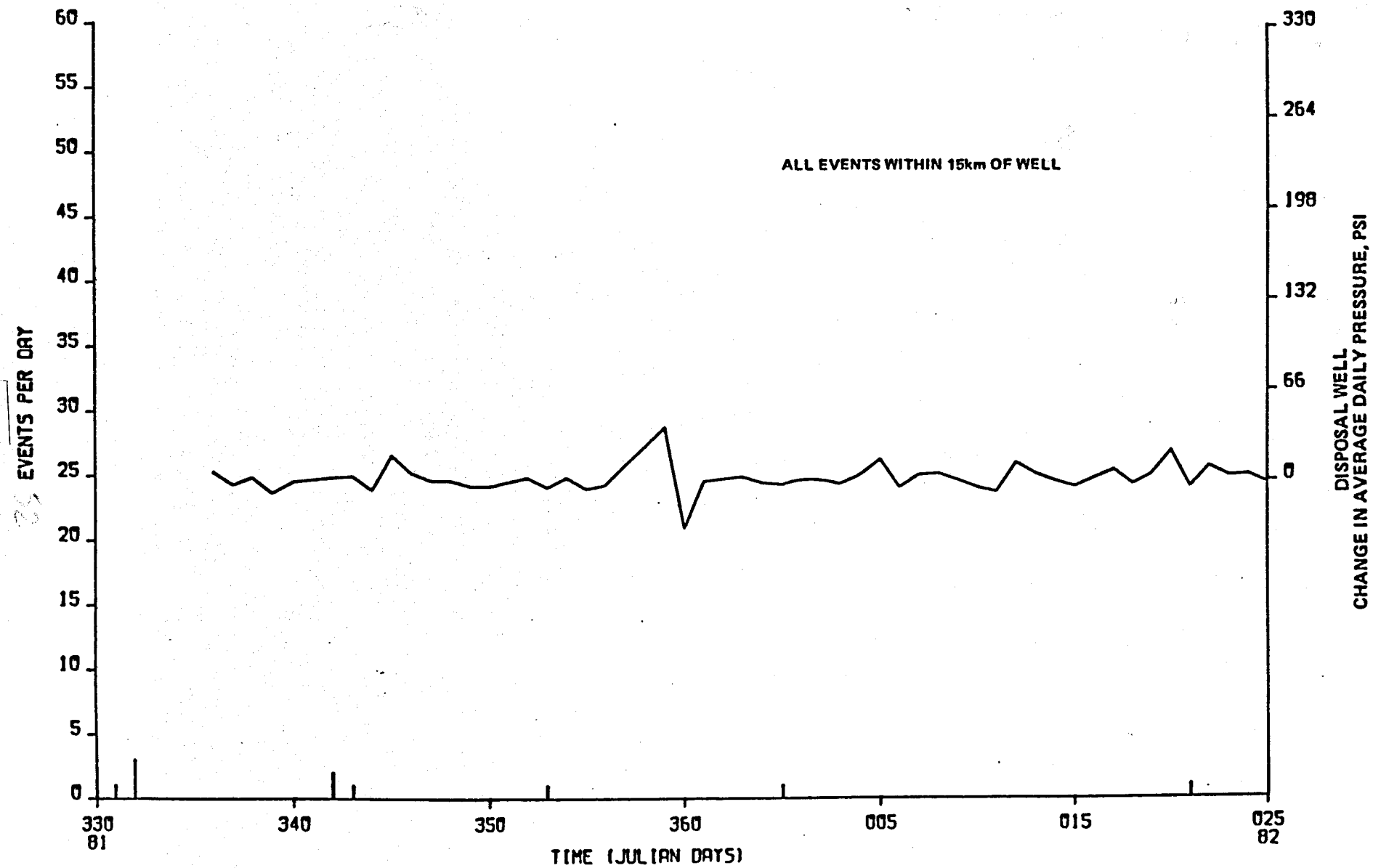

FIGURE 23. Seismic activity and changes in well pressure, Sweet Lake test well.

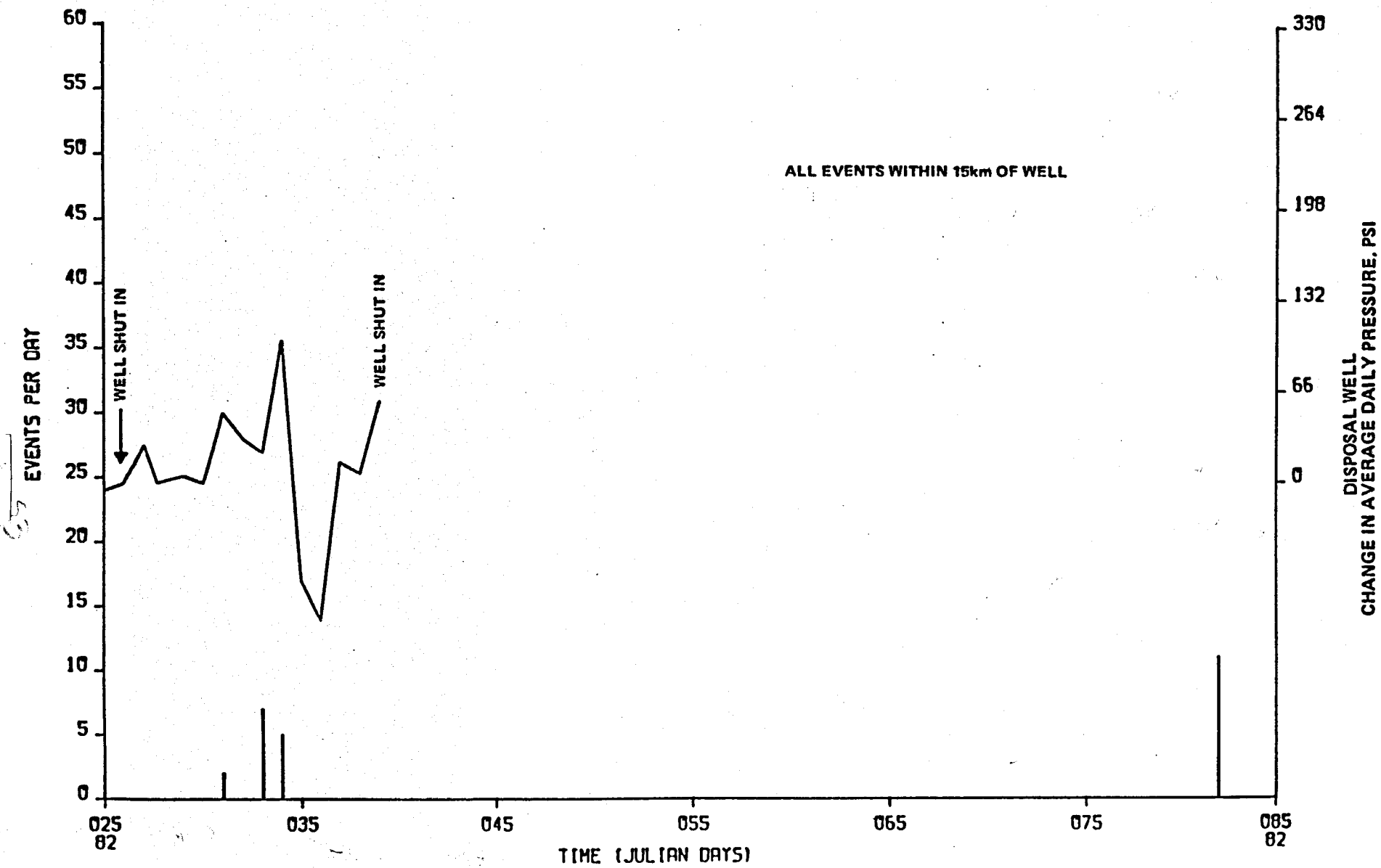

FIGURE 24. Seismic activity and changes in well pressure, Sweet Lake test well.

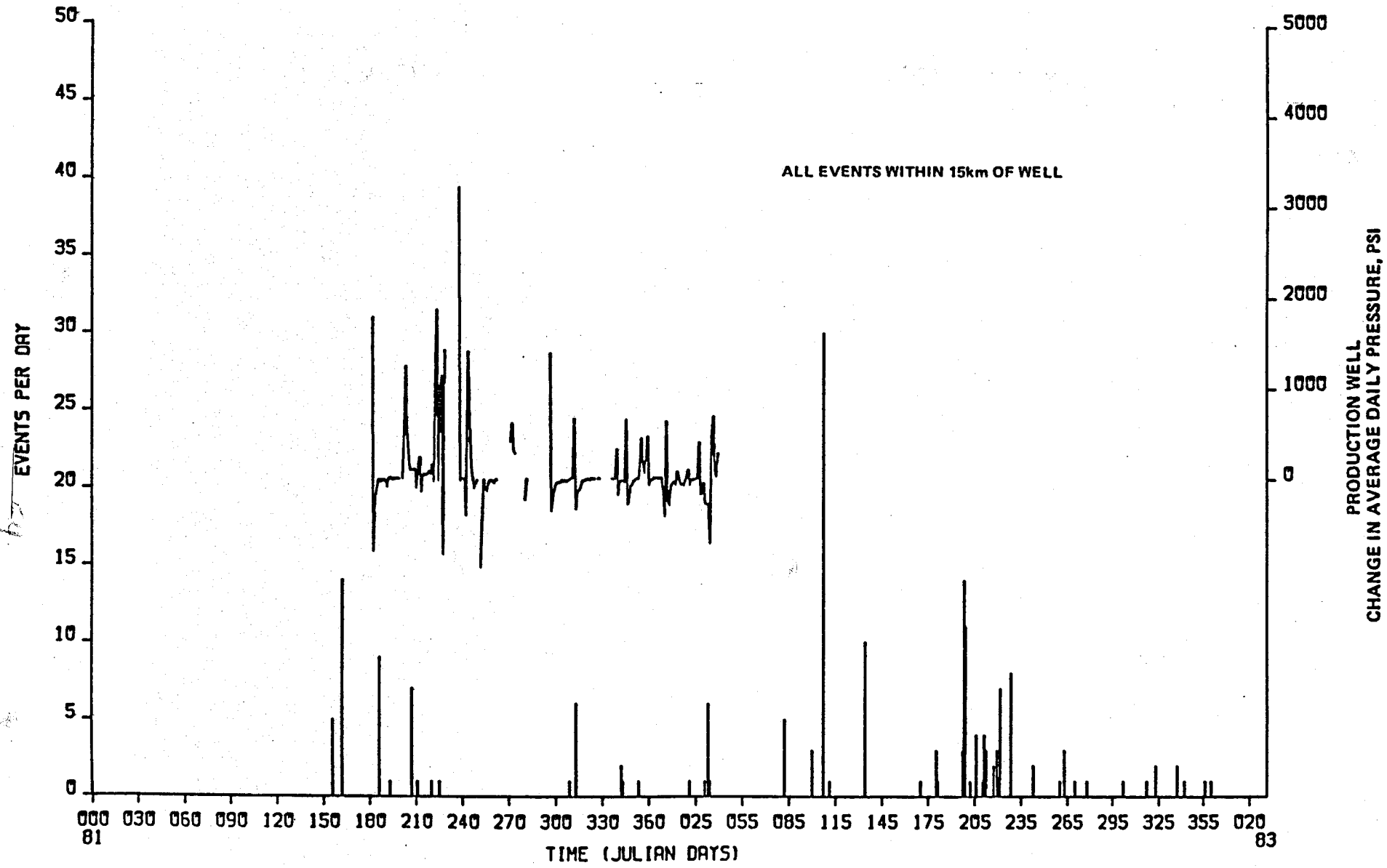

FIGURE 25. Seismic activity and changes in well pressure, Sweet Lake test well.

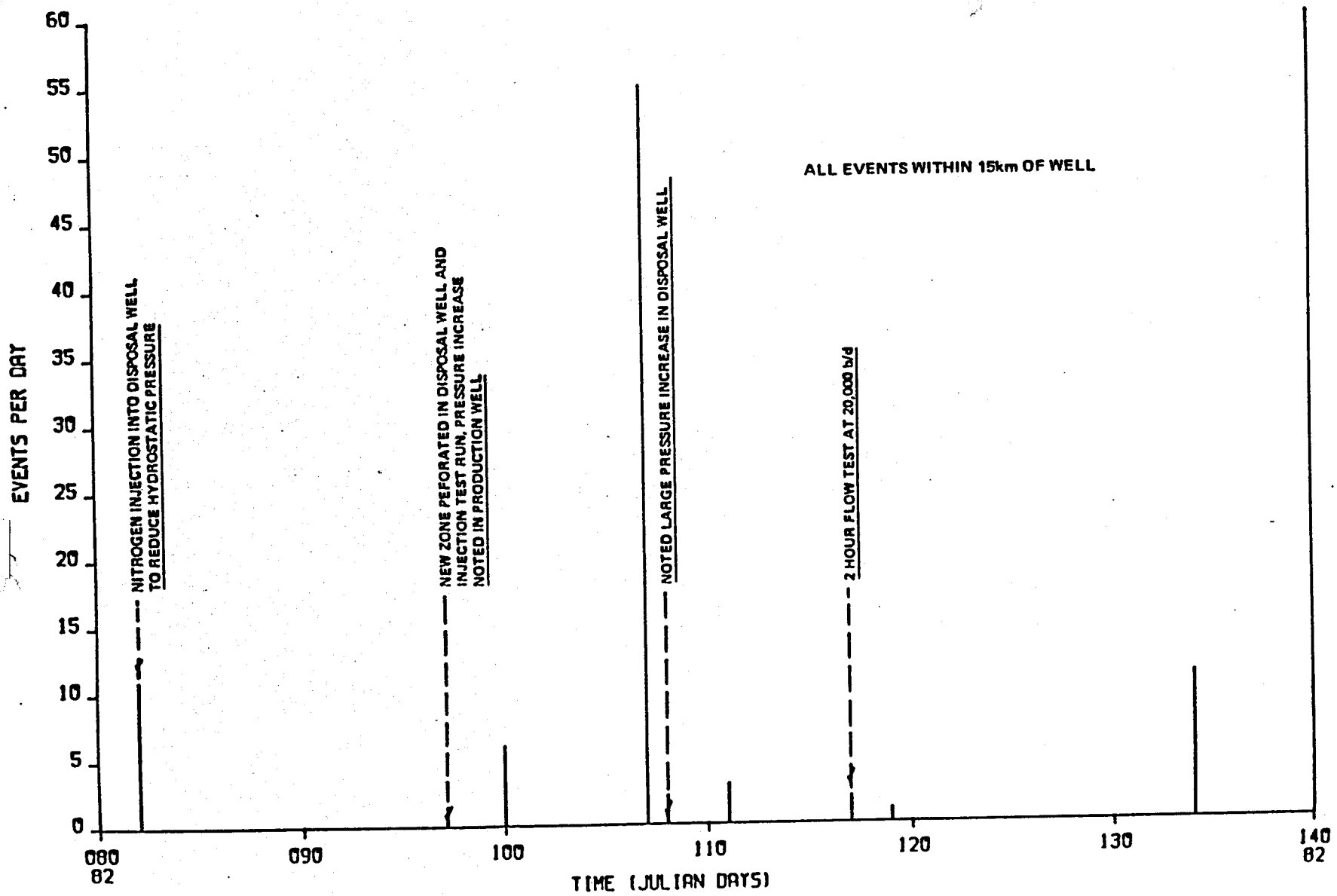

FIGURE 26. Seismic activity after reservoir limit testing, Sweet Lake test well.

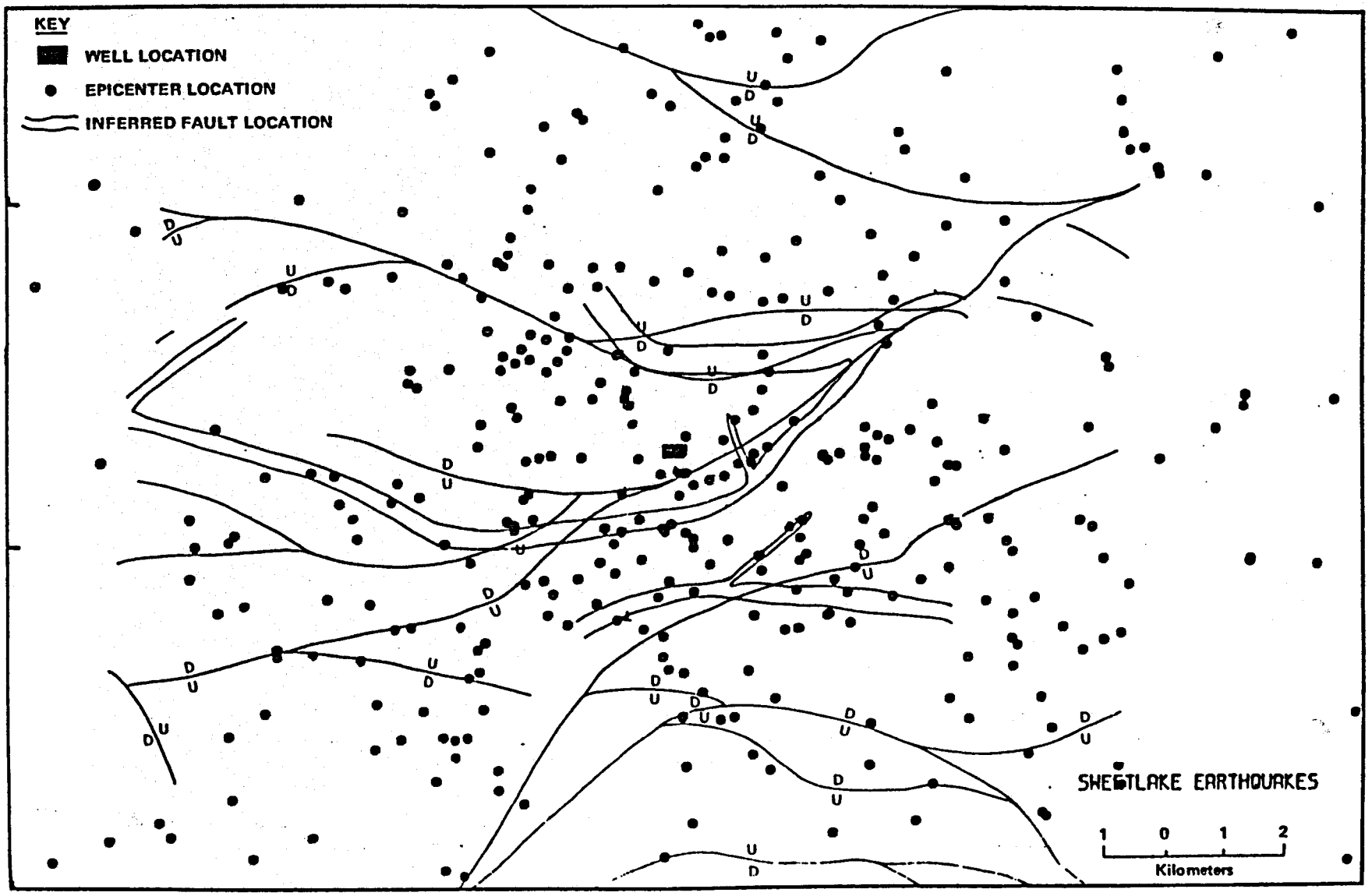

FIGURE 27. Locations of seismic activity, Sweet Lake test well, July 1980 to January 1983.

(Fig. 28). Even the bursts of seismicity that are tightly clustered in time do not show distinct spatial clustering about or along known structures, but they do appear to be distributed in spatial clusters about the well and within the area covered by the network. There does not appear to be any overall spatial migration of activity with time; however, the spatial clustering of activity occurring as bursts of seismicity does indicate potential locational constraints or preferences probably defined by specific changes occurring in the subsurface.

All of the best event locations within 6 km of the wells have computed depths between 0 and 8 km (Fig. 29). This suggests that microearthquakes are occurring within the range of depths at which the influence of fluid withdrawal and injection is to be expected. The spatial distribution of the microearthquakes as a function of depth may be related to the relative confinement of the reservoir fluids at both the depths of the withdrawal and injection. The geopressured-geothermal brine being withdrawn from the production well occurs in a graben that is bounded by growth faults. Withdrawal from this reservoir will affect the fluid pressures at the graben boundaries and perhaps those of other aquifers at similar depths. On the other hand, the injection of fluid in the disposal well occurs in relatively unbounded sands. Faults at this level are thought to have significantly smaller displacements with respect to the reservoir thickness. Hence, the more dispersed distribution of the shallower activity may be a reflection of the disposal horizon's unbounded character.

Seismic Monitoring and Seismicity October 1982 through September 1983

During the period of October 1982 through September 1983, 169 small events were detected by five or more stations of the Sweet Lake Seismic Monitoring Network (SLSMN). These events, which are believed to be of natural origin, are listed in Table 9, the event catalog for the period. Taking the highest

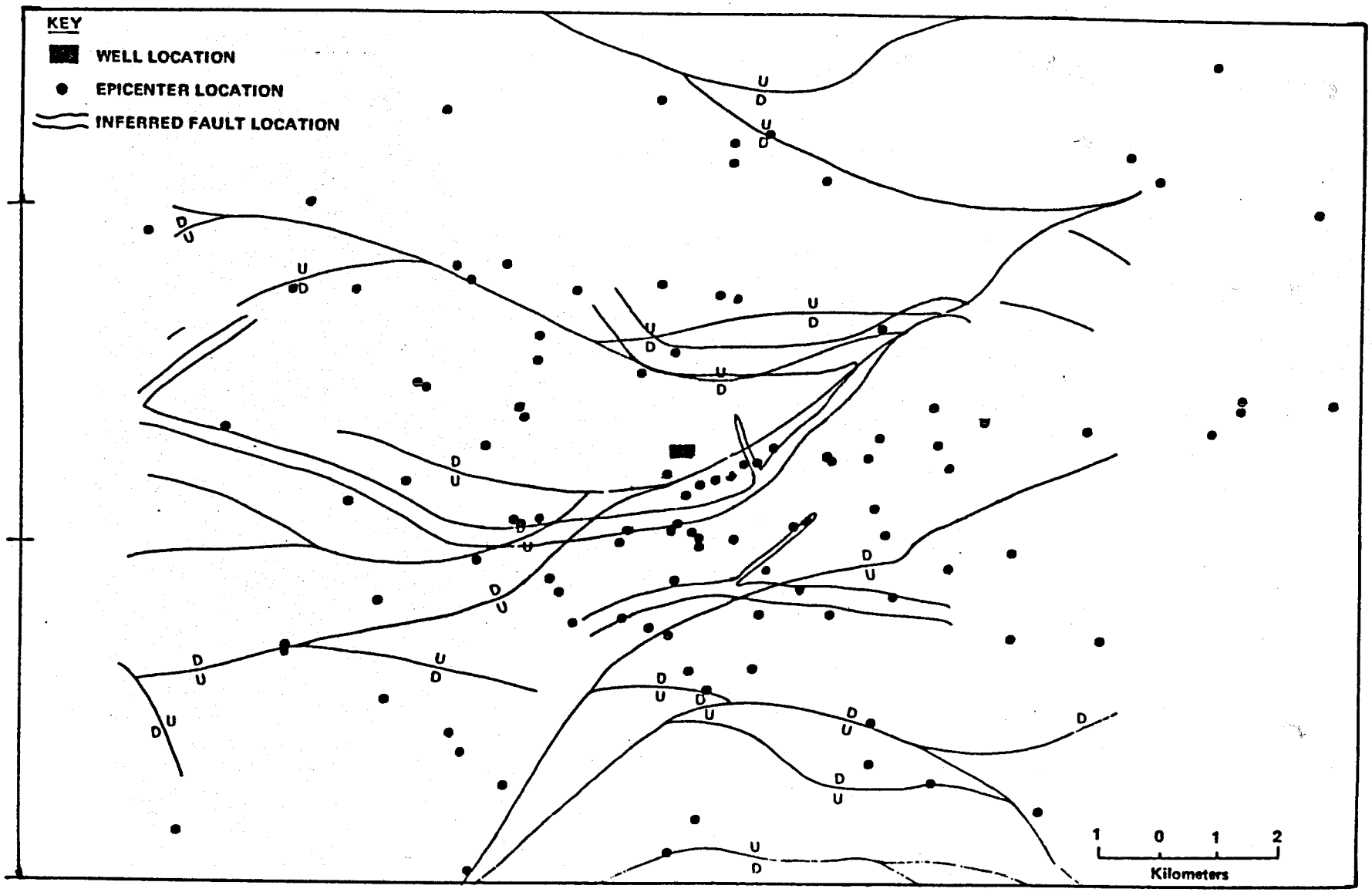

FIGURE 28. Locations of seismic activity during reservoir limit test, Sweet Lake test well, June 1981 to February 1982.

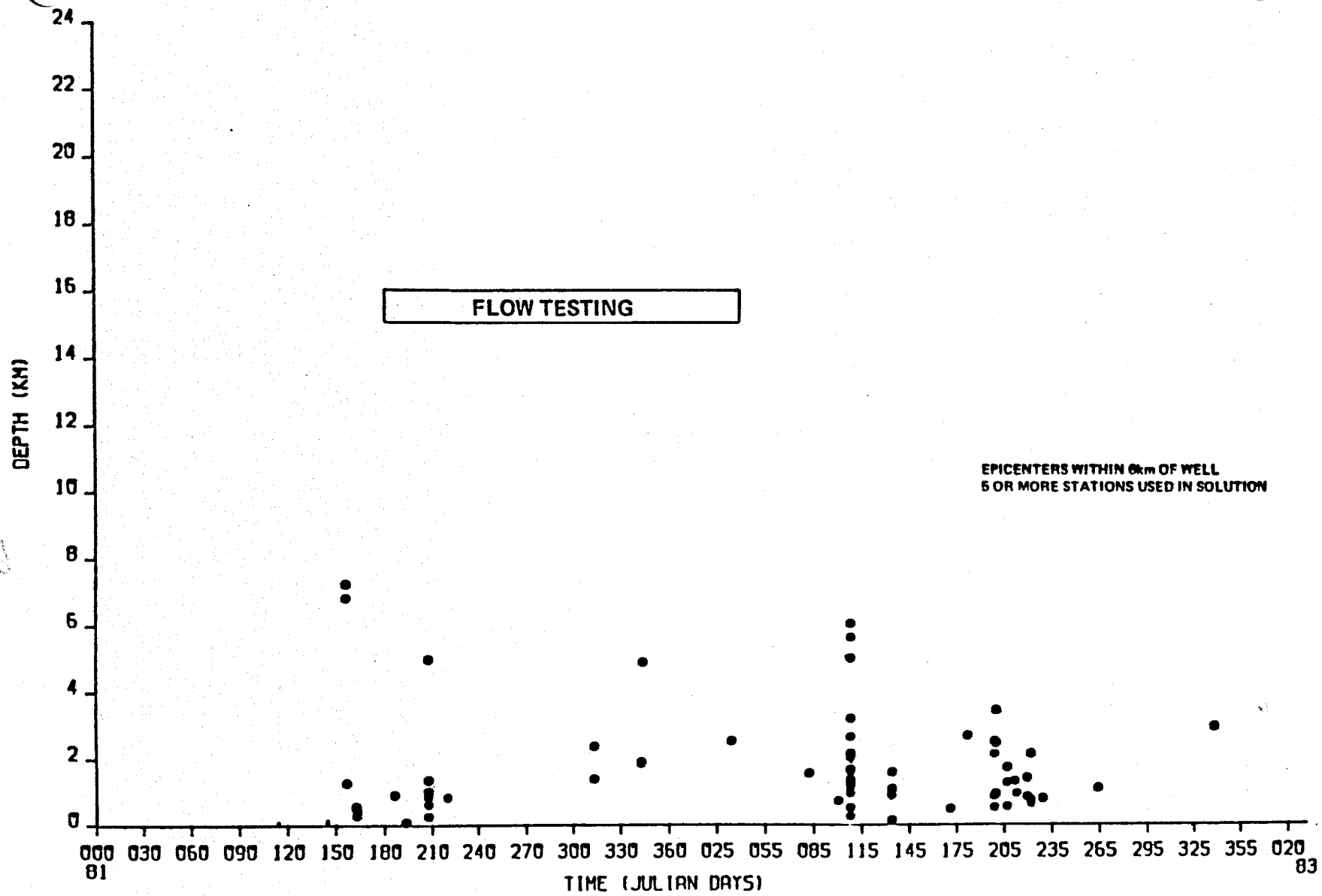

FIGURE 29. Distribution of computed depths, Sweet Lake test well.

TABLE 9. Sweet Lake events
(five or more stations reporting).

	YEAR	JULIAN DAY	LATITUDE	LONGITUDE	ERROR RMS	NO. OF STATIONS REPORTING
1	1982	278	29.9968	93.1061	0	5
2	1982	302	29.9280	93.1942	0	5
3	1982	319	30.2086	93.2606	0	6
4	1982	323	29.9125	93.1604	0	5
5	1982	323	30.0678	92.9666	0	5
6	1982	323	29.9012	93.0775	0	5
7	1982	331	29.7997	93.4454	0	5
8	1982	331	29.8667	93.3792	0	5
9	1982	334	30.1281	93.0254	0	5
10	1982	336	29.9384	93.3127	0	5
11	1982	337	29.8997	93.2169	0	5
12	1982	337	29.9672	93.1667	0	5
13	1982	337	30.2356	93.2877	0	5
14	1982	337	29.7622	92.9533	0	5
15	1982	339	29.8996	93.2250	0	5
16	1982	342	29.1920	93.8992	0	5
17	1982	342	29.9542	93.2087	0	5
18	1982	356	30.0006	93.2125	0	5
19	1982	360	29.9881	93.0710	0	5
20	1982	360	29.8042	93.1108	0	5
21	1982	361	30.2693	93.9411	0	5
22	1982	361	29.9788	93.3322	0	5
23	1982	364	29.5349	93.9202	0	5
24	1983	012	30.7798	93.0543	0	5
25	1983	013	29.3824	93.9042	0	5
26	1983	040	29.8808	93.4812	0	5
27	1983	041	30.0519	93.1101	0	5
28	1983	041	30.0773	93.0496	0	6
29	1983	041	29.9663	93.1152	0	5
30	1983	041	29.8882	93.1070	0	6
31	1983	046	29.6854	93.4793	0	5
32	1983	060	31.0936	92.6239	0.291	6
33	1983	064	29.9342	93.2169	1.064	5
34	1983	064	29.8869	93.2201	1.417	5
36	1983	064	29.6911	93.4411	1.166	5
37	1983	064	29.3904	93.6210	0.208	6
38	1983	064	29.2989	93.6867	0	6
39	1983	069	30.6743	92.8365	0.290	5
40	1983	080	30.1847	93.0963	0.490	5
41	1983	082	29.8256	93.6236	0	5
42	1983	082	29.8899	93.4451	1.050	6
43	1983	082	29.9093	93.0173	0.452	5
44	1983	089	29.9429	93.3615	0.377	6
45	1983	089	29.9139	93.3432	0.065	7
46	1983	089	29.9924	93.2388	1.171	6
47	1983	089	29.9705	93.1415	0.182	6

TABLE 9, cont.

	YEAR	JULIAN DAY	LATITUDE	LONGITUDE	ERROR RMS	NO. OF STATIONS REPORTING
48	1983	089	29.9815	93.1245	0.346	5
49	1983	089	29.8125	93.3597	0.346	6
50	1983	089	30.0503	93.1302	0.173	5
51	1983	089	30.0411	93.0605	0.299	5
52	1983	089	29.9985	93.1170	0.327	5
53	1983	089	30.1528	93.0828	0.166	5
54	1983	089	29.5185	93.8580	0.282	6
55	1983	090	29.2208	94.0377	0.434	5
56	1983	095	30.0283	93.1428	0.252	5
57	1983	099	29.9156	93.2660	1.552	6
58	1983	099	29.5214	93.5839	1.237	5
59	1983	099	30.0191	92.8948	0.084	5
60	1983	099	30.0033	92.7361	0.545	6
61	1983	117	30.1124	93.1021	0.049	5
62	1983	118	30.1408	93.1504	0.121	6
63	1983	118	30.0979	93.1580	0.142	6
64	1983	118	30.1197	93.1609	0.032	6
65	1983	118	30.1667	93.1785	0.037	5
66	1983	130	29.9317	93.0708	0.284	5
67	1983	130	29.9145	93.0848	0.144	5
68	1983	130	30.0581	93.1694	0.281	5
69	1983	139	29.8675	93.1908	0.812	5
70	1983	139	29.9462	93.1978	1.505	5
71	1983	139	29.8779	93.2190	0.791	5
72	1983	141	30.0009	93.1338	0.083	5
73	1983	141	30.0151	93.1169	0.203	5
74	1983	141	29.9948	93.1562	0.873	5
75	1983	141	29.9908	93.1665	0.169	5
76	1983	141	29.9885	93.0943	0.496	5
77	1983	141	30.0128	93.1155	0.135	5
78	1983	141	30.0746	92.9810	0.110	6
79	1983	141	30.0339	93.1428	0.070	6
80	1983	141	30.0344	93.1628	0.313	6
81	1983	141	30.0197	93.1580	0.200	5
82	1983	141	30.0185	93.1346	0.061	5
83	1983	142	29.9954	93.1147	0.088	5
84	1983	142	29.9959	93.1656	0.237	6
85	1983	142	29.9856	93.1299	0.202	5
86	1983	142	30.0038	93.1394	0.091	5
87	1983	159	30.0002	92.6664	1.269	5
88	1983	162	30.0299	93.0677	0.528	5
89	1983	169	29.8509	93.3157	0.221	5
90	1983	169	29.8452	93.0463	0.145	5
91	1983	176	29.8913	93.2284	0.382	5
92	1983	177	29.8428	93.1123	0.771	5
93	1983	177	29.9952	93.1873	0.273	5
94	1983	177	29.9743	93.1613	0.192	5
95	1983	177	29.9184	93.2488	0.160	5

TABLE 9, cont.

	YEAR	JULIAN DAY	LATITUDE	LONGITUDE	ERROR RMS	NO. OF STATIONS REPORTING
96	1983	177	29.9954	93.1667	0.084	5
97	1983	177	29.9994	93.1907	0.162	5
98	1983	177	29.9589	93.1731	0.035	5
99	1983	177	30.0545	93.0781	0.018	5
100	1983	177	30.0588	93.0902	0.263	5
101	1983	177	29.9792	93.1341	0.259	5
102	1983	177	29.9752	93.1559	0.466	5
103	1983	177	29.9815	93.1500	0.218	5
104	1983	177	29.9924	93.1212	0.144	5
105	1983	177	30.0043	93.1013	0.078	5
106	1983	177	30.0357	93.0932	0.032	5
107	1983	177	30.0331	93.1442	0.037	5
108	1983	177	30.0395	93.1485	0.028	5
109	1983	177	30.0393	93.1465	0.040	5
110	1983	177	30.0393	93.1453	0.074	5
111	1983	177	30.1291	93.2275	0.324	5
112	1983	177	29.9303	93.2965	0.342	5
113	1983	197	29.6976	92.7855	0.487	5
115	1983	199	30.0265	93.1173	0.203	6
116	1983	199	30.0185	93.1264	0.133	5
117	1983	199	30.0252	93.1225	0.285	5
118	1983	199	30.0132	93.1410	0.099	6
119	1983	199	29.8724	93.2757	0.099	5
120	1983	199	29.8626	93.2989	0.327	5
121	1983	199	29.8592	93.3284	0.264	5
122	1983	201	30.0359	93.1318	0.071	5
123	1983	201	30.0911	93.1734	0.058	5
124	1983	201	30.0008	93.1373	0.962	5
125	1983	201	30.0188	93.1430	0.264	5
126	1983	201	30.0118	93.1090	0.113	5
127	1983	201	30.0037	93.1525	0.038	5
128	1983	208	29.9038	92.8385	0.089	5
129	1983	210	30.0051	93.1258	0.119	5
130	1983	210	29.9698	93.1413	0.341	6
131	1983	210	29.9416	93.1465	0.197	6
132	1983	210	30.0017	93.1574	0.277	5
133	1983	210	29.9429	93.1402	0.481	5
134	1983	210	29.8110	93.3981	0.113	5
135	1983	216	29.9993	92.9149	0.612	5
138	1983	217	29.8109	93.2427	0.221	5
139	1983	217	29.8293	93.2457	0.361	5
140	1983	218	30.0201	93.0833	0.602	5
141	1983	221	29.9547	93.0817	0.055	5
142	1983	223	29.8830	93.1713	0.610	5
143	1983	223	29.8462	93.1750	0.368	5
144	1983	223	29.9967	93.1604	0.295	5
145	1983	223	30.0275	93.2892	0.351	5
146	1983	223	29.9386	93.1825	0.387	5

TABLE 9, cont.

	YEAR	JULIAN DAY	LATITUDE	LONGITUDE	ERROR RMS	NO. OF STATIONS REPORTING
147	1983	223	29.9847	93.1592	0.279	5
148	1983	223	29.9697	93.1268	0.149	5
149	1983	223	30.0017	93.0879	0.238	5
150	1983	223	29.9258	93.0819	0.196	5
151	1983	224	30.0718	93.1571	0.055	5
152	1983	242	30.6992	92.8239	0.242	5
153	1983	249	29.9895	93.0978	1.927	5
154	1983	249	29.9908	93.0543	0.095	5
155	1983	249	29.9981	93.1739	0.011	5
156	1983	249	30.0786	93.2425	0.083	5
157	1983	249	30.0741	93.2067	0.353	5
158	1983	249	30.0529	93.2166	0.010	5
159	1983	249	30.0506	93.2463	0.023	5
160	1983	249	30.0500	93.2457	0.198	5
161	1983	249	29.9440	93.1336	0.646	5
162	1983	249	29.9544	93.1594	1.086	5
163	1983	249	29.9890	93.1084	0.128	5
164	1983	254	30.0294	93.1717	0.117	5
165	1983	254	30.0290	93.1721	0.150	5
166	1983	261	29.9301	93.0157	0.237	5
167	1983	261	29.9908	93.0244	0.244	5
168	1983	262	29.9161	93.2111	0.097	5
169	1983	262	29.9757	93.1582	0.100	5
170	1983	262	30.0267	93.1589	0.153	5

quality locations of these 169 events, that is, the events with RMS values less than 0.1, we are left with 36 possible microearthquakes. Of these 36, 28 are located within the boundaries of the Sweet Lake location map (Fig. 30 and Table 9). Of these 28 events, 6 occurred within the boundaries of the SLSMN, as defined by its outermost stations.

Event 164, which occurred on 11 September 1983, had an estimated duration magnitude of $M_D = +0.83$ and estimated focal depth of 5.36 km. This event is unique to this study in that both P- and S-waves could be easily discerned on five stations. Velocity Model 1 (Table 10) was used to determine an epicentral location inside the SLSMN. This same event was relocated using a velocity model appropriate to the East Texas Basin (see Table 11, Velocity Model 3), as provided by Dr. Wayne Pennington of the University of Texas at Austin. This relocation of event 164 appears as event 165 in Table 9. The relocation pushed the estimated epicenter slightly north and west of that found with Velocity Model 1 and placed the focal depth slightly deeper at 7.29 km. The event, as located with Velocity Model 3, still lies within the SLSMN (Fig. 30). Since the actual seismic velocities for the sediments underlying the Sweet Lake area are unknown, both Velocity Models 1 and 3 are inaccurate estimates. However, the fact that both velocity models place this event within the SLSMN indicates that it probably is local and of natural origin.

Discussion

After examination of the apparently large number of events being detected at the SLSMN, it was decided to compare the event detection record of the best quality events to the climatological data of the area. Rainfall at two recording sites within 10 km of the SLSMN, Lake Charles Airport and Hackberry, Louisiana, has been plotted daily to get a more accurate indication of actual rainfall within the SLSMN. A plot of daily rainfall and daily seismicity (Fig. 31) reveals that a definite relation between events (best quality

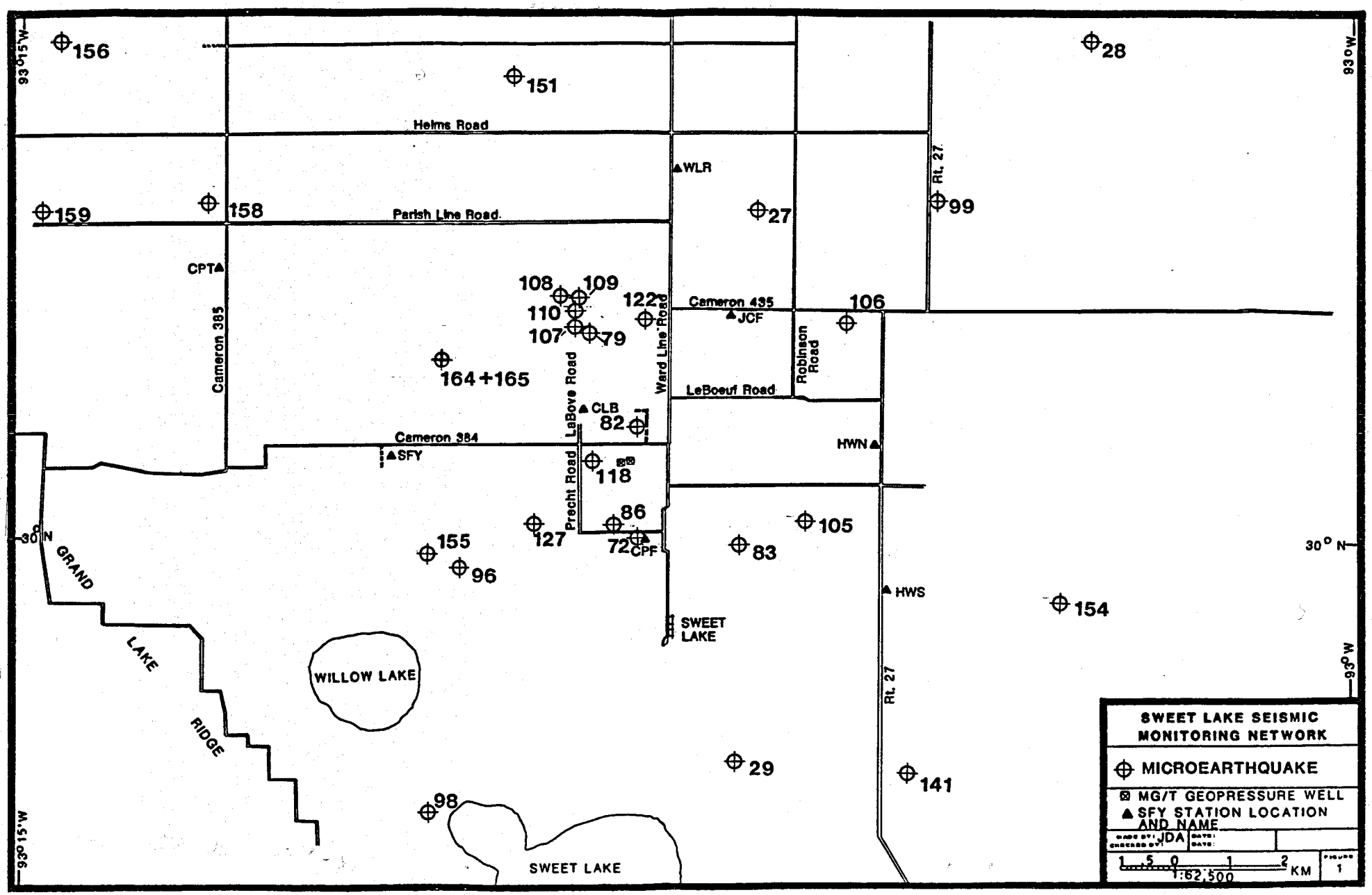

FIGURE 30. Location of microearthquakes within Sweet Lake map boundaries.

TABLE 10. Velocity Model 1 and alternative "slow wave"*
Velocity Model 2 for the Sweet Lake Seismic Monitoring Network.

MODEL 1

Velocity (km/s)	Depth Interval (km)
1.530	0.00 - 0.08
1.710	0.08 - 0.15
1.800	0.15 - 0.27
2.050	0.27 - 0.60
2.257	0.60 - 1.20
2.620	1.20 - 2.28
2.891	2.28 - 4.99
3.182	4.99 - 6.00
3.409	6.00 - 7.00
3.636	7.00 +

P-wave: S-wave velocity ratio equals 1.66:1.00.

MODEL 2

Wave velocity (km/s)	Depth Interval (km)
0.342	0.00+

*Slow waves are assumed to be long-period Rayleigh (L_R) waves, but could be S-waves since depth to focus can sometimes be determined.

TABLE 11. Velocity Model 3, East Texas Basin.

Velocity (km/s)	Depth Interval (km)
2.2	0.0 - 1.0
3.4	1.0 - 3.0
4.5	3.0 - 5.0
5.4	5.0 - 15.0
6.8	15.0 - 35.0
8.2	35.0+

67

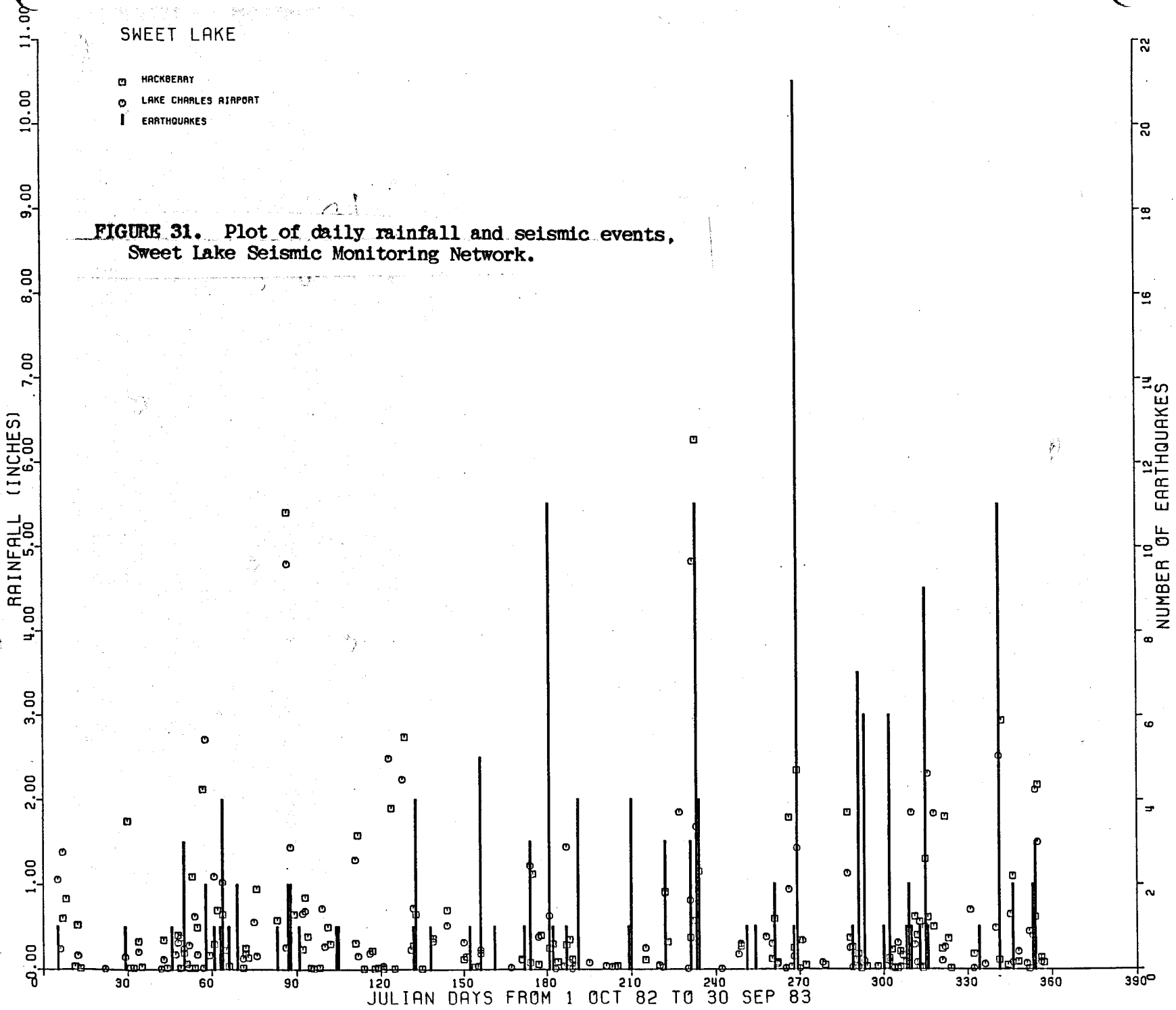

FIGURE 31. Plot of daily rainfall and seismic events, Sweet Lake Seismic Monitoring Network.

locations) and weather-related phenomena, such as rainfall (thunderstorms), cannot be ruled out.

Of the 139 events located in this reporting period, 93% occurred during periods of known rainfall. In addition, periods with the greatest number of events also had the greatest levels of rainfall. We believe that most of these events were induced by lightning. As further evidence of this, for many events a characteristic seismic "glitch" occurred at all stations simultaneously. This was followed by seismic wave arrivals traveling at approximately the speed of sound in air. The arrivals which followed the "glitch" must have necessarily been thunder if the "glitch" is lightning-induced electromagnetic interference in the telephone line or possibly in the amplifier electronics boxes at each seismic station.

Of all the suspected naturally occurring local seismic events detected during this time, only event 164 (Table 9) had a seismic signature typical of known earthquakes which occur in other parts of the country, that is, a clearly discernible P-wave followed by an S-wave. This event may have been a foreshock of a larger (m_{Blg} = 3.8) event which occurred 16 October 1983 in the Sweet Lake area.

Since the Sweet Lake DOE/M-G/T Amoco Fee #1 test well was shut in during June and July and only minor (nonpumping) work was done at the well site prior to event 164 on 11 September 1983, it would seem unlikely that this event is related to well activity, considering that the located depth is well below the production horizon.

Rockefeller Refuge

The Rockefeller Refuge microseismic monitoring network consists of eight permanent field stations (Fig. 32) which are maintained as Sweet Lake by the university's subcontractor, Woodward-Clyde Consultants. Location coordinates and other station data are given in Table 12. Each field station consists of a

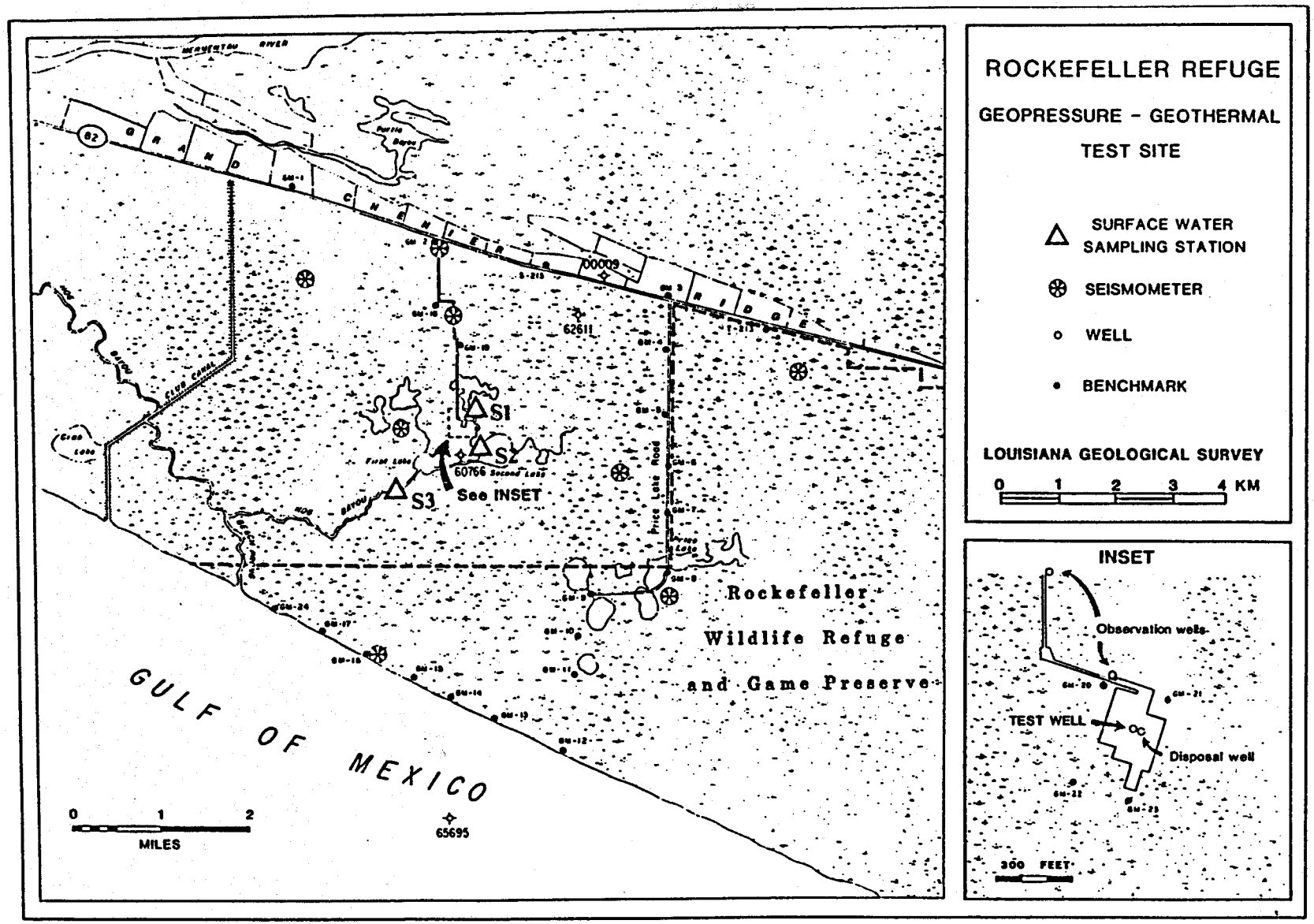

FIGURE 32. Area map of Rockefeller Refuge geopressured-geothermal test site showing locations of observation stations.

TABLE 12. Rockfeller Refuge seismic monitoring network.

Station Code	Station Name	North Latitude	West Longitude	Seismometer Depth (m)	Seismometer Installation (mo/d/yr)	On-Line to Baton Rouge Office (mo/d/yr)	First Recorded on Magnetic Tape (mo/d/yr)
BCH 680 Hz	Beach	29°40'38"	92°53'19"	10.67 m	6/24/81	7/9/81	7/20/81
LEV 1020 Hz	Levee	29°42'43"	92°52'54"	15.24 m	6/25/81	7/9/81	7/20/81
SHR 1360 Hz	Sohio Rd.	29°42'25"	92°50'31"	15.24 m	6/25/81	7/9/81	7/20/81
PLR 1700 Hz	Price Lake Rd.	29°41'14"	92°50'00"	15.24 m	6/25/81	7/9/81	8/22/81
ALP 2040 Hz	Alligator Ponds	29°43'13"	92°48'32"	15.24 m	6/26/81	7/9/81	7/20/81
GCS 2380 Hz	Grand Chenier School Property	29°44'05.3"	92°53'54"	15.24 m	1/25/82	5/24/82	5/24/82
WRD 2720 Hz	Well Road	29°43'52.42"	92°52'19.43"	15.24 m	1/26/82	5/22/82	5/22/82
HQS 3060 HZ	Equipment Shed	29°44'31"	92°52'27"	10.67 m	6/23/81	7/9/81	7/20/81

seismometer and a standard amplifier/VCO unit and power supply. The sensors, Mark Products L28LB 4.5 Hertz seismometers, were installed in boreholes ranging from 11 to 15 m below the ground's surface. Data collected at each field station are telemetered by high-frequency radio transmission to an equipment shed at the well site. From the equipment shed, data are multiplexed and transmitted over telephone lines to a central recording facility in Woodward-Clyde Consultants' office in Baton Rouge, Louisiana.

Seismic Monitoring and Seismicity October 1982 through September 1983

The characteristics of microearthquakes recorded by the seismic network at Gladys McCall, the procedure used to locate them, and the method used to determine their magnitudes are all similar to those at Sweet Lake. Only very limited flow testing has taken place at Gladys McCall. The observed seismicity can therefore be considered as normal background activity.

Seismic Monitoring and Seismicity

During this reporting period, 57 small events, believed to be of natural origin, were detected by the Rockefeller Refuge Seismic Monitoring Network (RRSMN) (Table 13). Of these small events, only 12 locations were of high enough quality to give their locations any validity. Of the 12, only 7 were located within the boundaries of our location map (Fig. 33, Table 13). Spatial distribution of seismicity is fairly dispersed. No limitations or migration of activity with time is apparent. Spatial distribution of all earthquakes does not show any clear relation to the locations of growth faults inferred in the area of brine production.

Discussion

As with the Sweet Lake events, analysis of recorded activity indicates that a relationship between events and weather-related phenomena, such as

TABLE 13. Rockefeller Wildlife Refuge
(five or more stations reporting).

	YEAR	JULIAN DAY	LATITUDE	LONGITUDE	ERROR RMS	NO. OF STATIONS REPORTING
1	1983	006	30.3594	92.5270	0	5
2	1983	012	29.5528	93.1041	0	5
3	1983	012	29.4342	93.1920	0	5
4	1983	012	30.0463	92.8922	0	5
5	1983	017	30.2492	92.5804	0	5
6	1983	039	29.5697	93.0354	0	5
7	1983	040	29.7009	92.9201	0	7
8	1983	040	29.7464	92.9107	0	5
9	1983	040	29.6525	92.8631	0	6
10	1983	040	29.7152	92.8728	0	5
11	1983	041	29.8690	92.7405	0	5
12	1983	041	29.9559	93.1441	0	5
13	1983	041	30.0657	92.4507	0	6
14	1983	046	29.5783	93.1088	0	6
15	1983	046	29.6310	92.9357	0	6
16	1983	060	30.2448	92.5964	0.343	5
17	1983	061	29.5851	93.2898	0.101	5
18	1983	064	29.5937	93.0642	0.797	6
19	1983	064	29.6358	92.9977	0.564	5
20	1983	064	29.6983	92.8690	0.250	5
21	1983	068	29.6437	93.2074	0.041	5
22	1983	069	30.1998	92.6230	0.231	5
23	1983	074	29.5462	93.1552	0.120	6
24	1983	075	29.4226	93.3435	0.384	5
25	1983	081	29.7327	92.8571	0.102	6
26	1983	081	29.3420	93.7104	0.702	6
27	1983	082	29.7227	92.8897	0.051	5
28	1983	082	29.7320	92.8491	0.188	6
29	1983	086	29.4427	93.0939	0.094	6
30	1983	089	29.5312	92.6875	0.072	6
31	1983	089	29.5081	92.9258	0.080	5
32	1983	089	29.6639	92.9456	0.215	6
33	1983	089	29.6112	92.9425	0.098	7
34	1983	089	29.6187	92.9334	0.134	6
35	1983	089	29.6341	92.9327	0.165	5
36	1983	089	29.6302	92.9117	0.151	7
37	1983	089	29.7261	92.7182	0.031	6
38	1983	089	29.7149	92.7758	0.593	6
39	1983	089	29.6375	92.8860	0.136	5
40	1983	089	29.6964	92.8512	4.033	6
41	1983	089	29.6681	92.8739	0.107	6
42	1983	089	29.6689	92.8646	0.123	7
43	1983	089	29.6950	92.8227	0.833	5
44	1983	089	29.6848	92.8163	0.125	7
45	1983	089	29.7184	92.7831	0.120	6
46	1983	089	29.6950	92.8456	0.059	5

TABLE 13, cont.

	YEAR	JULIAN DAY	LATITUDE	LONGITUDE	ERROR RMS	NO. OF STATIONS REPORTING
47	1983	099	29.5893	93.0942	0.106	6
48	1983	101	29.7603	92.8455	0.130	5
49	1983	130	29.7046	92.8537	0.054	5
50	1983	147	29.6959	92.9325	0.126	5
51	1983	147	29.6914	92.9368	0.080	6
52	1983	169	29.6487	92.8545	5.450	5
53	1983	169	29.7869	92.8716	0.216	5
54	1983	177	29.6593	92.8320	0.086	5
55	1983	249	29.6766	92.8698	0.554	6
56	1983	250	29.7313	92.8173	0.667	5
57	1983	254	30.2357	92.3921	0.502	5

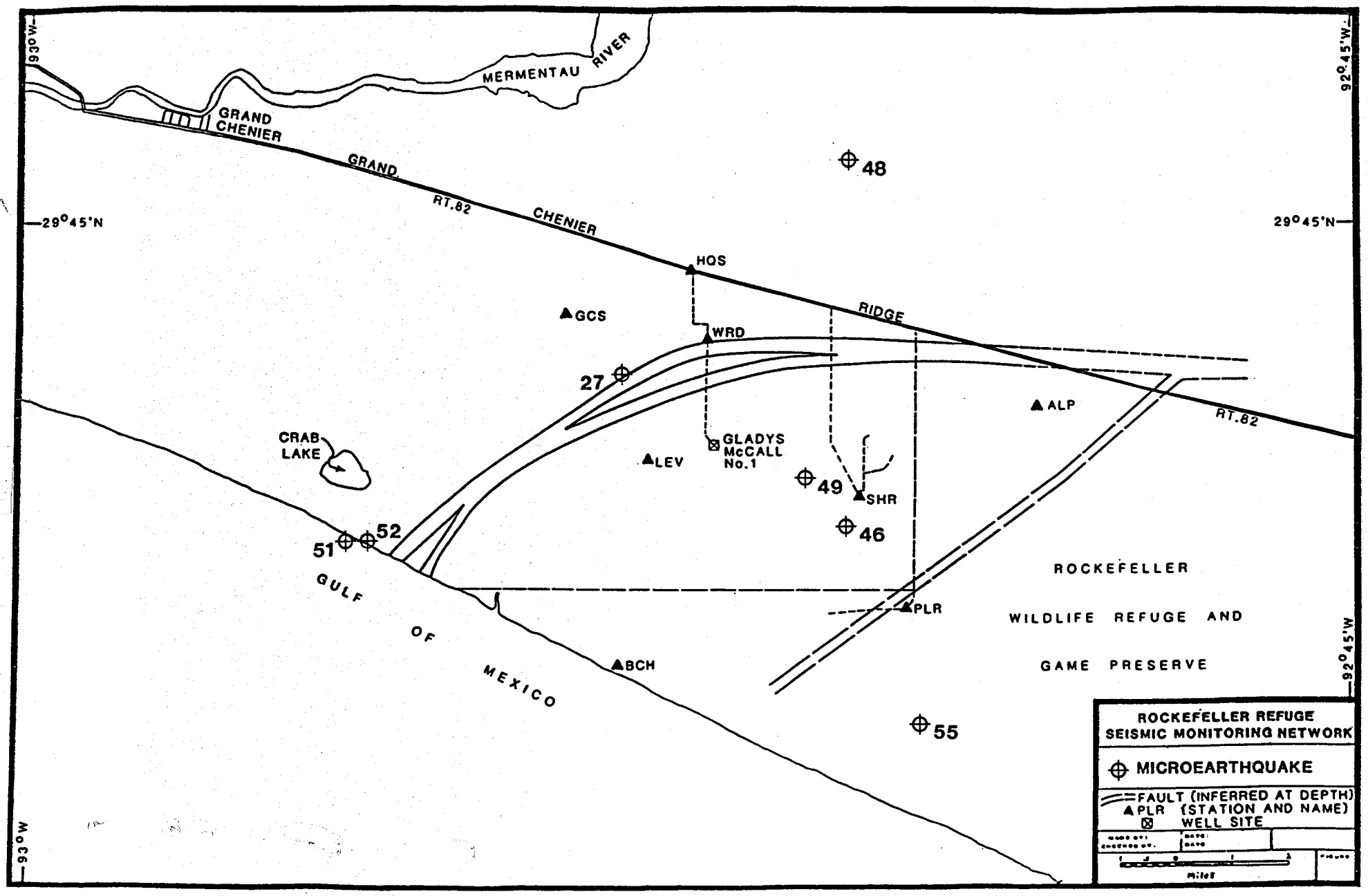

FIGURE 33. Location of microearthquakes within Rockefeller Refuge map boundaries.

rainfall, lightning, and thunder, cannot be ruled out. Figure 34 is a plot of rainfall versus seismic activity for the period 1 January 1982 to 1 October 1983. Although not as strong as that at Sweet Lake, a good correlation exists between rainfall and seismic activity.

As there was negligible production during the reporting period, no data correlating testing and seismic activity are available.

Conclusions

After three years of microseismic monitoring, our contractors have presented us with locations for more than 1000 microseismic events. For this report, we have used only the best quality event locations, thereby dropping the total considerably. By using the highest quality events, it was hoped that a true indication of seismicity could be observed. Through the course of data analysis, two problems have been encountered and are currently being studied. The first is that almost all of the located events are of the impulsive Rayleigh wave type. It must be pointed out that regardless of the quality of location as given by the computer program, locations using only Rayleigh wave arrivals are not as reliable as those using body waves. Furthermore, the depths for the locations are extremely questionable. It is because of this that attributing events to particular inferred growth fault locations at depth is impossible. We are currently working on methods of arriving at more reliable event locations and depths.

The second problem is that coincident rainfall and seismic activity have been observed at all three wells. At this time, it is unclear whether these slow-moving (290-350 m/s), impulsive Rayleigh wave events can be attributed to meteorological disturbances or indeed are of earth origin. Unfortunately, this slow velocity range is also occupied by acoustical transmissions through the air, and significant coupling of atmospheric acoustic and earth Rayleigh waves is highly probable. If, in fact, most of the observed signals are of earth

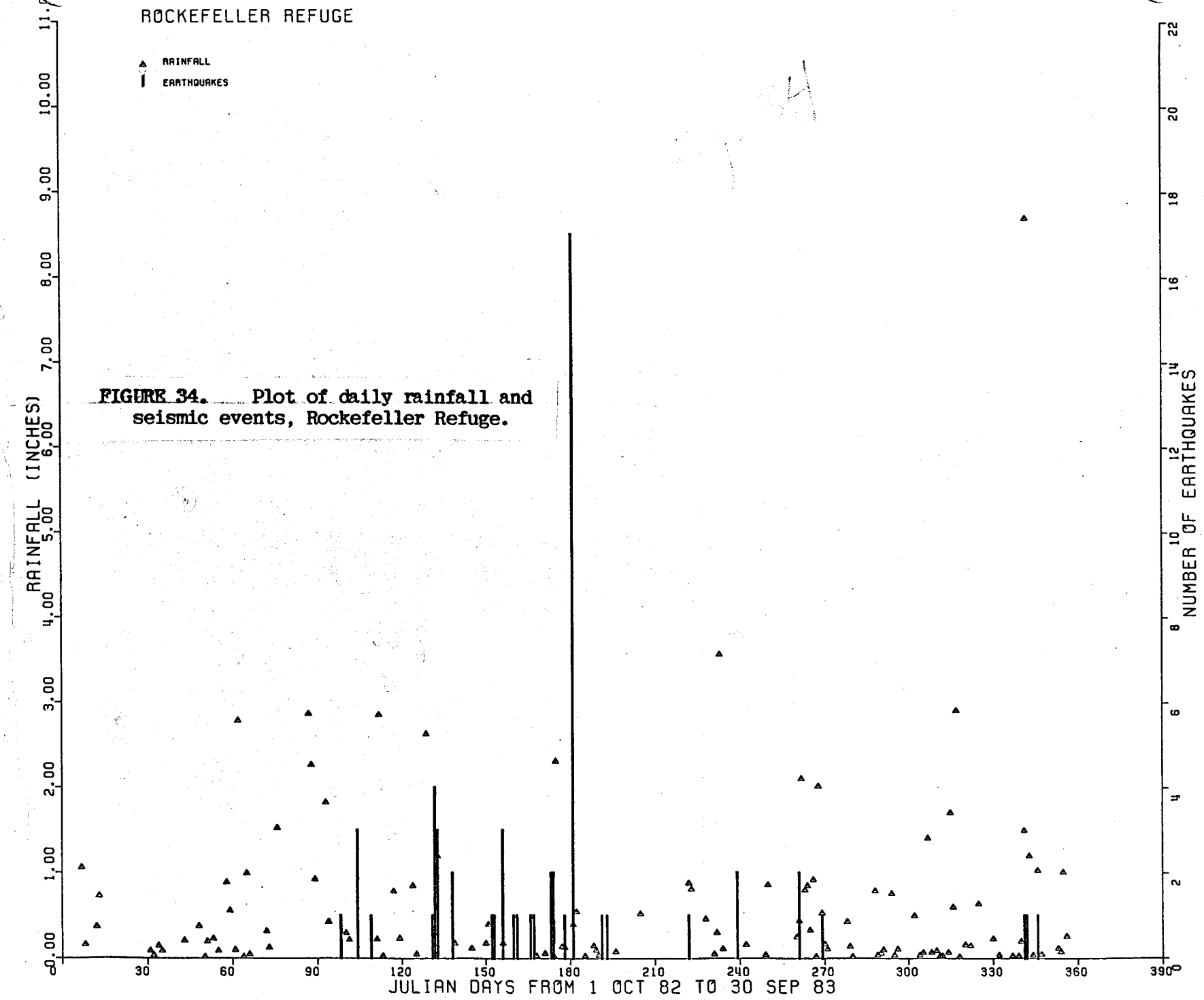

FIGURE 34. Plot of daily rainfall and seismic events, Rockefeller Refuge.

origin, it is extremely difficult to separate them from atmospheric acoustic events, such as thunderstorm activity, associated with times of rainfall and frontal passage.

After five months of flow testing at Parcperdue and seven additional months of seismic monitoring after well shut-in, it is still unclear whether brine production and disposal initiated any increase in seismic activity. There was indeed an increase in activity during the testing program with some 12 Rayleigh wave events and 1 body wave event recorded. However, in March 1983, three months after the last test, there was a spurt of 34 microseismic events located within the Parcperdue network. Another sequence of 17 events occurred in May and June 1983. What this postproduction activity means after shut-in is not clear. With only three years of data, it is impossible to say what the true background levels of activity are at Parcperdue over the long term.

At Sweet Lake, flow testing lasted seven months. During that time and for more than 1-1/2 years after the last flow test, seismic monitoring has shown no creditable correlation with flow testing. All activity seems to be at intermittent intervals throughout the three years. In the future, we hope to see longer terms and higher volumes of flow testing which will give us a true indication of coproduction seismicity.

References

Herrmann, R. B., 1979, FASTHYPO—A Fortran program for simple hypocenter determination: Earthquake Notes, vol. 50, no. 2.

REPORT DISTRIBUTION

Department of Energy
Nevada Operations Office
Attn: Robert D. Clarke (3 copies)
Energy Applications Division
P.O. Box 14100
Las Vegas, NV 89114

Department of Energy
Division of Geothermal Energy
Attn: D. B. Lombard (2 copies)
(CE-324/SG-064 FORSTL)
Washington, D.C. 20466

Department of Energy
Nevada Operations Office
Attn: Dorothy Nowack (2 copies)
for the NV Technical Library
P.O. Box 14100
Las Vegas, NV 89114

Technical Information Center
Document Control Branch (2 copies)
P.O. Box 62
Oak Ridge, TN 37830

R. D. Roop
Oak Ridge National Laboratory (1 copy)
Building 2001
Oak Ridge, TN 37830

APPENDIX A

REGIONAL AND LOCAL SUBSIDENCE IN LOUISIANA

TRAHAN, Drukell B.*

Abstract

Causes of subsidence in Louisiana range from local, man-induced events to regional, large-scale processes. The measurement of local, man-induced subsidence is especially critical in areas with high rates of land loss. To measure this subsidence, absolute historical geodetic movements have been estimated by adjusting all movements along the first-order vertical control network from northeast to southwest Louisiana as related to the Monroe uplift. The adjustment will serve as a base line by which local subsidence or uplift can be measured.

A generalized trend of increasing subsidence to the south in Louisiana probably reflects increasing sediment thickness and weight toward the axis of the Gulf Coast basin. Anomalous values as low as -17.6 mm/yr (-0.7 in./yr) occur in areas overlying Pleistocene and Holocene fluvial elements. Positive movement as high as +4.1 mm/yr (+0.2 in./yr), has been found to be associated with the Iberian structural axis in south-central Louisiana.

Land subsidence due to natural causes may far outweigh subsidence resulting from fluid withdrawal or depressurization of geopressured aquifers. The effects of regional and local natural processes should not be underestimated in any systematic approach to measuring subsidence.

---

*Louisiana Geological Survey, Box G, University Station, Baton Rouge, Louisiana 70893

Introduction

The U.S. Department of Energy is presently testing geopressured-geothermal energy reserves in southwestern Louisiana. The reserves are in areas where sandstones are enclosed between the shales of downthrown fault blocks in major depocenters. In these sandstone reservoirs, fluid pressure and temperature are high, a result of the encapsulation of pore waters under a heavy overburden. During the development of these reservoirs, hydraulic energy—up to 13,000 psia—is released. The resulting reduction in pressure may cause dewatering and compaction of the surrounding shales and subsidence at the land surface (Gustavson and Kreitler, 1976, p. 20).

Depressurization of deep geopressured aquifers is one of a host of factors which could cause subsidence of the land surface. Ground-water withdrawal and marsh reclamation by drainage are other potential causes. The effect of these local activities on the land surface may be determined by comparing historical subsidence rates. In addition, natural causes of subsidence must be ascertained and an attempt made to determine absolute movement.

Subsidence is widespread in south Louisiana. Besides the effect of deep crustal movement and surface compaction due to dewatering of marshy soils, the shales of the Gulf Coast basin are highly susceptible to compaction resulting from dewatering and compression. Subsidence is a critical concern in coastal areas already at or below sea level, where current rates of land loss are estimated to be 129 km^2/yr (50 mi^2/yr). Problems caused by subsidence are high rates of land loss, increased urban flooding, building foundation failures, and ecosystem imbalances.

Preliminary base-line subsidence monitoring in the areas of geopressured-geothermal energy development involved the adjustment of local lines of historical first-order leveling (Trahan, 1982). In each case, the data were referenced to a benchmark common to all epochs of leveling by numerically maintaining the common benchmark at a fixed elevation. The depicted relative movements are true, but misleading. The reference benchmarks, assumed to be steady for the purpose of determining relative motion, are probably subsiding, therefore introducing an error factor in the data presented by Trahan (1982). Most of the south Louisiana coastal plain is subsiding at some rate. Rates ranging from -0.5 to -4.3 cm/yr (-0.2 to -1.7 in./yr) were suggested by Swanson and Thurlow (1973, p. 2760). Holdahl and Morrison (1974, p. 381) calculated a range from -0.03 to greater than -0.05 cm/yr (-0.01 to -0.02 in./yr) for the coastal plain in south Louisiana. In both studies, the data were adjusted regionally, with assumptions based on sea level rise, and thus do not provide the scale necessary to monitor local subsidence.

Man-induced effects, such as depressurization of deep geopressured aquifers, will result in local subsidence over relatively small areas. The purpose of this study was to establish a local base line by which these movements may be measured.

Methodology

The method described here involves the tie-in and adjustment of leveling lines in a region of unknown actual movement to those in a region where uplift has been measured. Schumm, Watson, and Burnett (1982) used geomorphic evidence to measure movement of the Monroe uplift in northeast Louisiana. Changes in stream channel characteristics and differences between actual and theoretical valley gradients indicate that uplift in the area has been increasing, from +0.4 to +1.4 mm/yr (+0.02 to +0.06 in./yr), for the last 3500 years. Other investigators have also found evidence for continued activity of the Monroe uplift. The most recent movements are believed to have occurred at least during the Miocene (Fisk, 1939; Spooner, 1935). The uplift was a compensatory effect resulting from the deposition of thick deltaic masses in the Gulf Coast basin to the south (Spooner, 1935, p. 130). It is unlikely that this isostatic relationship ceased to exist into the Quaternary Period. The effects of continental glaciation and the continued, although cyclic, deltaic progradation in the Gulf Coast could only have served to continue uplift to the north.

A description of this relationship can be provided through an analysis of rates of vertical motion from north to south through Louisiana. Current mapping involves the first-order leveling network from northeastern Louisiana to southwestern Louisiana (Fig. 1), which has been adjusted to movement associated with the Monroe uplift. Where possible, loop closure adjustments (LCA) were made for all epochs of leveling along the network. Where closure errors existed, the loops were closed mathematically by averaging the elevations at the junction point and distributing the resulting difference around the loop. Loop spurs were adjusted by correcting benchmark heights along the spur for the elevation difference at the spur-loop junction. Interpolations were made, when necessary, at junctions of lines where years of leveling did not coincide; the relative rate of movement for the common benchmark served as the adjustment. Relative movements were plotted and adjusted to account for uplift ranging from +0.4 to +1.4 mm/yr (+0.02 to +0.06 in./yr) at Winnsboro, Louisiana, which is located on the southern flank of the Monroe uplift. The resulting profiles show changes in elevation between epochs and show the adjusted topographic expression of the land surface (Figs. 2-7). Geomorphic and structural elements were included in the profiles for reference and correlation.

Profiles

Winnsboro to Alexandria, Louisiana

This survey line extends from Winnsboro through Jonesville to the south and then continues in a southwesterly direction to Alexandria, Louisiana (Fig. 2). The benchmark at Winnsboro is the reference point for all movements depicted in this study. In the adjusted profile for the period 1934 to 1966, uplift increases to a point above the position of the Foules salt dome. To the south, uplift decreases where the survey line crosses the Tensas River-Little River-Catahoula Lake drainage system. West of this feature is a section of uplift which corresponds

to the structural position of the La Salle arch. Still farther to the west towards Alexandria, subsidence tends to dominate the profile and is greatest at a position within the Red River valley.

Monroe to Iowa, Louisiana

This survey line parallels the Ouachita River valley from Monroe to a point approximately 42 km (26 mi) south of Monroe (Fig. 3). The survey line then turns to the southwest away from the valley. The movement profile effectively parallels the topographic profile for some distance, depicting greater subsidence across the Little and Red River valleys and less subsidence in the uplands between the valleys. From the south valley wall of the Red River to Iowa, subsidence increases, corresponding presumably to thickening sediments of the Gulf Coast basin. A spike in the movement profile 4 km (2.5 mi) north of Iowa may be associated with the structure of the Woodlawn salt dome.

Orange, Texas, to Baldwin, Louisiana

Subsidence is depicted along the major portion of this profile from Orange, Texas, to Lafayette, Louisiana, for the period 1965-82 (Fig. 4). The greatest subsidence is in the shape of a trough along a segment of the line between the Mermentau and Vermilion rivers. The Mermentau River is about 65 km (40 mi) west of the Vermilion River, which flows through Lafayette. The line turns at Lafayette to the southeast and follows the Iberian structural axis (Barton, 1933) parallel to the Five Islands salt dome trend. Uplift is dominant along this segment of the line.

Sulphur to Holly Beach, Louisiana

Major subsidence, which is evident between Sulphur and Holly Beach, is greatest 4 km (2.5 mi) south of Sulphur (Fig. 5). This survey line crosses the contact between the Pleistocene Prairie Terrace and the Holocene coastal marshland at a point where subsidence is decreasing. This point occurs approximately 5 km (3 mi) south of the subsidence maximum. Subsidence is minimal from the Hackberry salt dome to a point 11 km (7 mi) north of Holly Beach, where the profile again deflects downward. Subsidence is indicated for the segment of the profile 12 km (7.5 mi) north of Holly Beach.

Iowa to Creole, Louisiana

The survey line from Iowa to Creole (Fig. 6) is about 32 km (20 mi) to the east of and parallel to the preceding transect (Fig. 5). The profiles are similar. Maximum and minimum rates of subsidence are at approximately the same geomorphic positions; correlations between movement extremes, however, are better. The position of the Sweet Lake salt dome and the Prairie Terrace-coastal marshland boundary both coincide with the point where the rate of subsidence is lowest.

Holly Beach, Louisiana, to Rockefeller Refuge

In general, subsidence decreases along this line from Holly Beach on the west eastward to Rockefeller Refuge (Fig. 7). Anomalous rates of subsidence occur in areas next to the Calcasieu and Mermentau River valleys, with the greatest amount of subsidence occurring in the Mermentau River valley.

Discussion

This report presents what is believed to be a best estimate for absolute geodetic movements in Louisiana. Holdahl and Morrison (1974, p. 378) based their regional analysis on a sea level rise of 1 mm/yr (0.04 in./yr). With the adjustment of all movements to the quantified movement of the Monroe uplift, assumptions based on recent sea level rise have presumably been circumvented. The profiles illustrate a general trend of increasing negative movement from northeast to southwest Louisiana. Except for the area southeast of Lafayette, these movements range from +2.3 mm/yr (+0.1 in./yr) south of Winnsboro to -17.6 mm/yr (-0.7 in./yr) south of Iowa. These extremes, however, are not normal; rather, they occur as anomalous values related to the positions of structural and geomorphic elements. If the average rate of uplift and subsidence along each line is used, the range can be generalized from +1.2 mm/yr (+0.05 in./yr) near the Monroe uplift to -6.7 mm/yr (-0.3 in./yr) in the coastal area of southwestern Louisiana. Uplift associated with the Iberian structural axis is as great as +4.1 mm/yr (+0.2 in./yr) and averages +2.8 mm/yr (+0.1 in./yr).

The depicted movements correlate with recent geomorphic elements. The thickest recent sediments, such as those found in recent alluvial valleys (Figs. 3 and 7), are susceptible to dewatering and compaction. Movements related to deeper structural elements are, for the most part, overshadowed by movements related to recent geomorphic features. The anomalous trough of subsidence depicted in Figure 4 correlates well with an area of Pleistocene Red River alluviation (Varvaro, 1957, p. 23, pl. 2). Where strong correlations exist between the movement profiles and major structural elements, recent activity of these structural elements may be substantiated (for example, the Iberian structural axis southeast of Lafayette, Fig. 4). However, some profiles exhibit negative correlations, which may also be a product of structural movement (Figs. 5-6). Greater subsidence would be expected south of the Prairie Terrace-coastal marshland boundary. The absence of pronounced subsidence here may be a result of continuing water saturation of sediments, since this land surface is at or below sea level in most places. Sediment dewatering may have been curtailed, or subsidence to the north may be an anomalous response to the compaction of a buried Pleistocene Red River fluvial system. On the other hand, natural subsidence may have been counteracted by movement associated with the Hackberry-Sweet Lake salt ridge.

The National Geodetic Survey, in its leveling work, uses several methods to correct elevations observed in the field (Balazs and Young, 1982). Random errors caused by instrument variations or human

inconsistencies have presumably been reduced by loop closure adjustments. Other corrections are based on natural orthometric and gravimetric variations. These are theoretically constant for each benchmark independent of time. When the change in elevation for a benchmark is documented, these variations are presumably eliminated (Balazs, 1983, personal commun.).

Other assumptions must be made when adjusting lines of leveling to determine movement. The reliance in this study on positive and measurable movement of the Monroe uplift has already been discussed. Furthermore, it has been assumed, in connecting lines and making adjustments, that relative movements during the last half-century have been incremental.

Summary

The coastal area of Louisiana is rapidly disappearing. Before the effects of geopressured-geothermal development or other causes of subsidence can be ascertained, ideally a base line of absolute historical and natural effects must be determined. Indications in this study are that natural effects in Louisiana are not to be underestimated and may far outweigh any man-induced effects.

The increase in negative movement rates to the south is believed to be related to the thickening of sediments in the Gulf Coast basin. The relationship may be a reflection of greater dewatering in the thicker sediments or isostatic adjustments resulting from loads and stresses placed on the basement by the weight of the sediment pile. Anomalies in the general trend are correlated with more recent geomorphic and structural elements. Pleistocene and Holocene fluvial deposits and salt domes contribute substantially to crustal motion in Louisiana.

This estimate of absolute geodetic movements in Louisiana is consistent with the range of movement suggested by Holdahl and Morrison (1974). Higher subsidence values are a result of local anomalies which were not detected in their regional evaluation.

Future work should include an expansion of this base line into other parts of the state and a tie-in to tide stations for further comparison. Consolidation of the vertical control network in selected areas with high rates of land loss will also aid in the understanding of local subsidence.

Acknowledgments

This work was sponsored in its entirety by the U.S. Department of Energy under contract number DE-AC08-81NV10174. I wish to express formal gratitude to the National Geodetic Survey in Rockville, Maryland, for its valuable assistance in acquiring survey data and continued support. Additional thanks go to the cartographic and editorial staffs of the Louisiana Geological Survey and to all the other professionals who have offered their input during various phases of the study. Special

gratitude is owed to Anna Babin and Steve Bennett for helping to assimilate the vast amounts of geodetic data into a workable format.

References

Anderson, E. G., 1979, Basic Mesozoic study in Louisiana, the northern coastal region and the Gulf Basin province: La. Geol. Survey, Baton Rouge, La., Folio Series no. 3, vol. 1, 58 p.

Balazs, E. I., 1983, Personal commun.: National Geodetic Survey, Rockville, Md.

Balazs, E. I., and G. M. Young, 1982, Corrections applied by the National Geodetic Survey to precise leveling observations: U.S. Dept. Commerce, Nat. Oceanic and Atmospheric Admin., NOAA Tech. Memorandum NOS NGS 34, 12 p.

Barton, D. C., 1933, The Iberian structural axis: Jour. Geology, vol. 41, no. 3, p. 225-42.

Fisk, H. N., 1939, Jackson Eocene from borings at Greenville, Mississippi: Bull., Am. Assoc. Petr. Geol., vol. 23, no. 9, p. 1393-1403.

Gustavson, T. C., and C. W. Kreitler, 1976, Geothermal resources of the Texas Gulf Coast: Environmental concerns arising from the production and disposal of geothermal waters: Univ. Texas, Austin, Bur. Econ. Geology, Austin, Tex., Geol. Circ. 76-7, 35 p.

Holdahl, S. R., and N. L. Morrison, 1974, Regional investigations of vertical crustal movements in the U.S., using precise relevelings and mareograph data, in R. Green, ed., Recent crustal movements and associated seismic and volcanic activity: Tectonophysics, vol. 23, p. 373-90.

Schumm, S. A., C. C. Watson, and A. W. Burnett, 1982, Investigation of neotectonic activity within the Lower Mississippi Valley Division: U.S. Corps of Engineers, contract no. DACW38-80-C-0096, 158 p.

Stanfield, C. P., 1976, A list of Louisiana oil and gas fields and salt domes including the offshore areas showing code numbers and abbreviations: La. Geol. Survey, Baton Rouge, La., Resources Inf. Series no. 1, 137 p.

Spooner, W. C., 1935, Oil and gas geology of the Gulf Coastal Plain of Arkansas: Ark. Geol. Survey, Little Rock, Ark., Bull. no. 2, p. 125-39.

Swanson, R. L., and C. I. Thurlow, 1973, Recent subsidence rates along the Texas and Louisiana coasts as determined from tide measurements: Jour. Geophysical Research, vol. 78, no. 15, p. 2665-71.

Trahan, D. B., 1982, Monitoring local subsidence in areas of potential geopressured fluid withdrawal, southwestern Louisiana: Trans., Gulf Coast Assoc. Geol. Socs., vol. 32, p. 231-36.

Varvaro, G. G., 1957, Geology of Evangeline and St. Landry parishes: Dept. Conservation, La. Geol. Survey, Baton Rouge, La., Geol. Bull. no. 31, p. 23, pl. 2.

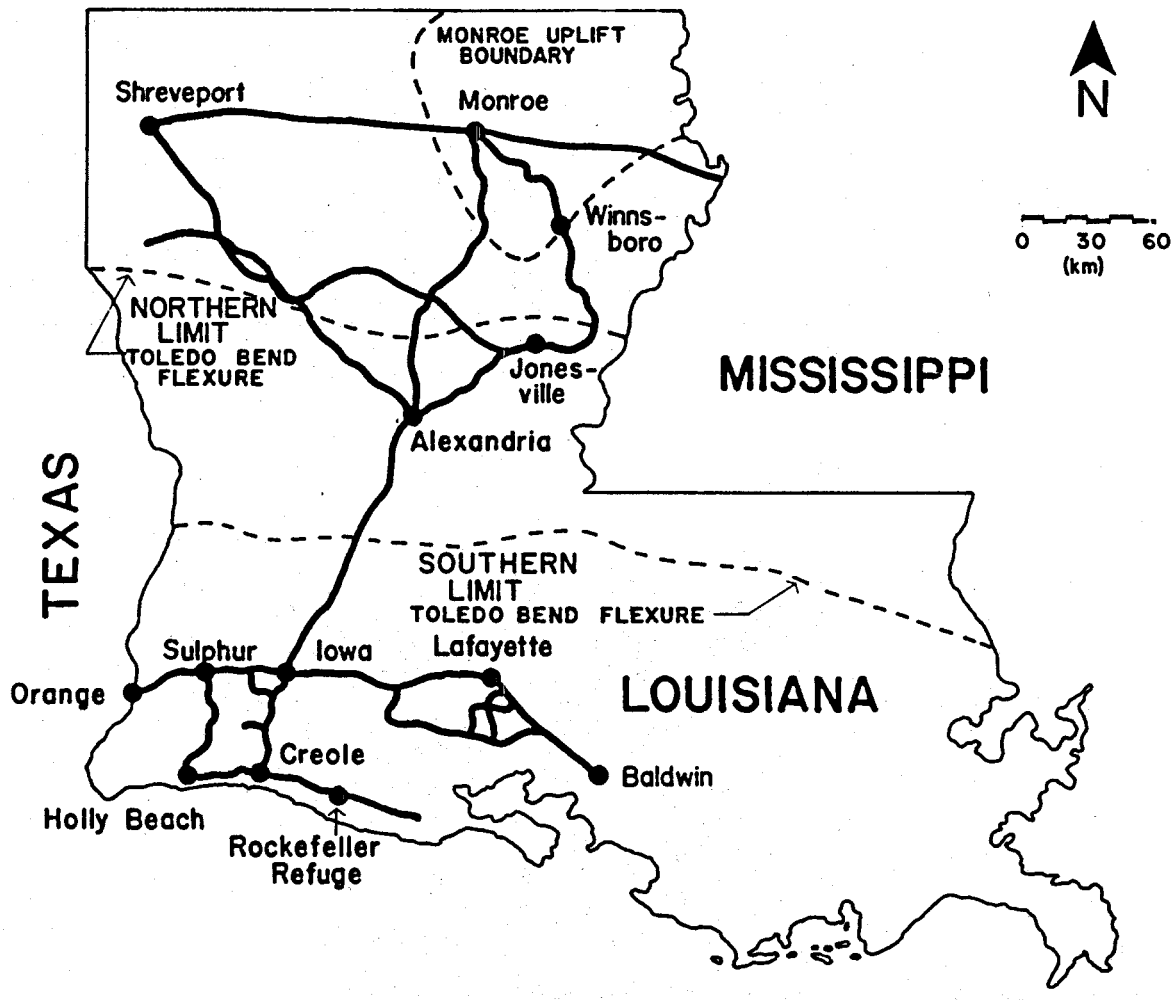

FIGURE 1. The Louisiana first-order leveling network showing positions of major junctions and the boundary of the Monroe uplift.

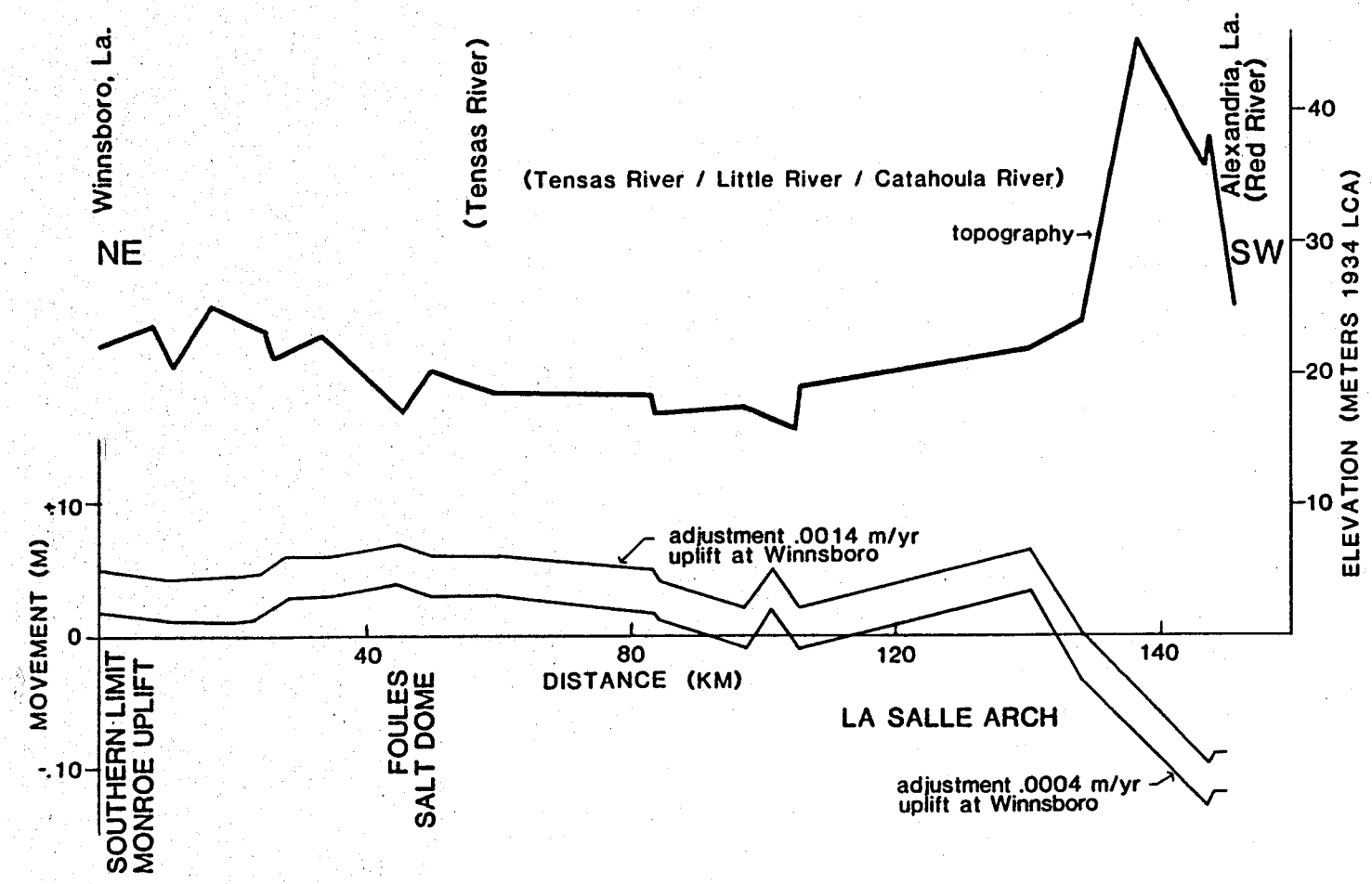

FIGURE 2. Total absolute change in elevation based on movement of the Monroe uplift, Winnsboro to Alexandria, Louisiana, 1934 to 1966. Geomorphic and structural features (Anderson, 1978; Schumm, Watson, and Burnett, 1982; Stanfield, 1976) indicated for reference and correlation.

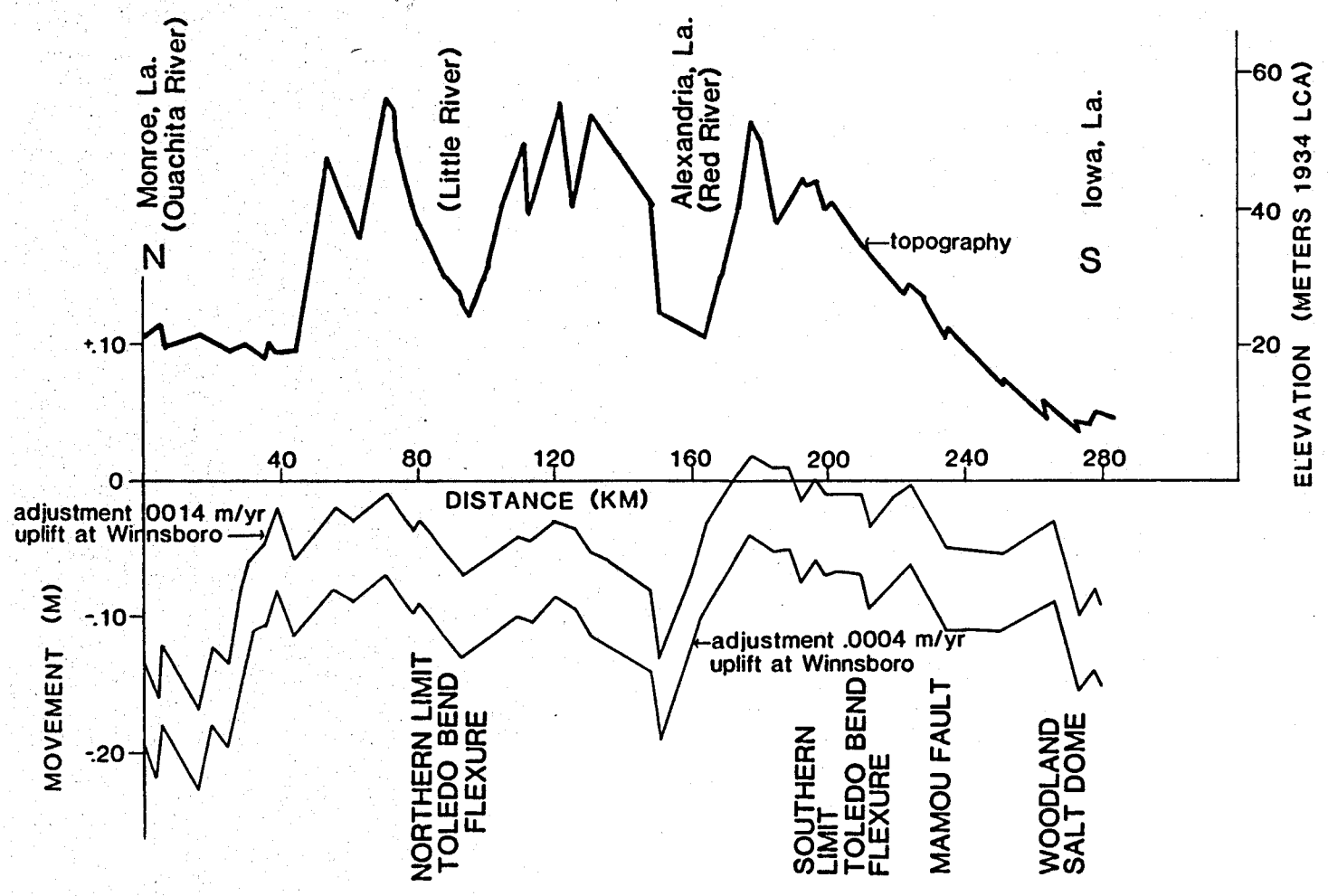

FIGURE 3. Total absolute change in elevation based on movement of the Monroe uplift, Monroe to Iowa, Louisiana, 1934 to 1966. Geomorphic and structural features (Anderson, 1979; Stanfield, 1976) indicated for reference and correlation.

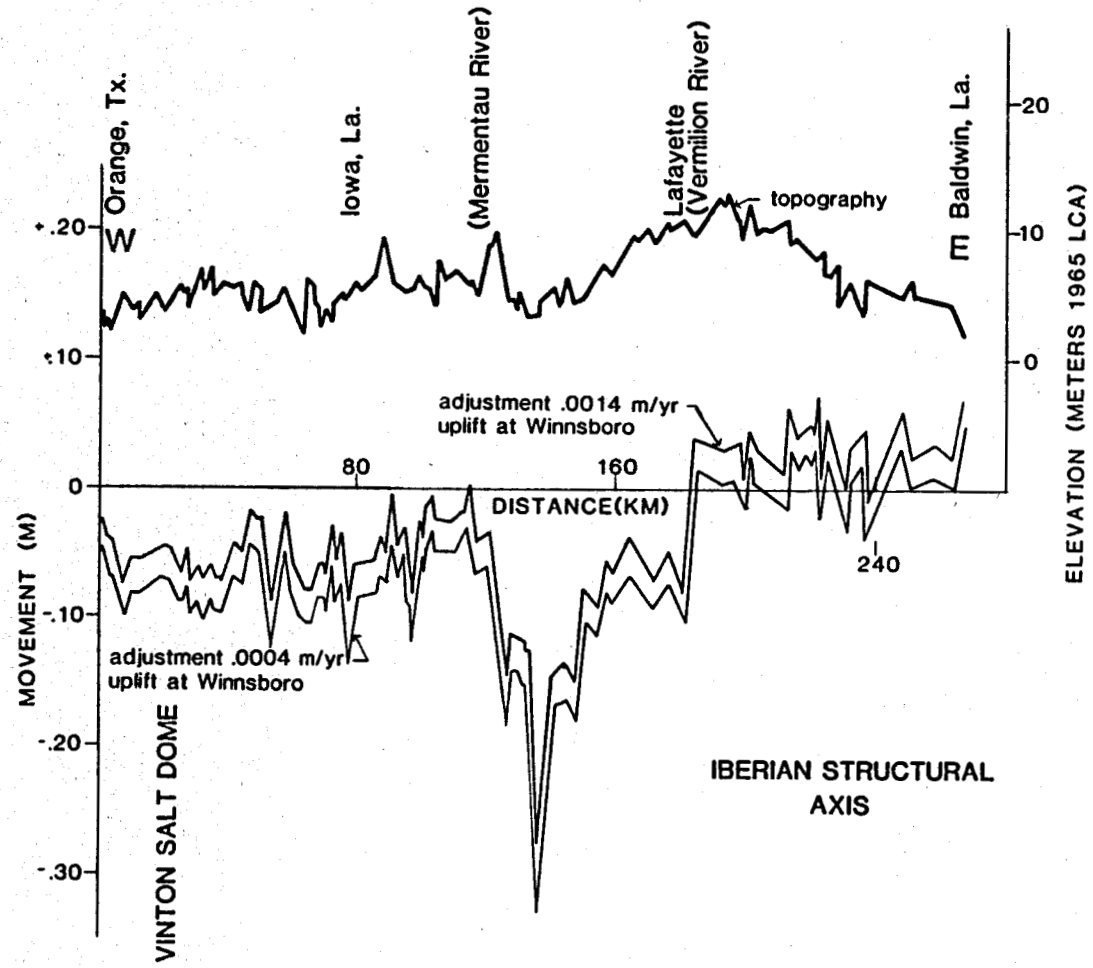

FIGURE 4. Total absolute change in elevation based on movement of the Monroe uplift, Orange, Texas, to Baldwin, Louisiana, 1965 to 1982. Geomorphic and structural features (Anderson, 1979; Stanfield, 1976) indicated for reference and correlation.

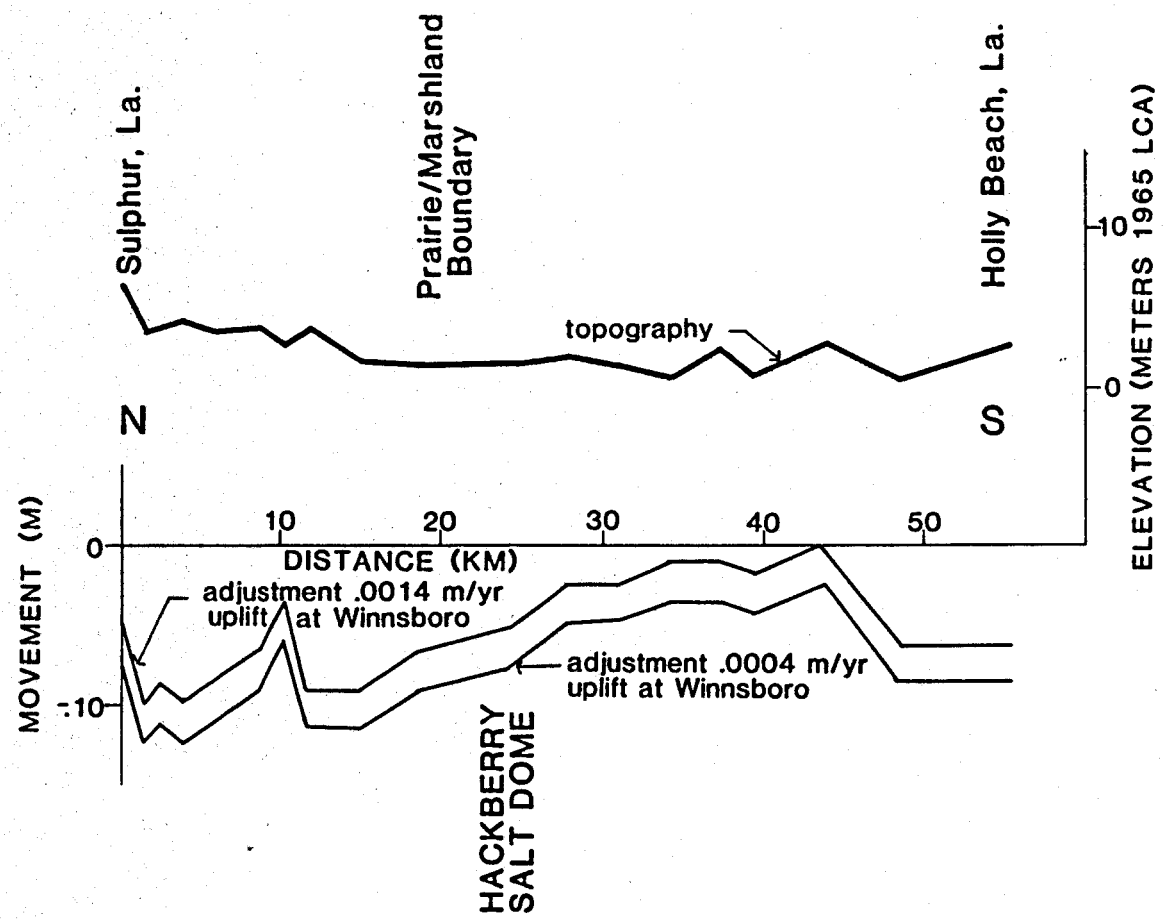

FIGURE 5. Total absolute change in elevation based on movement of the Monroe uplift, Sulphur to Holly Beach, Louisiana, 1965 to 1982. Geomorphic and structural features (Anderson, 1979; Stanfield, 1976) indicated for reference and correlation.

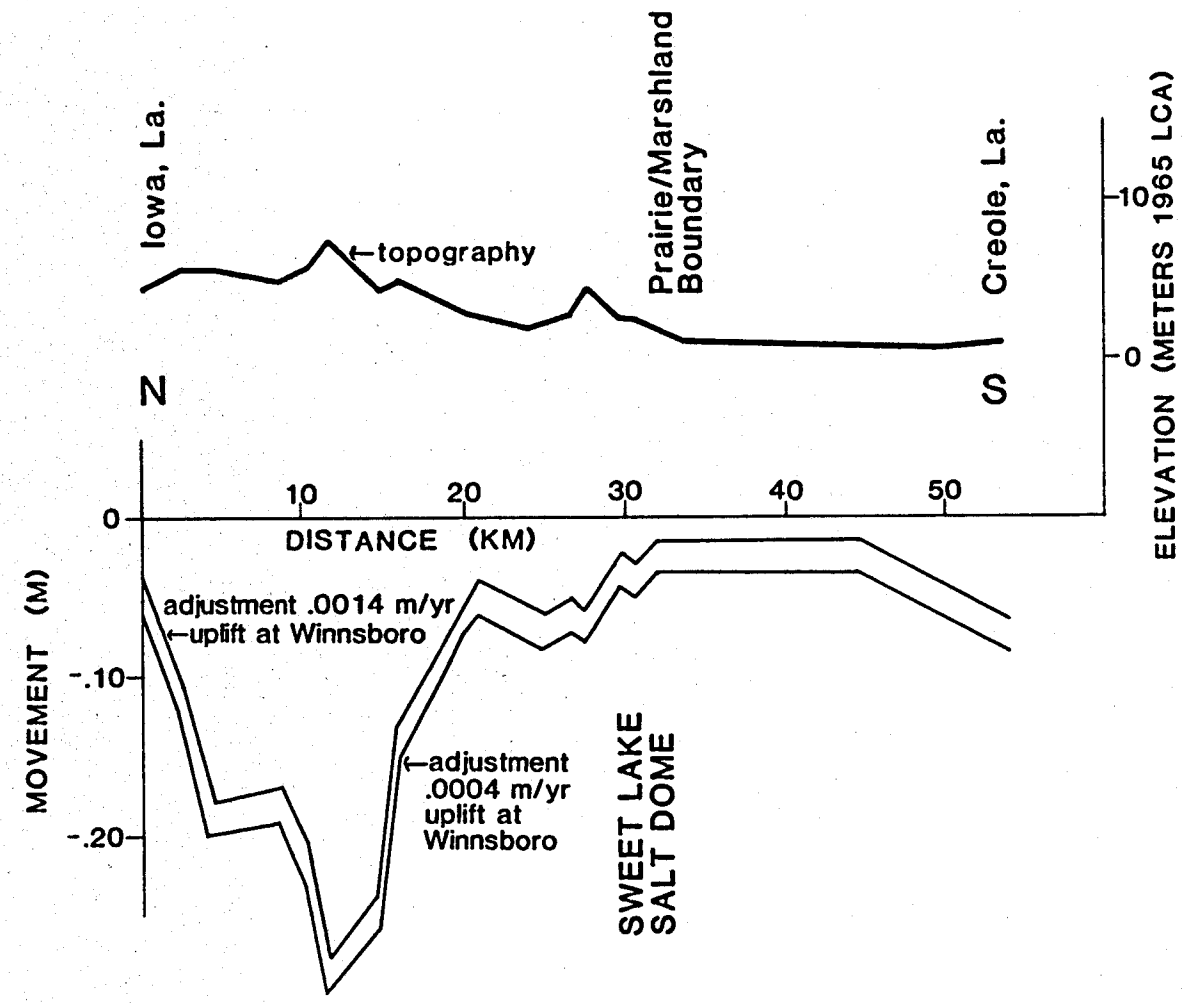

FIGURE 6. Total absolute change in elevation based on movement of the Monroe uplift, Iowa to Creole, Louisiana, 1965 to 1982. Geomorphic and structural features (Anderson, 1979; Stanfield, 1976) indicated for reference and correlation.

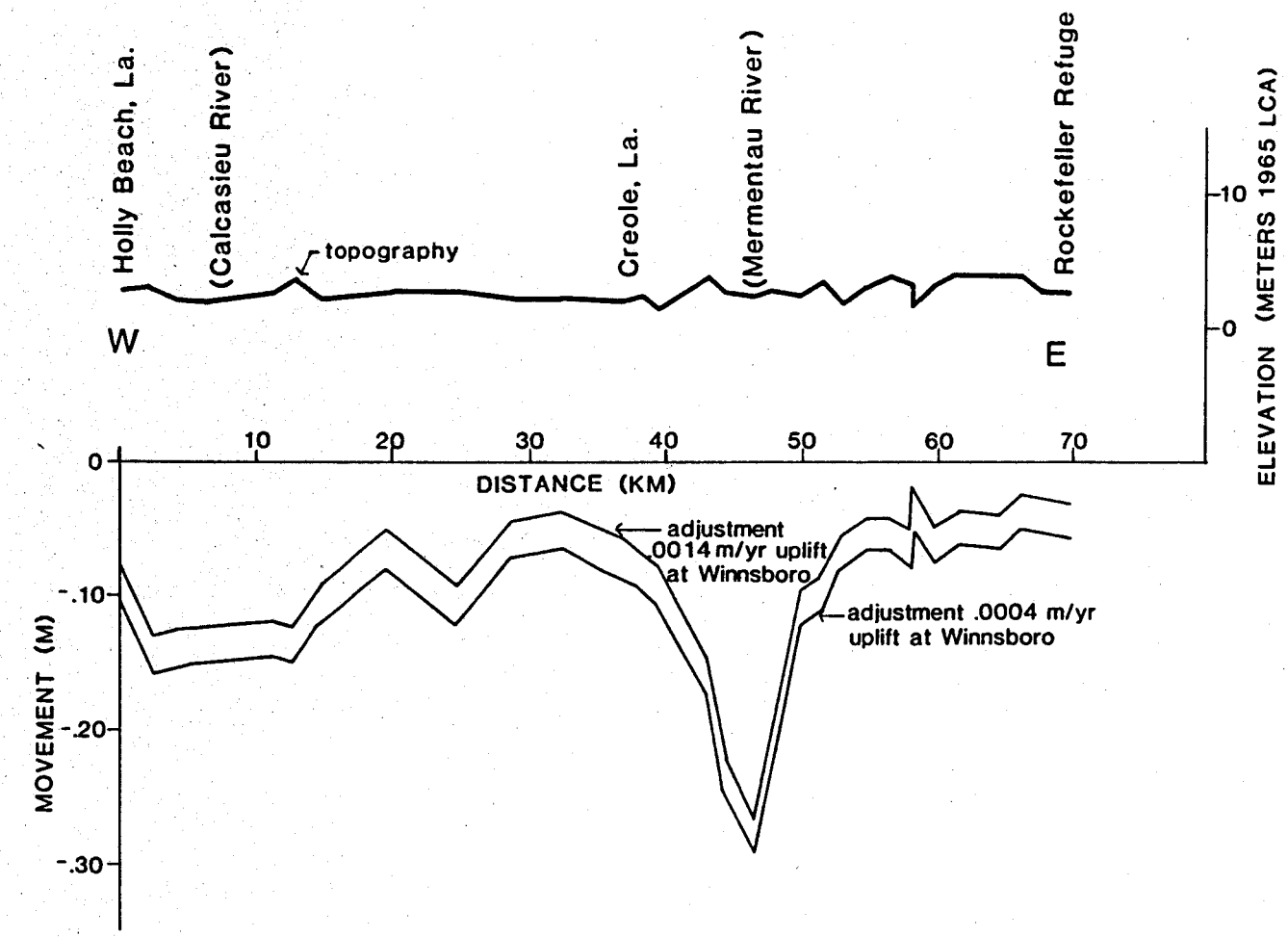

FIGURE 7. Total absolute change in elevation based on movement of the Monroe uplift, Holly Beach to Rockefeller Refuge, Louisiana, 1965 to 1982. Geomorphic features indicated for reference and correlation.

APPENDIX B

TECHNICAL REPORT NO. 84-2

MICROSEISMIC MONITORING OF BAYOU PARCPERDUE LOUISIANA: THE DOW L.R. SWEEZY NO. 1 GEOPRESSURED/GEOTHERMAL ENERGY TEST WELL PROGRAM

FINAL REPORT

Frederick J. Mauk
Billie Kimball
Robert Alan Davis

Prepared for

The Louisiana Geological Survey and the Louisiana
State University Department of Geology
Baton Rouge, Louisiana 70893

TELEDYNE GEOTECH
3401 Shiloh Road
Garland, Texas 75041

20 March 1984

380/1

CONTENTS

	Page
SUMMARY	1
INTRODUCTION	2
THE PARCPERDUE SEISMIC NETWORK, INSTRUMENTATION, DESIGN, AND SPECIFICATIONS	3
DATA ANALYSIS PROCEDURES	10
Body Wave Data	10
Surface Wave Data	11
Magnitude Determination	20
THE DOW L. R. SWEEZY NO. 1 TEST PROGRAM	23
DISCUSSION OF SEISMIC ACTIVITY NEAR THE L. R. SWEEZY SITE AUGUST 1980 - NOVEMBER 1983	31
REFERENCES	50
APPENDIX A - DISCUSSION OF OBSERVED ACTIVITY FOR OCTOBER AND NOVEMBER, 1983	

ILLUSTRATIONS

Figure		Page
1	Parcperdue, Louisiana seismic array	4
2	Block diagram of Parcperdue, Louisiana seismic array	5
3	Parcperdue velocity response	6
4	a. Spectral estimates of daytime background noise recorded at Parcperdue b. Spectral estimates of quiet (nighttime) background noise recorded at Parcperdue	7
5	Corner frequency versus seismic moment for central United States earthquakes (after Street, Hermann, and Nuttli, 1975)	9
6	Lithology, P-wave velocity and thermal profiles for Parcperdue, Louisiana, based on SP, sonic, dual induction, thermal and dipmeter logs of the DOW L. R. Sweezy No. 1 well	12
7	Rayleigh wave group velocity for six modes in Texas Gulf Coast sediments (after Ebeniro, Wilson and Dorman, 1982)	15
8	Velocities, density, and theoretical Rayaleigh wave amplitude-depth curves at 2.0 Hz, Apache, Oklahoma (after Douze, 1964)	16
9	a. Diagram illustrating transmission of an energetic ray across a velocity interface b. The propagation of a leaking mode from a trapping layer (V_2)	18
10	Velocity analysis of impulsive Rayleigh event 22 August 1982 at 18:52:28.7 UTC time	19
11	Microearthquake from the Lake Charles, Louisiana, area. OT = 19:40:46.1 UTC (CST + 5 hrs)	21
12	Cumulative brine and gas production from the DOW L. R. Sweezy No. 1 geopressured/geothermal test well from 26 April through 31 December 1982	25

ILLUSTRATIONS, Continued

Figure		Page
13	a. Production well withdrawal pressure histories at the Parcperdue geopressured/geothermal test site from 26 April through 31 August 1982	26
	b. Production well withdrawal pressure histories at the Parcperdue geopressured/geothermal test site from 30 August 82 through 31 December 82	27
14	Full stream flow rate versus time for the DOW L. R. Sweezy No. 1 geopressured/geothermal test well from 26 April through 31 December 1982	28
15	a. Disposal well injection history at the Parcperdue geopressured/geothermal test site from 26 April through 1 January 83	29
	b. Disposal well injection history at the Parcperdue geopressured/geothermal test site from 26 April through 1 January 83	30
16	Microearthquake 26 February 1982, 14:46:16.65 UTC (CST + 6 hrs) Magnitude M_D = 1.5, Depth = 1.55 km	40
17	Location of the microearthquake activity (presumed to be of natural origin) occurring in the vicinity of the Parcperdue array during the monitoring program	41
18	Rayleigh leaking mode event 23 March 1982 at 23:29:56.48 UTC, Velocity - 250 meters/second	42
19	Rayleigh leaking mode event 25 June 1982 at 21:04:52.08 UTC, Velocity - 330 meters/second	43
20	Rayleigh leaking mode event 17 August 1982 at 00:19:37.24 UTC, Velocity - 260 meters/second	44
21	Temporal distribution of seismic activity at Parcperdue for 1981 through 30 November 1983. Flow testing episodes at the L. R. Sweezy No. 1 are indicated	45
22	Correlation of microearthquake activity in the vicinity of the Parcperdue seismic monitoring array with soil moisture storage (1983 daily water budgets soil moisture storage 6" capacity from Louisiana Monthly Climate Review)	46
23	Distribution of seismicity at Parcperdue 1980 - 1983 and first-order releveling survey (1980 - 1968) along Route 339	47

APPENDIX ILLUSTRATIONS

Figure		Page
A1	Location of leaking mode events recorded during October 1983	A-3
A2	Rayleigh leaking mode event #8, 06:50:39.4 UTC 11 October 1983, Velocity = 100 meters/second	A-15
A3	Rayleigh/leaking mode event #9, 17:21:31.8 UTC 11 October 1983, Velocity = _____ meters/second	A-16
A4	Rayleigh/leaking mode event #21, 18:38:29.7 UTC 27 October 1983, Velocity = 125 meters/second	A-17
A5	Rayleigh/leaking mode event #23, 16:00:48.6 UTC 2 October 1983, Velocity = 200 meters/second	A-18

TABLES

Table		Page
1	Parcperdue Louisiana seismic array	3
2	a. Velocity structure for events inside the array b. Velocity structure for events outside the array	13
3	Descriptions of well test index arrows for figures 12 through 15	24
4	Summary of important seismic activity occurring near the Parcperdue monitoring array 1981-1983	32

APPENDIX TABLES

Table		Page
A1	Parcperdue data log for October and November 1983	A-6
A2	Parcperdue, Louisiana array log for October and November 1983	A-14

SUMMARY

Microseismic monitoring of the Bayou Parcperdue region around the L. R. Sweezy test well in Vermillion Parish, Louisiana, from 1980 through 1983 has resulted in the following observations.

1. Two dominant types of seismic events are observed, one with identifiable body phases, the other with only surface wave signatures. The latter event type is by far the more commonly observed signal.

2. The hypocenters of the microearthquakes located using body phases have depths apparently greater than 1.5 kilometers, but less than the production zone depth of the geopressured/geothermal test well. The epicenters of these events are spatially coincident with the position of known growth faults at a depth of 16,000 feet. The P-wave first motions of the events are rarely identifiable. Those which are clear suggest a dilitational first motion, i.e., down-dip slip of the fault plane.

3. Epicenters of microearthquakes located using surface waves concentrate near the L. R. Sweezy well. Mauk, Kimball and Davis (1984) report convincing evidence that these events have hypocentral depths between 300 and 800 meters. The locations of these events do not clearly associate with the position of growth faults; however, they are concentrated where a previous leveling survey indicated the highest rate of subsidence.

4. The magnitudes of the microearthquakes have all been less than 1.5 with the exception of an event hear Lake Charles, Louisiana. Neither the size nor number of events recorded constitute a seismic hazard due to accelerations. The coincidence of the seismic activity with an area of known relative high subsidence rates may suggest the seismicity could be used to identify regions where subsidence displacement could be a longer term risk.

5. The temporal distribution of microearthquakes may suggest that production from the L. R. Sweezy well resulted in accelerated activity. Prior to production, the rate of seismicity was extremely low. During brine production, the rate of seismicity increased dramatically from the previous ambient condition. The highest rate of activity was in the form of swarms post shut-in of the L. R. Sweezy well. Because the activity during shut-in occurred as swarms, it is uncertain whether the ambient condition prior to production was truly representative or merely a hiatus between swarms. An unequivocal causal relationship thus could not be demonstrated between specific production and/or disposal activities at the L. R. Sweezy test site and the occurrences of specific seismic activity. It seems likely, however, that brine production resulted in induced seismic activity.

INTRODUCTION

Commercial utilization of Gulf Coast geopressured/geothermal brines as an alternative energy source requires production and disposal of these environmentally hazardous fluids at rates exceeding 10,000 barrels per day per well. Fluid volume withdrawal and injection at these rates alters the state of subsurface stress, thereby potentially resulting in induced microearthquake activity and ground subsidence. To investigate the potential seismic risks associated with the production of brines from the DOW L. R. Sweezy No. 1 design well in Vermillion Parish Louisiana, Teledyne Geotech, with the authorization of the Louisiana Geological Survey and Louisiana State University, conducted a seismic monitoring program at Bayou Parcperdue from August 1980 through November 1983. The primary objective of the Parcperdue seismic monitoring program was to determine if production from the L. R. Sweezy No. 1 geopressured/geothermal energy well resulted in enhanced seismicity which would constitute a risk in itself or would indicate the longer term hazard of accelerated subsidence.

The results of this study have demonstrated that seismicity is enhanced by the brine production; however, neither the increased number of events, nor the size of the induced microearthquakes constitute a serious hazard or risk due to ground accelerations. Whether or not these microearthquakes cumulattively constitute a long-term subsidence risk is not answered by these data.

This is the final technical report of the Parcperdue seismic monitoring program. It is intended to define the experimental procedures, summarize the observations from 1980 through 1983, and discuss the results and conclusions drawn from analyses of the data. Although we believe the principal objective of the program has been accomplished, we also believe that many more questions have been raised than answered by this study. Additional research in the areas of seismic energy propagation through Gulf Coast sediments, growth fault mechanics, and the interaction of fluid transport and mechanical characteristics of faulted aquafers in the Gulf Coast is strongly indicated.

THE PARCPERDUE SEISMIC NETWORK, INSTRUMENTATION, DESIGN, AND SPECIFICATIONS

The Parcperdue seismic array consisted of five seismogram stations in the Parcperdue Bayou area of Vermillion Parish, Louisiana. The locations of these stations, local cultural features, and projected locations of growth faults at a depth of 16,000 feet are illustrated on figure 1. The aperture of the array is four kilometers. The latitudes, longitudes and elevations of the sensors are listed in table 1. Figure 2 is a block diagram illustrating the operation of the array. Each station consisted of a Teledyne Geotech S-500 seismometer which is locked in a borehole at a depth of approximately one hundred feet. The signal from the seismometer is magnified using a Teledyne Geotech 42.50 amplifier and then FM multiplexed to a voice-band carrier frequency for transmission to a common data collection point at Youngsville, Louisiana. Data transmission is via telephone telemetry circuits. At Youngsville, the signals from the five stations are amplitude conditioned and multiplexed together for transmission via AT&T long lines to the Teledyne Geotech Laboratory at Garland, Texas.

TABLE 1. PARCPERDUE LOUISIANA SEISMIC ARRAY

Site	Latitude (N) Deg	Min	Sec	Longitude (W) Deg	Min	Sec	Elevation Feet	Magnification x 1000 @ 5 Hz	VCO Hz
LSU1	30	04	23.7	91	58	55.5	-74	180	1020
LSU2	30	04	42.6	92	01	53.4	-80	198	1360
LSU3	30	02	57.0	92	00	25.5	-80	169	2040
LSU4	30	02	06.0	92	02	46.5	-72	155	2380
LSU5	30	04	02.4	92	03	15.3	-79	154	1700

In Garland, the five station signals were demultiplexed from their respective carriers using Teledyne Geotech 46.12 discriminators. The signals and precise time code were recorded on magnetic tape and on 16-mm film using a Teledyne Geotech Develocorder. The unity-gain velocity response of the system is illustrated in figure 3. The magnificiation at a frequency of five hertz of the individual stations is given in table 1. Variations in effective magnification reflect the variability of the ambient noise at the different sites.

Figures 4a and 4b illustrate daytime and nighttime (quiet) background noise levels typical for the Parcperdue monitoring array vicinity. These samples are shown relative to estimated system noise levels. The ambient background is shown to be well above system noise in the 3-30 hertz range.

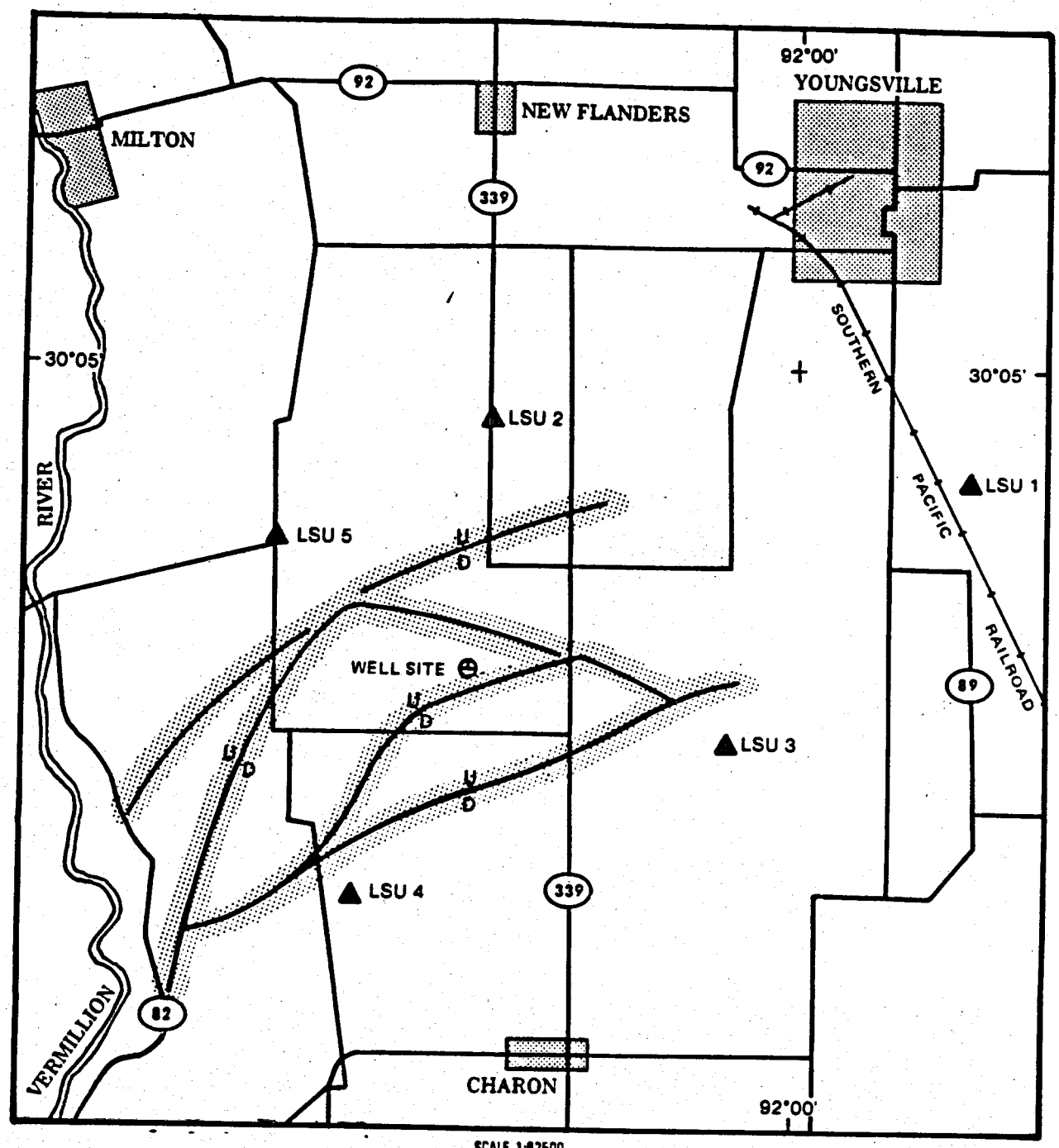

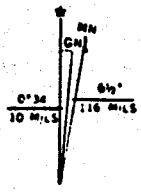

▲ SEISMOGRAPH STATIONS

⊖ TEST WELL

GROWTH FAULTS NEAR 16000 FT DEPTH

FIGURE 1. PARCPERDUE, LOUISIANA SEISMIC ARRAY

G 11905

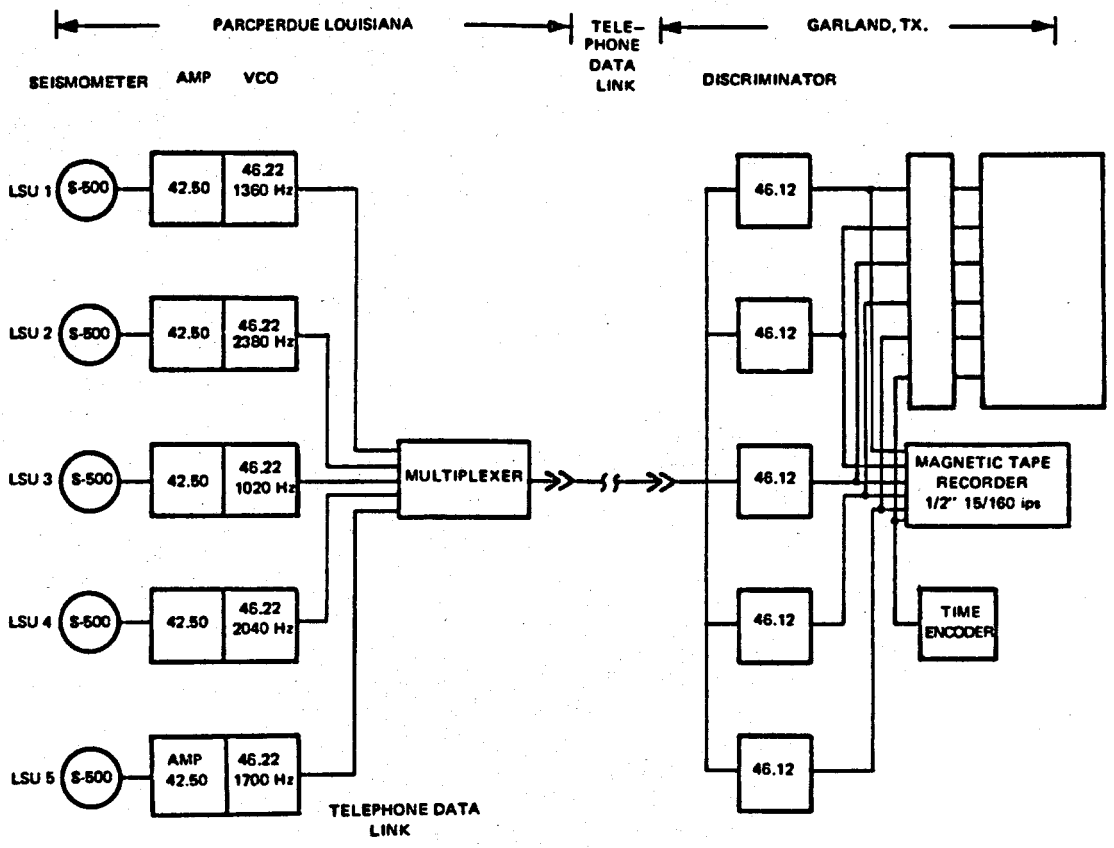

FIGURE 2. BLOCK DIAGRAM OF PARCPERDUE, LOUISIANA SEISMIC ARRAY

G 11908 A

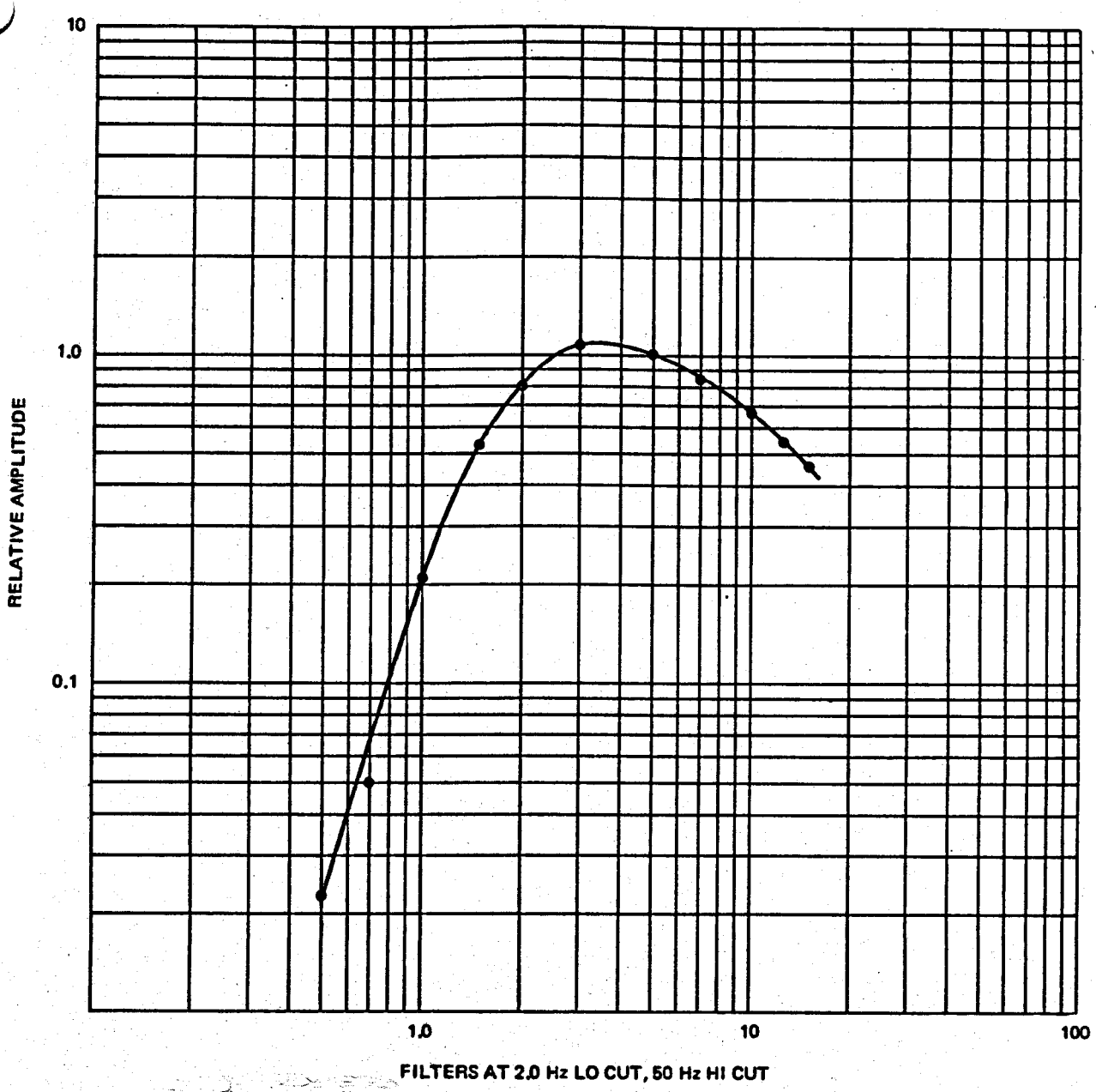

FIGURE 3. PARCPERDUE VELOCITY RESPONSE

G 11147C

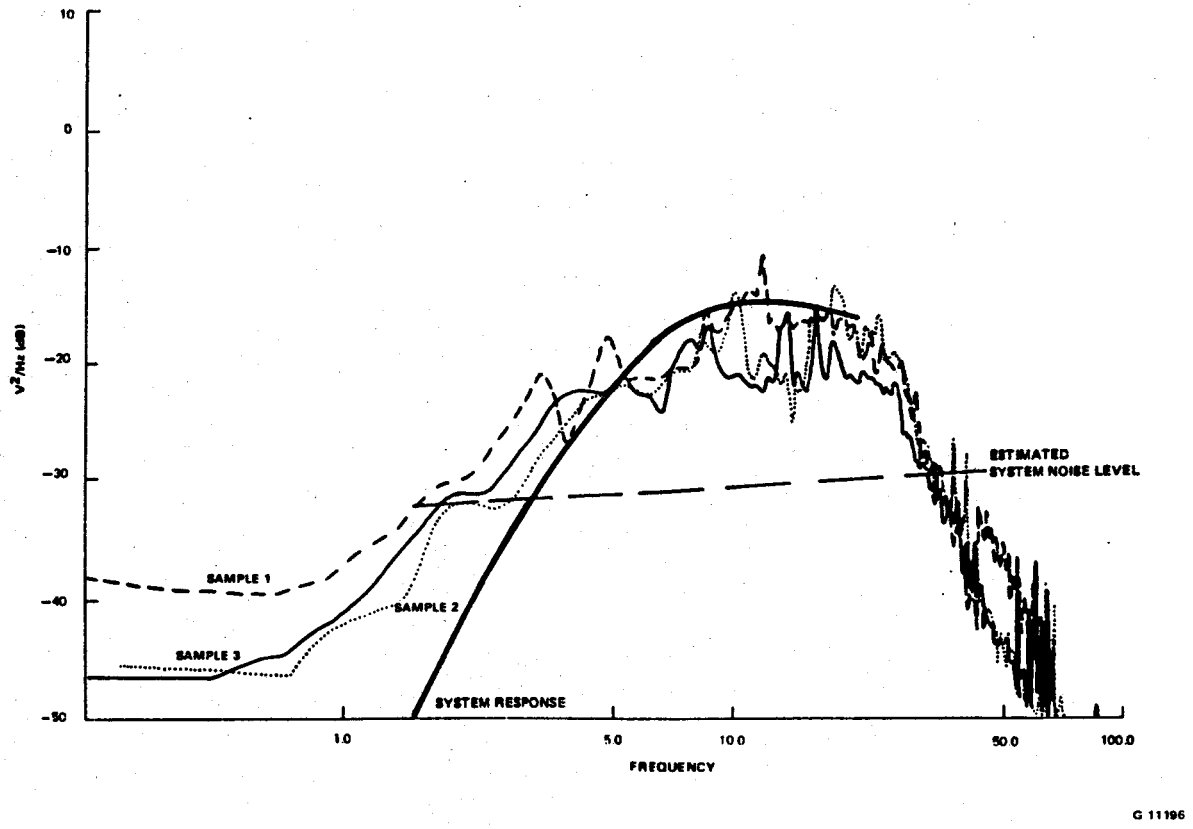

FIGURE 4a. SPECTRAL ESTIMATES OF DAYTIME BACKGROUND NOISE RECORDED AT PARCPERDUE

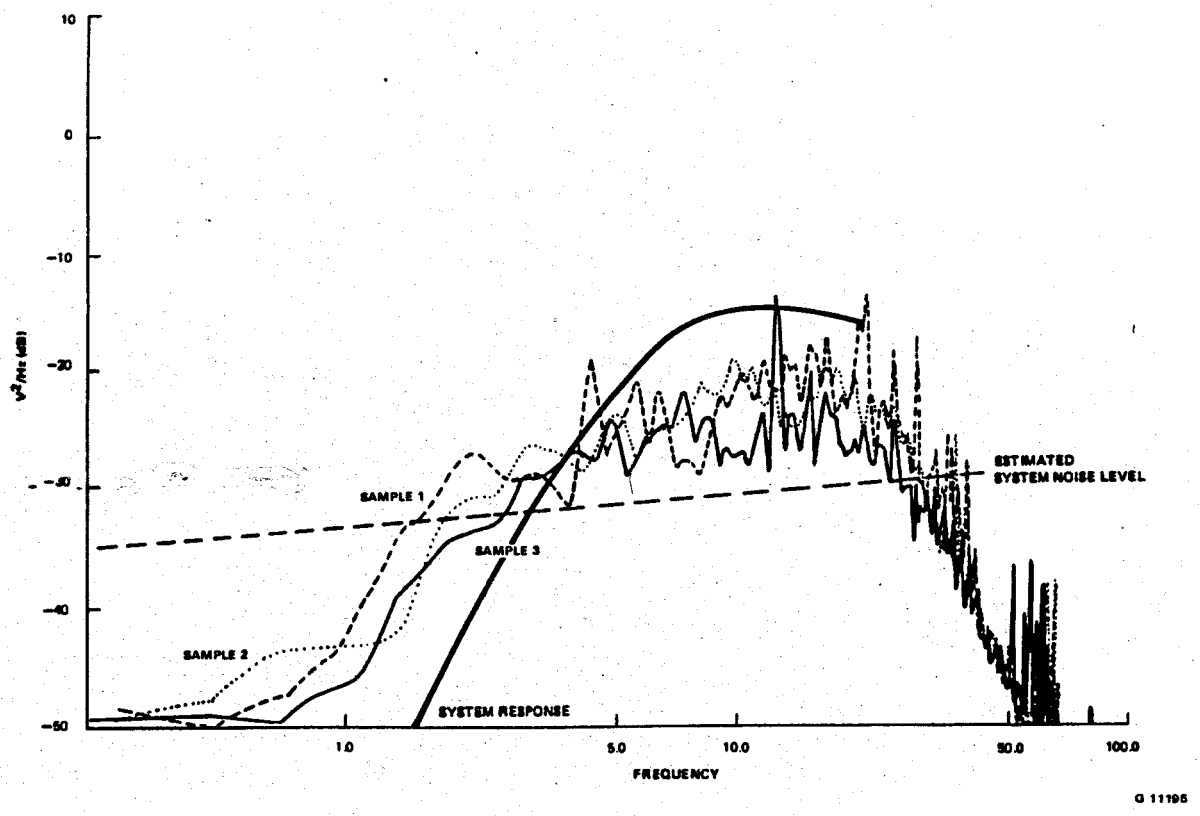

FIGURE 4b. SPECTRAL ESTIMATES OF QUIET (NIGHTTIME) BACKGROUND NOISE RECORDED AT PARCPERDUE

In general, the maximum (0-P) ground displacements observable with the Parcperdue seismograph instrumentation without significant distortion or clipping at one, five and ten hertz are respectively $7.4 * 10^5$, $2.6 * 10^6$, and $1.2 * 10^6$ meters. The minimum (0-P) ground displacements observable are between $1 * 10^9$ and $5 * 10^9$ meters depending upon ambient ground noise conditions. These observation limitations correspond to events with seismic moments between 10^{17} and 10^{20} dyne-cm or approximate local magnitudes between -0.5 and 2.5 (see figure 5).

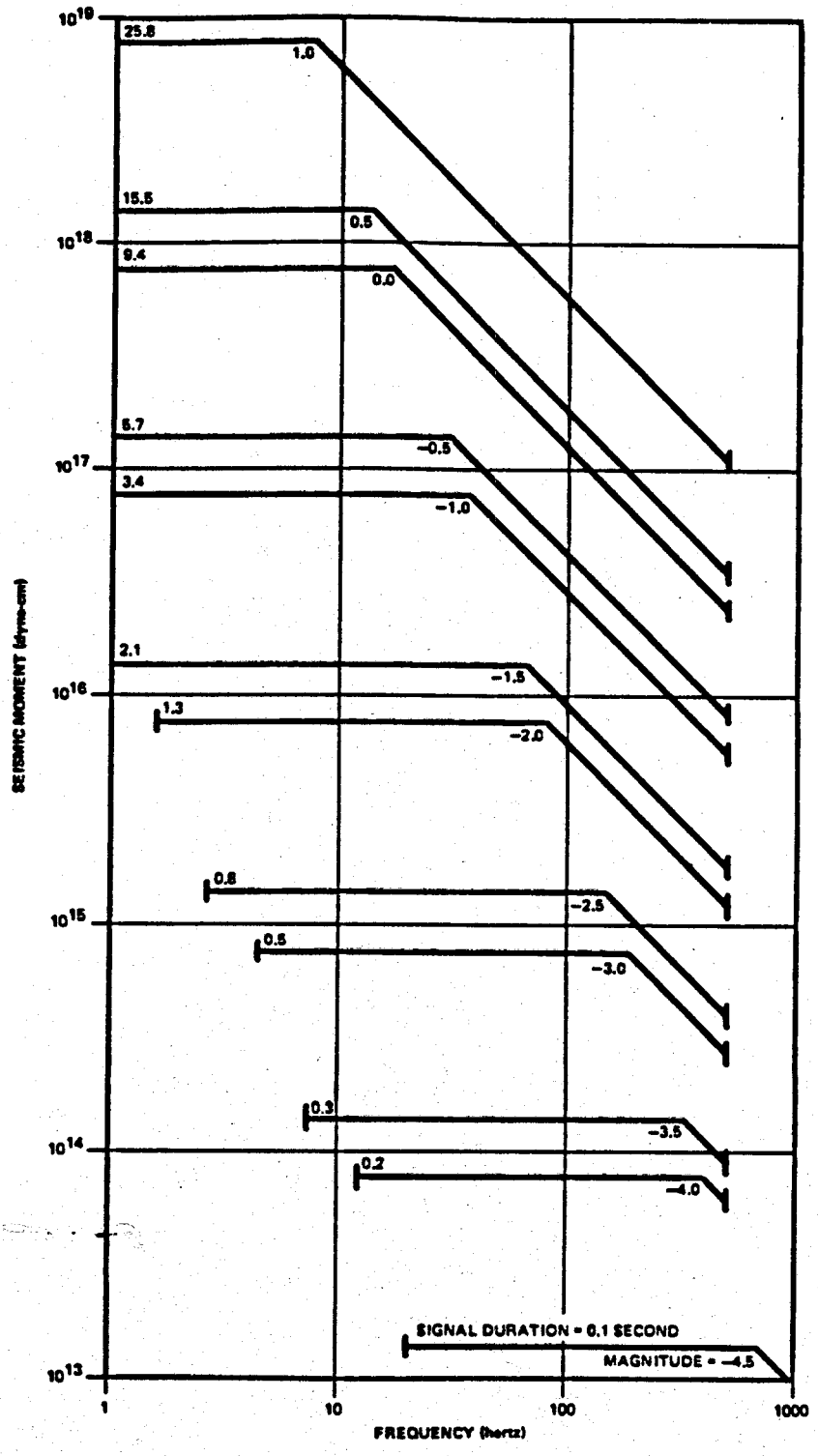

FIGURE 5. CORNER FREQUENCY VERSUS SEISMIC MOMENT FOR CENTRAL UNITED STATES EARTHQUAKES (AFTER STREET, HERMANN, AND NUTTLI, 1975)

G 13371

DATA ANALYSIS PROCEDURES

Two general types of signals were recorded by the Parcperdue seismic array, and each required specific data processing procedures. Type I events were signals which traversed the array with apparent velocities more nearly like body waves (that is, P-waves and S-waves). The analysis procedures for phase arrival timing and locating these events are discussed under the heading Body Wave Data. Type II events were signals which traversed the array with apparent velocities more nearly like surface waves. The analysis procedures for locating these events are discussed under the heading Surface Wave Data. Finally, the methodology for computing event magnitude is discussed under the heading of Magnitude Determination.

Body Wave Data

The data generated by the Parcperdue seismic array were analyzed using standard procedures to yield basic information about origin times, locations and magnitudes of observed events. The 16-mm film seismograms were reviewed carefully to detect any microseismic events that may have occurred. When an event was detected, the analyst measured the amplitude, period, and arrival times of the P (compressional), S (shear), and L_R (surface) wave of the event. The amplitude, period and arrival time data are stored for subsequent input into a computer code (MEHYPO) which estimates the origin times, source coordinates and local magnitudes of the observed events. The estimation algorithm is similar to that described (Lee and Lahr, 1972) in that it finds the origin time and set of source coordinates which minimizes the mean square difference between observed and predicted arrival times at the various sensor locations. The code also provides various location uncertainty estimates which are based upon the assumption that the arrival time errors are normally distributed and that the seismic velocity structure is known without error. The sensor frequency response data, the P-wave amplitude and period data are used to compute the local magnitudes of the observed events.

The lithologic column, P-wave velocity structure and thermal profile for the Parcperdue geopressured test well region are illustrated in figure 6. The lithologic column is based on interpretation of the Schlumberger SP, sonic and dipmeter logs and driller's documentation from the DOW L. R. Sweezy No. 1 well. The corresponding P-wave velocity structure is based on the sonic log. Mean velocities for lithologic units were derived by averaging velocities determined every ten feet for thick units and every two feet for thin units. Standard deviations of velocities from the means are shown on figure 6 as error bars with the mean velocity and standard deviation in meters per second given at the end of the error bars. The dual induction and caliper logs were used as measures of reliability for the sonic log. Wide departures of the deep and intermediate induction logs were taken as indications of significant formation penetration by drilling muds. The sonic log for these zones is probably not an accurate indication of the true velocity. The three sand units with every low velocities at depths less than 1200 meters had significant departures of the dual induction logs. Drilling reports for

13 January through 15 January indicate loss of mud to and subsequent influx of sand from these horizons supporting the geophysical observation of high porosity and permeability and low shear strength. Thus, although the true velocities for these units may not be as low as indicated by the sonic log, they are significantly different from the surrounding strata.

The P-wave velocity models used for hypocenter determination at the Parcperdue array are given in tables 2a and 2b. Two different velocity structures were necessary because of sharp velocity inversions in shallow layers. These velocity inversion layers can be included in the location computational schemes for array-interior events because the wave incidence angles are sufficiently high to permit transmission of the waves through the layers. However, array exterior events can have wave incidence angles to the low-velocity layers which do not permit theoretical transmission of the energy as a normal refracted wave and thus fail to converge to a location solution. Solutions exterior to the array can be obtained by smoothing these velocity inversions out of the structure as in table 2b. Comparisons of known and computed locations of explosions outside the array demonstrated that this smoothing procedure does not jeopardize the accuracy of the location. On the other hand, including the velocity inversion layers for array interior events improves both the precision and accuracy of the locations obtained.

The S-wave velocity structure was derived from the P-wave velocity structure using the formulation:

$$V_S = V_P \frac{1}{/(1 + 1-2\sigma)^{1/2}}$$

where: V_S = Shear wave velocity
V_P = Compressional wave velocity
σ = Poisson ratio

Water has a Poisson ratio of 0.5, and most competent rock has a Poisson ratio of 0.25. Lash (1980) has determined the Poisson ratio for surficial Gulf Coast sediments to be greater than 0.45 with the ratio decreasing with increasing depth. To utilize S-waves for hypocenter location, a fixed V_P/V_S ratio of 1.732 was used. Epicenters were computed only for events observed at four or more stations because of possible ambiguities of solutions based on data from fewer stations.

Surface Wave Data

Signals consisting entirely of surface (Rayleigh) waves and/or leaking modes were recorded commonly by the Brazoria, Parcperdue, Sweet Lake, and Rockefeller Refuge seismic arrays. Hypocenters of events generating these signals cannot be determined using standard Geiger least-squares inversion procedures. It is possible to determine approximate epicenters of these events, however, if an appropriate wave velocity for the observed phase arrivals can be determined.

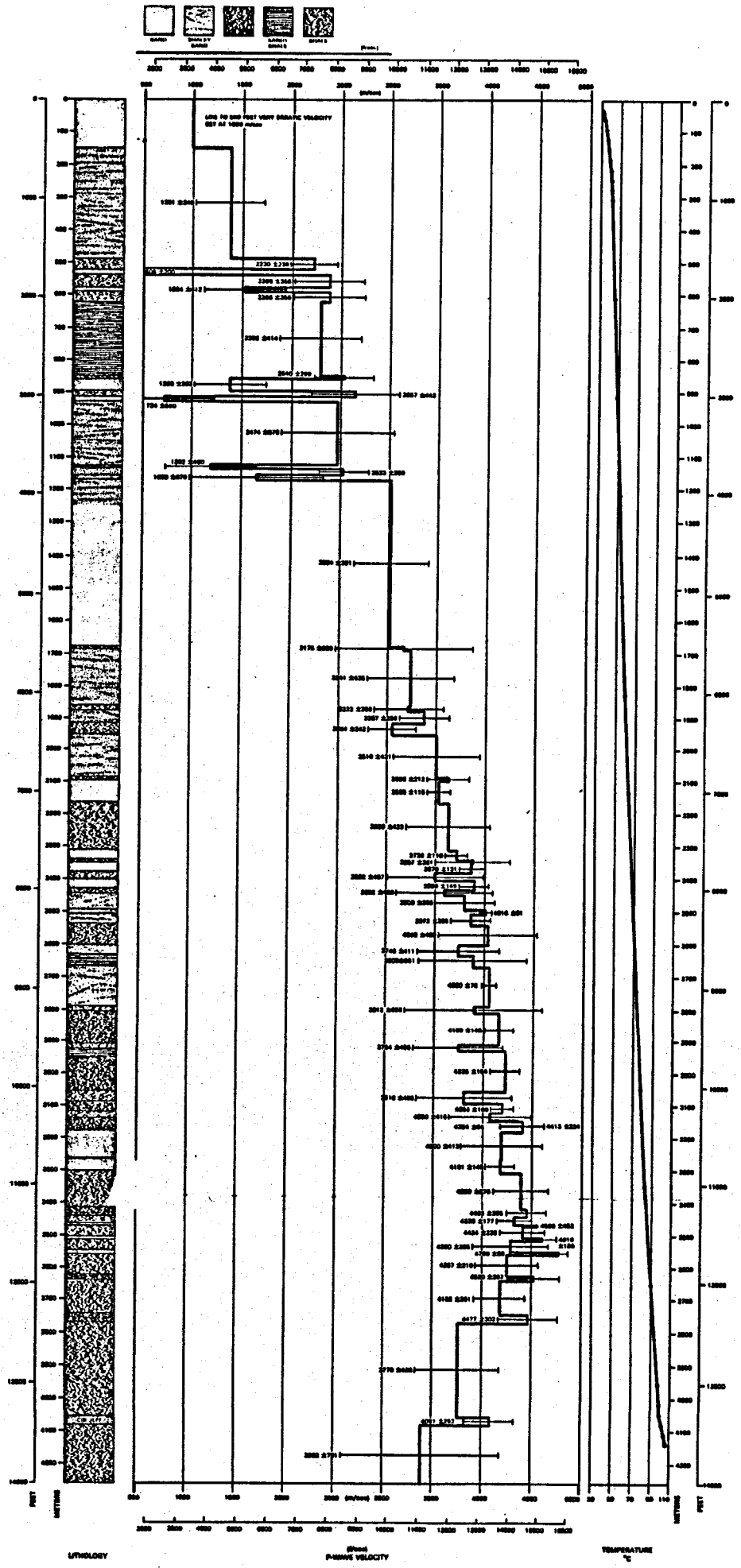

FIGURE 6. LITHOLOGY, P-WAVE VELOCITY AND THERMAL PROFILES FOR PARCPERDUE, LOUISIANA, BASED ON SP, SONIC, DUAL INDUCTION, THERMAL AND DIPMETER LOGS OF THE DOW L. R. SWEEZY NO. 1 WELL

G 12116

TABLE 2A. VELOCITY STRUCTURE FOR EVENTS INSIDE THE ARRAY

Layer Parameters	P-Wave Vel. (Km/sec)	S-Wave Vel. (Km/sec)	Thickness (Km)
1	0.6100	.352	0.0091
2	1.7070	.986	0.1000
3	1.7500	1.010	0.0400
4	1.8000	1.039	0.1500
5	2.0120	1.162	0.1220
6	2.0730	1.197	0.2140
7	2.2550	1.302	0.2900
8	2.2860	1.320	0.3100
9	2.6210	1.513	1.036
10	2.9260	1.689	1.0500
11	3.3530	1.936	0.5500
12	2.6210	1.513	0.5200
13	2.4380	1.403	0.3100
14	2.7430	1.584	0.3100
15	2.9260	1.689	0.3000
16	3.1700	1.830	0.3000
17	3.5000	2.021	0.3000
18	3.8000	2.194	1000.0000

TABLE 2B. VELOCITY STRUCTURE FOR EVENTS OUTSIDE THE ARRAY

Layer Parameters	P-Wave Vel. (Km/sec)	S-Wave Vel. (Km/sec)	Thickness (Km)
1	0.8000	0.4619	0.0600
2	1.1000	0.6351	0.0710
3	1.3910	0.8031	0.3270
4	2.2000	1.2702	0.2650
5	2.3500	1.3568	0.4500
6	3.5400	2.0439	1.6680
7	3.9600	2.2864	1.8140
8	4.2500	2.4538	0.6000
9	4.7000	2.7136	1.0000
10	4.9000	2.8291	5.0000
11	5.1000	2.9446	200.0000
12	5.3000	3.0600	1000.0000

The excitation of surface waves, particularly in an environment characterized by significant variations in velocity in three dimensions, is more complex than excitation of primary body waves. Surface waves, unlike body waves, propagate not only as fundamental mode oscillations, but also as higher mode oscillations. These higher modes are analagous to overtones produced by musical instruments. Both the velocities and amplitudes of the Rayleigh modes excited are critically dependent on the body-wave (both P- and S-waves) velocity structure. Figure 8 illustrates the relative excitation of the first four vertically-oriented, two-hertz Rayleigh modes as a function of depth for a location near Apache, Oklahoma, (Douze, 1964). Also illustrated are the density, P-wave, and S-wave profiles for the upper 3,000 meters of geological section. The relative amplitudes of the higher modes generally decline significantly as mode number increases when the velocity structure is free of low-velocity zone energy traps. If, on the other hand, the depth of a particular model maximum occurs in a low-velocity zone (LVZ), that mode will display an anomalous amplitude compared with that which would be excited if the LVZ were not present. The observed Rayleigh-wave energy at any particular frequency is dependent upon the depth of observation and the total energy integrated over all possible modes. Thus, for example, a seismogram from a location at a depth of 2,000 meters in the structure of figure 7 would display Rayleigh waves dominated by first, second and third higher mode arrivals with very little contribution by the fundamental mode.

The Gulf Coast sedimentary column is significantly more complex than the one illustrated in figure 8 and the relative importance of higher mode contributions, particularly at wave frequencies greater than two hertz, should not be underestimated. Figure 7 illustrates the computed and observed Rayleigh group velocities as a function of period for six Rayleigh modes in Gulf Coast sediments for Refugio County, Texas (Ebeniro and others, 1983). Note that fundamental third-, fourth-, and fifth-order harmonics are observed, and that first and second higher modes are not. The higher modes are strongly, normally dispersed (that is, phase and group velocities are inversely related to wave frequency). The fundamental mode, on the other hand, is relatively non-dispersed, or slightly inversely dispersed, in the frequency range from one to five hertz. This accounts for why the Rayleigh wave train frequently appeared as an impulsive arrival in the time domain. Since the density, bulk and shear moduli are all low for Gulf Coast sediments, the fundamental mode Rayleigh wave velocities are also low, ranging from 150 m/sec to 350 m/sec. Unfortunately, the velocity range also is occupied by acoustical transmissions through air, and significant coupling of atmospheric acoustic and earth Rayleigh waves is highly probable. Thus, it is very important to determine if observed signals are of atmospheric or earth origin. This discrimination is not necessarily obvious as will be shown in a later section.

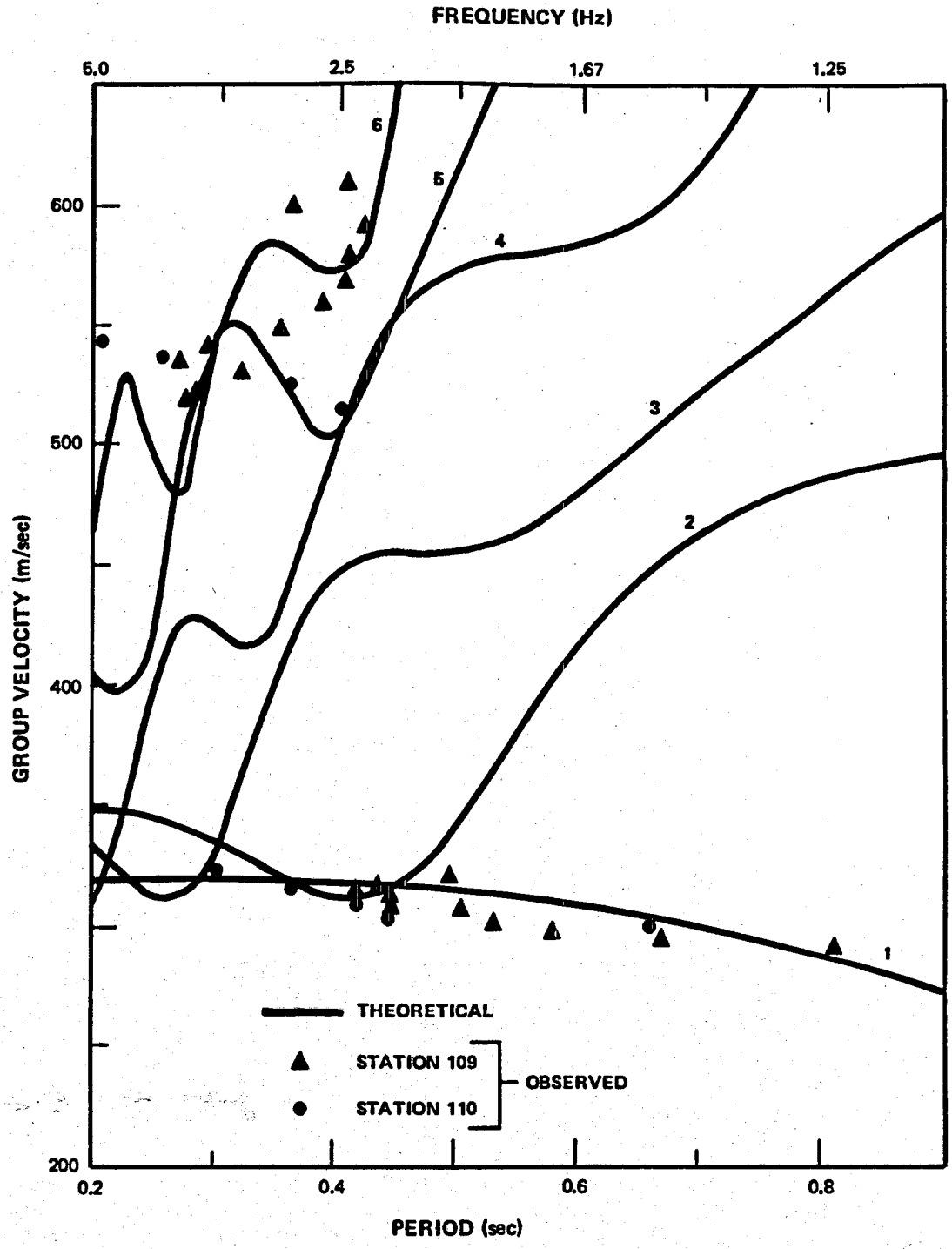

FIGURE 7. RAYLEIGH WAVE GROUP VELOCITY FOR SIX MODES IN TEXAS GULF COAST SEDIMENTS (AFTER EBENIRO, WILSON AND DORMAN, 1982)

G 13221

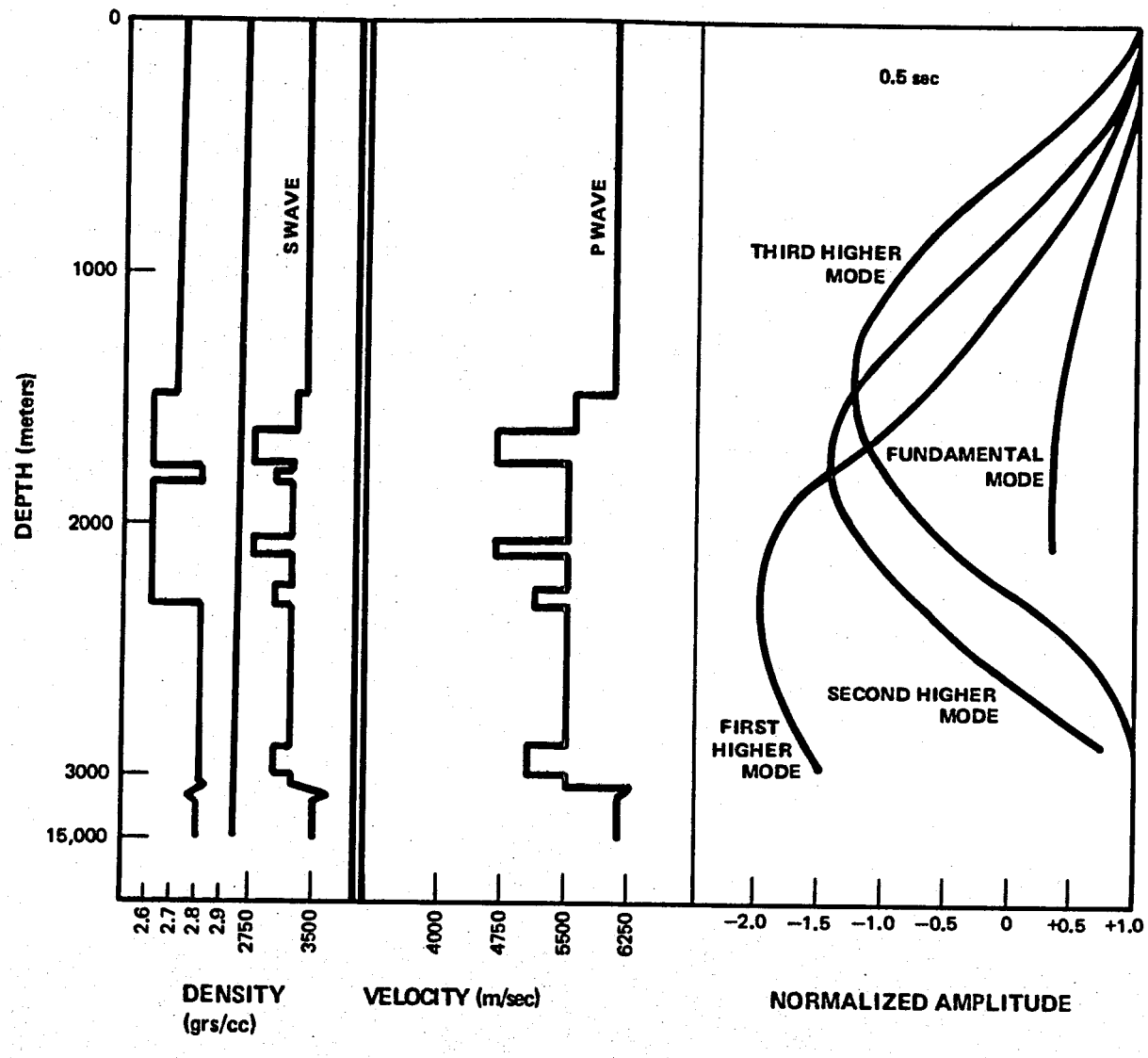

FIGURE 8. VELOCITIES, DENSITY, AND THEORETICAL RAYLEIGH WAVE AMPLITUDE - DEPTH CURVES AT 2.0 Hz, APACHE, OKLAHOMA (AFTER DOUZE, 1964)

124

G 13222

Unfortunately, strong evidence exists that the mode of propagation of type II events is not a simple surface wave. There are several energy traps (low velocity in the Bayou Parcperdue velocity structure at depths layers) between zero and one and a half kilometers, and the potential effect of these traps requires some explanation. In general, the propagation of energy across a discontinuity in velocity physically obeys Snell's law as illustrated in figure 9a. If there exists in the velocity structure one or more layers with velocities significantly less than the velocities of their bounding layers, then the conditions are ideal to create a wave guide or trapping layer as illustrated in figure 9b by the layer identified as V_2. If the velocity contrast between the bounding layers and the trapping layer is sufficiently large, the energy can never escape from the layer and continues to propagate down the layer as a series of reflected waves. Perfect traps, however, are exceedingly difficult to create, and more often the case is that, at each reflection, a little energy leaks off into the adjacent layers. This "leaked" energy can be observed as a leaking mode arrival on seismograms. If the type of wave trapped is S_v, in a poorly consolidated water-rich layer, the velocity could be exceedingly low (S-wave velocity in water is zero). Because the apparent surface velocity (V_a) is the surface distance between the source and receiver divided by the total travel time rather than the sum of the real ray path distances divided by the sum of the real ray segment velocities, the apparent velocity can appear to be much slower than it is in actuality.

If these observed impulsive arrivals are leaking mode S_v waves rather than surface waves (a subtle distinction which seems highly probable), then the location scheme utilized can result in both location and origin time biases. If the microearthquake occurs within the array, the bias would be as follows. Since the real velocity and real path length are unknown, the computed origin time would always be underestimated, that is, the real origin time would always be earlier than the apparent origin time. Similarly, the apparent location would be biased in a direction away from the real location toward the station or stations with the fastest velocities.

Because of the complexities in Gulf Coast modal excitation and propagation, type II event epicenters computed from described apparent velocities must be regarded with a greater caution than more complete body wave solutions. The procedure we follow to locate these events is to solve iteratively for the least-squares error associated with both the location and wave velocity simultaneously. The functional relationship between epicentral area uncertainty and half-space velocity typically assumes approximately hyperbolic shape (see figure 10).

We assume that the hyperbolic vertex corresponds with the best half-space velocity and that the computed location using this velocity is the best approximation of the epicenter. Depth is not resolved by this technique.

In principal, this location analysis technique permits the simultaneous determination of the best fit velocity and location; however, word of caution is appropriate here. When few arrival time observations (<10) exist with which to invert iteratively for an epicenter solution, it is possible to produce an intra-array alias location from an extra array source by fixing an

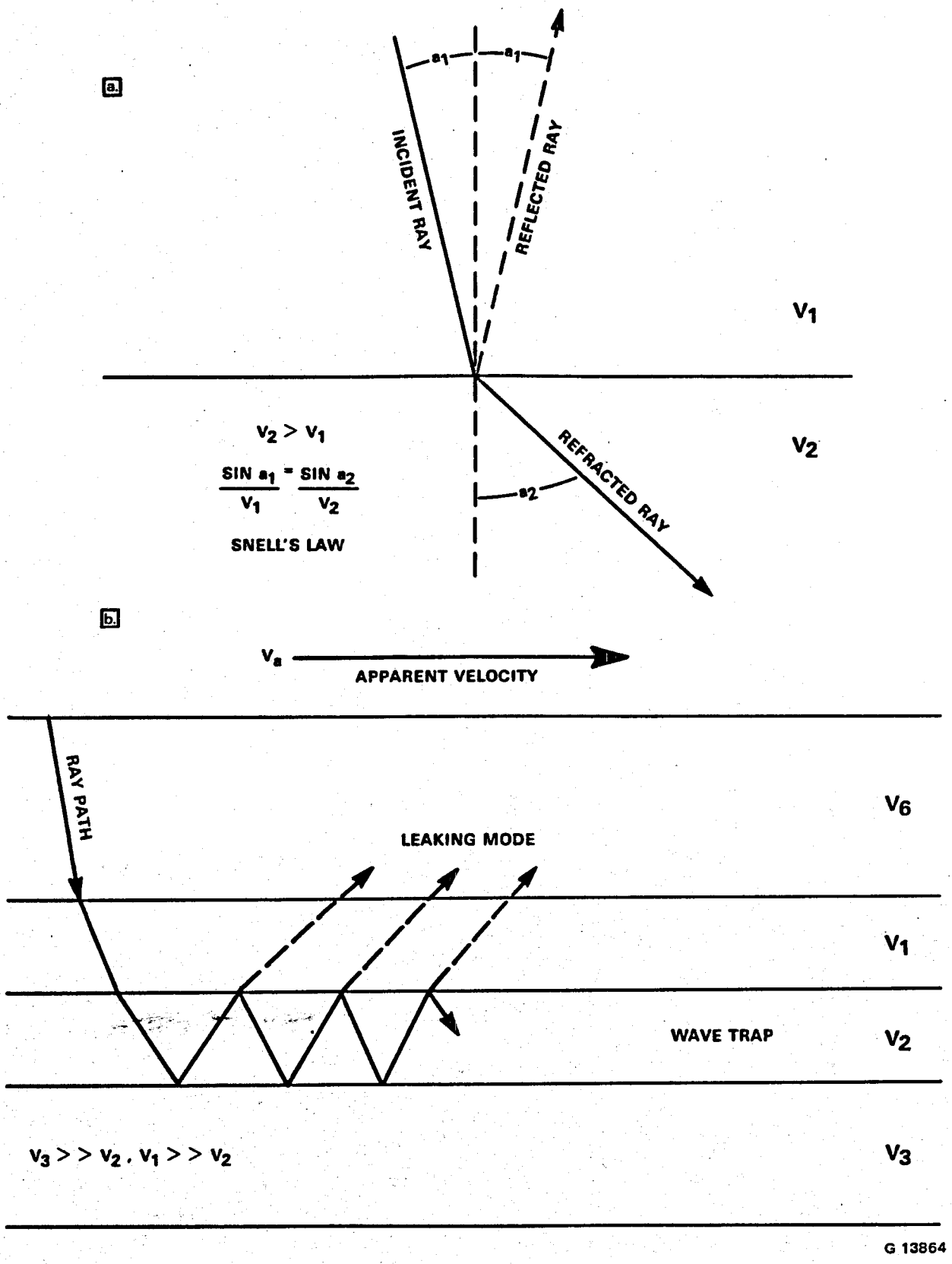

FIGURE 9. a. DIAGRAM ILLUSTRATING TRANSMISSION OF AN ENERGETIC RAY ACROSS A VELOCITY INTERFACE. b. THE PROPAGATION OF A LEAKING MODE FROM A TRAPPING LAYER (V_2)

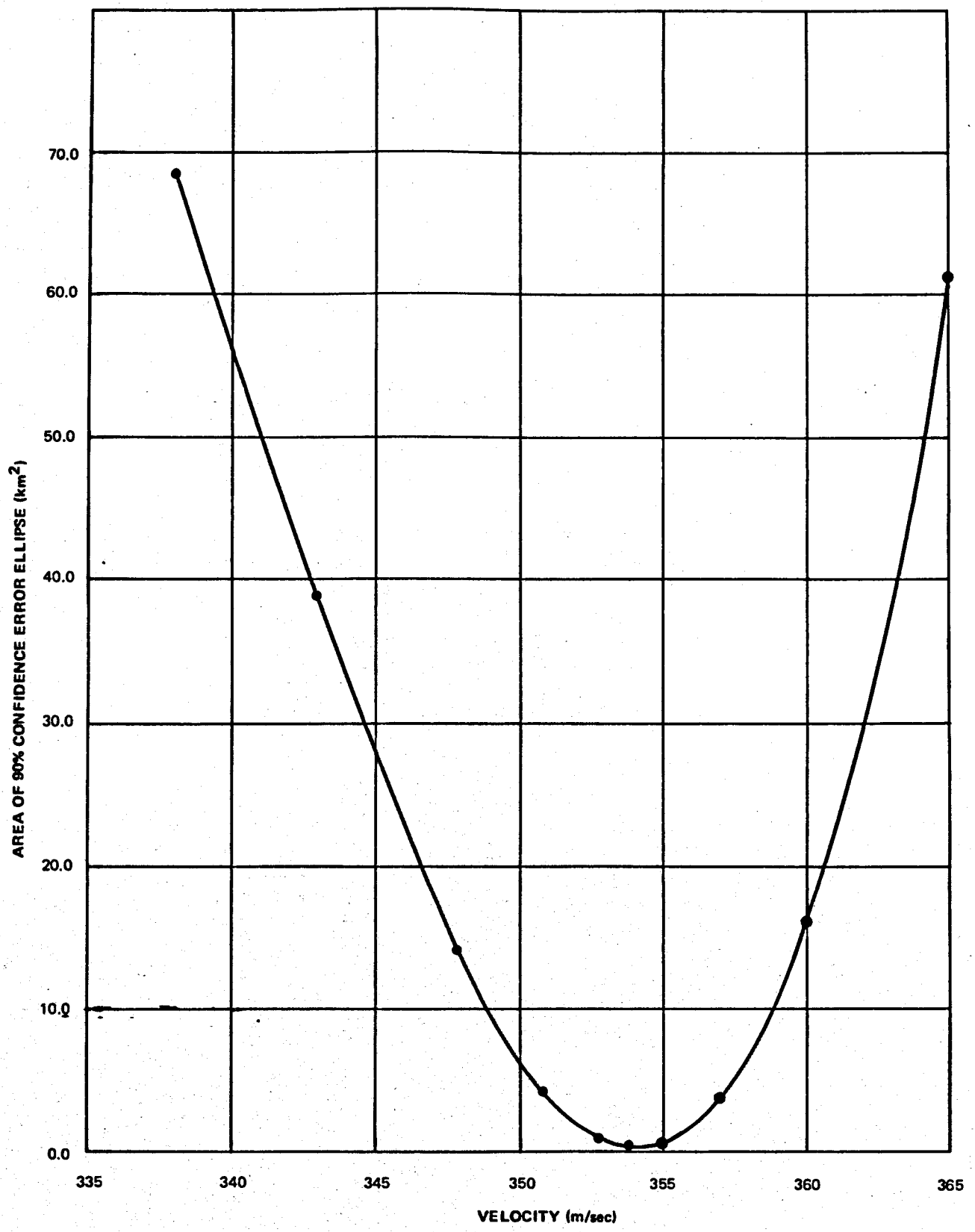

FIGURE 10. VELOCITY ANALYSIS OF IMPULSIVE RAYLEIGH EVENT 22 AUGUST 1982 AT 18:52:28.7 UTC TIME

G 13007

appropriate half-space velocity. The extreme example of this possibility is that the arrival times from a distant teleseism can yield a location solution within the array, if the interior velocity used for location is set sufficiently low. For this reason, epicenters of events located using this least-squares inversion technique, particularly when best-fit velocities are less than 350 meters/second, should be viewed with appropriate caution.

Magnitude Determination

Magnitudes have primarily been calculated using duration as

$$M_d = -2.22 + 2.28 \log (D)$$

where d is duration in seconds from onset of P to return of coda to ambient noise level. It has been shown by (Aki and Chouet, 1975; Chouet and others, 1978; Aki, 1981) that the duration of seismic coda is dependent on the number and distribution of potential back scattering sources. For this reason, coda duration magnitude formulations must be tailored specifically for each region where they were used. The duration magnitude formula we use is one for the Mississippi Embayment determined by the Tennessee Earthquake Information Center. Since a magnitude scale has not been developed for the Gulf Coast, it is possible that all quoted magnitudes are in error. The magnitudes quoted should agree approximately with normal Richter magnitudes.

Magnitudes may be calculated alternatively as local seismic magnitudes based upon maximum surface wave amplitude as

$$ML = \log10 (a/2) - 1.15 + 0.8 \log10 (x)2$$

where ML is the local magnitude
and A is the peak-to-peak surface wave amplitude in millimicrons
and X = [(epicentral distance) 2 + (hypocentral depth) 2]1/2
and X > 1.0

The constant -1.5 in the magnitude equation assumes a surface wave to P-wave amplitude ratio of 10. Thus, a magnitude 0 event at 1 km distance would generate surface waves with a peak-to-peak amplitude of about 2.8 millimicrons.

Throughout the duration of the monitoring program, there have been few opportunities ~~to subtantiate the~~ magnitude formulas of the Gulf Coast. Figure 11 is a microearthquake which occurred near Lake Charles, Louisiana, on 16 October 1983. This Gulf Coast earthquake was sufficiently large to be observed both on the local arrays and distant seismograph stations (see event 19, Table A1). This event provided an opportunity to test Gulf Coast magnitude computations from adjacent regions. The duration magnitude computed from the data of the Parcperdue seismic array stations illustrated is 3.02. This compares with an Mb (Lg) (magnitude based on the amplitude of the Lg, scattered wave) computed from distant stations of 3.8. This comparison suggests that the magnitudes reported for the Parcperdue array may be underestimated by approximately half a magnitude. However, it is equivalently important to realize that the majority of events observed at Bayou Parcperdue had focal depths apparently less than a kilometer. These

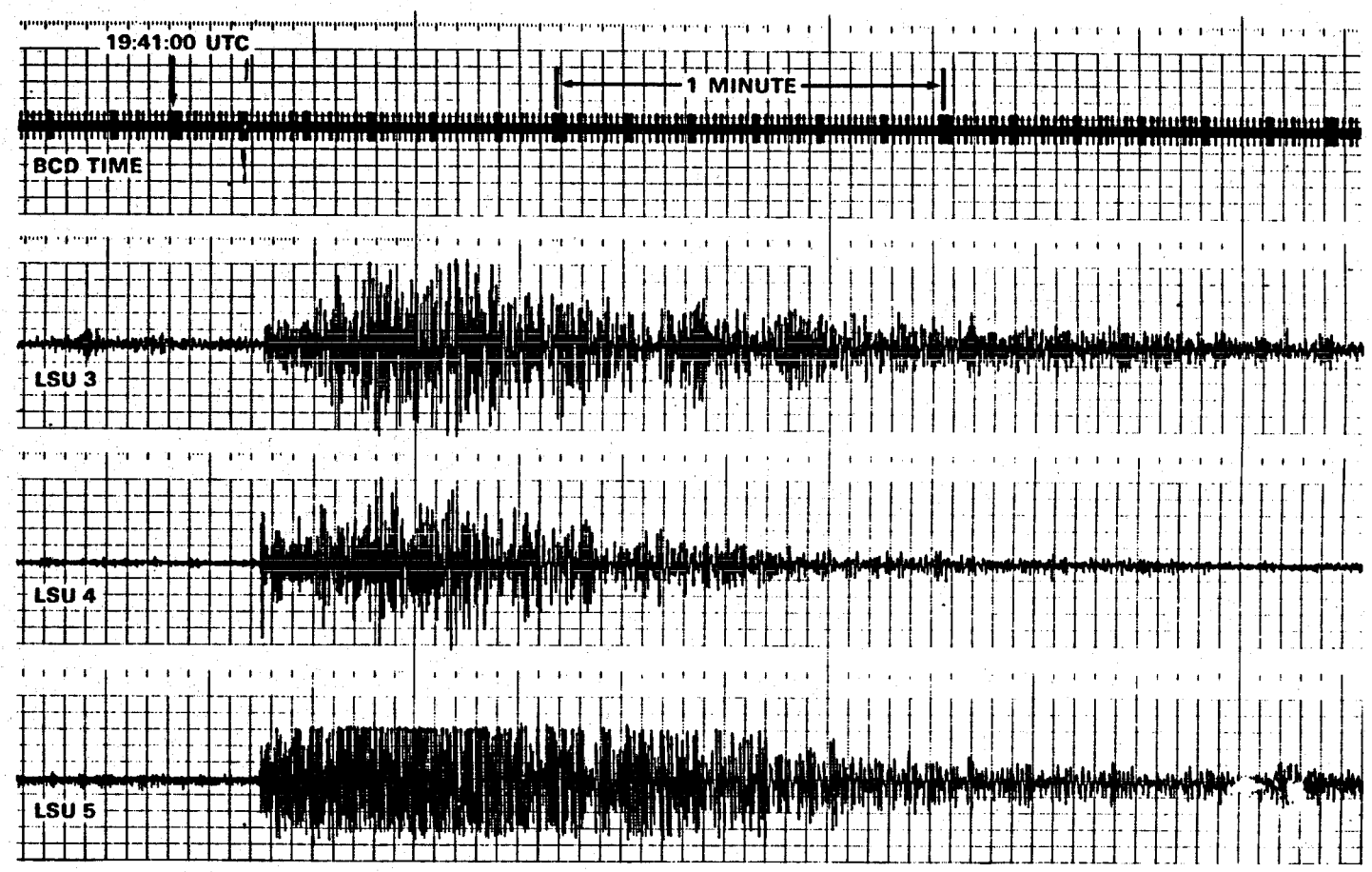

G 14351

FIGURE 11. MICROEARTHQUAKE FROM THE LAKE CHARLES, LOUISIANA, AREA. OT = 19:40:46.1 UTC (CST + 5 HRS) ON 16 OCTOBER 1983

are significantly less deep than the Lake Charles earthquake, and, thus, the comparison may be for deeper events only. The exact "size" of the events recorded by the Bayou Parcperdue array is not known. The reported magnitudes are internally consistent, and, if alternative calibration becomes available, it will be possible to rescale these magnitudes if it is of importance.

THE DOW L. R. SWEEZY NO. 1 TEST PROGRAM

Brine and gas were produced from the Cib Jeff zone of the Frio formation through the DOW L. R. Sweezy No. 1 well which was perforated at depth of 13,349 to 13,388 feet (4,074.6 - 4,080.7 m) and 13,395 to 13,406 feet (4,082.5 - 4,086.2 m). Brines were subsequently reinjected in the DOW L.R. Sweezy No. 2 well at depths of 4,520 to 4,640 feet (1,377.7 - 1,414.3 m) and 4,646 to 4,660 feet (1,416.1 - 1,420.4 m). Nearly 2,000,000 barrels of brine and 31,500 mcf of gas were produced during the test program. Production at Parcperdue terminated on 5 February 1983, when severe sanding of both the producing well and the injection well occurred. Both wells were plugged and abandoned due to excessive remedial costs required to continue operations.

Testing of the brine production capabilities of the DOW L. R. Sweezy well began with a short-term flow test of approximately 689 barrels on 26 April 1982. By 31 December 1982, nearly $1.7 * 10^6$ barrels of brine and $3 * 10^7$ cubic feet of gas had been produced in eight short-term and three long-term flow tests. Although flow rates exceeding 10,000 barrels/day were attempted on two brief occasions, excessive sand production precluded long-term brine production at such rates. The cumulative brine and gas productions from the L. R. Sweezy well from 26 April through 31 December, 1982 are illustrated in figure 12. The relatively constant production rate for all of the flow tests from 5 through 11 is obvious from the constant slope of each segment separated by the shut-in and build-up periods. Figure 12 also clearly indicates that the gas/brine production ratio has remained relatively fixed throughout the production history of the well.

Details of the production wellhead tubing and casing pressures as a function of time are illustrated in figures 13a and 32b. The corresponding flow rate versus time is illustrated in figure 14. The disposal well injection pressure history is illustrated in figures 15a and 15b. These figures were prepared from data provided by the DOW Chemical Company which have been entered in computer files. The purpose of these production/disposal logs is to provide a basis for comparison with the observed temporal distribution of the seismicity. Sixty-three significant perturbations in the test program history are indicated by numerically coded arrows along the time lines of figures 13a through 15b. Explanations of these indicated events are given in the associated tables. Times of shut-ins and build-up tests are shaded to help clarify when they occurred in the production history. The relationship of the observed seismicity to the DOW L. R. Sweezy test program is discussed in the next section.

TABLE 3. DESCRIPTIONS OF WELL TEST INDEX ARROWS FOR FIGURES 12 THROUGH 15

EVENT	CUM HR	DATE	TIME	EXPLANATION (DURATION)
1	4	26 APRIL 82	22:00	FLOW TEST NO. 1A (6 HRS) INJECTION PRESSURE PEAKS AT 74 PSI
2	46	28 APRIL 82	16:00	FLOW TEST NO. 1B, PEAK FLOW RATE 14970 BPD (8 HRS) INJ PRESS. 799
3	196	04 MAY 82	22:00	FLOW TEST NO. 2 BEGINS (4 HRS)
4	378	12 MAY 82	12:00	FLOW TEST NO. 3 BEGINS
5	410	13 MAY 82	20:00	BEGIN BUILDUP NO. 3 (36 HRS)
6	506	17 MAY 82	20:00	FLOW TEST NO. 4
7	532	18 MAY 82	22:00	BEGIN BUILDUP NO. 4 (34 HRS)
8	566	20 MAY 82	08:00	BEGIN FLOW TEST NO. 5
9	710	26 MAY 82	08:00	BEGIN BUILDUP NO. 5 (170 HRS)
10	886	02 JUNE 82	16:00	BEGIN FLOW TEST NO. 6
11	902	03 JUNE 82	06:34	SHUT-IN, THEN FLOW TO PIT
12	932	04 JUNE 82	13:00	SHUT-IN, THEN FLOW TO PIT
13	1000	07 JUNE 82	08:30	FLOWED TO PIT, BLED CASING TO 2000 PSI
14	1056	09 JUNE 82	18:00	SHUT-IN FOR FLOW TEST NO. 6
15	1144	13 JUNE 82	10:00	PIT FLOW (0.5 HR)
16	1218	16 JUNE 82	12:00	CHANGE FILTERS INJ WELL
17	1294	19 JUNE 82	16:00	INJ PRESS. READING LOST (10 HRS)
18	1384	23 JUNE 82	10:00	SHUT-IN TO RUN OTIS WIRELINE IN HOLE (2.5) BEGIN FLOW TEST 8
19	1464	26 JUNE 82	18:00	INSTRUMENT CALIBRATION (TUBING PRESSURE)
20	1508	28 JUNE 82	12:00	SHUT-IN FOR BUILD-UP TEST 8 (200 HOURS)
21	1538	29 JUNE 82	20:00	EQUIPMENT CALIBRATION (TUBING PRESSURE GAUGE)
TO	1566	01 JULY 82	02:00	
22	2054	21 JULY 82	08:00	ACID TREATMENT ON INJ WELL
23	2192	27 JULY 82	04:00	BRINE DUMP VALVE NOT WORKING
24	2198	27 JULY 82	07:23	SHUT-IN TO REPAIR DUMP VALVE (10 HRS)
25	2248	29 JULY 82	09:45	SHUT-IN TO REPAIR LEAKS (7 HRS)
26	2688	16 AUG 82	18:00	CHANGED INJ WELL FILTERS
27	2884	24 AUG 82	20:30	BACKFLUSHED INJ WELL – LINE TO PIT OPENED FOR 3 MIN WHILE NOT CLOSING INJ DSP TREE
28	2926	26 AUG 82	15:30	SHUT-IN TO RUN OTIS WIRELINE IN HOLE (3 HRS)
29	2944	27 AUG 82	9:30	SHUT-IN FOR BUILD UP 9 (100 HRS)
30	3068	1 SEPT 82	13:10	SHUT-IN TO REPAIR LEAKS IN MASTER VALVE – NO READINGS (144 HRS)
31	3234	8 SEPT 82	10:20	PIT FLOW – REPAIRED TURBINE METER (3 HRS)
32	3358	13 SEPT 82	12:00	PIT FLOW - TO LOWER INJ PRESS (0.5 HR)
33	3382	14 SEPT 82	12:34	SHUT-IN BY LEAK CONTROL PANEL – NO CAUSE FOUND (6 HRS)
34	3428	16 SEPT 82	10:52	PIT FLOW – TO LOWER INJ PRESS (0.5 HR)
35	3622	24 SEPT 82	12:00	BLED INJ PRESS DOWN TO 190 PSI
36	3758	30 SEPT 82	06:00	INJ PRESS JUMPED FROM 225 PSI TO 365 PSI IN 28 HRS – CAUSE UNKNOWN
37	3762	30 SEPT 82	10:30	BACKFLUSHED INJ WELL
38	3766	30 SEPT 82	14:40	PIT FLOW (0.33 HR)
39	3808	2 OCT 82	07:40	ACID TREATMENT ON INJ WELL
40	3886	5 OCT 82	13:00	BACKWASH NO. 1 FILER ON INJ WELL
41	4014	10 OCT 82	19:00	REPLACED PACKING IN INJ PUMP
42	4052	12 OCT 82	12:00	PIT FLOW (0.08 HR)
43	4084	13 OCT 82	22:00	PIT FLOW (0.24 HR)
44	4100	14 OCT 82	10:00	ACID TREATMENT ON INJ WELL
45	4110	14 OCT 82	20:00	PIT FLOW (2 HRS)
46	4138	14 OCT 82	22:00	ATTEMPTS TO LOWER INJ PRESS BY FLOWING
	4182	19 OCT 82	16:00	TO PIT (TOT OF 8 HRS)
47	4238	20 OCT 82	08:00	ACID TREATMENT ON INJ WELL
48	4308	23 OCT 82	06:00	PIT FLOW (0.4 HR)
49	4338	24 OCT 82	12:00	PIT FLOW (0.25 HR)
50	4362	25 OCT 82	10:00	ACID TREATMENT ON INJ WELL
	4526	1 NOV 82	06:00	
	3428	1 NOV 82	06:00	
	3420	31 OCT 82	24:00	
51	4526	1 NOV 82	08:45	SHUT-IN (2.25 HRS), PIT FLOW (12 HRS)
52	4530	1 NOV 82	13:00	SHUT-IN SIGNAL PROBLEMS (6 HRS)
53	4552	2 NOV 82	12:30	SHUT-IN FOR BUILD UP TO (71 HOURS)
54	4623	5 NOV 82	13:00	END BUILD UP 10. CONTINUE SHUT-IN FOR REPAIRS (TOT 325 HRS)
55	4872	15 NOV 82	15:30	BEGIN FLOW TEST 11
56	4884	16 NOV 82	07:00	SHUT-IN FOR REPAIRS (2 HRS)
57	5054	23 NOV 82	10:43	PIT FLOW (0.6 HR)
	5056		12:01	RIG UP OTIS FOR INJ WELL FALL OFF TEST (0.25 HR)
58	5058		14:55	PIT FLOW, FALL OFF TEST (0.25 HR)
	5064		20:04	FALL OFF TEST (0.5 HR)
	** NOTE: AT THIS SAMPLE INTERVAL THE FALL OFF TESTS ARE NOT REFLECTED IN THE INJ PRESS CURVE. LOWS WERE 70 PSI.			
59	5322	4 DEC 82	14:00	CITRIC ACID TREATMENT (16 HRS)
60	5383	7 DEC 82	02:56	SHUT-IN AIR COMPRESSOR FAILURE (2.5 HRS)
61	5437		09:25	CITRIC ACID TREATMENT
			09:30	INJECTION PRESS REACHED 600 PSI WHILE CHANGING FILTERS (NOT ON GRAPH) PIT FLOW (0.5 HR)
	5444		16:30	CITRIC ACID TREATMENT
62	5530	13 DEC 82	05:00	SHUT-IN AIR COMPRESSOR FAILURE (6 HRS)
63	5942	30 DEC 82	08:00	CITRIC ACID TREATMENT
	5988	1 JAN 83	06:00	

G 13509

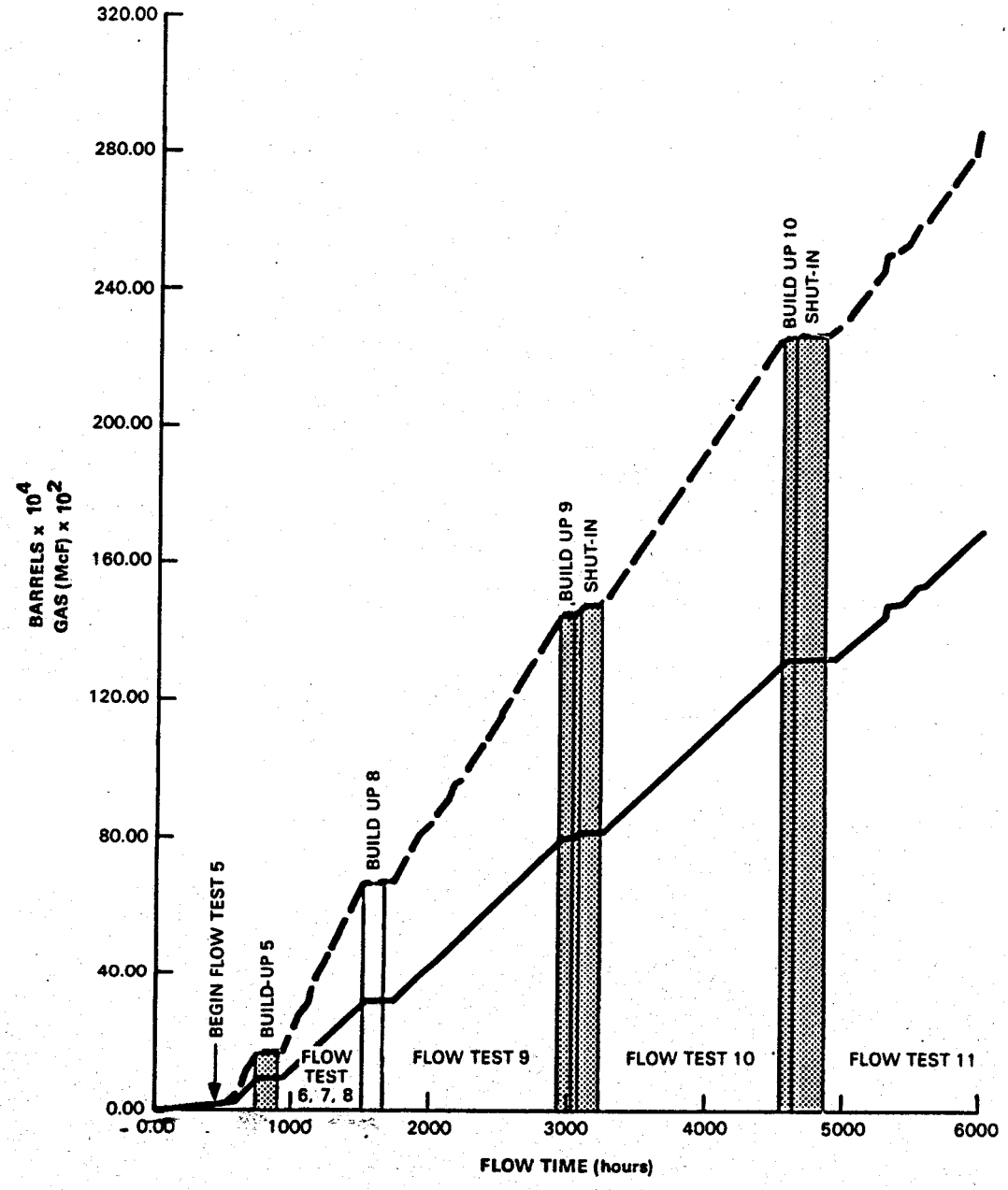

FIGURE 12. CUMULATIVE BRINE AND GAS PRODUCTION FROM THE DOW L.R. SWEEZY NO. 1 GEOPRESSURED/GEOTHERMAL TEST WELL FROM 26 APRIL THROUGH 31 DECEMBER 1982.

G 13504

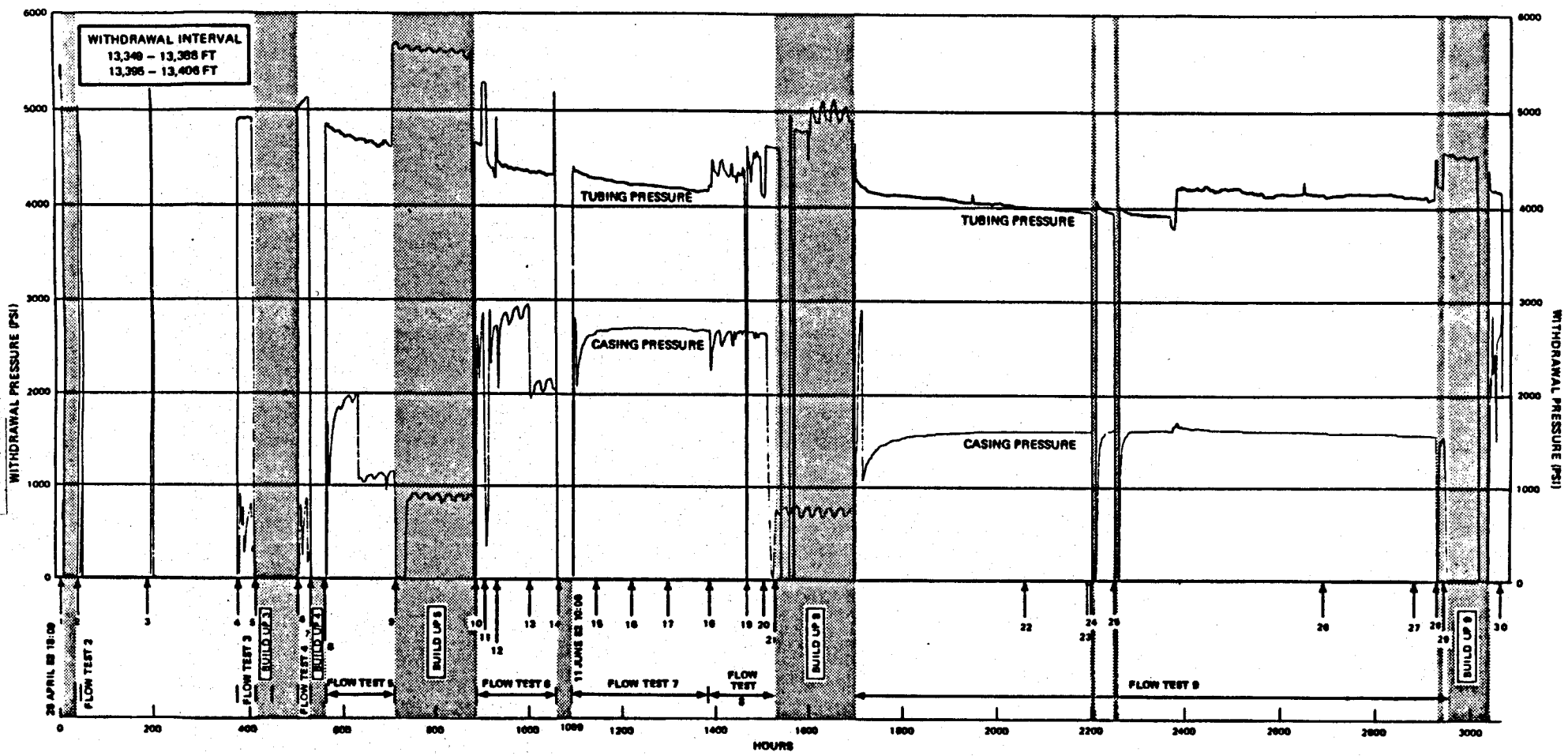

FIGURE 13a. PRODUCTIVE WELL WITHDRAWAL PRESSURE HISTORIES AT THE PARCPERDUE GEOPRESSURED/GEOTHERMAL TEST SITE FROM 28 APRIL TO 31 AUGUST 82.

G 13606A

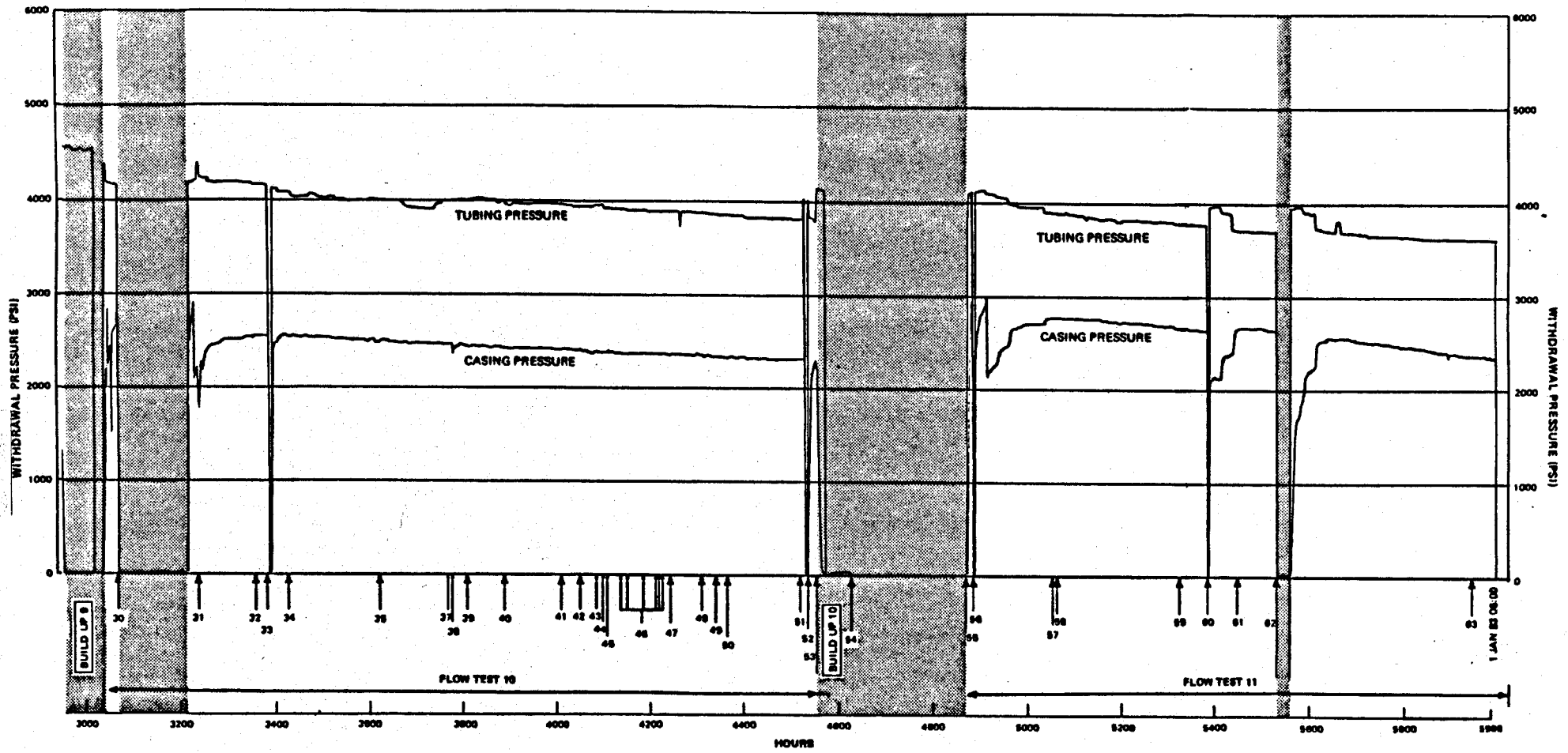

FIGURE 13b. PRODUCTION WELL WITHDRAWAL PRESSURE HISTORIES AT THE PARCPERDUE GEOPRESSURED/GEOTHERMAL TEST SITE FROM 31 AUGUST 82 THROUGH 31 DECEMBER 82

G 136068

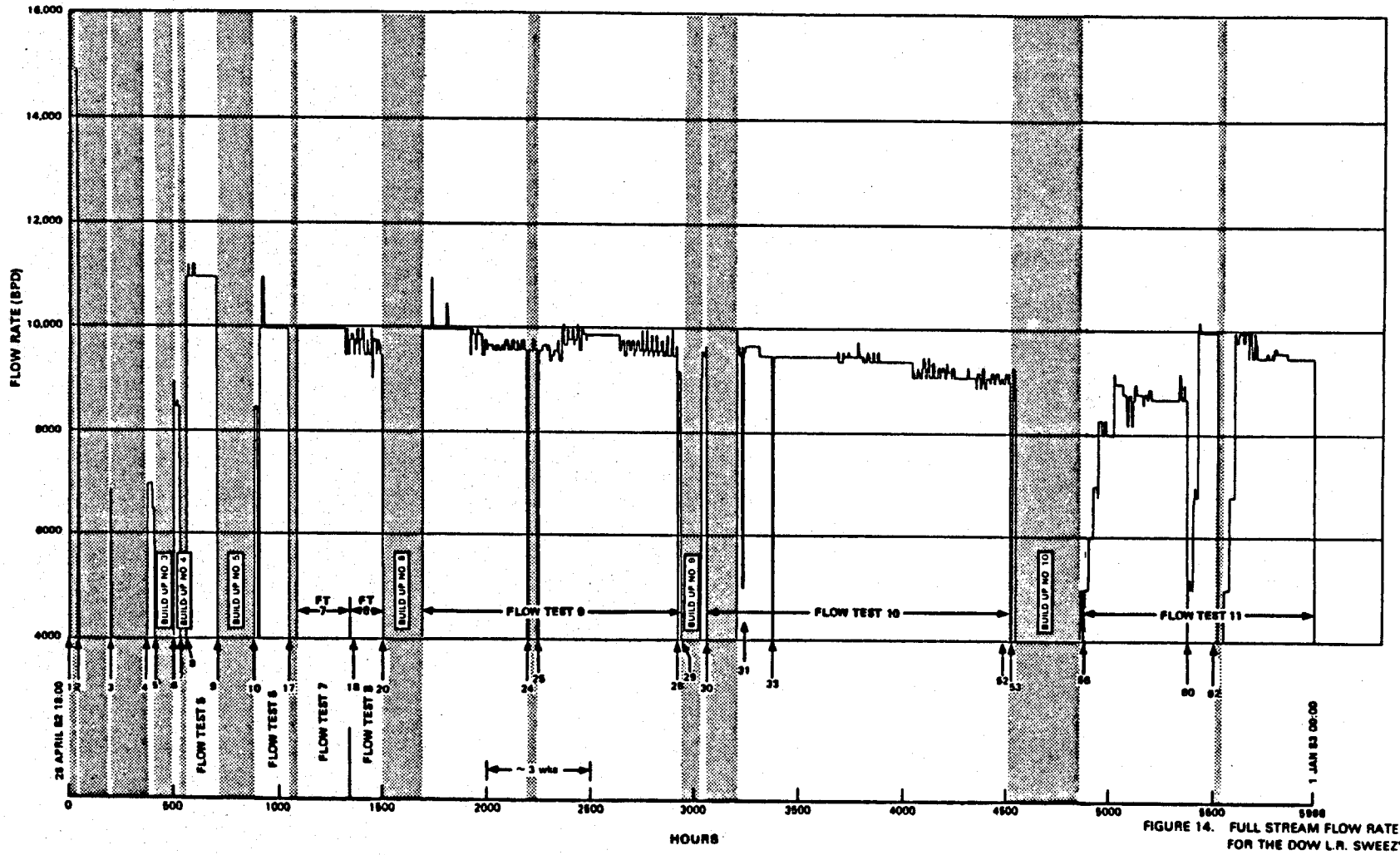

FIGURE 14. FULL STREAM FLOW RATE VERSUS TIME FOR THE DOW L.R. SWEEZY NO. 1 GEO-PRESSURED/GEOTHERMAL TEST WELL FROM 26 APRIL THROUGH 31 DECEMBER 1982

G 13607

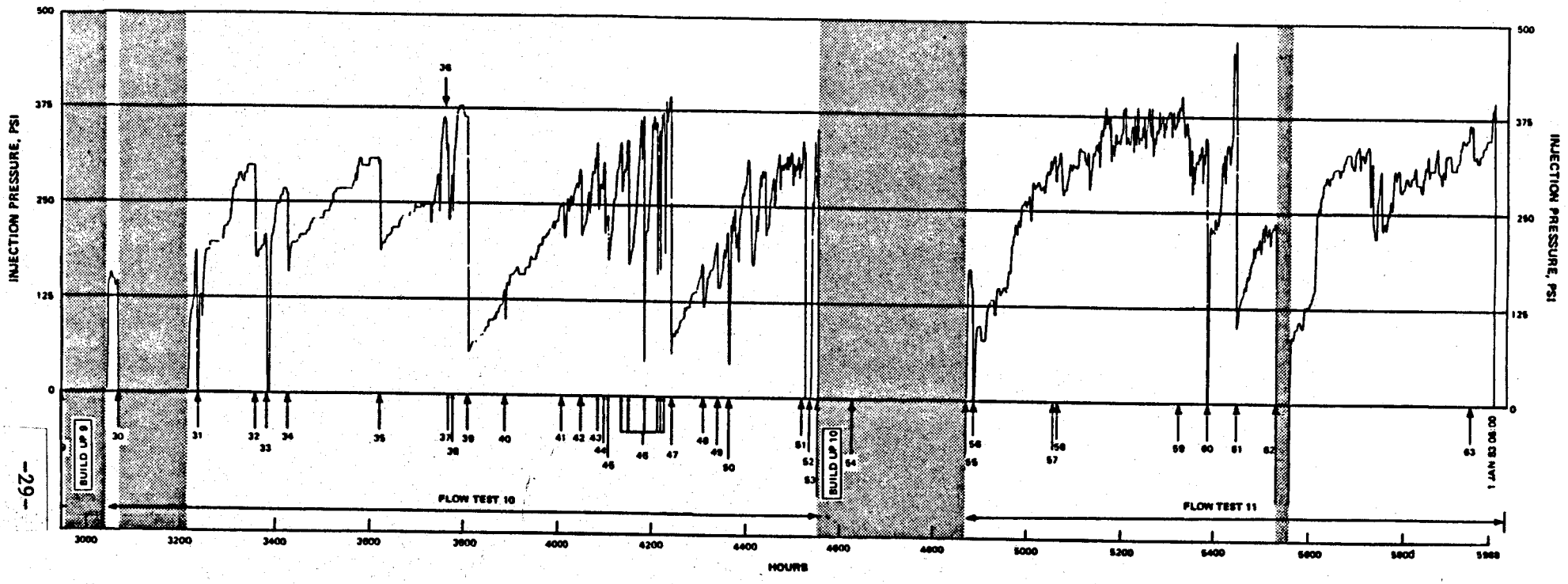

FIGURE 15a. DISPOSAL WELL HISTORY AT THE PARCPERDUE GEOPRESSURED/GEOTHERMAL TEST SITE FROM 26 APRIL THROUGH 1 JAN 83

G131948

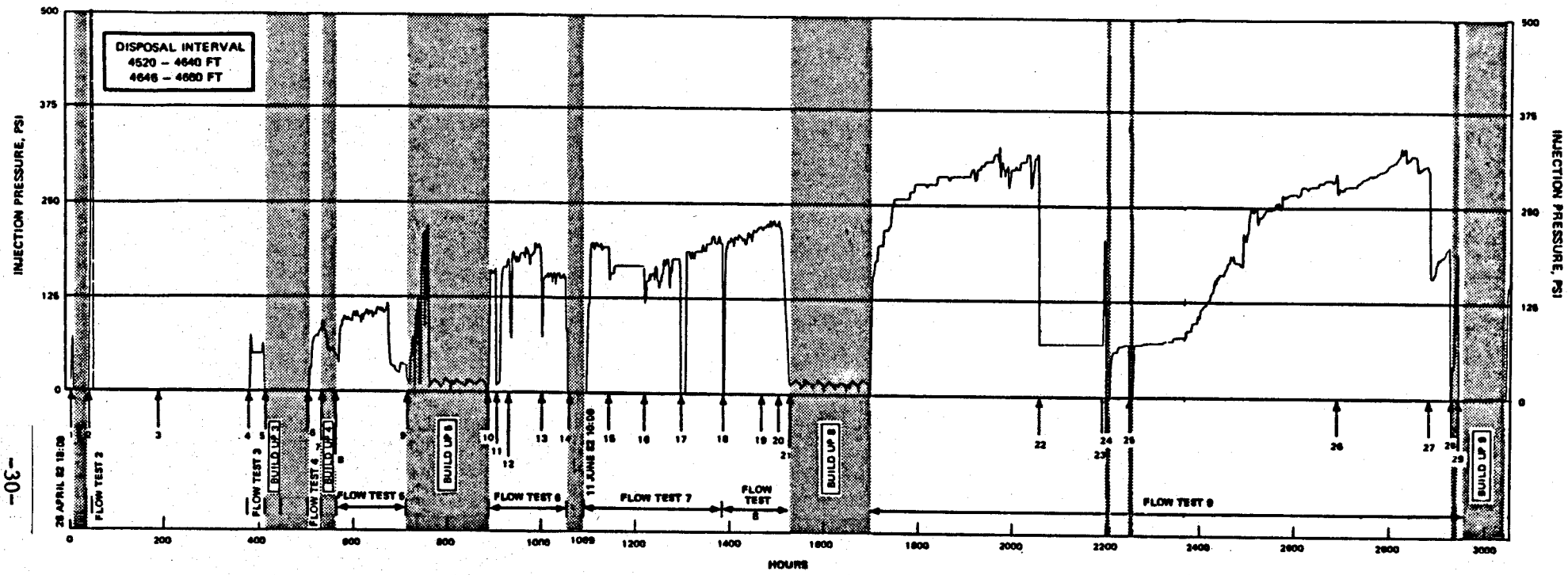

FIGURE 15b. DISPOSAL WELL INJECTION HISTORY AT THE PARCPERDUE GEOPRESSURED/GEOTHERMAL TEST SITE FROM 26 APRIL THROUGH 1 JAN 83

G 13194A

DISCUSSION OF SEISMIC ACTIVITY NEAR THE L. R. SWEEZY SITE
AUGUST 1980 - NOVEMBER 1983

In the data analysis section of this report, we indicated that two primary types of signals were observed throughout the monitoring program (see table 4). An example of an event with observed body waves (type I) is illustrated in figure 16. Note the relatively short time for the initial phase to move-out across the array. Arrival time data of this event type can be inverted by standard techniques (Lee and Lahr, 1972/1975) to determine hypocentral depth as well as epicentral location. It is important to note, however, that with small arrays having less than the ten elements, these depth determinations are not very precise. During the recording history of the Parcperdue seismic array, relatively few events of this type were recorded. With the exception of the Lake Charles, Louisiana, earthquake, 16 October 1983, all of the microearthquakes of this type had hypocentral depths greater than one and a half kilometers but less than the depth of the L. R. Sweezy production zone. Thus, these events could not be related definitively to production or injection operations. The epicentral distribution of the type I events in the vicinity of the L. R. Sweezy well is illustrated on figure 17 by asterisks. There is a relatively close spatial relationship between the location of these events and the proposed location of growth faults at a depth of 16,000 feet. In fact, the spatial correlation is sufficiently high to assume that these events were the result of small movements along these growth faults. The sense of initial motion, which is rarely determinable, is dilatational. This type of motion would be consistent with down-dip motion of the slips.

The more common seismic events recorded not only by the Parcperdue array, but also the Pleasant Bayou, Texas, Rockefeller Refuge, Louisiana, and Sweet Lake, Louisiana, arrays were of the type illustrated in figures 18, 19, and 20. These events are characterized by relatively low-velocity phase arrival move-outs across the arrays which generally are consistent with surface wave velocities. Arrival time data from events of this type cannot be inverted to determine hypocentral depths. Detailed theoretical analyses by Mauk, Kimball, and Davis (1984) in conjunction with analyses of similar events recorded by the Pleasant Bayou array, however, strongly suggest that hypocentral depths for events of this type are less than one kilometer. They obtained best fits between theoretical and observed signals for events with depths between three hundred and eight hundred meters.

The spatial distribution of type II signals recorded by the Parcperdue array is illustrated on figure 16 as solid circles. The spatial correlation of these events with the locations of the growth faults is not as apparent. There is a larger concentration of activity south-southeast of the L. R. Sweezy well, and the concentration of events apparently decreases with increasing distances from the L. R. Sweezy well. This concentration of activity near the geopressured/geothermal well may or may not be significant. Since the resolution of the seismic array also decreases with distance from the well, the decrease of activity with increased distance from the well could be an observational limitation of the array.

TABLE 4. SUMMARY OF IMPORTANT SEISMIC ACTIVITY OCCURRING NEAR THE PARCPERDUE MONITORING ARRAY 1981-1983

Date	UTC Time	Lat (N) Deg	Lat (N) Min	Lat (N) Sec	Long (W) Deg	Long (W) Min	Long (W) Sec	Event* Type	Estimated Depth (km)	Magnitude
81 05 31	19 21 00	No epicenter determined						2	0	0.06
82 02 09	17:44:47.0	No epicenter determined						1		
82 02 26	14:46:16.65	30	02	29.7	91	59	28.1	1	1.55	1.5
82 03 23	23:29:56.48	30	03	16.4	92	02	52.6	2	0	
82 06 10	08:14:00.43	30	02	31.4	92	02	48.7	2	0	
82 06 17	01:03:57.03	30	09	04.2	92	05	04.1	2	0	.46
82 06 17	01:11:45.17	30	09	08.4	92	04	54.0	2	0	
82 06 25	21:04:52:08	30	02	56.6	92	02	34.6	2	0	-.16
82 07 17	21:44:11.96	30	03	18.4	92	00	09.1	2	0	
82 07 23	11:45:27.41	30	01	38.2	92	00	26.1	2	0	
82 07 31	23:11:13.98	30	01	49.9	92	01	10.2	2	0	
82 08 06	23:33:38.64	30	03	50.3	92	00	32.9	2	0	
82 08 08	11:39:07.98	29	58	44.1	92	02	26.0	2	0	
82 08 16	19:16:09.20	30	03	10.30	92	02	48.5	2	0	

* 1 Events with identifiable body phases

2 Events with only surface waves

TABLE 4. SUMMARY OF IMPORTANT SEISMIC ACTIVITY OCCURRING NEAR THE PARCPERDUE MONITORING ARRAY 1981-1983 (continued)

Date	UTC Time	Lat (N) Deg	Lat (N) Min	Lat (N) Sec	Long (W) Deg	Long (W) Min	Long (W) Sec	Event* Type	Estimated Depth (km)	Magnitude
82 08 17	00:19:37.24	30	03	22.7	92	02	44.2	2	0	
82 08 17	00:21:48.70	30	03	18.9	92	02	58.7	2	0	
82 10 26	13:40:32.17	30	04	24.1	92	00	58.5	1	2.5	
83 02 23	18:30:05.90	30	03	31.3	92	02	32.0	2	0	
83 03 23	21:16:40.0	30	03	47.7	92	02	11.3	2	0	
83 03 23	21:17:28.2	30	03	57.6	92	02	22.4	2	0	
83 03 23	21:23:53.5	30	06	02.5	92	02	42.3	2	0	
83 03 30	06:23:09.0	30	04	07.3	92	01	58.8	2	0	
83 03 30	06:25:08.3	30	03	08.9	92	01	34.8	2	0	
83 03 30	06:34:50.2	30	01	16.0	92	02	17.0	2	0	
83 03 30	06:38:16.6	30	02	42.9	92	01	53.8	2	0	
83 03 30	06:39:12.8	30	02	34.6	92	01	54.7	2	0	
83 03 30	06:40:45.5	30	02	17.0	92	01	56.9	2	0	
83 03 30	06:44:08.1	30	02	22.4	92	01	51.1	2	0	
83 03 30	06:46:07.5	30	02	31.5	92	01	50.0	2	0	
83 03 30	06:54:07.6	30	03	38.8	92	01	48.9	2	0	

TABLE 4. SUMMARY OF IMPORTANT SEISMIC ACTIVITY OCCURRING NEAR THE PARCPERDUE MONITORING ARRAY 1981-1983 (continued)

Date	UTC Time	Lat (N) Deg	Lat (N) Min	Lat (N) Sec	Long (W) Deg	Long (W) Min	Long (W) Sec	Event* Type	Estimated Depth (km)	Magnitude
83 03 30	06:57:57.2	30	02	50.6	92	01	43.1	2	0	
83 03 30	07:00:37.3	30	02	17.9	92	03	04.6	2		
83 03 30	07:07:55.1	30	02	39.9	92	02	09.6	2		
83 03 30	07:09:09.7	30	02	34.3	92	02	13.1	2		
83 03 30	07:09:40.9	30	02	35.9	92	02	35.8	2		
83 03 30	07:10:40.1	30	02	46.5	92	02	24.2	2		
83 03 30	07:14:01.1	30	02	45.2	92	02	07.1	2		
83 03 30	07:16:38.1	30	02	05.7	92	02	16.0	2		
83 03 30	07:18:24.2	30	02	13.8	92	02	00.3	2		
83 03 30	07:22:07.2	30	02	21.9	92	01	49.3	2		
83 03 30	07:26:22.4	30	02	30.3	92	01	51.1	2		
83 03 30	07:27:13.1	30	02	51.4	92	01	48.2	2		
83 03 30	07:28:58.9	30	02	30.2	92	01	45.6	2		
83 03 30	07:30:36.3	30	02	41.1	92	01	43.6	2		
83 03 30	08:27:44.1	30	03	37.4	92	03	40.5	2		
83 03 30	09:17:11.3	30	03	56.6	92	01	23.2	2	0	

TABLE 4. SUMMARY OF IMPORTANT SEISMIC ACTIVITY OCCURRING NEAR THE PARCPERDUE MONITORING ARRAY 1981-1983 (continued)

Date	UTC Time	Lat (N) Deg	Lat (N) Min	Lat (N) Sec	Long (W) Deg	Long (W) Min	Long (W) Sec	Event* Type	Estimated Depth (km)	Magnitude
83 03 30	10:54:01.4	30	01	40.1	92	00	19.3	2	0	
83 03 30	11:00:09.9	30	02	47.2	92	01	46.0	2	0	
83 03 30	11:09:59.9	30	02	46.3	92	01	44.2	2	0	
83 03 30	11:10:51.1	30	02	58.8	92	01	42.4	2	0	
83 03 30	11:15:27.4	30	02	30.9	92	01	47.1	2	0	
83 03 30	17:34:19.5	30	04	15.6	92	01	18.4	2	0	
83 03 30	18:30:06.7	30	02	33.2	92	03	00.9	2	0	
83 03 30	19:32:52.2	30	03	07.3	92	02	13.6	2	0	
83 03 31	01:59:09.3	30	02	35.1	92	03	04.9	2	0	
83 05 19	13:51:47.1	30	01	03.0	92	03	06.1	2	0	
83 05 19	13:52:46.1	30	02	54.1	92	02	02.4	2	0	
83 05 19	13:54:11.1	30	02	56.6	92	02	06.6	2	0	
83 05 19	13:55:21.7	30	03	21.4	92	01	40.6	2	0	
83 05 19	13:57:13.0	30	02	46.3	92	01	46.0	2	0	
83 05 19	15:10:32.3	30	02	07.7	92	03	09.8	2	0	
83 05 19	15:16:50.0	30	01	23.9	92	03	10.0	2	0	

TABLE 4. SUMMARY OF IMPORTANT SEISMIC ACTIVITY OCCURRING NEAR THE PARCPERDUE MONITORING ARRAY 1981-1983 (continued)

Date	UTC Time	Lat (N) Deg	Lat (N) Min	Lat (N) Sec	Long (W) Deg	Long (W) Min	Long (W) Sec	Event* Type	Estimated Depth (km)	Magnitude
83 05 19	15:30:06.0	30	04	16.4	92	00	57.2	2	0	
83 06 28	01:30:10.5	30	02	38.3	92	01	43.4	2	0	
83 06 28	01:37:39.5	30	04	37.2	92	00	25.7	2	0	
83 06 28	01:39:31.6	30	04	55.1	92	00	14.8	2	0	
83 06 28	01:44:43.2	30	04	32.5	92	00	22.0	2	0	
83 06 28	01:48:12.2	30	02	48.3	92	01	31.4	2	0	
83 06 28	01:56:40.5	30	03	22.3	92	00	35.2	2	0	
83 06 28	02:02:01.2	30	03	47.8	92	00	26.1	2	0	
83 07 05	23:41:32.0	30	04	42.0	92	01	24.6	2	0	
83 08 03	05:52:47.2	30	04	26.2	92	01	27.1	2	0	
83 08 03	05:53:19.9	30	03	40.1	92	01	34.2	2	0	
83 08 03	05:54:40.0	30	03	18.4	92	01	36.3	2	0	
83 08 03	05:56:24.1	30	02	27.8	92	02	18.5	2	0	
83 08 03	06:04:11.3	30	03	45.9	92	00	41.0	2		
83 08 03	06:07:21.8	30	03	33.1	92	00	59.6	2		
83 08 03	06:12:01.9	30	04	46.8	92	01	38.4	2		

TABLE 4. SUMMARY OF IMPORTANT SEISMIC ACTIVITY OCCURRING NEAR THE PARCPERDUE MONITORING ARRAY 1981-1983 (continued)

Date	UTC Time	Lat (N) Deg	Lat (N) Min	Lat (N) Sec	Long (W) Deg	Long (W) Min	Long (W) Sec	Event* Type	Estimated Depth (km)	Magnitude
83 08 03	06:37:43.8	30	03	45.8	92	02	20.1	2		
83 08 03	06:39:42.2	30	03	49.5	92	02	19.7	2		
83 08 03	06:46:41.1	30	03	23.9	92	02	26.8	2		
83 08 03	06:49:39.3	30	04	09.5	92	00	33.4	2		
83 08 03	06:58:58.4	30	04	26.2	92	00	53.8	2		
83 08 03	07:01:03.9	30	04	20.5	92	01	55.9	2		
83 10 03	22:03:19.5	30	03	19.2	92	01	58.5	2	0	-0.10
83 10 03	22:24:05.3	30	03	18.9	92	01	58.7	2	0	-1.42
83 10 06	19:05:29.0	30	03	00.6	92	02	00.7	2	0	0.72
83 10 06	21:18:51.8	30	03	06.6	92	02	16.0	2	0	0.70
83 10 12	10:11:53.3	30	03	00.6	92	01	57.2	2	0	-0.63
83 10 12	10:13:16.5	30	03	25.3	92	02	03.0	2	0	-0.97
83 10 12	10:34:43.9	30	02	51.0	92	01	45.1	2	0	-0.59
83 10 12	10:39:30.0	30	03	18.6	92	01	40.5	2	0	-0.26
83 10 13	11:50:45.0	30	03	15.2	92	01	59.1	1		
83 10 14	01:08:30.4	30	03	16.1	92	02	05.5	2	0	0.75

TABLE 4. SUMMARY OF IMPORTANT SEISMIC ACTIVITY OCCURRING NEAR THE PARCPERDUE MONITORING ARRAY 1981-1983 (continued)

Date	UTC Time	Lat (N) Deg	Lat (N) Min	Lat (N) Sec	Long (W) Deg	Long (W) Min	Long (W) Sec	Event* Type	Estimated Depth (km)	Magnitude
83 10 14	01:11:46.0	30	03	04.2	92	02	12.8	2	0	0.13
83 10 14	02:13:24.7	30	03	08.6	92	02	19.7	2	0	0.08
83 10 16	19:40:46.1	Lake Charles, Louisiana								
83 10 27	18:38:29.7	30	03	38.1	92	01	46.7	2	0	1.26
83 11 02	16:00:48.6	30	03	52.1	92	01	46.6	2	0	1.16
83 11 03	18:45:18.8	30	04	00.8	92	01	42.1	2	0	.89
83 11 10	20:54:33.4	30	03	17.4	92	01	56.7	2	0	.51
83 11 16	11:10:08.7	30	03	06.5	92	02	30.2	2	0	-.46
83 11 16	17:43:41.9	30	03	37.1	92	02	08.2	2	0	.72

Computation of event magnitudes generally was based on signal duration. The largest near-regional event to occur during the operational period of the network was the Lake Charles, Louisiana, earthquake with a magnitude of 3.2 - 3.4. All type I events generally had magnitudes less than 1.0. Events of this magnitude do not attain accelerations sufficiently high to constitute a short-term hazard or risk.

One of the principal objectives of this study has been to assess the likelihood that production of the geopressured/geothermal brines would result in enhanced local seismicity. Such an assessment assumes that the ambient seismicity can be characterized prior to production sufficiently well to recognize significant differences in activity level. Approximately fourteen months of nearly continuous monitoring preceded flow testing of the L. R. Sweezy well. The temporal distribution of seismic activity at Parcperdue for this period, during flow testing, and for seven months post shut-in is illustrated in figure 21. An examination of this diagram clearly shows that activity during production and shut-in are at a much higher level than prior to production of the geopressured/geothermal brines. If it is assumed that no significant production changes occurred from other wells in the vicinity of the Bayou Parcperdue test (an assumption unconfirmed by the authors), then production from the L. R. Sweezy well did result in enhanced local seismicity, predominantly from very shallow depths. Similar results have been reported for the Pleasant Bayou test program in Texas (Mauk, Kimball, and Davis, 1984).

It is interesting to note several points about the temporal distribution of seismicity at Parcperdue. (1) The seismicity is sporadic, and does not display any characteristics associated with particular fine details of the production or injection history of the well. Prior to production, events generally occurred individually scattered randomly in time. Post production, and particularly post shut-in, the seismicity occurred in swarms. The timing of several of these swarms was coincident with times of heavy rainfall (see figure 22) suggesting the likelihood that the swarms may have been triggered by other conditions. No similar swarm activity was reported for the Pleasant Bayou geopressured/geothermal well test site. This significant change in behavior punctuated by the production testing of the L. R. Sweezy well could be interpreted as a definite cause/effect relationship. However, considering the overall character of the seismicity, it is equally plausible that the level of activity prior to production was merely a hiatus of seismicity following some previous and unrecorded period of swarms. Thus, although the former interpretation is favored by the authors, the likelihood of the latter interpretation cannot be discounted.

Although the Bayou Parcperdue microearthquakes do not constitute a seismic hazard or risk due to associated accelerations, their cumulative displacements may pose a local hazard due to increased subsidence rates. VanSickle and Groat (1981) reported the results of a first-order leveling survey along route 339 in Vermillion Parish between 1968 and 1980. The reported relative differential displacements in the vicinity of the L. R. Sweezy test well are given on figure 23. The epicenters of the microearthquakes recorded by the Parcperdue array from 1980 through 1983 are illustrated on this figure as solid circles. Although the first-order leveling survey and the seismicity

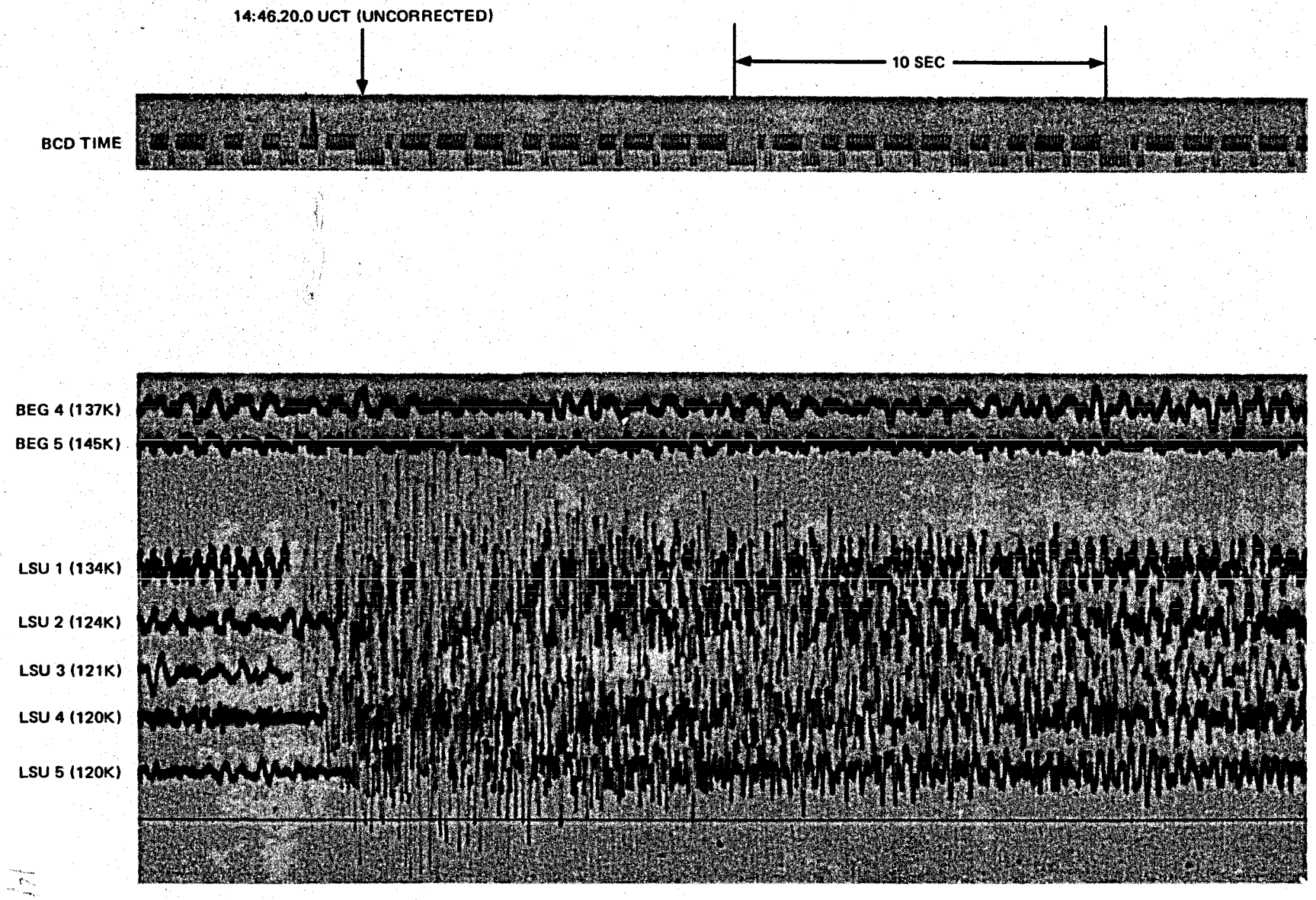

FIGURE 16. MICROEARTHQUAKE, 26 FEBRUARY 1982, 14:46:16.65 UTC (CST + 6 HRS), MAGNITUDE $M_D = 1.5$, DEPTH = 1.55 km.

G 12611

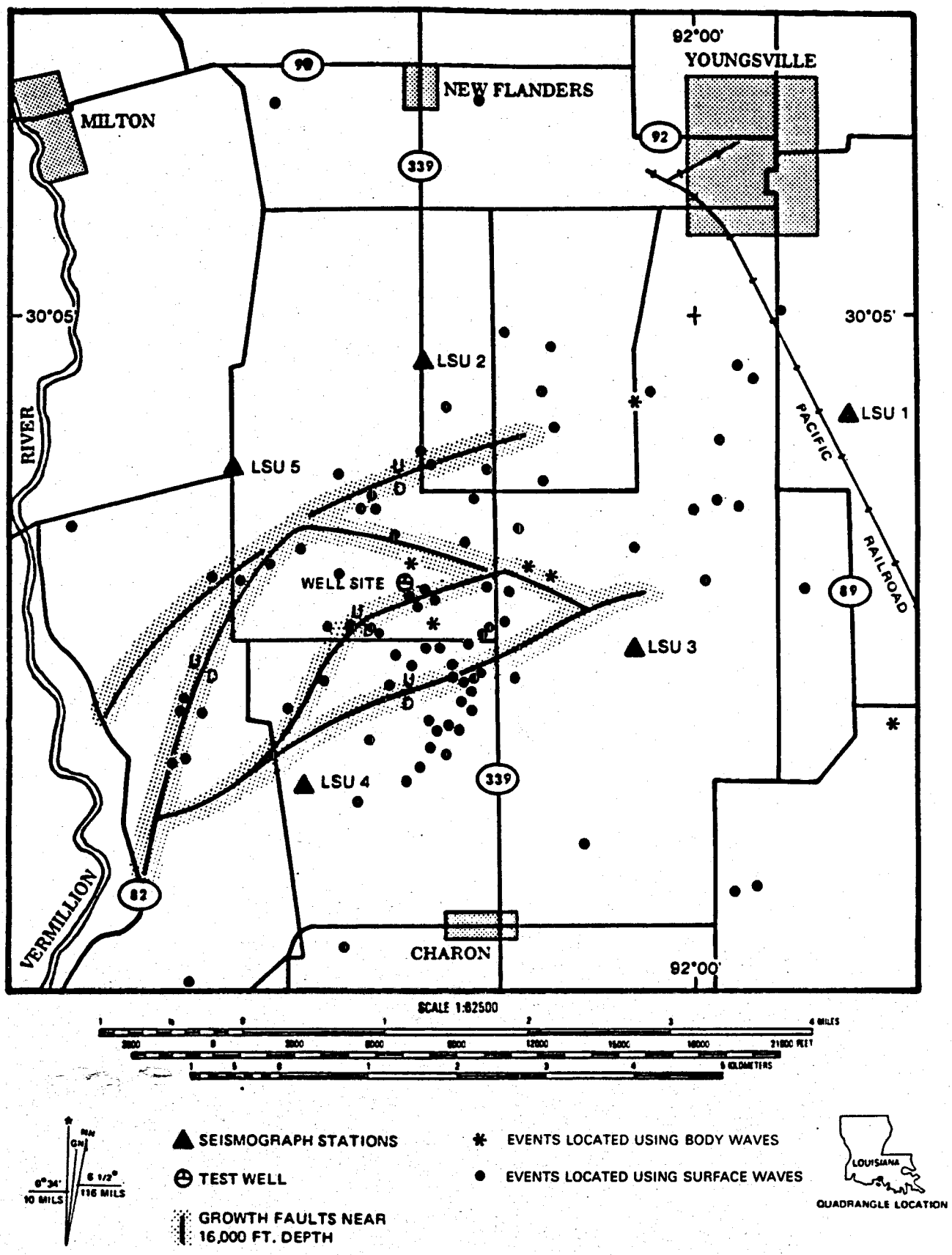

FIGURE 17. LOCATION OF THE MICROEARTHQUAKE ACTIVITY (PRESUMED TO BE OF NATURAL ORIGIN) OCCURRING IN THE VICINITY OF THE PARCPERDUE ARRAY DURING THE MONITORING PROGRAM

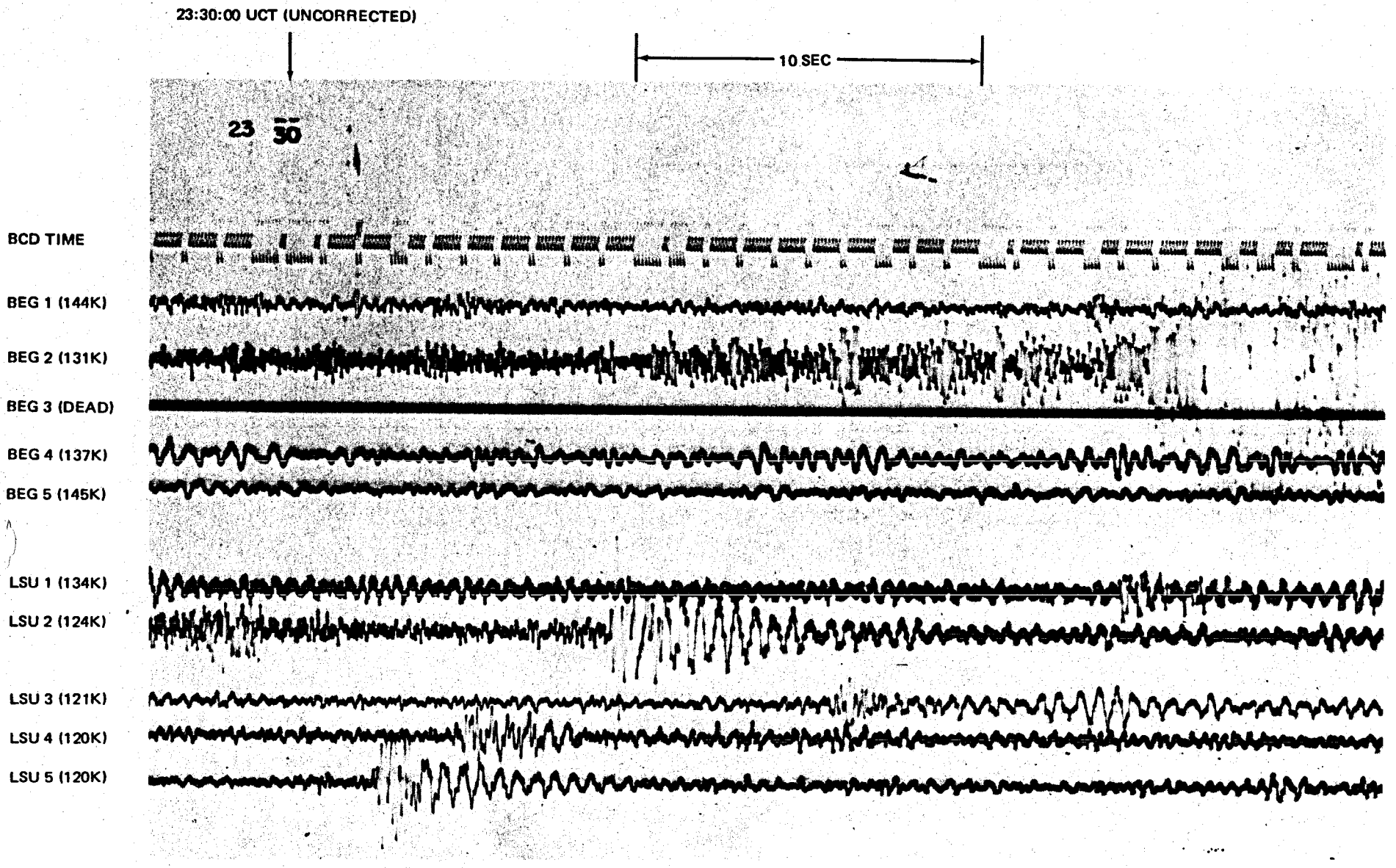

FIGURE 18. RAYLEIGH SURFACE WAVE EVENT, 23 MARCH 1982 AT 23:29:56.48 UTC.
VELOCITY - 250 METERS/SECOND

G 13491

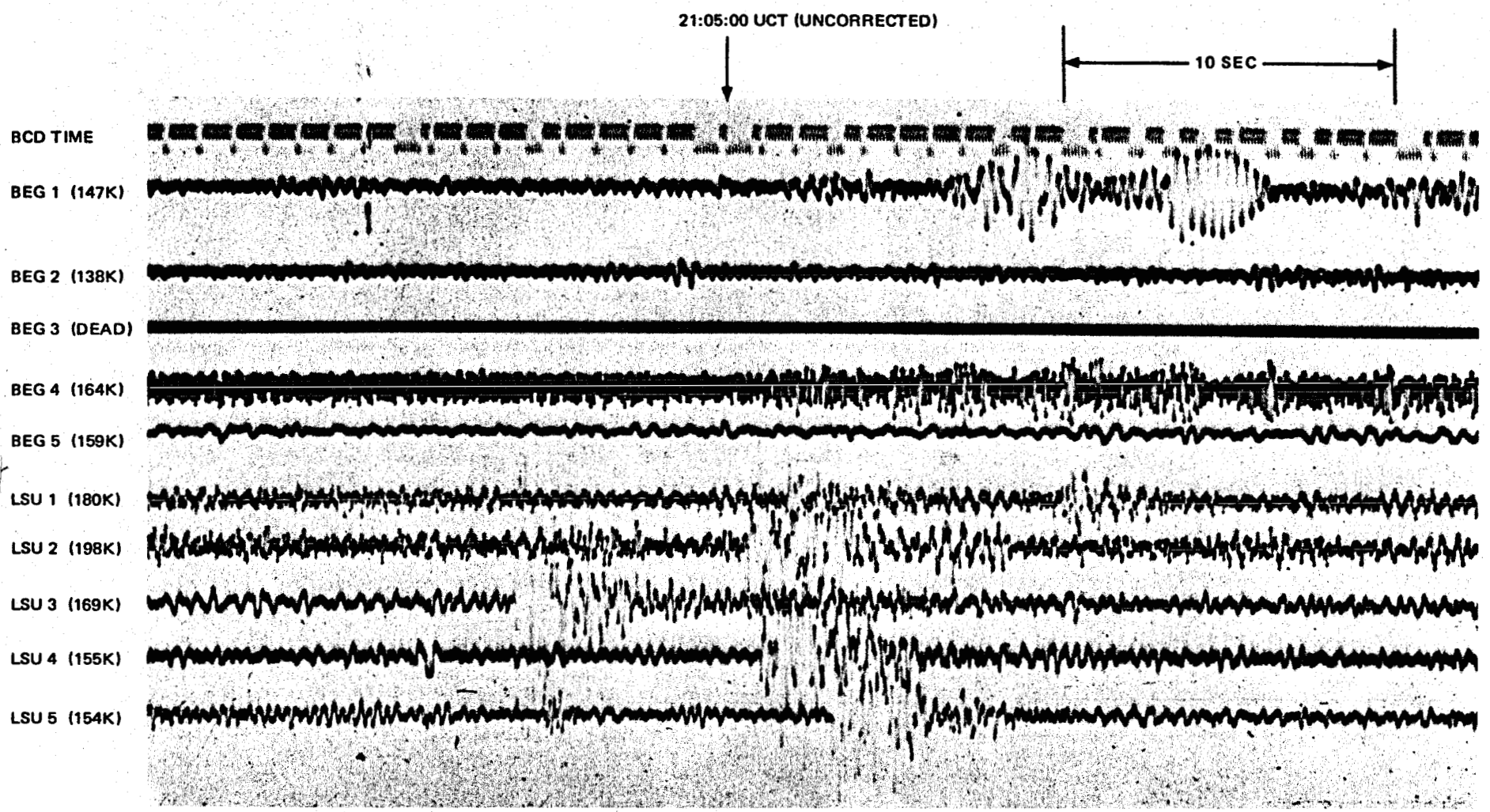

G 12916

FIGURE 19. RAYLEIGH LEAKING MODE EVENT, 25 JUNE 1982 AT 21:04:52.08 UTC, VELOCITY - 330 METERS/SECOND

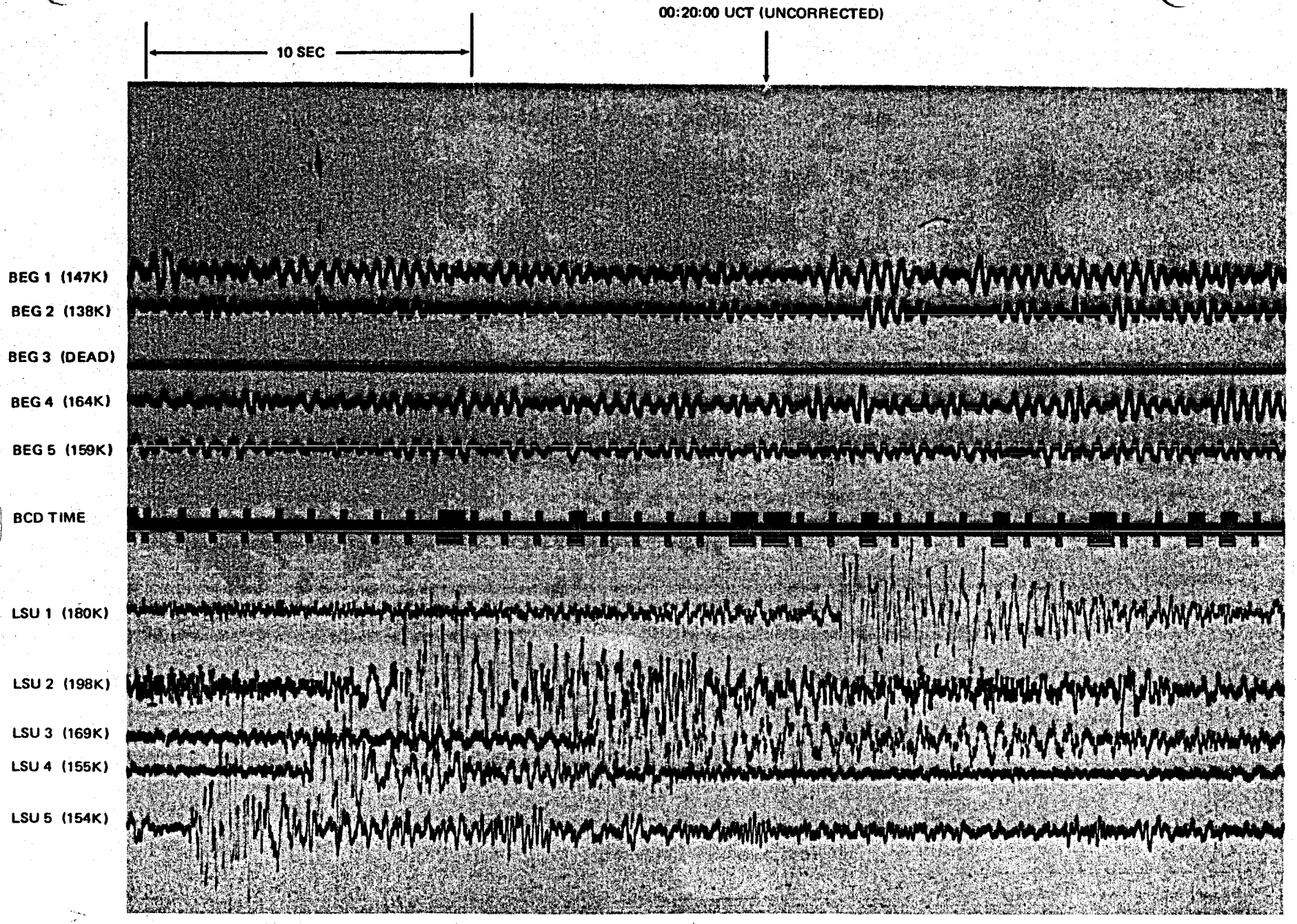

FIGURE 20. RAYLEIGH LEAKING MODE EVENT, 17 AUGUST 1982 AT 00:19:37.24 UTC, VELOCITY - 260 METERS/SECOND

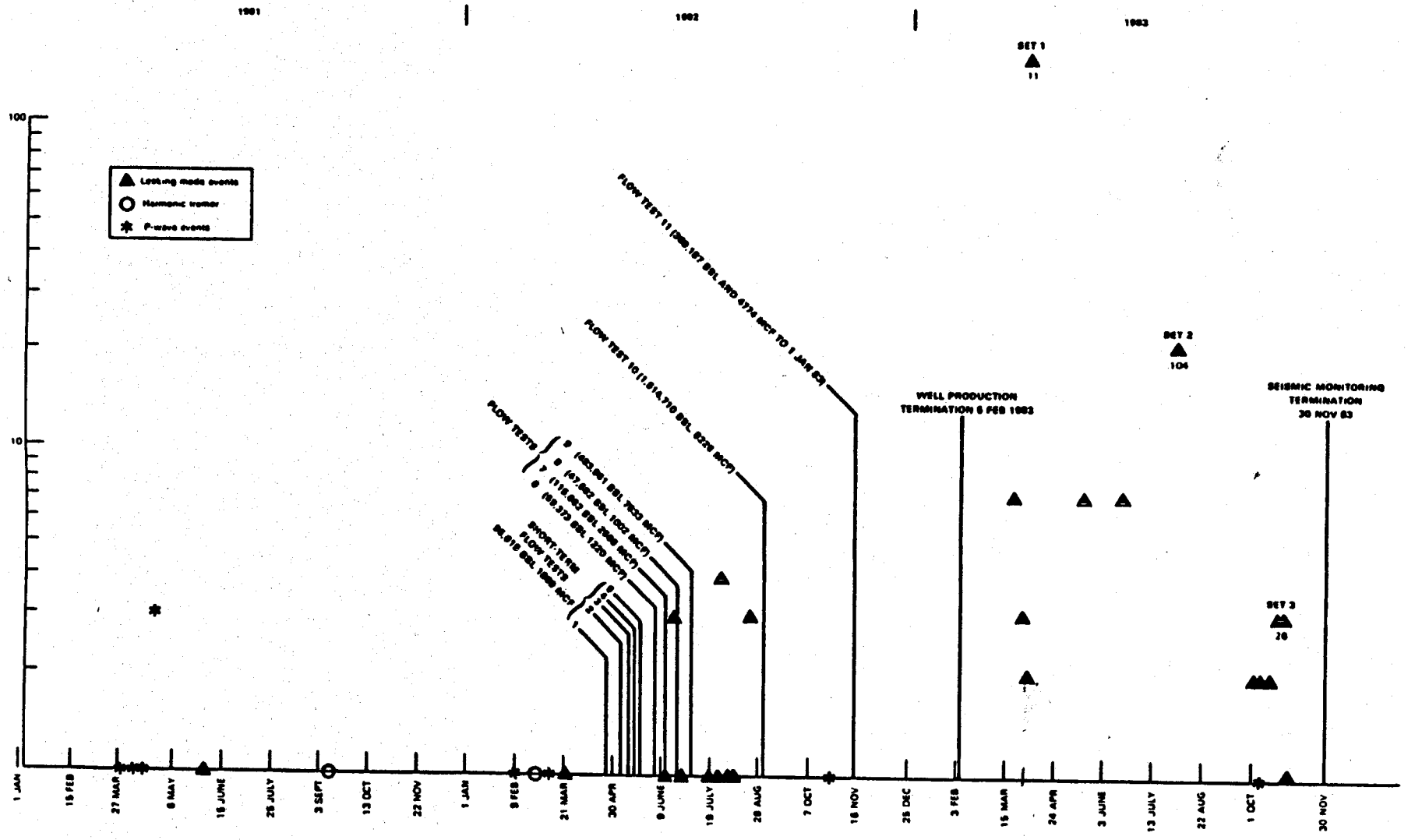

FIGURE 21. TEMPORAL DISTRIBUTION OF SEISMIC ACTIVITY AT PARCPERDUE FOR 1981 THROUGH 30 NOVEMBER 1983. FLOW TESTING EPISODES AT THE L.R. SWEEZY NO. 1 ARE INDICATED. G14029

748

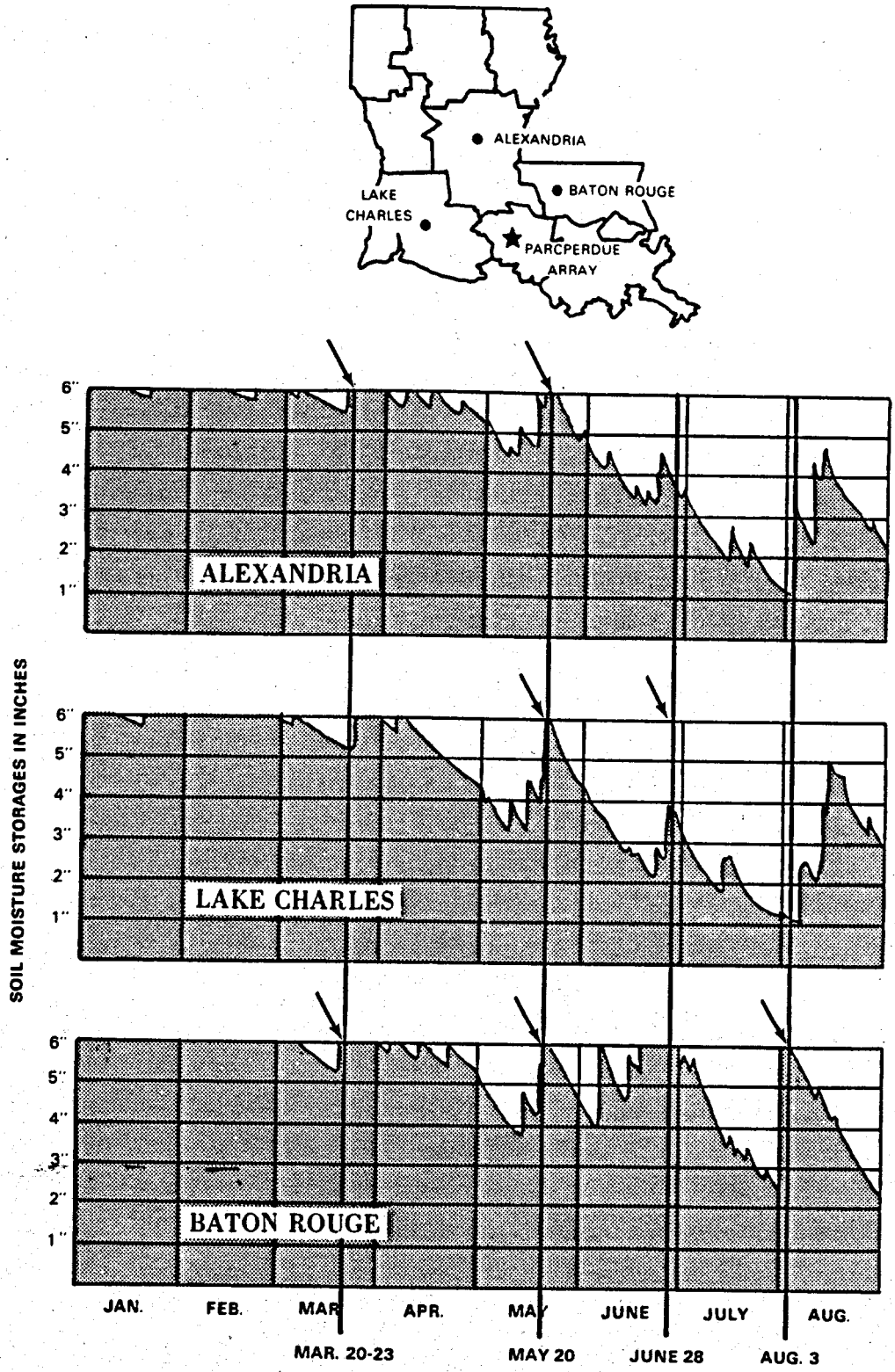

FIGURE 22. CORRELATION OF MICROEARTHQUAKE ACTIVITY IN THE VICINITY OF THE PARCPERDUE SEISMIC MONITORING ARRAY WITH SOIL MOISTURE STORAGE (1983 DAILY WATER BUDGETS SOIL MOISTURE STORAGE 6" CAPACITY FROM LOUISIANA MONTHLY CLIMATE REVIEW)

G 14305 A

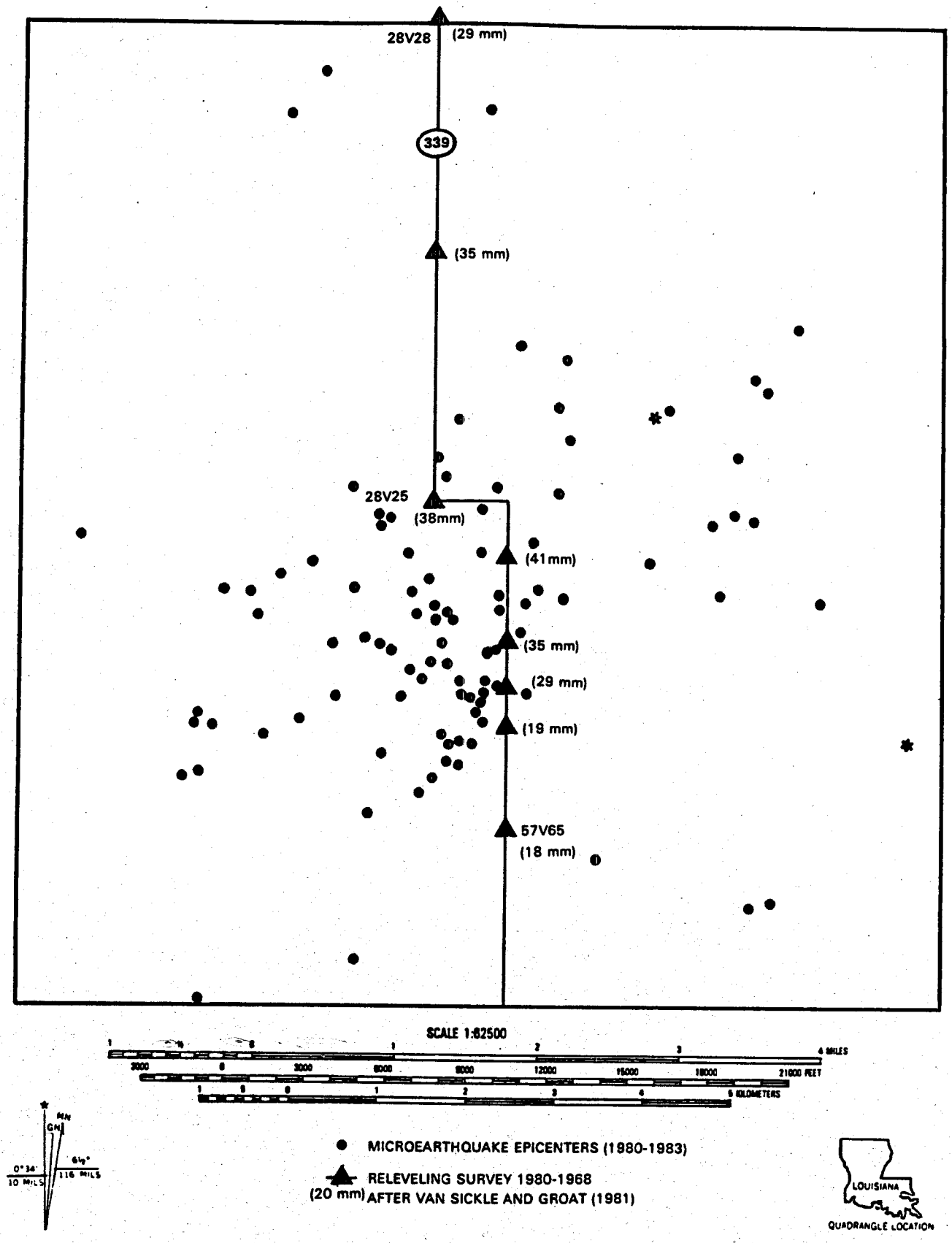

FIGURE 23. DISTRIBUTION OF SEISMICITY AT PARCPERDUE 1980 - 1983 AND FIRST ORDER RELEVELING SURVEY (1980 - 1968) ALONG ROUTE 339.

G14901

distribution cover independent but continuous time periods, it is obvious that the location of the greatest subsidence and highest density of epicenters are coincident. Since the first-order leveling was performed prior to production from the L. R. Sweezy well and clearly demonstrates a high rate of subsidence near the test well site, it is not possible to conclude that brine production resulted in accelerated subsidence. However, the results of the seismic monitoring program do suggest that the subsidence may not occur completely aseismically. If this is true, seismic monitoring of regions of interest in the Gulf Coast may indicate specific sites where accelerated subsidence problems might be occurring. Seismic monitoring, therefore, could be an extremely cost-effective method to locate sites for intensive study.

In conclusion, microseismic monitoring of the Bayou Parcperdue region around the L. R. Sweezy test well in Vermillion Parish, Louisiana, from 1980 through 1983 has resulted in the following observations.

1. Two dominant types of seismic events are observed, one with identifiable body phases, the other with only surface wave signatures. The latter event type is by far the more commonly observed signal.

2. The hypocenters of the microearthquakes located using body phases have depths apparently greater than 1.5 kilometers, but less than the production zone depth of the geopressured/geothermal test well. The epicenters of these events are spatially coincident with the position of known growth faults at a depth of 16,000 feet. The P-wave first motions of the events are rarely identifiable. Those which are clear suggest a dilitational first motion, i.e., down-dip slip of the fault plane.

3. Epicenters of microearthquakes located using surface waves concentrate near the L. R. Sweezy well. Mauk, Kimball and Davis (1984) report convincing evidence that these events have hypocentral depths between 300 and 800 meters. The locations of these events do not clearly associate with the position of growth faults; however, they are concentrated where a previous leveling survey indicated the highest rate of subsidence.

4. The magnitudes of the microearthquakes have all been less than 1.5 with the exception of an event hear Lake Charles, Louisiana. Neither the size nor number of events recorded constitute a seismic hazard due to accelerations. The coincidence of the seismic activity with an area of known relative high subsidence rates may suggest the seismicity could be used to identify regions where subsidence displacement could be a longer term risk.

5. The temporal distribution of microearthquakes may suggest that production from the L. R. Sweezy well resulted in accelerated activity. Prior to production, the rate of seismicity was extremely low. During brine production, the rate of seismicity increased dramatically from the previous ambient condition. The highest rate of activity was in the form of swarms post shut-in of the L. R. Sweezy well. Because the activity during shut-in occurred as swarms, it is

uncertain whether the ambient condition prior to production was truly representative or merely a hiatus between swarms. An unequivocal causal relationship thus could not be demonstrated between specific production and/or disposal activities at the L. R. Sweezy test site and the occurrences of specific seismic activity. It seems likely, however, that brine production resulted in induced seismic activity.

REFERENCES

Aki, K., (1981), Source and Scattering Effects on the spectra of small local earthquakes, Bull. Seis. Soc. Amer., 71, pp 1687-1701.

Aki, K., and Chouet, L. B., (1975), Origin and Coda Waves: Source, Attenuation and Scattering Effects, Jour. Geophys. Res., 80, pp 3322-3342.

Chouet, B., Aki, K., and Tsujiura, M., (1978), Regional Variation of the Scaling Law of Earthquake Source Spectra, Bull. Seis. Soc. Amer., 68, pp 49-79.

DOW Chemical Company (1982), Geopressured/Geothermal Drilling and Testing Plan Volume II Testing Plan DOW Chemical Co.-Department of Energy DOW-DOE Sweezy No. 1 Well Vermillion Parish Louisiana, February 1982, Publication No. NVO-216, vol. 2.

Jardetzky, W. S., and Press, F., (1952), Rayleigh Wave Coupling to Atmospheric Compression Waves, Bull. Seis. Soc. Amer., 42, pp 135-144.

Lee, W. H. K., and Lahr, J. C., (1972/1975), HYPO71 (revised): A computer program for determining hypocenter, magnitude and first motion pattern of local earthquakes, U.S.G.S Open file report 75-311.

Mauk, F. J., (1984), Microseismic Monitoring of Chocolate Bayou, Texas, the Pleasant Bayou No. 2 Geopressured/Geothermal Energy Test Well Program, Final Report, Teledyne Geotech Technical Report No. 84-1, 70 p.

Street, R. L., Herrmann, R. B., and Nuttli, O. W., (1975), Spectral Characteristics of the Lg-Wave generated by Central United States Earthquakes, Geophys. Jour., 41, pp 51-63.

VanSickle, V. R., and Groat, C. G., (1981), Subsidence and Induced Faulting: Key Environmental Issues in Geopressured/Geothermal Resource Development, in Proceedings of the Fifth Conference on Geopressured/Geothermal Energy, U. S. Gulf Coast, edited by D. G. Bebout and A. L. Bachman, October 13-15, 1981, Louisiana State University, Baton Rouge, Louisiana, pp 325-330.

APPENDIX A

DISCUSSION OF OBSERVED ACTIVITY FOR OCTOBER AND NOVEMBER, 1983

APPENDIX A

DISCUSSION OF OBSERVED ACTIVITY FOR OCTOBER AND NOVEMBER, 1983

During the fourth quarter of FY83 monitoring period, several types of events were recorded by the Parcperdue seismic array. Exploration shot series were recorded on eleven separate days during the quarter. In addition to the exploration shots, nine sonic booms, three teleseisms, one P-wave type local event and twenty-one Rayleigh type events were recorded. Seventeen of the Rayleigh events yield hypocenter locations within ten kilometers of the array center. Twelve of these events originating in the immediate vicinity of the monitoring array occurred in October, five occurred during November. Figure A1 shows the epicenter locations of the events. Origin time of the events and station arrival times are documented in Table A1. Table A2 lists geographical coordinates of events shown in figure A1. Typical examples of the seismograms are illustrated in figures A2 through A5.

The monitoring program final report discusses the iterative method of determining a velocity for Rayleigh/leaking mode event epicenter location, and the uncertainty associated with these locations. October and November 1983 events shown in figure A-1 are located using velocities ranging from 100 to 250 meters/second. These extremely low velocities produce the minimum least-squares error epicenter location solution, but are difficult to explain by physical laws of propagation.

Assuming that the epicenter locations shown in figure A-1 are correct, events occurring in October and November are generally localized in the vicinity of the well site. Duration magnitudes (M_d) of the events range from -1.4 to 1.3, with a mean magnitude near 0.26.

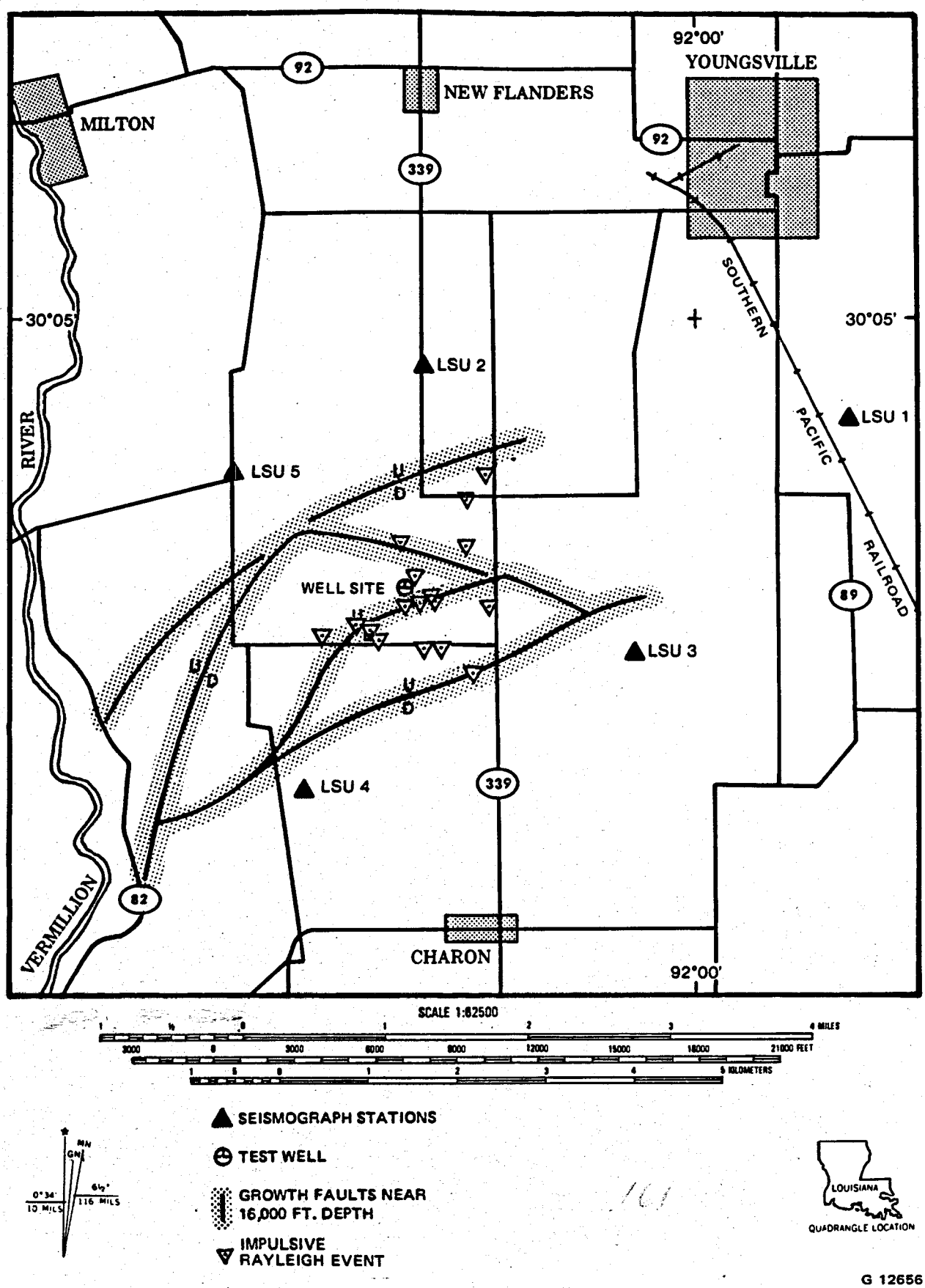

FIGURE A-1. LOCATION OF LEAKING MODE EVENTS RECORDED DURING OCTOBER 1983

Entries for the table A-1 data log utilize the following notation conventions:

Station Identification

LSU1, LSU2, LSU3, LSU4, LSU5

Phase Identification

P - compressional wave

S - shear wave

LR - Rayleigh surface wave

i - impulsive first motion

e - emergent first motion

c - compressional first motion

d - dilatational first motion

? - ambiguity of designation

pP - P-wave reflected at the crust near the epicenter

sS - S-wave converted to P-wave at reflection like pP

Airy - Airy phase (minimum group velocity) of Rayleigh wave.

Phase Timing

Times are designated in Universal Coordinated Time (UTC) which is equivalent to Central Standard Time + six hours. Explosions in a sequence may be designated by hour and minute only.

Phase Amplitude and Period

A_m = maximum 0-peak amplitude of the phase in mm observed on develocorder review (20 x magnification)

A = sustained 0-P amplitude in mm observed on develocorder review (20 x magnification) of a train of waves.

T = period of the wave in seconds.

D = duration of signal in seconds from onset of P to code = ambient noise.

C = number of cycles in a wave train.

Example Data Entry

LSU1	iPC	04:24:15.1, T = 0.5, A_m = 20.0, A = 13.0;
	eS	04:24:20.3, T = 1.0, D = 35

Station LSU1 recorded an impulsive-compressional P-wave at 04:24:15.1 UTC. The sustained amplitude was 13 mm zero to peak, the maximum amplitude was 20 mm, the period of the wave was 0.5 seconds. An emergent S wave was recorded at 04:24:20.3 UTC with a period of 1.0 seconds. The total event duration was 35 seconds.

TABLE A1. PARCPERDUE DATA LOG FOR OCTOBER AND NOVEMBER 1983

1. 83-10-03
   22:03:19.4 UTC
   Impulsive Rayleigh event, velocity = 100 meters/second

LSU1	iLR	Inoperative;
LSU2	iLR	22:03:44.60;
LSU3	iLR	22:03:44.90;
LSU4	iLR	22:03:44.90;
LSU5	iLR	22:03:45.40

2. 83-10-03
   22:14:00 UTC
   Impulsive Rayleigh event, velocity = 100 meters/second

LSU1		Inoperative;
LSU2	iLR	22:14:05.30;
LSU3	iLR	22:14:05.30;
LSU4	iLR	22:14:05.75;
LSU5	iLR	22:14:05.05

3. 83-10-03
   22:24:05.3 UTC
   Impulsive Rayleigh event, velocity = 100 meters/second

LSU1	iLR	Inoperative;
LSU2	iLR	22:24:30.25;
LSU3	iLR	22:24:33.90;
LSU4	iLR	22:24:31.00;
LSU5	ILR	22:24:30.45

4. 83-10-04
   16:16:00 UTC
   Exploration shot series from outside the array

   Additional exploration shots:

   83-10-04: 22:27:30, 23:34:50, 22:46:00
   83-10-05: 15:31:31, 15:46:40, 16:04:00, 18:17:15

5. 83-10-06
13:27:39 UTC
Acoustic-coupled Rayleigh event - Sonic Boom

LSU1		Inoperative;
LSU2	iLR	13:28:42.40;
LSU3		Inoperative;
LSU4	iLR	13:28:41.50;
LSU5	iLR	13:28:39.20

Additional acoustic-coupled Rayleigh events:

83-10-20:	15:12:40
83-10-24:	15:49:03
83-10-25:	16:47:15
83-10-26:	16:25:00
83-11-14:	14:08:29

6. 83-10-06
19:05:29.0 UTC
Emergent Rayleigh event, velocity = 100 meters/second

LSU1	iLR	Inoperative;
LSU2	iLR	19:06:03:80;
LSU3	iLR	19:05:52.60;
LSU4	iLR	19:05:52.60;
LSU5	iLR	19:04:54.60

7. 83-10-06
21:18:51.8 UTC
Emergent Rayleigh event, velocity = 100 meters/second

LSU1	iLR	Inoperative;
LSU2	iLR	21:19:11.50;
LSU3	iLR	21:19:22.80;
LSU4	iLR	21:19:11.50;
LSU5	iLR	21:19:14.80

8. 83-10-11
06:50:39.4 UTC
Emergent Rayleigh event from outside the array

LSU1		Inoperative;
LSU2	iLR	06:51:10.40;
LSU3	iLR	06:50:57.50;
LSU4	iLR	06:51:06.00;
LSU5	iLR	06:51:12.80

165

9. 83-10-11
17:21:31.8 UTC
Large emergent Rayleigh event from outside the array

LSU1		Inoperative;
LSU2	iLR	17:22:03.00;
LSU3	iLR	17:21:48.90;
LSU4	iLR	17:22:00.00;
LSU5	iLR	17:22:04.20;

10. 83-10-12
10:11:53.3 UTC
Impulsive Rayleigh event, velocity = 125 meters/second

LSU1		Inoperative;
LSU2	iLR	10:12:18.80;
LSU3	iLR	10:12:12.20;
LSU4	iLR	10:12:10.70;
LSU5	iLR	10:12:16.80

11. 83-10-12
10:13:16.5 UTC
Impulsive Rayleigh event, velocity = 100 meters/second

LSU1		Inoperative;
LSU2	iLR	10:13:39.80;
LSU3	iLR	10:13:44.10;
LSU4	iLR	10:13:43.50;
LSU5	iLR	10:13:39.70

12. 83-10-12
10:34:43.9 UTC
Impulsive Rayleigh event, velocity = 150 meters/second

LSU1		Inoperative;
LSU2	iLR	10:35:07.50;
LSU3	iLR	10:34:56.70;
LSU4	iLR	10:34:59.30;
LSU5	iLR	10:34:07.20

166

13. 83-10-12
10:39:30.0 UTC
Impulsive Rayleigh event, velocity = 100 meters/second

LSU1		Inoperative;
LSU2	iLR	10:39:55.90;
LSU3	iLR	10:39:48.80;
LSU4	iLR	10:39:59.80;
LSU5	iLR	10:40:02.40

14. 83-10-13
11:50:45.0 UTC
Micro-earthquake

LSU1		Inoperative;
LSU2	iLR	11;51:12.20;
LSU3	iLR	11;51:09.90;
LSU4	iLR	11:51.10.30;
LSU5	iLR	11:51:10.70

15. 83-10-13
15:47:00 UTC
Impulsive Rayleigh event from outside the array

LSU1		Inoperative;
LSU2	iLR	15:47:09.60;
LSU3	iLR	15:47:13.80;
LSU4	iLR	15:47:09.50;
LSU5	iLR	15:47:06.80

16. 83-10-14
01:08:30.4 UTC
Emergent Rayleigh event, velocity = 100 meters/second

LSU1		Inoperative;
LSU2	iLR	01:08:59.50;
LSU3	iLR	01:08:56.40;
LSU4	iLR	01:08:55.90;
LSU5	iLR	01:08:51.90

17. 83-10-14
01:11:46.0 UTC
Emergent Rayleigh event, velocity = 100 meters/second

LSU1		Inoperative;
LSU2	iLR	01:12:17.50;
LSU3	iLR	01:12:15.50;
LSU4	iLR	01:12:05.60;
LSU5	iLR	01:12:10.10

18. 83-10-14
02:13:24.7 UTC
Impulsive Rayleigh event, velocity = 100 meters/second

LSU1		Inoperative;
LSU4	iLR	02:13:55.40;
LSU4	ILR	02:13:57.00;
LSU4	iLR	02:13:44.70;
LSU5	ILR	02:13:46.10

19. 83-10-27
19:40:50.83 UTC ±0.32 sec
30.243 N ±3.3 km 93.393 W ±2.2 km
Depth = 5.0 km (geophysicist)
Lake Charles, Louisiana (504) mblg 3.8 (TUL), 3.4 (SLM), 3.5 (BLA). Felt (III) at Hackberry and Hayes. Also felt at Sulphur, Westlake and in the Lake Charles area.

LSU5	1.17	98	P	41 13.50
LSU4	1.18	100	P	41 13.90
LSU3	1.22	99	P	41 14.20
HKT	2.14	263	iP	41 27.80
			iS	41 54.50
NSLM	2.19	323	iP	41 29.50
ATX	3.87	272	eP	41 50.80
			iS	42 37.50
STAR	3.89	20	iP	41 53.19
			iS	42 37.45
BHO	4.31	344	iPnc	41 58.40
			i	41 59.20
SHA	4.55	83	e(P)	42 00.00
LGAR	4.97	27	iP	42 07.40
			iS	43 04.70
PGM	5.04	33	eP	42 08.70
			iS	43 04.40
WLA	5.42	24	eP	42 14.05

TABLE A1. PARCPERDUE DATA LOG FOR OCTOBER AND NOVEMBER 1983, Continued

OLY	5.49	17	iPc	42	14.90
			S	43	15.90
JCT	5.54	274	eP	42	14.00
			eS	43	16.50
GBO	5.79	345	iPn	42	20.30
SFTN	5.84	28	eP	42	19.40
TUL	6.00	341	iPnc	42	23.00
	0.8s		73.50nm		5.5mb
SIO	6.01	337	iPn	42	22.90
RLO	6.06	347	iPn	42	23.70
POW	6.18	17	eP	42	24.00
PWLA	6.52	42	iPC	42	28.04
			iS	43	38.30
PCO	7.10	336	e(P)	42	37.70
ELC	7.83	25	e(P)	42	47.00
FVM	8.10	17	e(P)	42	50.00
RSCP	8.46	49	eP	42	53.00
BHT	9.03	50	eP	43	02.50
			S	44	37.70
GBTN	9.42	53	eP	43	08.00
			eS	44	46.20
TKL	9.72	54	eP	43	10.00
			eS	44	53.50
PRM	10.10	65	eP	43	12.80
ALQ	11.97	296	ePc	43	43.50
	0.6s		1.83nm		4.6mb
GOL	13.61	317	eP	44	04.30
BDW	18.00	318	eP	45	05.00
	1.0s		4.40nm		3.5mb
DUG	18.68	307	eP	45	14.80
RSON	20.60	359	eP	45	32.00
	0.7s		4.96nm		4.0mb
COL	48.08	332	eP	49	32.00
	0.9s		4.10nm		4.5mb

S.D = 0.8 on 21 of 35 obs.

20. 83-10-27
~~18~~:38:~~29~~.7 ~~UTC~~
Large impulsive Rayleigh event, velocity = 125 meters/second

LSU1		Inoperative;
LSU2	iLR	18:38:45.60;
LSU3	iLR	18:38:48.80;
LSU4	iLR	18:38:48.60;
LSU5	iLR	18:38:57.00

169

21. 83-10-28
14:11:11 UTC
Idaho quake
OT = _____ UTC, H = 122 km, mb = 5.7

22. 83-11-02
16:00:48.6 UTC
Large impulsive Rayleigh event, velocity = 200 meters/second

LSU1	iLR	Inoperative;
LSU2	iLR	16:00:56.30;
LSU3	iLR	Inoperative;
LSU4	iLR	16:01:07.70;
LSU5	iLR	16:01:01.70

23. 83-11-02
17:56:14 UTC
Exploration shot series from outside the array

Additional exploration shots:

83-11-02: 17:57:59, 18:00:10, 18:03:34, 18:05:20, 18:08:10, 18:15:43, 18:17:11, 18:23:00, 18:23:00, 18:29:30, 18:35:32

24. 83-11-03
18:45:18.8 UTC
Impulsive Rayaleigh event, velocity = 250 meters/second

LSU1		Inoperative;
LSU2	iLR	14:45:24:10;
LSU3		Inoperative;
LSU4	iLR	14:45:35:40;
LSU5	iLR	14:45:29.90

25. 83-11-10
20:54:33.4 UTC
Impulsive Rayleigh event, velocity = 100 meters/second

LSU1		Inoperative;
LSU2	iLR	20:55:00.10;
LSU3	iLR	20:54:57.50;
LSU4	iLR	20:55:00.00;
LSU5	iLR	20:54:59.20

TABLE A1. PARCPERDUE DATA LOG FOR OCTOBER AND NOVEMBER 1983, Continued

26. 83-11-16
11:10:08.7 UTC
Impulsive Rayleigh event, velocity 175 meters/second

LSU1		Inoperative;
LSU2	iLR	11:10:27.30;
LSU3		Inoperative;
LSU4	iLR	11:10:19.30;
LSU5	iLR	11:10:20.10

27. 83-11-16
17:43:41.9 UTC
Impulsive Rayleigh event, velocity = 100 meters/second

LSU1		Inoperative;
LSU2	iLR	17:44:02.50;
LSU3		Inoperative
LSU4	iLR	17:44:12.10;
LSU5	iLR	17:44:12.10

TABLE A2. PARCPERDUE, LOUISIANA ARRAY EVENT LOG FOR OCTOBER AND NOVEMBER, 1983

Event No.	Month	Day	Hr	Min	Sec	Latitude (N) Y	Longitude (W) X	Depth	Magnitude	90% Confidence Ellipse Sem. Major Axes	Velocity (m/sec)
1	10	03	22	03	19.5	-0.092 30 03 19.2	0.287 92 01 58.5	—	-.1		100
3	10	03	22	24	05.3	-0.102 30 03 18.9	0.179 92 01 58.7	—	-1.42		100
6	10	06	19	05	29.0	-0.707 30 03 00.6	0.204 92 02 00.7	—	.72		100
7	10	06	21	18	51.8	-0.510 30 03 06.6	-0.383 92 02 16.0	—	.70		100
10	10	12	10	11	53.3	-0.707 30 03 00.6	0.337 92 01 57.2	—	-.63		125
11	10	12	10	13	16.5	.111 30 03 25.3	.115 92 02 03.0	—	-.97		100
12	10	12	10	34	43.9	-1.024 30 02 51.0	0.798 92 01 45.1	—	-.59		150
13	10	12	10	39	30.0	-0.113 30 03 18.6	0.974 92 01 40.5	—	-.26		100
14	10	13	11	50	45.0	-0.224 30 03 15.2	0.265 92 01 59.1	—			100
16	10	14	01	08	30.4	-0.196 30 03 16.1	0.019 92 02 05.5	—	.75		100
17	10	14	01	11	46.0	-0.587 30 03 04.2	-0.259 92 02 12.8	—	.13		100
18	10	14	02	13	24.7	-0.444 30 03 08.6	-0.523 92 02 19.7	—	.08		100
19	10	27	18	38	29.7	0.533 30 03 38.1	0.738 92 01 46.7	—	1.26		125
21	11	02	16	00	48.6	0.998 30 03 52.1	0.744 92 01 46.6	—	1.16		200
23	11	03	18	45	18.8	1.286 30 04 00.8	.914 92 01 42.1	—	.89		250
24	11	10	20	54	33.4	-0.149 30 03 17.4	0.354 92 01 56.7	—	.51		100
25	11	16	11	10	08.7	-0.511 30 03 06.5	-0.924 92 02 30.2	—	-.46		175
26	11	16	17	43	41.9	0.502 30 03 37.1	-0.086 92 02 08.2	—	.72		100

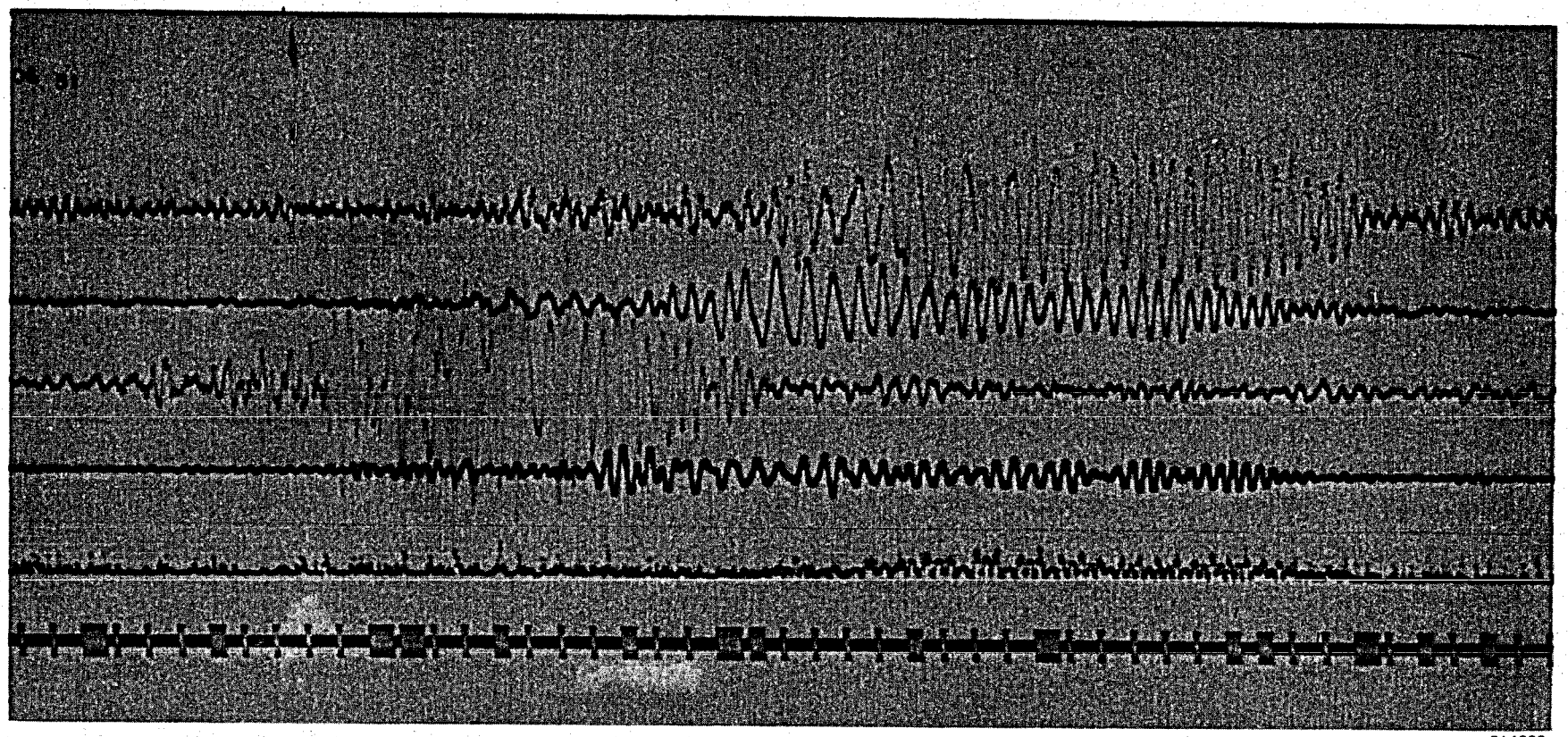

G14833

FIGURE A2. RAYLEIGH/LEAKING MODE EVENT #8, 06:50:39.4 UTC. 11 OCTOBER 1983, VELOCITY = 100 METERS/SECOND

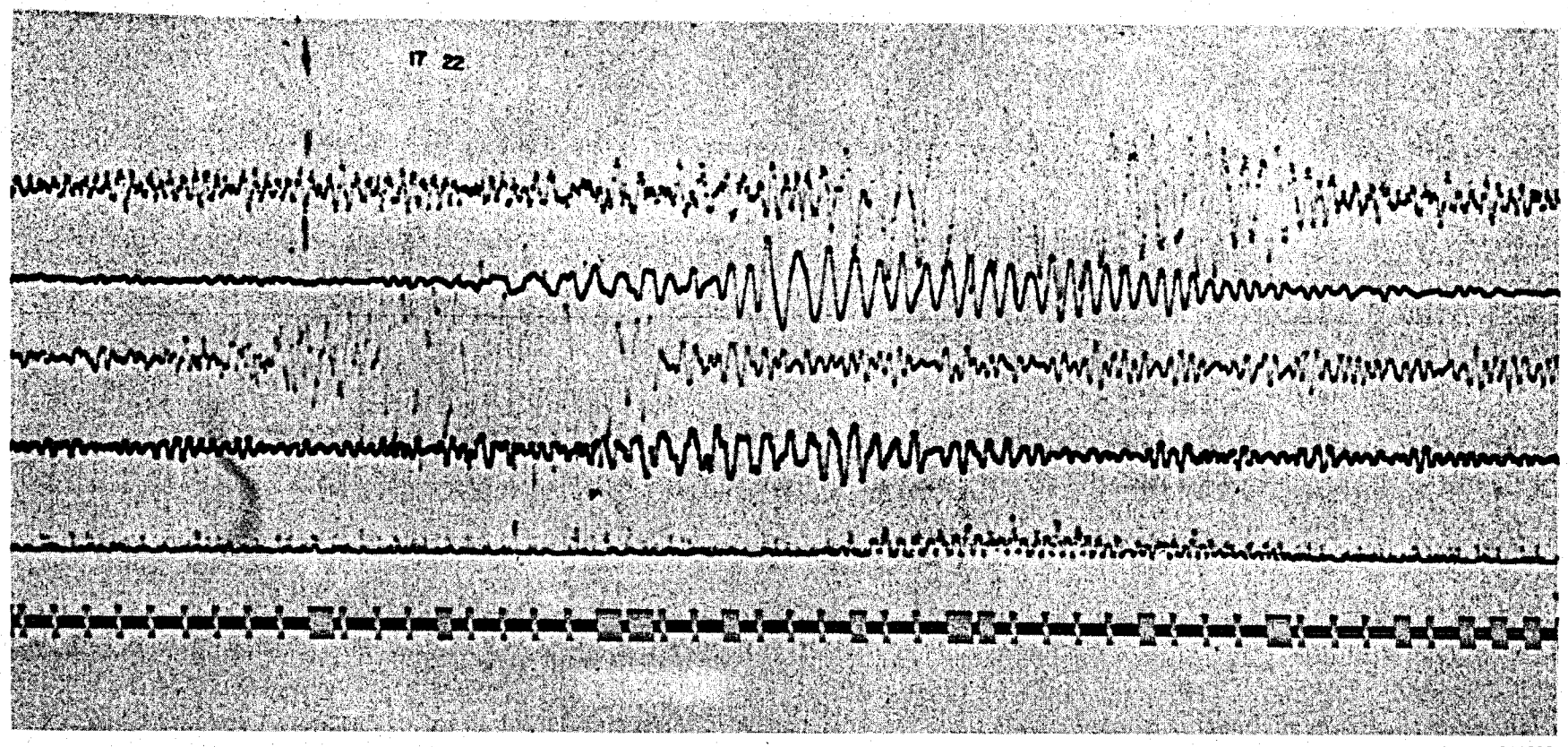

G14832

FIGURE A3. RAYLEIGH/LEAKING MODE EVENT #9, 17:21:31.8 UTC, 11 OCTOBER 1983, VELOCITY = 100 METERS/SECOND

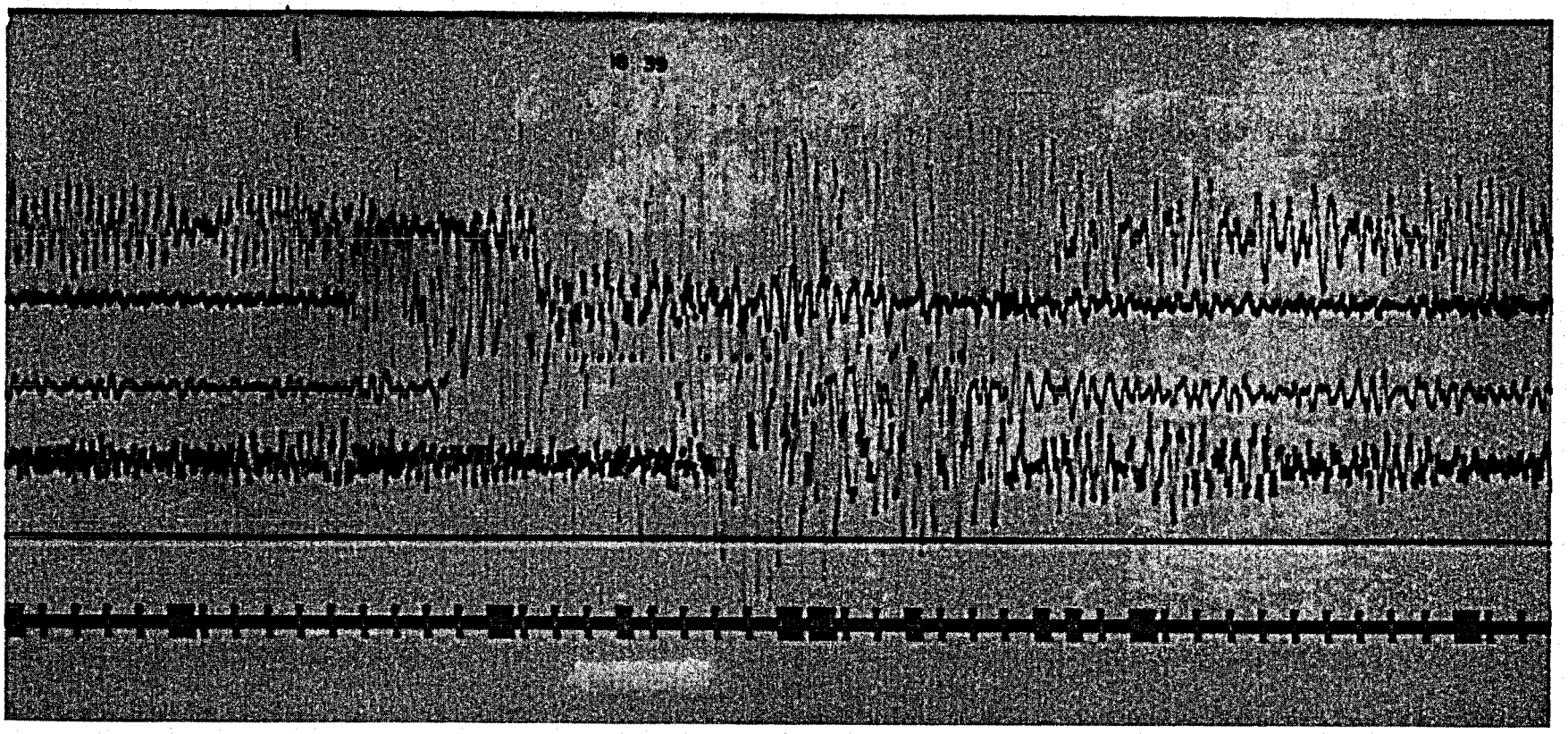

G14831

FIGURE A4. RAYLEIGH/LEAKING MODE EVENT #20, 18:38:29.7 UTC, 27 OCTOBER 1983, VELOCITY = 125 METERS/SECOND

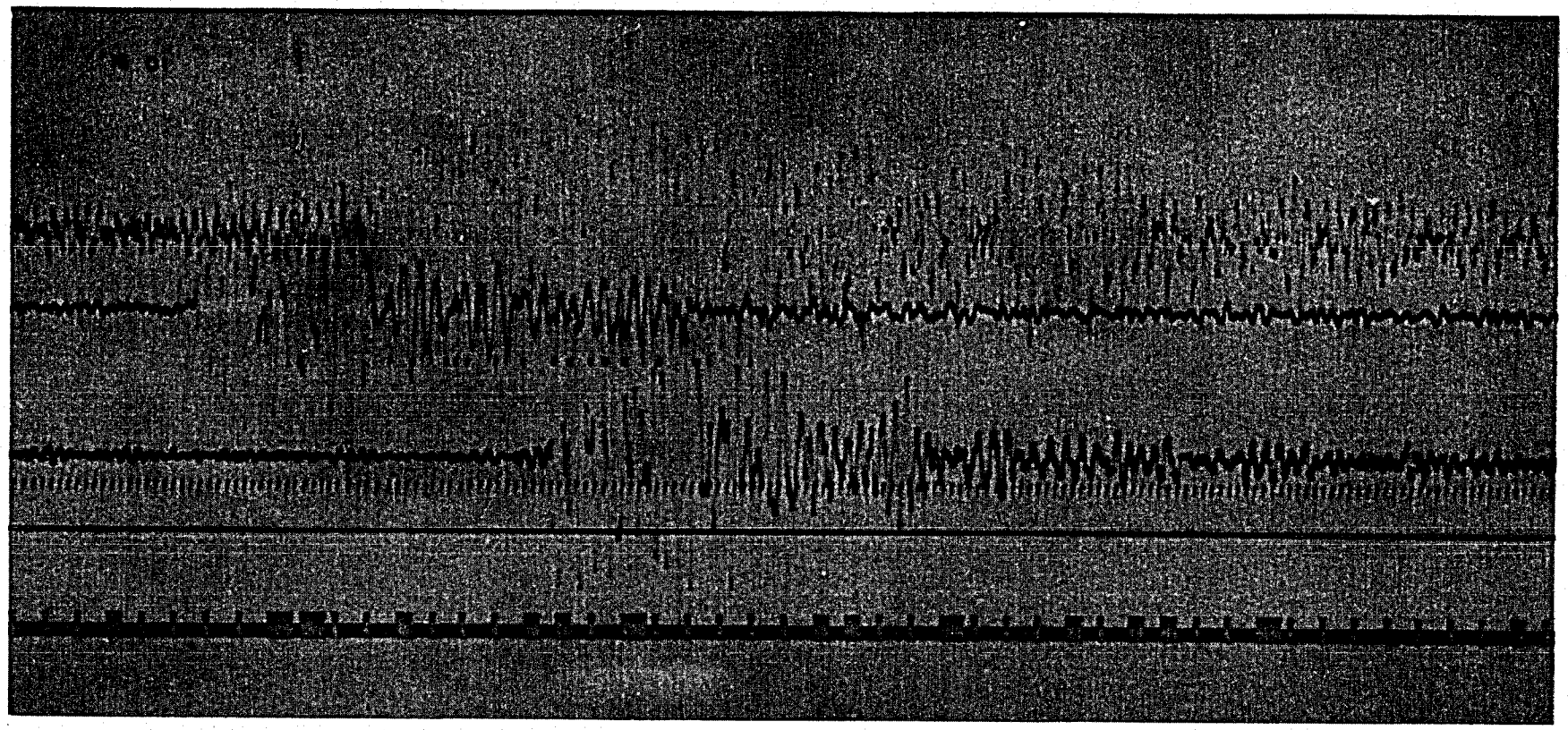

G14830

FIGURE A5. RAYLEIGH/LEAKING MODE EVENT #22, 16:00:48.6 UTC, 2 NOVEMBER 1983, VELOCITY = 200 METERS/SECOND